UNIVERSITAT DE BARCELONA

Connecting biodiversity and biogeochemical role by microbial metagenomics

Tomàs Llorens Marès

Tesi Doctoral

Universitat de Barcelona

Facultat de Biologia – Departament d'Ecologia

Programa de doctorat en Ecologia Fonamental i Aplicada

Connecting biodiversity and biogeochemical role by microbial metagenomics

Vincles entre biodiversitat microbiana i funció biogeoquímica mitjançant una aproximació metagenòmica

Memòria presentada pel Sr. Tomàs Llorens Marès
per optar al grau de doctor per la Universitat de Barcelona

Tomàs Llorens Marès

Centre d'Estudis Avançats de Blanes (CEAB)
Consejo Superior de Investigaciones Científicas (CSIC)

Blanes, Juny de 2015

Vist i plau del director i tutora de la tesi

El director de la tesi
Dr. Emilio Ortega Casamayor
Investigador científic
del CEAB (CSIC)

La tutora de la tesi
Dra. Isabel Muñoz Gracia
Professora al Departament
d'Ecologia (UB)

Llorens-Marès, T., 2015. *Connecting biodiversity and biogeochemical role by microbial metagenomics*. PhD thesis. Universitat de Barcelona. 272 p.

Disseny coberta: Jordi Vissi Garcia i Tomàs Llorens Marès.
Fletxes coberta: Jordi Vissi Garcia.
Fotografia coberta: Estanys de Baiau (Transpirinenca 2008), fotografia de l'autor.

La ciència es construeix a partir d'aproximacions que s'acosten progressivament a la realitat

Isaac Asimov (1920-1992)

Agraïments

Tot va començar l'estiu de 2009, just acabada la carrera de Biotecnologia. Com sovint passa quan acabes una etapa i n'has de començar una altra, els interrogants s'obren al teu davant i la millor forma de resoldre'ls és provar. Vaig fer una col·laboració al departament d'Enginyeria de Bioprocessos de la UAB en optimització de fermentacions (un tema clarament aplicat), però no em va convèncer. Jo sóc blanenc de tota la vida, els meus pares i avis tenen un botiga de pesca a on hi van a comprar coses la gent del Centre d'Estudis Avançats de Blanes i sabia que feien ciència a la muntanya i al mar. I així va ser com l'Àngel (responsable de manteniment del CEAB), em va dirigir a l'Emili, qui posteriorment seria el meu director de tesi. I aquí cau el primer agraïment, si l'Àngel no s'hagués interessat en preguntar-ho i dir-ho als meus pares, segurament no hauria escrit aquesta tesi, moltes gràcies Àngel! Doncs bé, casualitats de la vida, el grup de l'Emili es dedicava a estudiar l'ecologia dels llacs de muntanya (ja sabeu que m'apassiona la muntanya) i a més, utilitzant tècniques moleculars, que segurament era la única via d'entrada al CEAB tenint en compte la carrera que havia estudiat. Allò va resultar en una col·laboració durant el mes d'Agost i el repte d'escriure un projecte per a obtenir una beca per a fer el doctorat en el seu grup. Aquell any vaig marxar d'octubre a març a fer unes pràctiques a una empresa biotecnològica a Slough (al costat de Londres), en uns mesos que em va servir per escriure el projecte i adonar-me'n que fer el doctorat era la decisió correcta.

En tornar, vaig seguir col·laborant tot l'estiu amb l'Emili i després vam saber que no ens havien donat la beca. De totes formes, l'Emili va confiar en mi, i em va contractar a través d'un projecte per a que pogués fer la tesi. Això s'ha anat repetint any rere any fins acabar la tesi i no puc fer res més que estar eternament agraït d'haver pogut fer una tesi doctoral sense disposar de beca, una cosa que només depenia de l'Emili. Aprofito per agrair-te tot el

temps que has dedicat a la meva tesi, sobretot aquests darrers mesos (per no dir setmanes) i també per ensenyar-me tantes coses sobre la ciència i sobretot com transmetre un missatge, ja sigui en un article o en una xerrada, moltíssimes gràcies!

Aquell primer any també va ser el del màster en Ecologia Fonamental i Aplicada, un any on vaig fer la meva primera incursió en l'Ecologia (una branca que no es toca massa a Biotecnologia) i també em va servir per fer classes a la UdG, cosa que em va fer molta il·lusió. Moltes gràcies als magnífics companys d'aquell màster amb qui vam compartir molts bons moments i als professors que em van ensenyar una forma diferent de mirar el món. Merci Marc per l'ajuda en aquell mostreig al Redó i per ensenyar-me com funciona el món de l'esquí de muntanya! Espero que ens seguim trobant per aquestes muntanyes perdudes arreu del món!

El segon any va ser el de l'estada al JCVI de San Diego, California. Van ser tres mesos apassionants, on vaig aprendre moltíssim de la gent d'allà, però també amb la Maria, que va estar-hi un mes fent-me costat i ajudant-nos mútuament per comprendre com funcionava aquest món de la *metagenòmica*. Gràcies Maria per aquells dies i pel que ens hem ajudat després! Qui ens havia de dir que aniríem a casa del mateix Craig Venter a celebrar el seu aniversari, o que coneixeríem en persona un parell de premis Nobel, se'ns dubte allò va ser un gran moment d'aquesta tesi! Allà hi vaig conèixer molta altra gent, i tots em van ajudar moltíssim en cada pas que s'havia de fer. *Shibu you were the person that supported me in most bioinformatics problems, thank you very much for your time! And Chris, thanks for everything during my stay there, for your knowledge on global ecology and metagenomics that was very important during this PhD. Jeroen you were a fantastic friend in and out of the JCVI and it was a pleasure to share with you some great adventures!*

L'equador de la tesi també va comptar amb una estada internacional a la Penn State University (State College, Pennsylvania),

una col·laboració que es va gestar en un congrés a Holanda, on vaig presentar els resultats de l'estada a San Diego. *Thanks Don to host me and believe in the Chl. luteolum CIII genome! It was a short but intense month in which I learned everything about green sulfur bacteria and its genomes with the incredible support of Jay!*

El quart any va ser per encarar la segona part de la tesi, on vaig fer una part de feina de laboratori (que finalment no ha sortit a la tesi) i on vam anar a mostrejar l'estany Redó! Quina il·lusió que em va fer! A principis d'any també vaig tenir la oportunitat de fer una de les xerrades d'Aula Blanes. Gràcies Pep per donar-me aquesta oportunitat, per poder acostar la ciència a la gent del poble i a la família, i poder ensenyar la feina que estava fent al CEAB i que ara es veu reflectida en aquesta tesi doctoral. Feu una molt bona feina amb Aula Blanes, no deixeu mai de fer-ho!

Com molt bé sabeu, m'agrada fer curses de llarga distància, i en aquestes curses, quan més es pateix és cap al final, quan s'acumula tot el cansament psicològic i físic; però tot i que el final sol ser duríssim, també és quan te n'adones que acabaràs i en els darrers quilòmetres és quan gaudeixes més i et sents més ple, orgullós i feliç de l'esforç realitzat. Doncs no hi ha un símil millor per descriure aquest darrer any, ha estat duríssim, sobretot els darrers dos mesos on he concentrat moltíssima energia per acabar d'escriure aquesta tesi que teniu a les vostres mans, però alhora, ara, escrivint aquests agraïments i quan ja veig que arriba el final, és el moment de sentir-se feliç i orgullós d'aquest llarg camí recorregut durant aquests 5 anys.

I durant aquest camí, amb qui més he compartit a nivell científic ha estat amb els companys de grup. Els primers anys, vaig aprendre moltíssim de tres fenòmens com en Jean-Chris, l'Albert i l'Antoni, ha estat un honor poder compartir hores de treball amb vosaltres, em vau transmetre una autèntica passió per la ciència. No m'oblido tampoc de la Natalia, la Carmen, l'Anna, l'Ade i la Clàudia que tot i compartir-hi poc temps també han suposat un gra de sorra

per aquesta tesi. Amb en Xevi vam compartir l'organització d'un congrés a Santa Susanna i la paraula que em ve al cap per definir-lo és "mestre", gràcies per totes les hores que t'he tret del teu temps i per ser una persona que sempre està disposada a ajudar i aconsellar-te amb saviesa sobre qualsevol assumpte. I en Gela, que sempre sap trobar una solució per a treure el màxim rendiment del *cluster* i amb qui un dia haurem d'anar a volar amb parapent! Amb l'Steffi vam compartir unes quantes hores refent els càlculs de les qPCRs... Vaia tela! Moltes gràcies pels teus consells i el genial cap de setmana a Taüll! I els darrers anys s'han incorporat en Rüdi i en Vicente, un parell que apunten molt alt i que han sigut de gran suport en aquest final de tesi!

El CEAB està ple de gent fantàstica que ho fan tot molt fàcil, des de la gent d'administració fins a tots els que fan que el centre tiri cada dia endavant, moltes gràcies a tots vosaltres per tots els moments en què us he necessitat. Gràcies Xavi per les sortides amb bici... jo que em pensava que em coneixia el territori! Amb en Guillem i en Miquel vam començar compartint el cinquè nivell d'anglès a l'EOI i han acabat per ser dos grans empentes en aquest final de tesi, teniu molta culpa de que hagi pogut acabar la tesi abans d'agost perquè m'heu facilitat molts del passos "burrocràtics"! I a tots aquells amb qui he compartit algun moment de lleure, ja sigui un soparet, una sortida amb bicicleta, un partidet de futbol o un te a la terrassa del CEAB, gràcies per haver-me acollit tan bé tot i ser un "outsider" de Blanes!

La meva colla d'amics de Blanes tindrà alguna culpa d'aquest doctorat, a més, aviat en serem tres de doctors! Heu de saber que sou uns cracks i que les nostres converses filosòfiques (no per arreglar el món, sinó per arreglar-nos a nosaltres) han estat imprescindibles per tirar-ho endavant i entendre el sentit de tot plegat! Igual que passa amb els companys d'universitat, van ser només quatre anys, però d'aquella promoció en va sortir un grup especial que crec que va més enllà de simples companys

d'Universitat... Gràcies perquè cada trobada amb vosaltres és un pou de coneixement que s'encomana com un virus!

I, evidentment, la *family*: pares, avis, tiets, cosins... els que sempre hi sou i sort de vosaltres que mai heu tingut un no i sempre m'heu ajudat en tot, això sí que és tenir un gran suport! I volia acabar amb tu, que no només has hagut d'aguantar les meves "neures" *doctorals*, sinó que també has d'aguantar dia rere dia les *esportives*, *cauístiques*, *musicals, existencials*... i malgrat tot, segueixes aguantant-me i donant-me suport!

S'acaba una etapa i en comença una altra que segur que serà tan o més emocionant que totes les que han vingut fins ara.

Blanes, Juny de 2015

Informe del director

El Dr. Emilio Ortega Casamayor, Investigador Científic del Centre d'Estudis Avançats de Blanes (CSIC), i director de la Tesi Doctoral elaborada per Tomàs Llorens Marès i que porta per títol "***Connecting biodiversity and biogeochemical role by microbial metagenomics***"

INFORMA

Que els treballs de recerca portats a terme per Tomàs Llorens Marès com a part de la seva formació pre-doctoral i inclosos a la seva Tesi Doctoral han donat lloc a dos articles publicats, i tres manuscrits addicionals a punt de ser enviats a revistes d'àmbit internacional. A continuació es detalla la llista d'articles així com els índexs d'impacte (segons el SCI de la ISI Web of Knowledge) de les revistes on han estat publicats els treballs.

> *1. Llorens-Marès T, JC Auguet, EO Casamayor (2012) Winter to spring changes in the slush bacterial community composition of a high mountain lake (Lake Redon, Pyrenees). Environ Microbiol Reports 4 (1): 50-56. doi: 10.1111/j.1758-2229.2011.00278.x.*

L'índex d'impacte de la revista *Environmental Microbiology Reports* es de 3.264. Aquesta revista pertany a la categoria "Environmental Sciences" a la posició 35 de 216 revistes, quedant inclosa al grup de revistes del 1er quartil.

> *2. Llorens–Marès T, S Yooseph, J Goll, J Hoffman, M Vila-Costa, CM Borrego, CL Dupont, EO Casamayor (2015) Connecting biodiversity and potential functional role in modern euxinic environments by microbial metagenomics. ISME J 9: 1648-1661. doi:10.1038/ismej.2014.254.*

L'índex d'impacte del *ISME Journal* al 2014 va ser de 9.267. Tenint en compte aquest índex d'impacte la revista ocupa el 4rt lloc de la categoria ISI "Ecology", i el 9è a la categoria ISI "Microbiology", quedant inclosa en les revistes del primer decil en tots dos casos.

Alhora, FA CONSTAR

Que en Tomàs Llorens ha participat activament en el desenvolupament del treball de recerca associat a cadascun d'aquests treballs així com en la seva elaboració a les diferents fases, participant en el plantejament inicial dels objectius i liderant el processament de les dades, aplicació de la metodologia i optimització del processos bioinformàtics, filogenètics i d'assignació funcional, així com en la redacció dels articles i seguiment del procés de revisió dels mateixos.

Que cap dels co-autors dels articles abans esmentats ha utilitzat o bé té present utilitzar implícita o explícitament aquests treballs per a l'elaboració d'una altra Tesi Doctoral.

Signat a Blanes, 23 de Juny 2015

Dr. Emilio Ortega Casamayor

Contents

Connecting biodiversity and biogeochemical role by microbial metagenomics

Part I: Anoxic and suboxic systems with prevalent euxinia

Part II: Oxic system with oligotrophic waters

General overview

Bibliography

Appendix

Connecting biodiversity and biogeochemical role by microbial metagenomics

I

General introduction

Antonie van Leeuwenhoek (1632-1723) unveiled the microbial world at the end of the 17th century using handcrafted microscopes, a revolutionary methodological advance by that time. During the 18th, 19th and early 20th centuries, the study of microorganisms increased at a slow but constant pace hand in hand with technological improvements that initially promoted the study of microscopic life forms under two main perspectives, i.e. laboratory culturing and biochemical studies on a few bacterial strains, and structural descriptions by light and, late in 1930, electronic microscopy. Simultaneously, Ernst Haeckel (1834-1919) coined the word ecology in 1866, combining two Greek words for "household" and "knowledge" in what we now define as "the branch of biology dealing with the relations and interactions between organisms and their environment." The idea that microbes are ubiquitous and that microbiology could contribute to a universal theory of life began to flourish in the beginning of the 20th century by Martinus Beijerinck (1851-1931) and Lourens Baas Becking (1895-1963) (O'Malley 2008). However, it was not until the late 1960s that Thomas D. Brock (Ohio, 1926) wrote the first textbook with the term *microbial ecology* (Brock 1966), trying to integrate all the different disciplines studying microorganisms and its influence on ecology in the same global field.

Because of the technical difficulties to study microorganisms *in situ*, microbial ecology has always been a methods-driven discipline. In this PhD dissertation we explore the potential and limitations of the application of *metagenomics* for the study of microorganisms *in situ*.

1.1 Microbial biodiversity and evolution

The revolutionary vision of Carl Woese (1928-2012), using the divergence between nucleotide sequences of the small subunit of the ribosomal DNA (16S rRNA) as a 'molecular clock', allowed him to discover a completely new branch of life (Woese and Fox 1977), and changed the historical and classical view of the five kingdoms of life to a new paradigm based on three domains: Archaea, Bacteria and Eukarya (Woese et al. 1990). But it was Norman Pace and his team that combining a reverse transcriptase with DNA cloning techniques (Lane et al. 1985), and later improved by the polymerase chain reaction (PCR) protocol (Mullis and Faloona 1987), provided an easy methodology to obtain 16S rRNA sequences from field samples and popularized the study of microbes *in situ*. Thanks to these techniques, molecular microbial ecology flourished as an important field to help unveiling the biogeochemical interactions mediated by microbial communities and thus, understand the role of microorganisms in the evolution of life on Earth (O'Malley and Dupre 2007).

Currently, aerobic processes are prevalent both on land and oceanic ecosystems. However, early ocean and atmosphere were totally anoxic, and the emergence of life took place under anaerobic conditions (Kasting and Siefert 2002). Anoxic conditions dominated during the first half of Earth's history, until the appearance of oxygenic photosynthesis, the biological process by which cyanobacteria obtained energy and reducing power from light and water, respectively, and released O_2 as "waste" product. Microbial activity changed the air composition in what is know as the great oxygenation event (GOE). However, the deep ocean remained

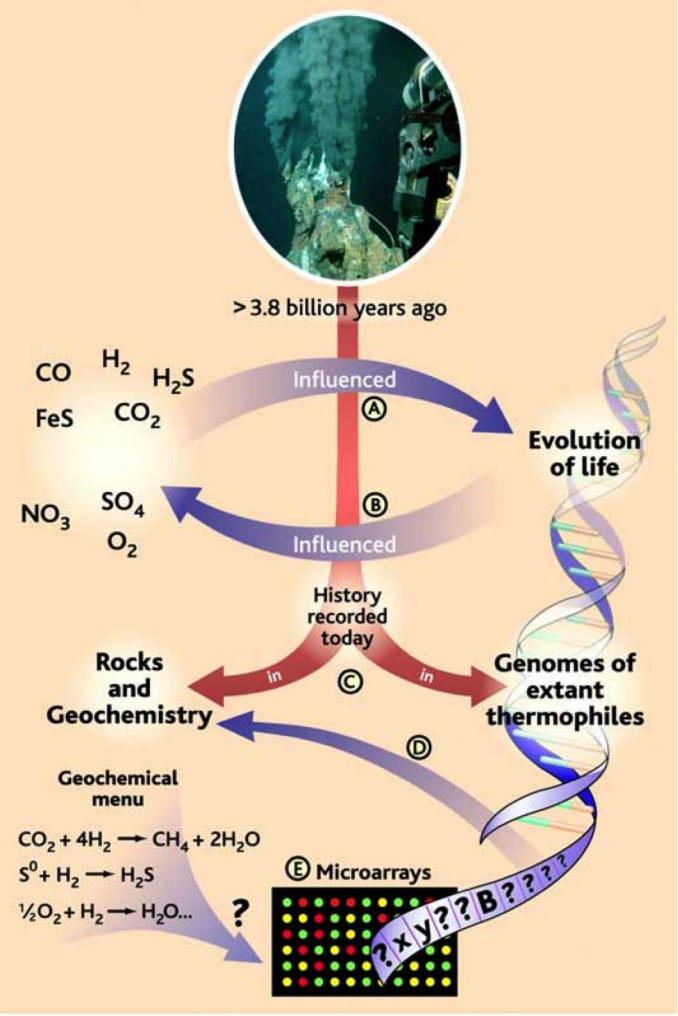

Figure 1.1: Conceptual framework of the link between biogeochemical cycles and microorganisms and how using NGS technologies we can reconstruct the history of evolution of life on Earth. Figure from Reysenbach and Shock (2002).

dominantly anoxic and the sink of organic matter from productive areas (mostly along continental margins), favoured the development of highly reduced environments where euxinic conditions (oxygen-free waters with dissolved hydrogen sulfide (H_2S)) were abundant, in what is known as the "Canfield Ocean" (Meyer and Kump 2008, Lyons et al. 2014). Overall, the "chemical soup" in early stages of Earth influenced the evolution of microbial life, which in turn changed the biogeochemistry of the atmosphere and ocean (Fig. 1.1). Thus,

the study of current environments with contrasting redox conditions may help to better understand the early evolution of life on Earth, and unveil the evolutionary history by which biogeochemical interactions turned hot water and rocks into habitats (Reysenbach and Shock 2002).

The evolution of life is driven by changes in the DNA (i.e., mutation, duplication, truncation…), which may lead to a different or new aminoacidic sequence with the improvement in a specific function of the cell. However, the fast adaptation of prokaryotic species to new conditions cannot be only explained by molecular evolution (Ochman et al. 2000). Prokaryotes have the ability to exchange DNA with highly divergent organisms, i.e. horizontal gene transfer (HGT), which allows acquiring specific functions by the direct transfer of genetic material (Wiedenbeck and Cohan 2011). Various mechanisms may explain HGT (i.e. phage-mediated transduction, transformation or conjugation), and it is a major mechanism for bacterial innovation and adaptation to colonize new ecological niches. As a consequence of HGT among highly diverse microorganisms, it is very difficult to define "prokaryotic species" as uniform entities, and we now understand that there are various forces driving microbial speciation, which include genetic variation (mutations), population dynamics (HGT), and ecological processes (niche-adaptation) that effect the evolution of prokaryotes and shape the current microbial world (Doolittle and Zhaxybayeva 2009) and the ecological success of a given population (Aminov 2011).

The use of environmental genetic methods unveiled the diversity and importance of microorganisms *in situ*, but it was not until the 21st century when the massive use of next-generation sequencing (NGS) techniques, has produced an exponential growth in the number of both 16S rRNA gene sequences (16S-tag community profiling) and microbial genomes available in databases (Fig. 1.2). According to 16S rRNA gene phylogenies, at least 60 major prokaryotic phyla have been identified (Rinke et al. 2013),

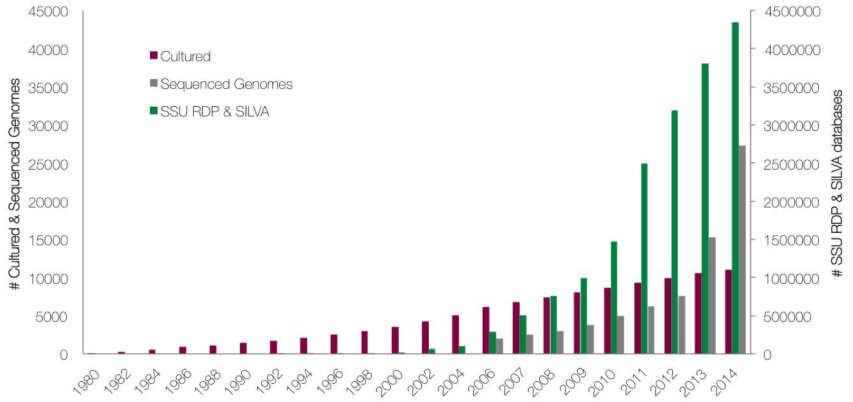

Figure 1.2: Increase in cultured sequences (purple), sequenced genomes (grey) and number of 16S rRNA sequences in RDP & SILVA databases (green) over the last 35 years. Note the different scale for SSU sequences (two orders of magnitude higher).

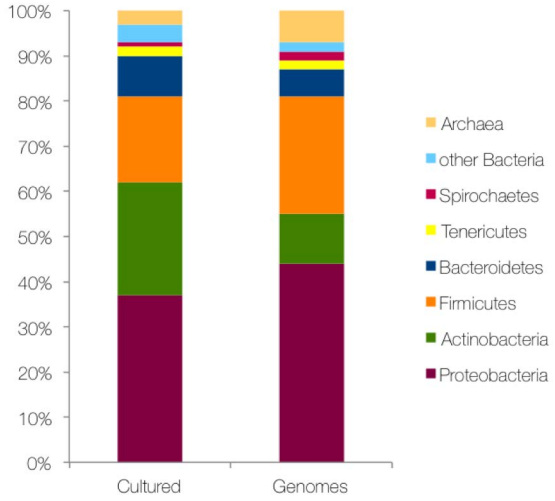

Figure 1.3: Phylum-level distribution of prokaryotic cultured isolates, compared to sequenced genomes. Figure adapted from Rinke et al. (2013).

although probably many more will be discovered in the coming years (Brown et al. 2015, Spang et al. 2015). Conversely, around 90% of all microbial strains cultured in the laboratory only belong to four main bacterial phyla, i.e., *Proteobacteria*, *Actinobacteria*, *Firmicutes* and *Bacteroidetes* (Fig. 1.3). The titanic task of culturing and a bias to a few prokaryotic groups restricts the global understanding of

metabolic diversity. Accordingly, available sequenced genomes are also biased to these four main phyla (Fig. 1.3).

1.2 Microbial metagenomics

The application of NGS technologies for the analysis of genomic DNA has been successfully applied to both complex environmental samples (metagenomics) and individual organisms or cells (genomics). However, metagenomics has the potential to provide genomes *in silico* from uncultivated microorganisms (see the exponential increase of sequenced genomes in 2013 and 2014, doubling the number of cultured species; Fig. 1.2) by the analysis of either low-complexity environmental samples (Tyson et al. 2004) or previously sorted single-cells (Rinke et al. 2013) offering the possibility to unveil the genetic potential of uncultured but abundant microbial species.

Metagenomics also provides an excellent framework in order to explore and understand the role of the whole microbial community into the functioning of a given ecosystem. The initial major contributions of metagenomics were on the ubiquity and energetic role of proteorhodopsins (Fuhrman et al. 2008), and on the importance of archaeal ammonia oxidizers (Treusch et al. 2005, Prosser and Nicol 2008). This approach also permitted ambitious environmental sequencing challenges such as the Global Ocean Sampling (GOS) expedition carried out by the J. Craig Venter Institute, which sampled from the northwest Atlantic to the eastern tropical Pacific in a vast and pioneering metagenomics study (Rusch et al. 2007) that helped to substantially expand the universe of protein families (Yooseph et al. 2007).

Metagenomic studies easily generate billions of sequences that need to be sequentially processed in order to extract information and knowledge. This high computing demand consolidated *Bioinformatics* as a separated discipline from computational biology

to facilitate massive sequence processing and data analyses from metagenomic studies (Kunin et al. 2008) to meet an ever growing high performance computing needs. After samples collection, DNA extraction, preparation and sequencing, sequence reads processing is crucial to refine the information in a process that requires a high demand of computational power (Fig. 1.4). First, reads need to be trimmed to remove low-quality bases and sequence adapters. A second optional step is assembly, which is the process of combining sequence reads in order to obtain longer stretches of contiguous DNA, which are called *contigs*. Assembly is a crucial step in genome sequencing to obtain both the lowest number and the largest fragments from a genome. It becomes easier when a close previously described reference genome is available (co-assembly). Otherwise, *de novo* assembly from complex environmental samples is a very difficult task because of the lack of sequence similarity between reads. Recently, methods based on sequence composition (Wrighton et al. 2012) or differential coverage binning of multiple metagenomes (Albertsen et al. 2013) have been used in order to circumvent this limitation and obtain reasonable *de novo* genome assemblies. Either for assembled or unassembled reads the next

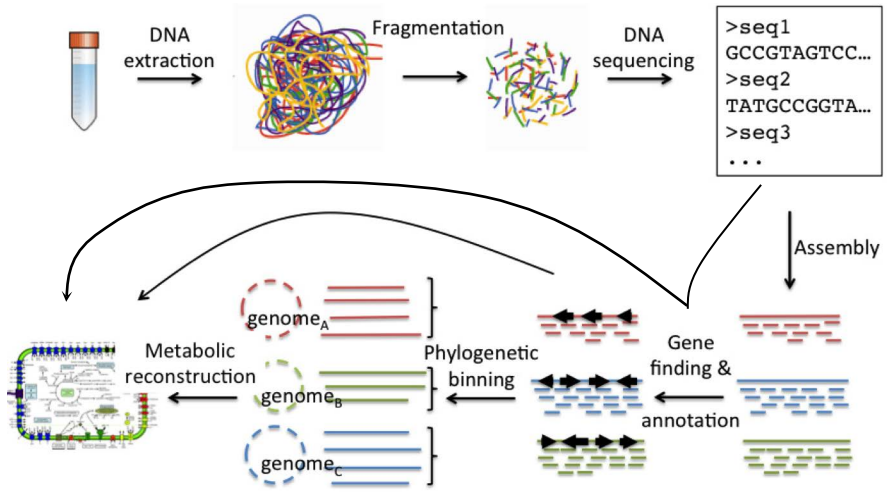

Figure 1.4: General environmental metagenomics workflow. Figure taken from http://envgen.github.io/metagenomics.html.

computational demand is annotation, which comprises a first step where genes or open reading frames (ORFs) are predicted (i.e. protein coding sequences (CDS) and a second step, which allows the assignment of putative gene functions and taxonomic neighbours of ORFs by a process based on homology searches against databases (Thomas et al. 2012). The correct annotation of ORFs with curated protein databases is essential in order to obtain a correct picture of the metabolic potential in the community.

There are some drawbacks however, that need to be kept in mind when metagenomics studies are carried out (Gilbert and Dupont 2011). First, the length of reads generated by NGS is a limiting factor for a correct identification of the sequences. Second, the annotation of proteins is based on previously identified sequences (i.e. cultured microorganisms). This is why most metagenomics studies are only able to annotate ~20% of the reads and there will be always a bias to cultured organisms in genes identification. Finally, as mentioned above, HGT is a common mechanism for prokaryotic innovation and adaptation (Ochman et al. 2000, Wiedenbeck and Cohan 2011), thus the functional taxonomic assignment should be carefully considered. In addition, metagenomics only provides the genomic potential of the community, but not the *in situ* activity of the microbial community, and should be complemented by mRNA extraction (gene expression) and metatranscriptomics for the identification of those genes that are being transcribed *in situ* (Gifford et al. 2011, Vila-Costa et al. 2013).

A key application of metagenomics is focused on the links between biogeochemical cycles and microbes driving energy and matter transformations in the ecosystems. A comprehensive understanding of the individual role of microbial populations in the biogeochemical cycling, and its influence in the dynamics of the ecosystem is a need to predict the ecosystem response to current environmental challenges (e.g., climate and global change, contamination, oil spills, etc.).

1.3 Biogeochemical cycling

The most important elements for life are carbon, nitrogen, phosphorus and sulfur, and understanding how microorganisms mediate the biogeochemical processes driving the transformations of these elements and the key genes performing each step of the cycle is of major interest. To obtain usable energy for the cell, oxygen (O_2) is the preferred electron acceptor because of the higher reduction potential obtained from the redox couple O_2/organic matter, from which more energy can be obtained. In the absence of oxygen, other compounds may be used as electron acceptors. The reduction potential of each redox couple, determines the preferred sequence of electron acceptors under anoxic conditions, which mainly are nitrate (NO_3^-), iron (Fe^{3+}), sulfate (SO_4^{2-}) and carbon dioxide (CO_2), respectively. The biochemical transformations taking part in most ecosystems have been largely described by biochemistry; however, the main drivers of these transformations are not well understood and remain unknown for most environments. Metagenomics may provide a better understanding on these processes, but in order to fully decipher metagenomics into a comprehensive biogeochemical framework, we need to have a complete view on the metabolic processes involved in the biogeochemical cycling and on the functional genes driving each transformation.

Carbon compounds form the basis of all known life forms on Earth, but, apart from the geological record, carbon is mostly found as CO_2 in the atmosphere or inorganic carbon dissolved in the oceans. It is difficult to evaluate all processes in which carbon takes part, however, the major biological processes involve the assimilation of CO_2 into organic matter and the respiration to CO_2 as a residual product (Fig. 1.5). The environmental availability of organic carbon compounds is the main driver of productivity and thus it is very important to understand how microorganisms link C recycling by the antagonist processes of photosynthesis and respiration either aerobic or anaerobic. CO_2 can be used for both oxygenic and

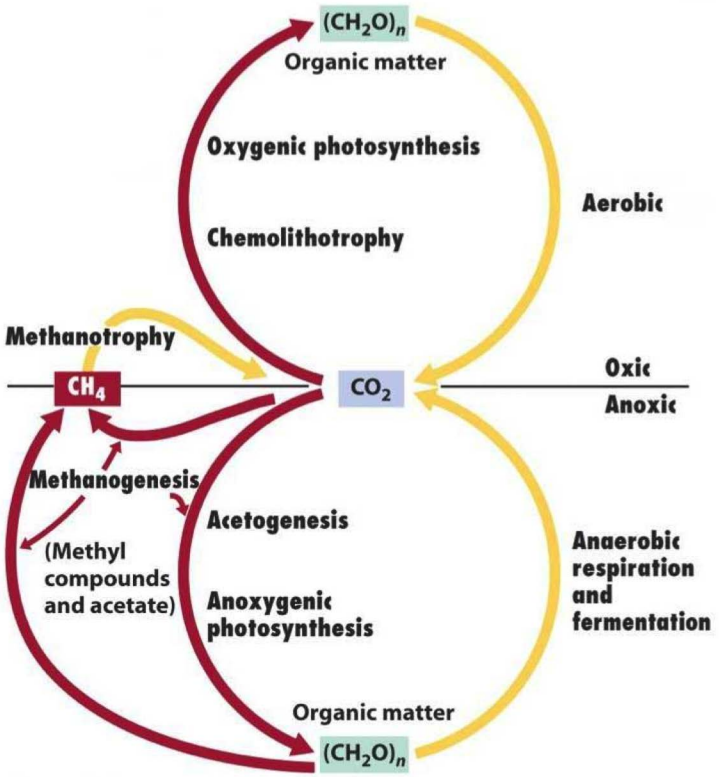

Figure 1.5: Redox cycle for the carbon cycle. Figure from Madigan (2012).

anoxygenic photosynthesis, but it can be also used as an electron acceptor in anaerobic respiration by methanogenic archaea. The energy yield through methanogenesis is very low, but this process might have been very important in early stages of life (Reysenbach and Shock 2002). Several studies have reported the genetic inventory for carbon cycling such as carbon fixation (Fuchs 2011) or aerobic respiration (Schmetterer et al. 2001).

The nitrogen cycle is also very important on Earth, not only for organisms, but also because it is probably the most altered cycle by human activities (Galloway et al. 2008). In the absence of oxygen, nitrates are the main alternative as final electron acceptors, and play an important role in the oceanic oxygen minimum zones (OMZs) and in coastal areas as a consequence of anthropogenically induced

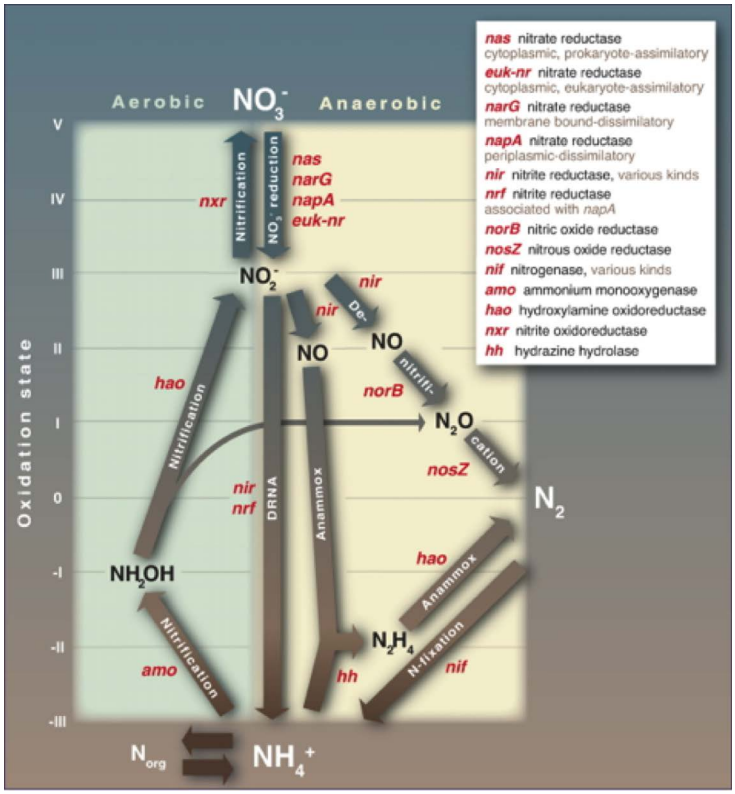

Figure 1.6: Major biological nitrogen transformation pathways and their associated genes. Figure from Canfield et al. (2010).

coastal eutrophication (Lam and Kuypers 2011). The understanding and functional relationships among the nitrogen cycle has changed substantially in the last years, with recently discovered processes like dissimilatory nitrogen transformations in eukaryotes, anaerobic ammonium oxidation coupled to nitrite reduction (anammox) or anaerobic methane oxidation with nitrite (Thamdrup 2012), highlighting that new metagenomics studies may provide new evidence for different and more diverse transformations within any metabolic cycle. The whole set of genes participating in the nitrogen cycle have been mainly identified and are available in databases for metagenomics annotation (Fig. 1.6).

Sulfur is another essential element for life, and all organisms have assimilatory pathways in order to incorporate sulfur into aminoacids and polymers. However, its major biogeochemical implications rely on the dissimilatory pathways leading to energy production coupled to sulfate respiration. These dissimilatory pathways only take place in the absence of oxygen, when sulfate is used as an alternative final electron acceptor in reduced environments, producing large amounts of sulfide that can be used as electron donor by sulfur-oxidizing bacteria both phototrophic and chemotrophic. These conditions were common in the early stages of life on Earth. Thus, understanding the links and players of the sulfur cycle may help to understand early evolution of life (Meyer and Kump 2008) and the early connections among the different biogeochemical cycles. The key enzymes driving the sulfur cycle have been identified and are also well understood (Fig. 1.7).

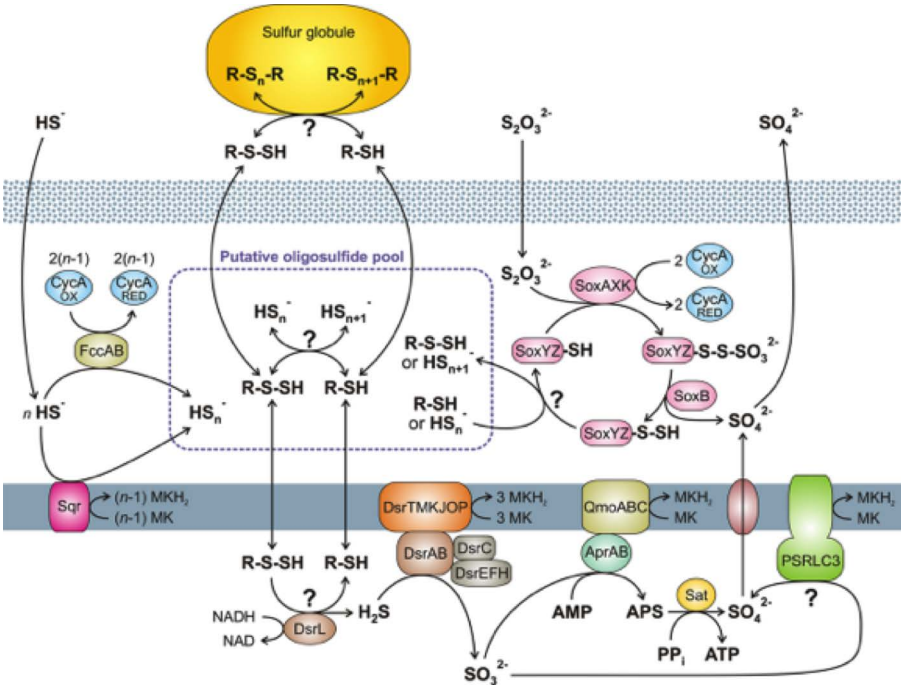

Figure 1.7: Overview of oxidative sulfur metabolism in green sulfur bacteria. Figure from Gregersen et al. (2011).

Finally, phosphorus is not used in dissimilatory pathways coupled to energy production, but it is very important in oligotrophic ecosystems where it has emerged as one of the main limiting factors (Dyhrman et al. 2007). Thus, the assimilation of either inorganic or organic phosphorus, and its storage in the cell are properties that will be of great relevance for microorganisms living in phosphorus-limited environments. Various studies provide the major genes involved in phosphorus transport and metabolism (Martiny et al. 2006, Vila-Costa et al. 2013, Carini et al. 2014).

1.4 Connecting biodiversity and biogeochemical role: two case studies

In order to explore the potential and limitations of metagenomics to unveil the main drivers of biogeochemical processes, two contrasted and widely studied ecosystems with global ecological interest were selected. First, the Banyoles karstic system, a mirror to the past euxinic conditions where three different lakes provide different euxinic situations where reduced compounds and sulfate were highly available: Lake Cisó, a small eutrophic lake with high carbon inputs, permanent anoxia and high euxinia; Lake Vilar, a meromictic mesotrophic lake; and Lake Banyoles basin CIII, a meromictic deep oligotrophic basin. And second, the ultraoligotrophic Lake Redon, with three contrasted situations to study: the slush, an oxygenated environment with labile carbon from algal exudates; the epilimnion oxygenated layer with low availability of reduced compounds; and the hypolimnion, a dark layer under the influence of the mineralization microbial processes from the sediment.

1.4.1 Banyoles karstic system with euxinic waters

Euxinic conditions (i.e. anoxic conditions with the presence of dissolved hydrogen sulfide) were common in the oceans during long periods of Earth history (Anbar 2008, Meyer and Kump 2008,

Reinhard et al. 2013). Nowadays, only some specific environments mimic those conditions found in early stages of life. The Banyoles karstic system (BKS) contains a group of lakes with sulfate-rich underlying waters, which harbours an active community of anaerobic sulfate-reducing bacteria producing large amounts of sulfide and creating the necessary conditions for euxinia. BKS offers a diverse range of conditions to study lakes with different stratification conditions and nutrient levels from eutrophy to oligotrophy.

The first microbial ecology studies on Banyoles area date back to the 1970s, when the physiological adaptations and competition between green and purple sulfur bacteria were initially studied. The ecological niches of green and purple are mostly determined by sulfide concentration and light (Guerrero et al. 1980), and pure cultures demonstrated that light quality plays a selective role on the competition between green and brown sulfur bacteria (Montesinos et al. 1983). Detailed vertical *in situ* distribution analyses showed sulfide- and light-limitation as main drivers for the massive development of phototrophic sulfur bacteria in the lakes (Guerrero et al. 1985) with the diel cycle playing an important role in their metabolism (Van Gemerden et al. 1985). A comprehensive review on the microbial ecology of Lake Cisó also described quantitatively the interactions among different microbial populations (Pedros-Alio and Guerrero 1993). The distribution and adaptations of green sulfur bacteria were explored in detail through HPLC and pigment analysis (Borrego et al. 1999). Lately, these environments have been used as a model system to explore the performance and potential of genetic fingerprinting methods with natural samples (Casamayor et al. 2000, Casamayor et al. 2001a, Casamayor et al. 2001b, Casamayor et al. 2002). Conspicuous blooms of brown sulfur bacteria have been recurrently found in these lakes along many years (Guerrero et al. 1985, Borrego et al. 1999), being an appropriate model ecosystem to apply genomic sequencing on naturally blooming populations. Recently, studies on dark carbon fixation showed the importance of the chemolithoautotrophic guild to this process (Garcia-Cantizano et

al. 2005), forming a taxonomically and not fully understood complex group of microaerophilic and anaerobic microorganisms coexisting in the same water layers and potentially competing for the same substrates (Casamayor 2010, Lliros et al. 2011).

1.4.2 Deep oligotrophic high-mountain Lake Redon

Oxygen is the main driver of microbial energetics in the modern world, and thus it is important to understand the functioning of aerobic ecosystems linked to the different microbial roles in the present biogeochemical cycling. Alpine lakes with low direct human influence are considered excellent study sites for plankton ecologists and act as sentinels to predict the responses of whole ecosystems to global change (Catalan et al. 2002). Lake Redon, is a deep oligotrophic lake situated in the middle of the Pyrenees at an altitude of 2240m, presenting a strong dynamism in water stratification, a dimictic regime with mixing periods in spring and autumn, and ice-covered during 6 months a year, adding yet another level of complexity in the limnological variability along the year.

The lake has been extensively studied and its physical properties (Catalan 1988), limnological and seasonal changes of water chemistry and primary production are well understood (Catalan and Camarero 1991, Catalan 1992, Camarero and Catalan 1993, Catalan et al. 1994). The dynamics of the ice cover, which consists of a superposition of different layers of ice and slush (a mixture of water and snow), have been also studied (Catalan 1989), and the slush layers are predicted to be microbial activity hotspots (Felip et al. 1995). The eukaryotic microbial assemblages of the slush and water column were described by fluorescence and microscopic analysis in late 1990s (Felip et al. 1999a, Felip et al. 1999b, Felip et al. 2002). Recent molecular microbial ecology studies have focused on the detection of airborne bacteria and its influence in the microbial community composition of the bacterioneuston (Hervas and Casamayor 2009), and on the role of archaea in the nitrification in

oligotrophic cold lakes (Auguet et al. 2012, Restrepo-Ortiz and Casamayor 2013, Restrepo-Ortiz et al. 2014).

2
Objectives

The main objective of this PhD dissertation was to unveil the link between biogeochemistry and microbial diversity using metagenomics functional potential under a biogeochemical cycling framework as a proxy to connect a mechanistic perspective with whole-system ecology.

Comparative analysis of biodiversity and microbial nutrient cycling of two contrasted situations (i.e. anoxic and suboxic systems with prevalent euxinia, and an oxic system with oligotrophic waters) were used as a proxy to provide a new view to whole-ecosystem functioning of ancient and modern environments. The previous knowledge on the biogeochemistry, ecology and functioning of these ecosystems, offered an excellent framework to *connect the biodiversity and biogeochemical role by microbial metagenomics*.

The detailed objectives of each chapter and the structure of this PhD Thesis are as follows:

Part I: Anoxic and suboxic systems with prevalent euxinia

Chapter 3: The main objective was to unveil an unknown but large fraction of microbial diversity that remained hidden due to the low resolution of the techniques used in previous studies (i.e. culturing or DGGE). A 16S-tag community profiling was used to describe the bacterial diversity of the metalimnion and hypolimnion of Lake Banyoles basin CIII, Lake Cisó and Lake Vilar (Submitted manuscript to FEMS Microbiology Ecology).

Chapter 4: The main goal was to explore the links between microbial composition and functionality for the carbon, nitrogen and sulfur cycling after phylogenetic and functional identification. A metagenomics approach was used to describe the genetic potential of the metalimnion and hypolimnion of Lake Banyoles basin CIII and Lake Cisó in order to unveil the biogeochemical functioning under fully anoxic conditions (Llorens-Mares et al. 2015).

Chapter 5: Blooming populations of GSB have been recurrently found in Lake Banyoles CIII basin. We used this opportunity to show an example how the culture limitation can be overcomed in natural populations and used assembly and comparative genomics analysis to reconstruct the genome of a green sulfur bacteria population and understand the main genetic factors explaining its ecological success (Submitted manuscript to ISME Journal).

Part II: Oxic system with oligotrophic waters

Chapter 6: The slush and water column microbial communities of the high-mountain Lake Redon had been mainly studied by microscopy methods. In this chapter, we aimed to unveil the bacterial diversity through CARD-FISH and 16S rRNA clone libraries. The main community changes from winter to spring were characterized (Llorens-Mares et al. 2012).

Chapter 7: The main objective was to explore the functional and taxonomic links as a proxy of the potential of each biogeochemical cycle in Lake Redon. The microbial genetic potential of the slush, the epilimnion and the hypolimnion were described through metagenomics (Manuscript in preparation).

Part I: Anoxic and suboxic systems with prevalent euxinia

3

High bacterial diversity and phylogenetic novelty in euxinic waters of karstic lakes analyzed by 16S-tag community profiling[1,2]

Abstract

Microbial communities developed under extreme low redox conditions use to grow in sulfide-rich environments, and experience limitation of electron acceptors. We explored the bacterial composition in the metalimnia and hypolimnia of three sulfurous lakes from the Lake Banyoles karstic area (NE Spain) through 16S rRNA tag sequencing. High relative abundances of *Actinobacteria* was observed in the metalimnion of the three lakes, and of *Alphaproteobacteria* of the SAR11 group in samples with the lowest sulfide concentrations. *Betaproteobacteria* of the order *Burkholderiales* were highly represented being more abundant in metalimnia than in hypolimnia. Abundant and well-known sulfate

[1] Llorens-Marès T, CM Borrego, CL Dupont, EO Casamayor. Manuscript submitted to FEMS Microbiology Ecology.

[2] See supplementary material in Appendix A

reducers and sulfide oxidizers (e.g., *Chromatiales and Chlorobiales*) were detected, indicating the potential for an active sulfur cycle, and high diversity indices were found in all samples but the hypolimnion of basin C-III where a *Chlorobi* bloom dominated. We noticed a systematic underestimation of *Epsilonproteobacteria* abundance with the currently available 907R "universal" primer and we argue for the need of a modified primer version. The novelty patterns showed a higher proportion of OTUs of the "highest novelty" for the hypolimnia (38% of total sequences) than for the metalimnia (17%). *Elusimicrobia*, *Chloroflexi*, *Fibrobacteres* and *Spirochaetes* were the taxa with the highest proportion of novel sequences.

Introduction

Anoxic and sulfurous (euxinic) waters in aquatic systems are a consequence of both the stratification of the water column and the depletion of oxygen in deep waters due to aerobic microbial respiration of organic matter in the sediments. As a consequence, anaerobic respiration and fermentation prevail leading to the accumulation of reduced compounds (*e.g.* NH_4, H_2S, CH_4, H_2, among others) in the bottom water compartment. Euxinic conditions may occur at different scales both in marine systems (*e.g.* microbial mats, sediments, estuaries, fjords, stagnant marine basins, coastal lagoons) and in continental areas (lakes and reservoirs, eutrophic shallow forest ponds, lacustrine sediments) in response to stratification conditions and large nutrient inputs from natural or anthropogenic sources. Although locally restricted, recent studies have raised concerns on the expected increase of anoxic conditions under a global change scenario (warming, eutrophication and marine intrusions) (Diaz and Rosenberg 2008, Wright et al. 2012).

Anoxic, sulfide-rich waters have traditionally been considered as "dead zones" because anoxia and sulfide accumulation strongly limit the eukaryotic life (Vaquer-Sunyer and Duarte 2008, Ekau et al. 2010). Conversely, euxinic waters are hot spots of prokaryotic

diversity and activity (Pedros-Alio and Guerrero 1993, Garcia-Cantizano et al. 2005, Barberan and Casamayor 2011). The dynamic nature of physico-chemical gradients along the water column and the wide range of organic and inorganic compounds that accumulate in oxic-anoxic interfaces and bottom waters are impossible to mimic under laboratory conditions. This inability to reproduce *in situ* conditions *in vitro* has limited our success in recovering cultured representatives of many microbial groups, especially those that are not among the most abundant but have a key role for ecosystem functioning (Lynch and Neufeld 2015).

Most previous studies carried out in karstic lakes with euxinic bottom waters have focused on the diversity and activity of the abundant taxa and their impact into prevalent biogeochemical cycles (*i.e.* sulphur and carbon) (Camacho and Vicente 1998, Tonolla et al. 2004, Lehours et al. 2007, Casamayor et al. 2012). Particularly, many studies carried out in different lakes and lagoons of the Banyoles Karstic System (BKS, NE Spain) dealt on the seasonal dynamics and activity of anoxygenic photosynthetic sulfur bacteria (Borrego et al. 1999, Casamayor et al. 2007, Bañeras et al. 2010). Further studies aimed to gain a first view on the planktonic microbial diversity using 16S rRNA gene fingerprinting, showed that euxinic bottom waters harbored very diverse bacterial and archaeal communities that differed among lakes and seasons (Casamayor et al. 2000, Casamayor et al. 2001b, Casamayor et al. 2002, Lliros et al. 2008). In all these cases, an unknown but probably large fraction of microbial diversity remained hidden due to the low resolution of the technique used (i.e. DGGE). In this regard, a recent study using pyrotag sequencing of archaeal 16S rRNA genes revealed archaeal communities mainly composed of uncultured groups, whose distribution is mainly driven by sulfide and DOC concentrations (Fillol et al. 2015). In the present work, we have investigated the sulfurous waters of three karstic lakes of the BKS to unveil the phylogenetic novelty of bacterial groups inhabiting euxinic waters of varying sulfide. Our results show that cold, anoxic, sulfide-rich hypolimnetic waters harbor a high degree of novelty in 16S rRNA gene sequences, largely

exceeding that found at the oxic-anoxic interface and with large metabolic potential.

Materials and methods

Study area and sampling

Lakes Cisó, Vilar, and Lake Banyoles-basin III (C-III) are located in the Banyoles Karstic System, northeastern Spain (42°8'N, 2°45'E). The three lakes have an oxic-anoxic interface, or redoxcline, located at different depths in the water column. C-III is a meromictic, oligotrophic basin with a maximal depth of 32 m, and a redoxcline between 18 and 21 m depending on the season, where a conspicuous population of brown-colored GSB seasonally blooms (Borrego et al. 1999). Lake Vilar is a meromictic, mesotrophic lake formed by two circular basins of 9 m and 11 m depth and a surface area of 11,000 m^2. In Vilar, the oxic-anoxic interface is usually located between 4.5 m to 6 m depth. Lake Cisó is a small monomictic eutrophic lake (650 m^2), located 1 km away from Lake Vilar, with a maximum depth of 6.5 m, and a redoxcline at 1.5 m below the surface.

The lakes were sampled on May 2010, and vertical profiles of temperature, conductivity, oxygen, and redox potential, were measured *in situ* with a multiparametric probe OTT-Hydrolab MS5 (Hatch Hydromet, Loveland, CO, USA). Sulfide was measured following Trüper and Schlegel (1964). Photosynthetic pigments were analyzed by HPLC as previously reported (Borrego et al. 1999). Water samples for DNA extraction were pre-filtered through a 200 µm nylon mesh and collected on 0.1 µm Supor 293 mm membrane disc filters (Pall Life Sciences, IL, USA). DNA was extracted using the phenol/chloroform method in lysis buffer followed by ethanol precipitation (Zeigler Allen et al. 2012).

DNA extraction, pyrosequencing and sequence processing

Bacterial community composition was analyzed by PCR-amplified 16S rRNA gene tag sequencing with the primer pair 341F-907R matching the V3–V5 hypervariable regions (Van de Peer et al. 1996). Amplicons were sequenced using 454 FLX system technology (454 Life Sciences, Branford, CT, USA) at the Research and Testing Laboratory (Lubbock, TX). PCR and sequencing methods were done according to RTL protocols (http://www.researchandtesting.com). Sequences were quality filtered and edited with Mothur (Schloss et al. 2009), and denoised and chimera filtered using OTUPIPE (Edgar 2010, Edgar et al. 2011). Overall, 36,130 final sequences of >200 bp in length were clustered into Operational Taxonomic Units (OTUs) at 97% identity with OTUPIPE. OTUs were then aligned with SINA (Quast et al. 2013) and classified according to the SILVA108 SSURef database (Pruesse et al., 2007). Extremely novel sequences (identity in 16S RNA gene to previously reported sequences < 92% and with at least 5 sequences present in the dataset for each lake) were deposited in GenBank with accession numbers HG764771 to HG764781. The pyrotag 16S rRNA gene sequence dataset was deposited in the European Nucleotide Archive facility of the EMBL-EBI (http://www.ebi.ac.uk/) under accession number PRJEB5429.

The 16S rRNA gene novelty was explored by BLASTn identity searches against the GenBank database (search on January 2015). The identity of each single sequence was related to both the closest environmental match (CEM) and the closest cultured match (CCM) available in GenBank. Novelty patterns were presented via dispersion plots (del Campo and Massana 2011, Triado-Margarit and Casamayor 2013). The degree of phylogenetic novelty between the metalimnetic and hypolimnetic compartments for those OTUs with ≥80% of the sequences present in each compartment was compared. The closest match was used to explore the novelty within both different taxa and rare and abundant OTU categories. The non-parametric test of the Kruskal-Wallis one-way analysis of variance

was used in the R environment (R Core Team 2014) to test for significance between categories and multiple pairwise comparisons using the "pgirmess" package.

Results and discussion

Physico-chemical characterization of the water column

The water columns of the three lakes showed stable stratification with two water compartments separated by a well-defined redoxcline around the oxic-anoxic interface (Fig. 3.1, shaded area). Sulfide concentrations ranged between maximal concentrations in the hypolimnetic waters of Lake Cisó (600 µM) and a few micromols sulfide in the metalimnion of the three lakes (Table 3.1). Sulfide was undetectable in the upper, well-oxygenated epilimnion of all lakes. Higher nitrate and nitrite concentrations were always measured at the metalimnetic water layers. Oxidized nitrogen species were always

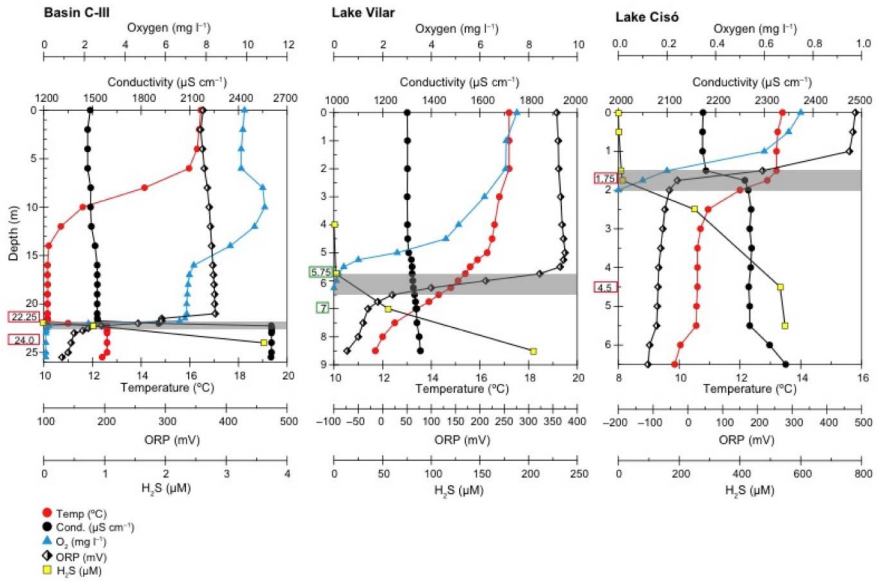

Figure 3.1: Vertical profiles of physico-chemical data for Banyoles basin C-III, Lake Vilar, and Lake Cisó. The 16S rRNA pyrotag analyses were carried out at two selected depths in each lake covering the redoxcline zones and the anoxic sulfurous hypolimnia. ORP: oxidation / reduction potential (Redox potential).

Table 3.1: Biogeochemical and pyrotag data for Lake Cisó, Banyoles basin C-III and Lake Vilar. ML: metalimnion; HL: hypolimnion. nd: not detected.

		Cisó ML	Cisó HL	C-III ML	C-III HL	Vilar ML	Vilar HL
Biogeochemistry	Depth (m)	1.74	4.5	22.25	24	5.75	7
	Eh (mV)	-30	-86	195	145	323	-30
	Oxygen (mg L^{-1})	0.10	0	0.25	0	0.19	0
	H_2S (µM)	12.83	531.90	0.81	3.60	1.35	54.90
	NH_4 (µM)	44.39	50.99	25.04	37.52	36.02	60.72
	NO_2 (µM)	0.75	nd	0.21	0.00	1.42	nd
	NO_3 (µM)	2.20	1.44	6.20	0.54	6.43	0.33
	TDP (µM)	1.05	2.83	0.33	0.37	0.61	2.42
	TOC (mg L^{-1})	5	3	1.5	3	4.5	9
	Chl *a* (µg L^{-1})	1.7	22.5	1.1	0.8	5.3	1.3
	BChl *a* (µg L^{-1})	2.4	123.7	1.1	1.6	0.1	0.1
	BChl *c* + *d* (µg L^{-1})	5.4	39.3	0	0	0	0
	BChl *e* (µg L^{-1})	0.8	13.6	25.8	40.6	0.2	1.1
16S rRNA gene pyrotag analysis	16S sequence tags	4472	6217	9868	6420	5086	4067
	OTUs (97% identity)	238	441	345	274	315	298
	S_{Chao1}	304	458	389	336	388	376
	Coverage (%)	98	99	99	99	98	98
	Shannon	4.1	4.4	4.0	3.1	4.4	4.2

below 2.2 µM in hypolimnetic waters, where ammonia accumulated to reach concentrations of up to 60 µM (Table 3.1). In Lake Cisó and basin C-III photosynthetic pigments specific for Green Sulfur Bacteria (GSB, Bacteriochlorophylls *c*, *d* and *e*) and Purple Sulfur Bacteria (PSB, BChl *a*) were measured (Table 3.1). The highest concentration of BChl *e* was measured in the hypolimnion of basin C-III.

Phylogenetic structure of planktonic bacterial assemblages

To test for the performance of the methodology used, amplicon 16S rRNA gene pyrotag results were compared with the 16S rRNA gene obtained from metagenomic data available from the same dataset

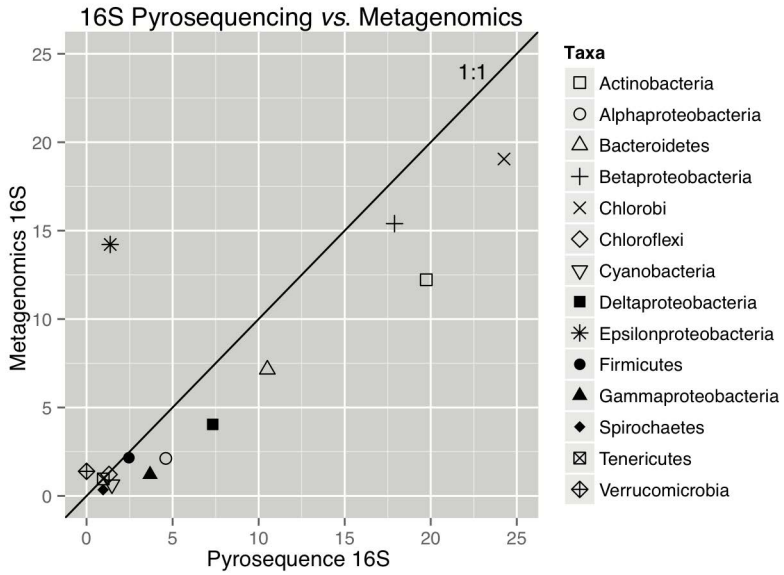

Figure 3.2: Relationship between the relative abundance for the bacterial 16S rRNA gene found in the amplicons pyrotags (present study) and in the metagenomic shotgun analysis for Lake Cisó and Banyoles basin C-III (Llorens-Marès et al. 2015).

(Llorens-Mares et al. 2015). Relative abundances showed a high degree of concordance for the different taxa (Fig. 3.2) but noticeable discrepancies were observed for the *Actinobacteria* (possibly overestimated in PCR-pyrotag analyses) and for the *Epsilonproteobacteria* (probably underestimated). In fact, the reverse primer used for the preliminary PCR step (907R) showed one mismatch to 16S rRNA gene sequences from members of the Class *Epsilonproteobacteria* (5'-CCG TCA ATT CMT TTR AGT TT-3'). The *in silico* coverage of this primer against the ARB database only detected 2% of the epsilonproteobacterial sequences whereas a full coverage was obtained in silico using a modified version of this reverse primer (5'-CCG TCT ATT CMT TTR AGT TT-3'.) A similar underestimation of *Epsilonproteobacteria* in 16S-pyrotags compared to the metagenomic dataset was observed in samples from the Baltic Sea (Dupont et al. 2014), pointing to a systematic underestimation of *Epsilonproteobacteria* abundance by pyrotag analyses using the

currently available 907R primer. Accordingly, the use of alternative primers targeting other hypervariable regions (*e.g.* V1–V4) of the 16S rRNA gene or a modified version of the 907R primer are needed for surveying bacterial diversity in aquatic systems where *Epsilonproteobacteria* are present.

The average number of OTUs (97% identity cutoff) per sample was 318 (range 238–441 OTUs) with a sampling coverage close to 99% (Table 3.1). Overall, most abundant OTUs affiliated to *Betaproteobacteria* of the order *Burkholderiales*, *Actinobacteria* of the orders *Frankiales* and *Micrococcales*, *Alphaproteobacteria* of the SAR11 cluster (*Pelagibacterales*), *Bacteroidetes* (mainly *Flavobacteriales*), *Chlorobiales* (GSB), *Deltaproteobacteria* (*Syntrophobacterales*, probably sulfate-reducers, SRB), and *Gammaproteobacteria* (*Chromatiales*, PSB). These populations were differentially distributed between water layers and among lakes (Fig. 3.3 and Supplementary Table A.C3.1) and corresponded to taxa commonly found in freshwater lakes (Tamames et al. 2010, Newton et al. 2011). Shannon diversity index was fairly similar in the metalimnion and hypolimnion of lakes Vilar and Cisó, contrasting with the less diverse community in the hypolimnion of basin C-III due to the dominance of GSB (67.6% of total tag reads, Table 3.1 and Supplementary Table A.C3.1). Several studies carried out in meromictic lakes reported the occurrence of very rich and diverse microbial communities at oxic-anoxic interfaces and euxinic waters in comparison to those inhabiting the upper, well oxygenated water layers (Barberan and Casamayor 2011, Gies et al. 2014). In this regard, several authors have pointed out that hypolimnia of stratified lakes may promote endemism of microbial communities due to the isolation of bottom water (Shade et al. 2008, Barberan and Casamayor 2011).

The high relative abundance of *Actinobacteria* observed in the metalimnion of the three lakes (average 31.6%±5.6%) is consistent with the widespread distribution of this taxa in freshwater systems, where they constitute a diverse and dominant fraction of the heterotrophic bacterioplankton (Glockner et al. 2000, Barberan and

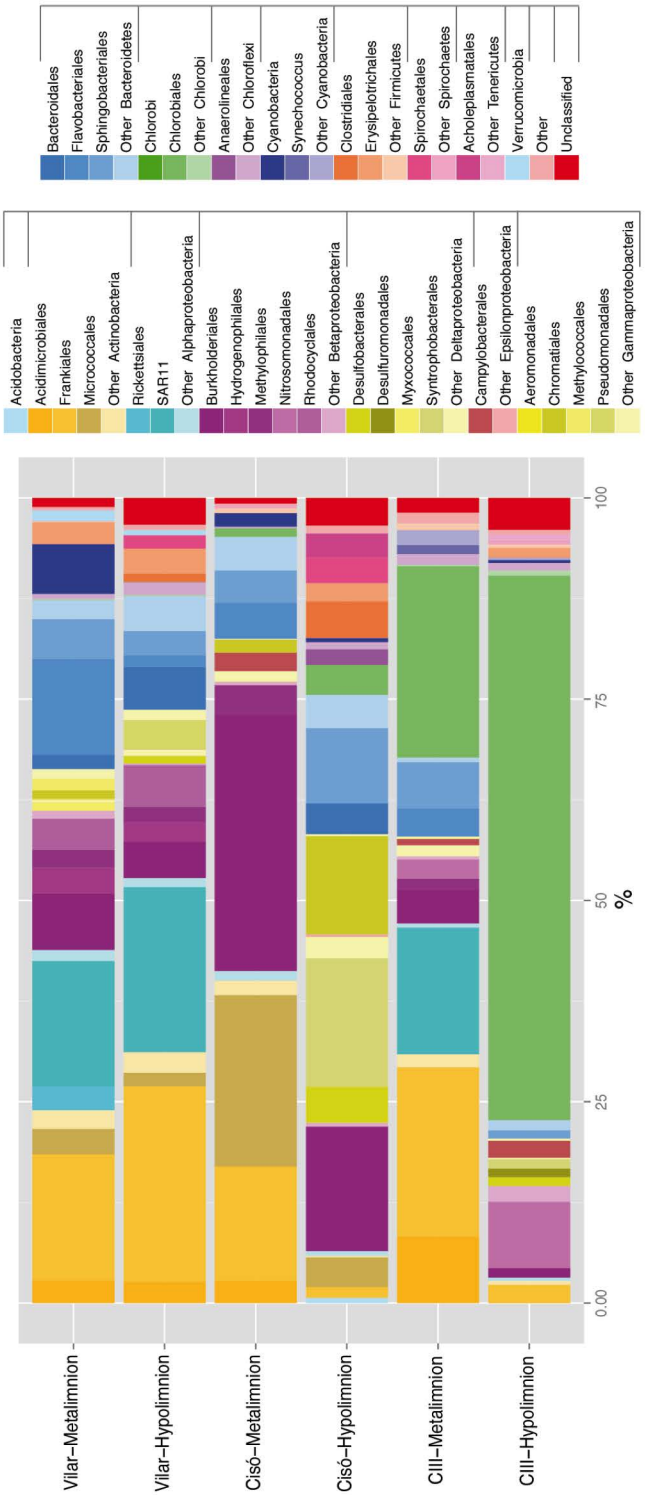

Figure 3.3: Order level bacterial community structure (relative abundances in the 16S rRNA gene amplicon mixture) in the metalimnia and hypolimnia of lakes Cisó, Vilar and Banyoles basin C-III.

Casamayor 2010). Of special relevance is also the phylogenetic richness and abundance of sequences affiliated to well-known groups of sulfate reducers and sulfide oxidizers, indicating the potential for an active sulfur cycle at both the metalimnion and hypolimnion of basin C-III and Lake Cisó. The anoxic conditions and high sulfate concentrations present in this karstic area makes it a suitable environment for the growth and activity of planktonic SRB (23% of 16S rRNA amplicon genes affiliated to *Deltaproteobacteria* in Cisó-Hypolimnion). In this regard, metagenomic analyses of samples from the hypolimnion of Lake Cisó identified a substantial contribution of genes for sulfate reduction (c. 16% of total reads) from *Desulfobacterales* and *Syntrophobacterales* (Llorens-Mares et al. 2015). Similar contribution of planktonic SRB in euxinic bottom water layers has been reported for other meromictic lakes with active sulfur cycling such as Lake Mahoney (Klepac-Ceraj et al. 2012) and Arctic lake A (Comeau et al. 2012). The predominant sulfur oxidizers detected in the studied lakes were the anoxygenic photosynthetic sulfur bacteria of the phylum *Chlorobi* in basin C-III and the purple sulfur bacteria (i.e. *Chromatiaceae*) in Lake Cisó. Both groups have consistently been found in lakes of the Banyoles karstic system where they account for most of the biomass and C photoassimilation rates at the oxic-anoxic interfaces and hypolimnetic waters (Garcia-Cantizano et al. 2005). In the studied lakes, the predominance of anoxygenic sulfur bacteria over non-photosynthetic gamma- or epsilonproteobacterial sulfur oxidizers that are prevalent in oceanic Oxygen Minimum Zones or anoxic marine basins (Grote et al. 2008, Wright et al. 2012, Dupont et al. 2014) might be probably explained by the shallower location of sulfidic redoxclines at photic depths that favours the blooming of anoxygenic phototrophs. In turn, the low recovery of sequences affiliated to epsilonproteobacterial sulfur oxidizers might be related, in addition to the underestimation caused by the primer pair used (see above), to a low representativeness during spring and summer in comparison to winter season, where they constitute active population in the O_2/H_2S interface of basin C-III (Borrego et al. in preparation). In fact, metagenomic analyses of the

same dataset detected genes from chemolithotrophic, sulfur oxidizing *Epsilonproteobacteria* related to C fixation (Arnon cycle), sulfide oxidation and denitrification in metalimnetic and hypolimnetic samples of basin C-III and Lake Cisó (Llorens-Mares et al. 2015). Interestingly, previous studies had reported that different types of anoxygenic photosynthetic bacteria dominate in the different lakes due to different ecophysiological strategies in pigment composition and use of light spectra, motility and carbon storage strategies (Guerrero et al. 1985, Van Gemerden et al. 1985), but our analyses extend this to sulfide oxidizers, sulfate reducers, denitrifying bacteria, and other functional guilds. Conversely, phylogenetically closer groups may belong to different functional guilds, as in the case of Actinobacteria that were predominant in the metalimnia of both lakes but whereas the family *Microbacteriaceae* dominated sulfur mineralization processes in Lake Cisó, *Sporichthyaceae* (*Frankiales*) were mostly involved in assimilatory sulfate reduction in Lake Banyoles. Understanding how the environmental conditions and community composition influence which taxa succeeds and the ultimate ecophysiological reasons are major challenges for future studies.

The metalimnetic and hypolimnetic genetic novelty

To assess the phylogenetic novelty of the 16S rRNA gene sequences found in the meta- and hypolimnia we analyzed their identity against their first BLAST hit to both the closest environmental match (CEM) and closest cultured representatives (CCM) in databases (Fig. 3.4). Both water layers have c. 60% of the OTUs placed in the "cultured gap" area (Table 3.2). However, two major differences were observed in the novelty patterns of metalimnia *vs.* hypolimnia. First, a larger number of well-known OTUs of limited novelty (both CEM and CCM ≥97% identity) were found in the metalimnia (21%) than in the hypolimnia (6%). And second, a higher proportion of OTUs in the "highest novelty" area (both CEM and CCM

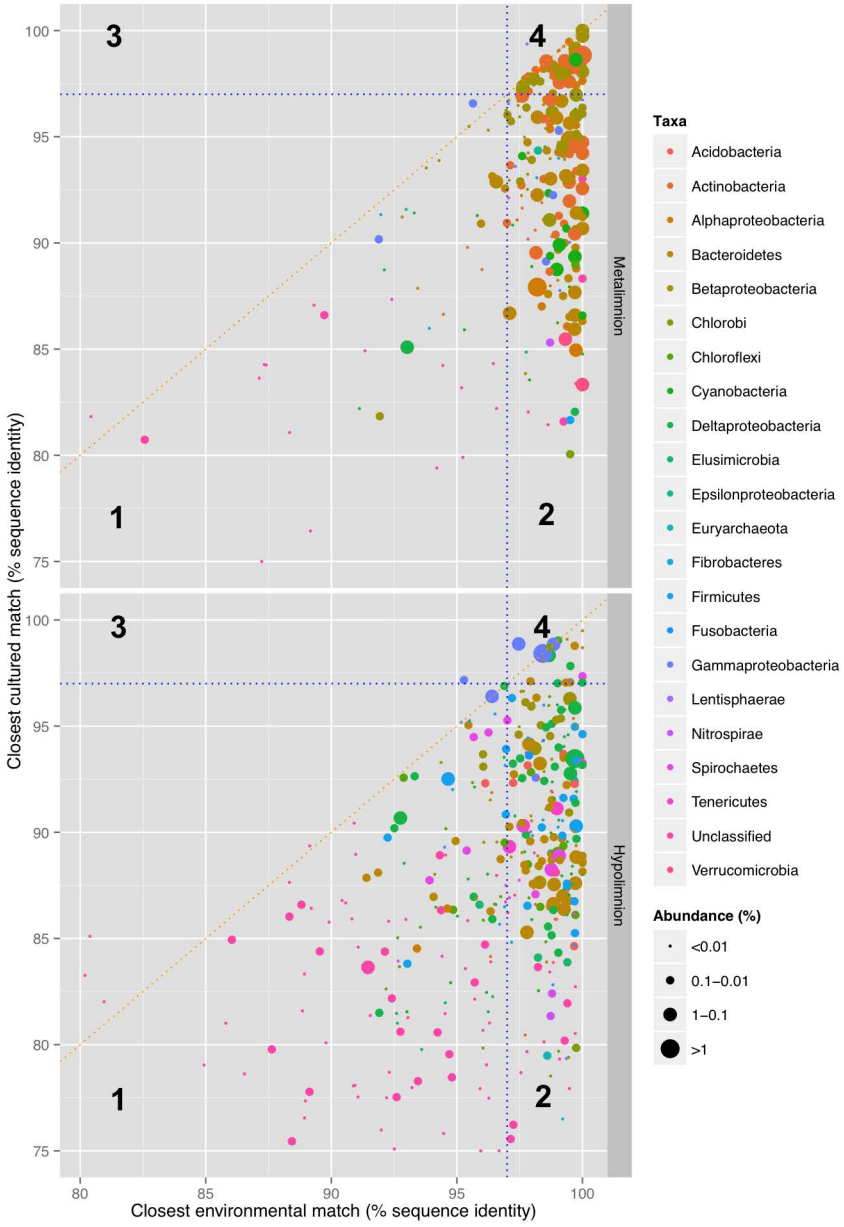

Figure 3.4: Novelty pattern plots for the different classes found in the metalimnia (upper plot) and hypolimnia (bottom plot) of lakes Cisó, Vilar and Banyoles basin C-III. The closest environmental match (CEM) and the closest cultured match (CCM) as available in GenBank (BLAST search, January 2015). Dots size proportional to the relative abundance in the amplicon mixture. Numbering (1-4) in the plot areas according to Table 3.2.

Table 3.2: Percentages and total number of OTUs in the two data subsets (metalimnion vs. hypolimnion) assigned to the different plot areas established in the novelty patterns (see also Fig. 3.4). The different plot areas were named according to the identity values to both the closest environmental match (CEM) and cultured representatives (CCM) in databases.

	Plot area 1[a]	Plot area 2[b]	Plot area 3[c]	Plot area 4[d]
Metalimnion	17.2% (46)	61.4% (164)	0.0% (0)	21.3% (57)
Hypolimnion	37.9% (148)	56.0% (219)	0.3% (1)	5.9% (23)

a) The highest novelty plot area: contains phylotypes matching < 97% identity to both CEM and CCM.
b) The cultured gap plot area: contains phylotypes matching > 97% identity to CEM and < 97% to CCM.
c) The environmental gap plot area contains phylotypes with sequence identity < 97% to CEM and > 97% to CCM.
d) The limited novelty plot area: contains phylotypes matching > 97 % to both CEM and CCM.

According to a class/phylum-level novelty distribution, *Elusimicrobia* and *Chloroflexi* were the taxa with the highest number of novel sequences with 81% and 35% of the OTUs below the 97% identity cutoff, respectively, and secondarily *Fibrobacteres* and *Spirochaetes* (Fig. 3.5). *Elusimicrobia* (formerly known as Termite Group-1) is a deeply branching, highly diverse bacterial group, which members have consistently been found in the most disparate environments (soil, wastewater, sediments and, particularly, the hindgut of termites) (Herlemann et al. 2007). According to the genomic analysis of the first cultivated representative (*Elusimicrobium minutum*), *Elusimicrobia* are capable of anaerobic growth by fermentation of sugars and amino acids and exhibit some tolerance to molecular oxygen (Herlemann et al. 2009). The occurrence of *Elusimicrobia* in the anoxic water layers of the studied lakes is thus in agreement with the physico-chemistry of the lakes and the large number of genes related with fermentative pathways recently

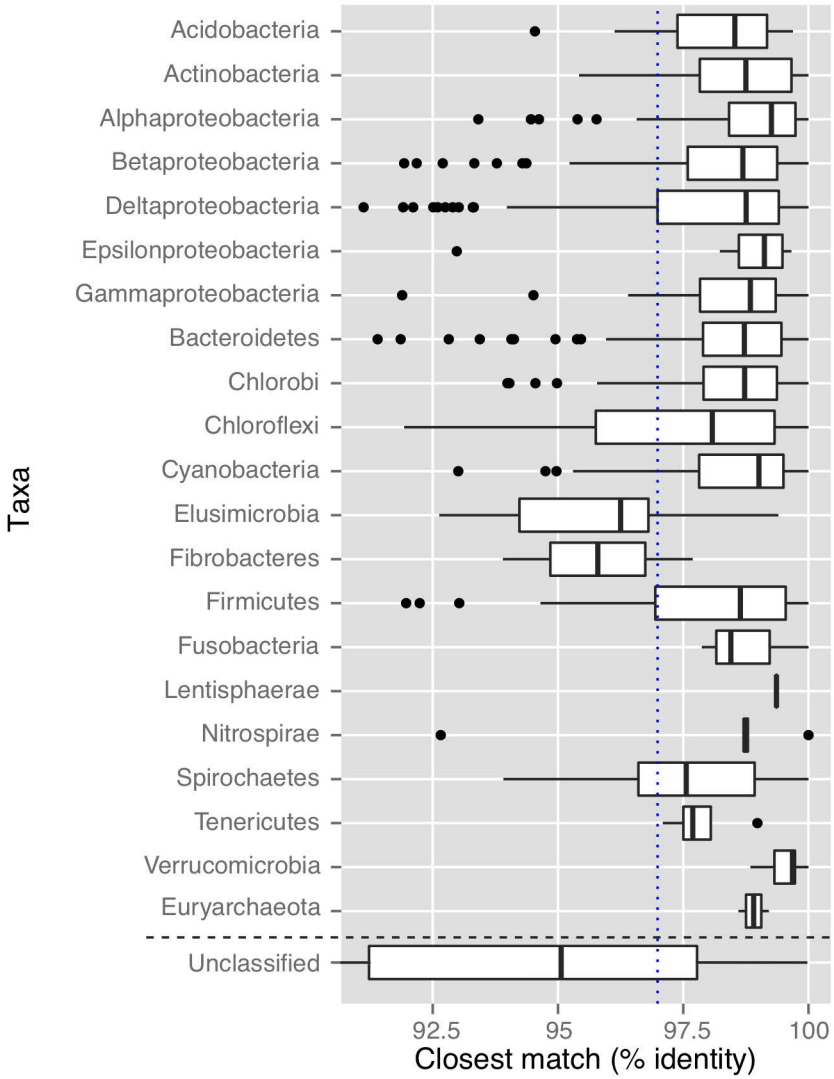

Figure 3.5: Class-level novelty distribution for the phylotypes found in lakes Cisó, Vilar and Banyoles basin C-III. The closest match identity as available in GenBank (BLAST search, January 2015).

identified in Lake Banyoles (Llorens-Mares et al. 2015). The presence of *Chloroflexi* is common in freshwater lakes, where they usually exhibit a large morphological and phylogenetical diversity, including green non-sulfur photosyntethic bacteria (Gich et al. 2001). In fact, the *Chloroflexi* is among the most abundant groups identified in euxinic water layers of stratified lakes (Lehours et al. 2007, Comeau

et al. 2012, Gies et al. 2014). Remarkably, other bacterial groups commonly found in aquatic systems such as *Betaproteobacteria*, *Deltaproteobacteria* and *Bacteroidetes* showed several phylotypes of high novelty (Fig. 3.5). High diverse populations of *Deltaproteobacteria* have also been identified in sulfide-rich waters of a meromictic Arctic lake (Comeau et al. 2012) and Lake Mahoney (Klepac-Ceraj et al. 2012).

Several OTUs that remained unclassified showed not only a very low abundance (<0.01% of total counts) but also the greatest phylogenetic novelty. These highly novel OTUs had as their closest phylogenetic relatives members of *Bacteroidetes* (*Bacteroidales* and *Sphingobacteriales*), *Firmicutes* (*Erysipelotrichi)*, *Deltaproteobacteria* (*Myxococcales*) and the candidate divisions BD1-5 and RF3 (Supplementary Fig. A.C3.1). The *in situ* roles carried out by these novel bacterial groups are unknown. Interestingly, the closest relatives for such rare and unclassified hypolimnetic OTUs were recovered from very diverse environments but mainly characterized by anoxia and high nutrient content (marine sediments, anaerobic digesters, soils and animal faeces; Supplementary Fig. A.C3.1). Of particular interest was the affiliation of some OTUs from Vilar and Cisó-Hypolimnion to candidate divisions BD1-5 and RF-3. Whereas BD1-5 is known to include strict anaerobic heterotrophs with a fermentative metabolism that are prevalent in anoxic, organic carbon-rich environments (Wrighton et al. 2012, Wrighton et al. 2014), less information is available for members of the candidate phylum RF3. Recently, Gies and co-workers reported an increase in the number of OTUs affiliated to RF3 at the sulfate methane transition zone of meromictic lake Sakinaw, suggesting a potential role in sulfur or methane cycling (Gies et al. 2014). These candidate divisions had a substantial presence in our lakes (0.5% in Cisó-Hypolimnion), and the occurrence in euxinic water layers might support a potential involvement in the sulfur cycle that deserve further investigations.

Acknowledgements

X Triadó-Margarit is acknowledged for data analyses. This research was funded by grants GOS-LAKES CGL2009-08523-E and DARKNESS CGL2012-32747 to EOC and ARCANOX CGL2009-13318-C02-02 to CBM from the Spanish Office of Science (MINECO) and from financial support by the Beyster Family Fund of the San Diego Foundation and the Life Technologies Foundation to the J. Craig Venter Institute.

4

Connecting biodiversity and potential functional role in modern euxinic environments by microbial metagenomics[1,2]

Abstract

Stratified sulfurous lakes are appropriate environments for studying the links between composition and function in microbial communities and are potentially modern analogues of anoxic conditions prevailing in the ancient ocean. We explored these aspects in the Lake Banyoles karstic area (NE Spain) through metagenomics and *in silico* reconstruction of carbon, nitrogen, and sulfur metabolic pathways that were tightly coupled through a few bacterial groups. The

[1] Original publication in Appendix B: Llorens-Marès T, S Yooseph, J Goll, J Hoffman, M Vila-Costa, CM Borrego, CL Dupont, EO Casamayor (2015) Connecting biodiversity and potential functional role in modern euxinic environments by microbial metagenomics. ISME J 9:1648-1661. doi:10.1038/ismej.2014.254.

[2] See supplementary material in Appendix A

potential for nitrogen fixation and denitrification was detected in both autotrophs and heterotrophs, with both nitrogen and carbon fixation being found in *Chlorobiaceae*. *Campylobacterales* accounted for a large percentage of denitrification genes, while *Gallionellales* were putatively involved in denitrification, iron oxidation and carbon fixation and may have a major role in the iron cycle. *Bacteroidales* were also abundant and showed potential for dissimilatory nitrate reduction to ammonium. The very low abundance of genes for nitrification, the minor abundance of anammox genes, the high potential for nitrogen fixation and mineralization, and the potential for chemotrophic CO_2 fixation and CO oxidation all provide potential insights to anoxic zone functioning. We observed higher gene abundances of AOB than AOA that may have a geochemical and evolutionary link related to the relative abundance of Fe and Cu in these environments. Overall, these results offer a more detailed perspective on the microbial ecology of anoxic aquatic environments and may help to develop new geochemical proxies to infer biology and chemistry interactions in ancient ecosystems.

Introduction

Linking microbial community composition and ecological processes such as carbon (CO_2 fixation and respiration), nitrogen (nitrification, denitrification, and N_2 fixation), and sulfur cycling (sulfur assimilation, anaerobic sulfate respiration, and sulfide oxidation) is a primary goal for microbial ecologists. This information is needed to improve our understanding on the structure and functioning of microbial communities, to properly guide experimental research efforts, to promote our ability to understand fundamental mechanisms controlling microbial processes and interactions *in situ* (Prosser 2012), and to approach the study of earlier interactions biosphere-hydrosphere-geosphere (Severmann and Anbar 2009). However, A detailed comprehension of biological interactions in highly complex systems is difficult (Bascompte and Sole 1995).

Stratified lakes with euxinic (anoxic and sulfurous) bottom waters are simplified study systems to explore current biodiversity-biogeochemistry interactions because of its high activity, large biomass, and low microbial diversity (Guerrero et al. 1985). Usually, oxic-anoxic interfaces contain conspicuous blooms of photosynthetic bacteria, which are often macroscopically visible because of the high intracellular content of pigments, and additional microbial populations also tend to accumulate (Pedrós-Alió and Guerrero 1993). These blooms are, in fact, natural enrichment cultures that facilitate physiological studies *in situ* (Van Gemerden et al. 1985). At such interfaces, fine gradients of physicochemical conditions are present and tight coupling between different biogeochemical cycles (mainly carbon, nitrogen and sulfur) are established. Microbes adapted to such gradients are difficult to culture because *in situ* conditions are very difficult to mimic in the laboratory, and their study has improved perceptibly by culture-independent methods (Casamayor et al. 2000).

Stratified euxinic lake systems may also provide potential modern day analogue ecosystems for the oceans during long periods of Earth history. The planet was essentially anoxic until 2.7-2.4 billion years ago, with a ferruginous ocean (Anbar 2008, Reinhard et al. 2013). With the advent of oxygenic photosynthesis, atmospheric oxygen began to rise, as did the oxygen content in the surface oceans. The deep oceans remained anoxic, but entered a period of temporal and spatial heterogeneity. Strong euxinic conditions might be expected in ancient coastal areas, with merely anoxic conditions in the open ocean, though high Fe deep ocean conditions would have been maintained (Reinhard et al. 2013). By contrast, Fe is low in the deep waters of the modern ocean and, therefore, it is difficult to find appropriate ancient ocean analogues in the current marine realm. With this in mind, stratified aquatic systems with high Fe concentrations in deep waters could be more appropriate modern day analogues of the Proterozoic ocean. Karstic lacustrine systems with a gradient of organic carbon delivery and sulfide concentrations generated by sulfate reduction, as well as

being rich in iron, would provide reasonable biogeochemical analogues for ancient coastal to open ocean gradients.

In this study, we explored the oxic-anoxic interface (metalimnion) and bottom waters (hypolimnion) from two sulfurous lakes in the Banyoles karstic area (NE Spain) through shotgun metagenomics and *in silico* analysis of several metabolic pathways. In the framework of paleoreconstruction of anoxic conditions in ancient marine systems, one lake would be representative of strong euxinic conditions (Lake Cisó) and the other of low euxinia and an active iron cycle (basin III of Lake Banyoles). We explore the links between microbial composition and functionality for the carbon, nitrogen, and sulfur cycling after phylogenetic and functional identification. The taxonomic identity assigned to each functional step was determined by the closest match in databases, and the relative abundance and distribution of marker genes was comparatively analyzed among samples as a proxy of the potential *in situ* relevance of these pathways under the specific environmental conditions studied. Because of the lack of oxygen, large microbial biomass, and high contribution of deep dark fixation processes to overall CO_2 incorporation (Casamayor 2010, Casamayor et al. 2008, 2012), we hypothesized a high genetic potential for chemotrophic CO_2 fixation and a tight redox coupling between carbon, nitrogen and sulfur biogeochemical cycling. In addition, because of its euxinic nature we also expected a low contribution of both methanogens and ammonia oxidizers in the biogeochemical cycles prevailing in these environments.

Materials and methods

Environment and samples collection

Lake Cisó and basin III of Lake Banyoles (Banyoles C-III) are in the Banyoles karstic area, northeastern Spain (42°8'N, 2°45'E), and the microbial communities inhabiting these water bodies have been extensively studied by limnologists and microbial ecologists (e.g.,

Garcia-Gil and Abellà 1992, Guerrero et al. 1980, Pedrós-Alió and Guerrero 1993). The lakes were sampled on May 8–9, 2010. Vertical profiles of temperature, conductivity, oxygen, and redox potential were measured *in situ* with a multiparametric probe OTT-Hydrolab MS5 (Hatch Hydromet, Loveland, CO, USA). The different water compartments (oxic epilimnion, metalimnion with the oxic-anoxic interface, and anoxic hypolimnion) were determined for each lake according to the physico-chemical profiles recorded *in-situ* (Fig. 4.1). For sulfide analyses, 10 ml of subsamples were collected in screw-capped glass tubes and immediately alkalinized by adding 0.1 ml of 1 M NaOH and fixed by adding 0.1 ml of 1 M zinc acetate. Sulfide was analyzed in the laboratory according to Trüper and Schlegel (1964). For pigments, water samples were processed as described by Guerrero and colleagues (1985) and analyzed by HPLC as previously reported (Borrego et al. 1999). Iron (Fe^{+2}) concentrations were obtained from Garcia-Gil (1990).

These lakes are stratified and have incoming sulfate-rich water seeping in through bottom springs resulting in deep waters rich in reduced sulfur compounds. An oxic-anoxic interface, or redoxcline, is established in the water column where light and sulfide usually coexist. Lake Banyoles is a gypsum karst spring area consisting of 6 main basins covering a surface area of 1.1 km^2. The basin III (C-III) is meromictic with a maximal depth of 32 m, and a redoxcline between 18 and 21 m, depending on the season. Blooms of brown-colored photosynthetic green sulfur bacteria (*Chlorobiaceae*) and purple sulfur bacteria (*Chromatiaceae*) have been periodically reported (Garcia-Gil and Abellà 1992). Lake Cisó is a small monomictic lake (650 m^2), located 1 km away from Lake Banyoles, with a maximum depth of 6.5 m. The thermocline is at 1.5 m, where different bacterial populations accumulate (Casamayor et al. 2000). The presence of aerobic chemoautotrophic sulfur-oxidizing bacteria, and substantial fixation of CO_2 in the dark have been previously reported in sulfurous lakes (Casamayor 2010). Lake Cisó is a small eutrophic water body fully surrounded by trees that strongly limit the incident irradiance on the lake and the landscape provide continuous allochthonous

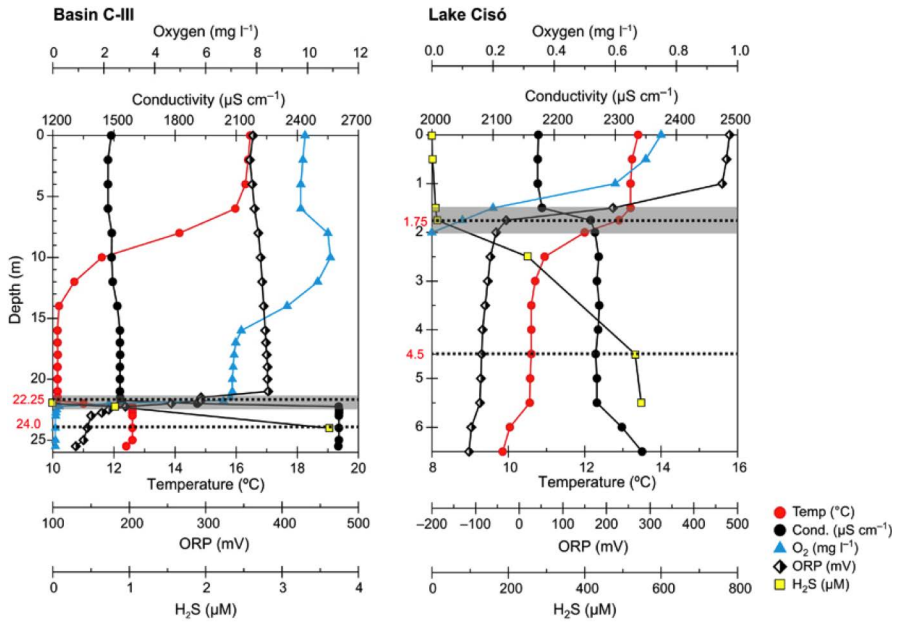

Figure 4.1: Vertical profiles of physico-chemical data for Lake Banyoles basin C-III and Lake Cisó. Metagenomic analyses were carried out at two selected depths (dotted lines): the oxic-anoxic interface (shadowed areas indicate the redoxcline zone) and the anoxic and sulfurous (euxinic) hypolimnia.

organic matter inputs both by leaching from the littoral zone and submerged vegetal debris. The system is therefore prone to a dominance of aerobic respiration and mineralization in surface layers overlying sulfate respiration, fermentation, and anaplerotic pathways at depth. In addition, the conspicuous presence of photosynthetic organisms and dissolved and particulate organic matter causes a strong light extinction and quality filtering in the first two meters that severely limits the development of oxygenic and anoxygenic green phototrophs (Vila and Abellà 1994). Conversely, the open-basin Banyoles C-III is oligotrophic, with a lower influence of the littoral zone. The basin maintains a stable, sharp chemocline that oscillates in depth between 19 and 21 m depending on the season, being shallower during summer. Active sulfate reduction occurring at the permanent anoxic monimolimnion causes sulfide accumulation below the chemocline, usually reaching concentrations of up to 1 mM

during summer and late fall. Lower sulfide concentrations are common however during spring. Light intensities reaching the O_2/H_2S interface are generally low (between 1% and 0.1% of surface incident light in winter and summer, respectively) despite the transparency of the epilimnetic waters of Lake Banyoles. The brown-pigmented green sulfur bacteria are better adapted to low irradiances than the green-pigmented (Garcia-Gil and Abellà 1992) and massively bloom in C-III.

The oxic-anoxic metalimnion interface and the euxinic (anoxic and sulfurous) hypolimnion samples for metagenomic analyses were determined *in situ* according to the vertical physico-chemical profiles. Samples were pre-filtered in the field through a 200 µm nylon mesh and kept in the dark in 25 L polycarbonate carboys until further processing in the lab 2–4 hours later. The plankton was collected using serial filtration onto 3.0, 0.8, and 0.1µm Supor 293 mm membrane disc filters (Pall Life Sciences, Port Washington, NY, USA), and stored in liquid nitrogen or -80ºC until DNA extraction. DNA extraction and pyrosequencing was carried out at the J Craig Venter Institute in Rockville, MD, USA as recently reported (Zeigler Allen et al. 2012).

DNA sequences analyses

A shotgun metagenomics approach was applied on all three size fractions of four samples from Lakes Cisó and Banyoles C-III. Identical reads were removed using CD-HIT (Li and Godzik 2006). Annotation of metagenomic reads was conducted through the JCVI prokaryotic annotation pipeline (Tanenbaum et al. 2010) using Uniref100, PFAM, TIGRfam and KEGG Orthologs (KO) databases for taxonomic and functional annotation. JCVI Metagenomics reports (http://jcvi.org/metarep) was used for analysis and comparative metagenomics (Goll et al. 2010). KO annotation was used for functional analysis and KO counts were normalized according to the length of the read and the length of the target gene (Sharon et al. 2009b). The communities and functional profiles found in each size fraction were highly similar (Supplementary Fig. A.C4.1) and, therefore, we pooled all reads after normalizing for sequencing depth

for subsequent analyses, which allows for a better comparison of metagenomes.

The functional analyses focused on the three main biogeochemical cycles for this type of lakes, i.e., carbon (C), nitrogen (N) and sulfur (S) cycling. The genetic potential of the microbial community was analyzed following the C, N, and S marker genes (KOs) as reported by (Lauro et al. 2011) with a few modifications. We amended this previous rubric by adding the anaerobic carbon fixation carried out through the Calvin cycle by *Chromatiaceae* and additional genes for polysulfide reduction, nitrate reduction, and nitrite oxidation. In addition, the genes pyruvate:ferredoxin oxidoreductase (*porA/B*) were not considered as marker genes for fermentation as in Lauro et al. (2011), because they are key genes in the rTCA cycle used for carbon fixation by *Epsilonproteobacteria* abundant in our study lakes (Campbell and Cary 2004, Takai et al. 2005). Because both sulfide oxidation and dissimilatory sulfate reduction pathways are mediated by the same set of genes (*aprA*, *aprB*, and *dsrA*) but are found in different families of bacteria, we assigned metagenomic reads to each pathway according to phylogeny, i.e., sulfate reduction for *Firmicutes* and *Deltaproteobacteria* reads, and sulfide oxidation for *Alphaproteobacteria*, *Betaproteobacteria*, *Chlorobiaceae*, and *Chromatiaceae*. Finally, for the sulfur-oxidizing *Epsilonproteobacteria* of the order *Campylobacterales* we specifically searched for *sox* genes (coding for thiosulfate oxidation) not currently available in the KEGG database. Marker genes used in the present work are shown in supplementary material (Supplementary Table A.C4.1). Hierarchical clustering and heatmap plots were generated with R (R Core Team 2014) using the library 'seriation'. Metagenomic data has been deposited at CAMERA (Sun et al. 2011) under accession number CAM_P_0001174.

Results

Environmental parameters

At the time of sampling (spring 2010), the water column was thermally stratified with thermoclines spanning from 1.5 to 3 m in Lake Cisó, and 7 to 14 m in basin C-III (Fig. 4.1). Chemical stratification was disconnected from thermal stratification in basin C-III, where a sharp chemocline was detected at 21 m depth based on the higher conductivity of incoming sulfate-rich waters. The epilimnion of C-III showed oxygen concentrations > 6 mg l^{-1}, with rapid drawdowns in the hypolimnion, and the sharp oxic-anoxic interface caused an abrupt decrease in the redox potential and generated of a pronounced redoxcline (Fig. 4.1, shaded area). In Lake Cisó, the epilimnion (0–1.5 m depth) was oxygen deficient (0.2 -1 mg l^{-1}) and the water column became completely anoxic below 2 m depth. In this case, the redoxcline and the oxic-anoxic interface were located in a narrow water layer of 0.5 m width (1.5–2 m depth). The concentration of nitrogen and sulfur species changed according to these physico-chemical gradients with high concentrations of ammonia mainly in the hypolimnia (up to 60 µM) and sulfide concentrations ranging between 532 µM in Lake Cisó and <1 µM in C-III in agreement with redox potential (Eh) measurements (Table 4.1, and Supplementary Fig. A.C4.2). The concentration of Chl *a* measured in the lakes agreed with their traditional trophic status (oligotrophic for C-III, and mesotrophic for Lake Cisó). Biomarker pigments for green sulfur (BChl *c*, *d* and *e*) and purple sulfur bacteria (BChl *a*) were detected in the metalimnion and hypolimnion of Lake Cisó and basin C-III. Particularly, conspicuous concentrations of BChl *e*, the characteristic pigment of brown-colored species of *Chlorobium*, were measured between 22 and 24 m depth in basin C-III (Table 4.1). An active Fe^{2+} cycle has been previously reported in Lake Banyoles with concentrations 8-10 µM in both the resurgence of groundwater (bottom spring) and water column of basin C-III, inflow velocity of 0.8 mmol total Fe/hour, and concentrations up to 8 mg

Table 4.1: Biogeochemical data for Lake Cisó and Banyoles basin C-III. Abbreviations: BChl, bacteriochlorophyll; b.d.l., below detection limits; Chla, chlorophyll a; HL, hypolimnion; ML, metalimnion; Eh, redox potential; TOC, total organic carbon; TDP, total dissolved phosphorus.

	Cisó ML	Cisó HL	C-III ML	C-III HL
Depth (m)	1.75	4.5	22.25	24
Temperature (ºC)	12.9	10.6	12.6	12.6
Conductivity (µS cm^{-1})	2260	2268	2603	2604
Eh (mV)	-30	-86	195	145
Oxygen (mg l^{-1})	0.10	0	0.25	0
H_2S (µM)	12.8	531.9	0.8	3.6
Light (% incident)	1%	<0.1%	1%	<0.1%
TOC (mg L^{-1})	5	3	1.5	3
pH	7.40	7.23	7.14	7.15
TDP (µM)	1.05	2.83	0.33	0.37
NH_4 (µM)	44.39	50.99	25.04	37.52
NO_2 (µM)	0.75	b.d.l.	0.21	0.00
NO_3 (µM)	2.20	1.44	6.20	0.54
Urea (µM)	4.84	0.17	1,91	1.08
Si (µM)	185.0	168.1	144.8	114.5
Chl *a* (µg l^{-1})	1.7	22.5	1.1	0.8
BChl *a* (µg l^{-1})	2.4	123.7	1.1	1.6
BChl *c* and *d* (µg l^{-1})	5.4	39.3	0	0
BChl *e* (µg l^{-1})	0.8	13.6	25.8	40.6

total Fe/g in sediment (dry weight) (Garcia-Gil 1990). Interestingly, we also observed substantial concentrations of nitrate in the bottom of the basin, coming from the groundwater, and high concentration in surface waters originating from the surrounding crop fields and farms (Supplementary Fig. A.C4.2).

Taxonomic structure of the microbial communities

The overall taxonomic breakdown of the communities was assessed using the phylogenetic annotation of the metagenomic reads. The Domain *Bacteria* numerically dominated the genetic composition of

the microbial communities, both at the oxic-anoxic interfaces and at the anoxic hypolimnia (Table 4.2). More than 95% of all taxonomically assigned metagenomic reads matched bacteria, with a few representatives of archaea (range 0.7-3.5%), phages (0.8-4.0%), and eukaryotes (0.7-2.8%). Archaeal metagenomic reads were more abundant in the hypolimnion (2.67±1.21% of total reads) than in the metalimnion (1.09±0.47%). Most of the archaeal metagenomics reads matched methanogens within *Euryarchaeota* (c. 88%), with a few additional representatives within *Thermococci*, *Thermoplasmata*, *Archaeoglobi*, and *Haloarchaea* (Supplementary Fig. A.C4.3). The 16S rRNA gene in the metagenomics dataset agreed with the broad taxonomic picture provided by the functional genes (Table 4.2), i.e., 98–100 % of the 16S rRNA gene affiliated to *Bacteria* whereas Archaea were a minor component more abundant in the hypolimnion (1.4±0.7%) than in the metalimnion (0.2±0.2%).

Table 4.2: Total number of metagenomic reads (averaged c. 1 million per sample) for Lake Cisó, and Banyoles basin C-III. Abbreviations: HL, hypolimnion; ML, metalimnion.

	Cisó ML	Cisó HL	C-III ML	C-III HL
Total number of reads	869947	991056	1071206	1077431
Taxonomically assigned reads (%)	46.7	53.5	54.2	62.4
Bacteria (%)	92.5	94.6	91.9	93.7
Archaea (%)	0.7	3.5	1.4	1.7
Eukarya (%)	2.8	1.1	2.7	0.7
Viruses (%)	4.0	0.8	4.0	3.9
16S rRNA genes in the metagenomic pool	465	578	690	787
Bacteria (%)	99.6	97.9	100	99.4
Archaea (%)	0.4	2.1	0	0.6
Functionally assigned metagenomic reads (%)	25.8	27.5	30.5	32.6
Reads of key genes in C, N, and S cycles	2392	3574	4773	5162

Interestingly, we observed higher proportion of functional reads affiliated to *Crenarchaeota-Thaumarchaeota* at the oxic-anoxic interface (12.3±0.4% of total archaeal reads) than at the anoxic and sulfurous bottom of the lakes (8.6±0.5%). *Thaumarchaeota* metagenomic reads putatively assigned to ammonia-oxidizers were 0.03% of total reads but were not detected in the 16S rRNA pool. Conversely, ammonia-oxidizing bacteria (AOB, *Nitrosomonadales*- and *Nitrosococcus*-like) and nitrite-oxidizing bacteria (NOB, *Nitrospirae*-like) metagenomic reads were detected at ten times higher concentration (0.3% of total reads). AOB were also detected in the 16S rRNA pool at similar concentrations (0.1% of total 16S rRNA gene). Overall, the most abundantly recovered 16S rRNA gene from the metagenomic dataset matched *Chlorobiales* (green sulfur bacteria; 20%, range 5-50%), *Campylobacterales* (epsilon-Proteobacteria; 14%, range 11-21%), *Burkholderiales* (beta-Proteobacteria; 12%, range 0.5-35%), OD1 (8%, range 4-13%), and *Frankiales* (Actinobacteria; 5%, range 0.3-12%), among others (Fig. 4.2, and Supplementary Table A.C4.2). These populations were differentially distributed between layers and lakes (Fig. 4.2, and see details in Supplementary Table A.C4.2) and yielded a taxonomic clustering according to the redox potential, with samples with higher redox (> -30 mV) and lower sulfide concentrations (sulfide <13 µM) closer each other than to the most euxinic sample (Lake Cisó hypolimnion, sulfide >500 µM, redox -86 mV; Table 4.1).

Functional structure of the microbial communities

The metagenomic dataset comprised four million reads of average length 377 bp and 54 % of the metagenomic reads were taxonomically assigned based on the APIS or BLAST, while 22% could be assigned KO numbers and thus putative functions (e-value 10^{-5}). From the identified KOs, we selected marker genes related to carbon (C), nitrogen (N), and sulfur (S) cycling (Supplementary Table A.C4.1). Anaerobic C fixation, nitrogen fixation, and assimilatory sulfate reduction genes accounted for a substantial percentage of annotated reads in the hypolimnia, whereas genes for aerobic

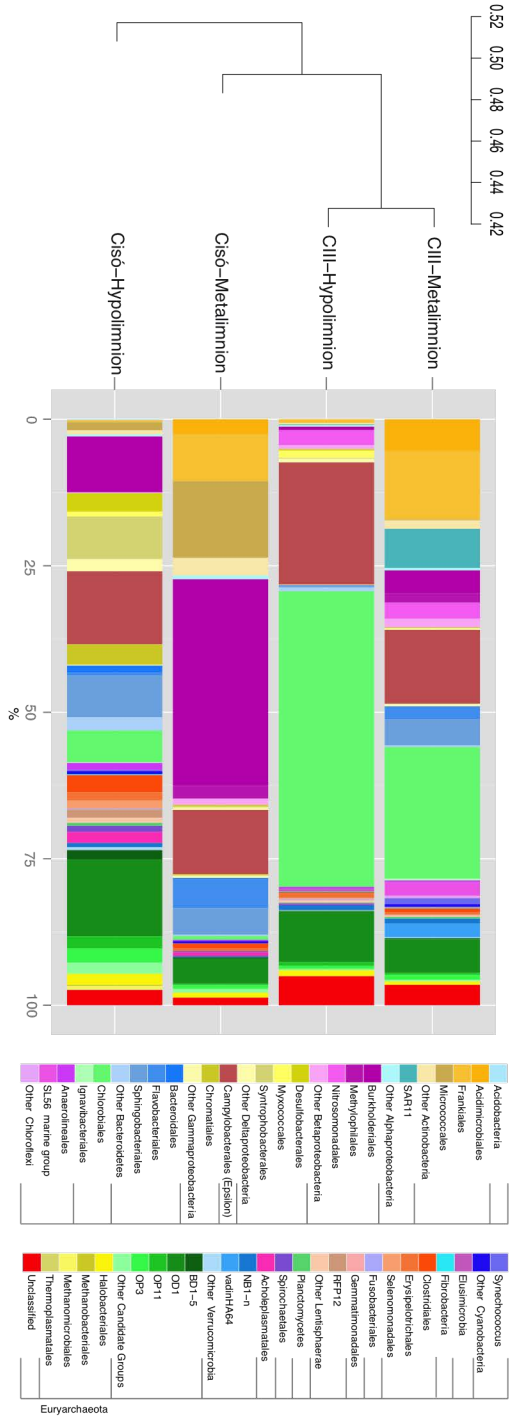

Figure 4.2: Prokaryotic community structure (relative abundances at the Order level) of Lake Banyoles basin C-III and Lake Cisó obtained from the 16S rRNA gene present in the metagenomic pool. See detailed information in Supplementary Table A.C4.2. Hierarchical clustering based on Bray-Curtis dissimilarity matrices.

respiration, nitrogen assimilation, and sulfur mineralization were more abundant at the oxic-anoxic interfaces (Supplementary Table A.C4.3). Other less abundant metabolic pathways such as ammonification, anammox-SRAO (sulfate-reducing anaerobic ammonia oxidation, Rikmann et al. 2012), and dissimilatory sulfate reduction were detected,mostly in the hypolimnion of Lake Cisó. Such differences were globally captured by a functional level (hierarchical analysis; C, N and S pathways were examined) that grouped the samples according to presence/absence of oxygen (Fig. 4.3). This clustering analysis produced the same result using multiple other functional annotations, including KEGG (EC), GO terms, and MetaCyc. Similarly, repeating this analysis with all size fractions as separate libraries (data not shown), and housekeeping genes

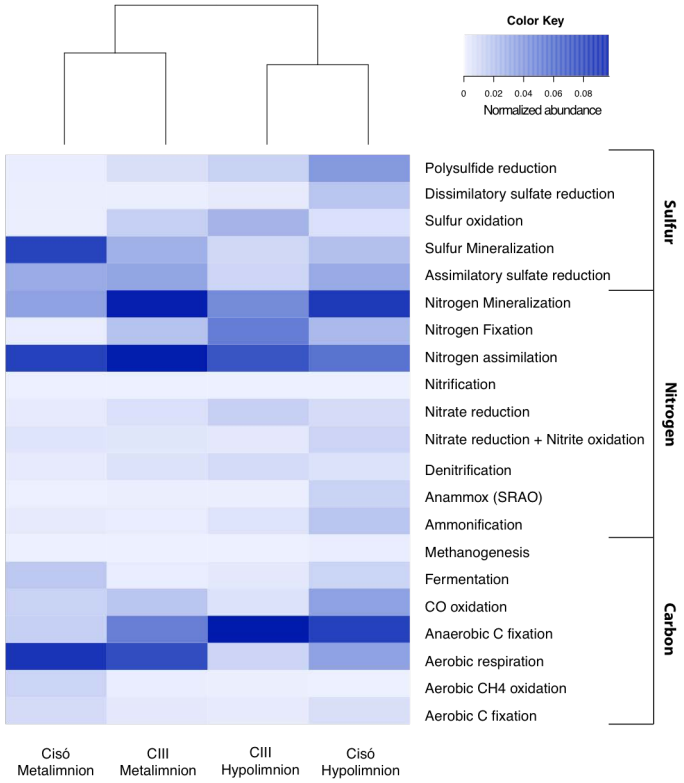

Figure 4.3: Heatmap plot and functional clustering of the selected KEGG Orthologs for the predicted ORFs from the metagenomic reads for Lake Cisó and Banyoles basin C-III.

(Supplementary Fig. A.C4.4) gave similar results with redox being a more structuring factor than geographical distribution.

As Bacteria and Archaea accounted for most of total metagenomic reads we focused on the prokaryotes for a comparative study of the geochemistry of carbon (Fig. 4.4), nitrogen (Fig. 4.5), and sulfur (Fig. 4.6) along the redoxcline. We used the relative abundance of the detected functional genes as a proxy of the potential relevance of each pathway *in situ* without considering the role of microscopic algae. For the C cycling, the main pathway detected in the oxic-anoxic interface was aerobic respiration by heterotrophic *Actinomycetales* and *Burkholderiales* in Lake Cisó, and by *Actinomycetales* and *Pelagibacterales* (SAR11-like) in Lake Banyoles C-III. In the hypolimnion, the abundant pathways were various forms of anaerobic carbon fixation: by *Chromatiales* (anoxygenic phototrophy by the Calvin cycle), *Bacteroidales* (probably anaplerotic) and sulfate-reducing bacteria (SRB) (probably the reductive citric acid cycle/Arnon pathway, Fuchs 2011) in Lake Cisó, and *Chlorobiales* (anoxygenic phototrophy by the Arnon cycle) in Banyoles C-III (Table 4.3). Chemolithotrophic aerobic carbon fixation via the Calvin cycle, which was rare, was mostly related to *Betaproteobacteria* of the genus *Hydrogenophilales* (*Thiobacillus*-like) and *Gallionellales* (*Syderoxydans*-like). Chemolithotrophic *Epsilonproteobacteria* with genes for the Arnon cycle (*Campylobacterales* on Fig. 4.4) were found related to the genera *Arcobacter, Sulfuricurvum,* and *Sulfurimonas* (Table 4.3). CO oxidation marker genes were also present (3-14 % of those targeted marker genes selected for the carbon cycle, Supplementary Table A.C4.3) and related to heterotrophic bacteria. The potential for fermentation was mostly observed in Lake Cisó. Both methanogenesis and methane oxidation specific marker genes had low abundances in all four environments, and even in those samples where such genes were not specifically detected (Fig. 4.4, dotted lines) we found additional metagenomic reads matching methanogens and methane oxidizers.

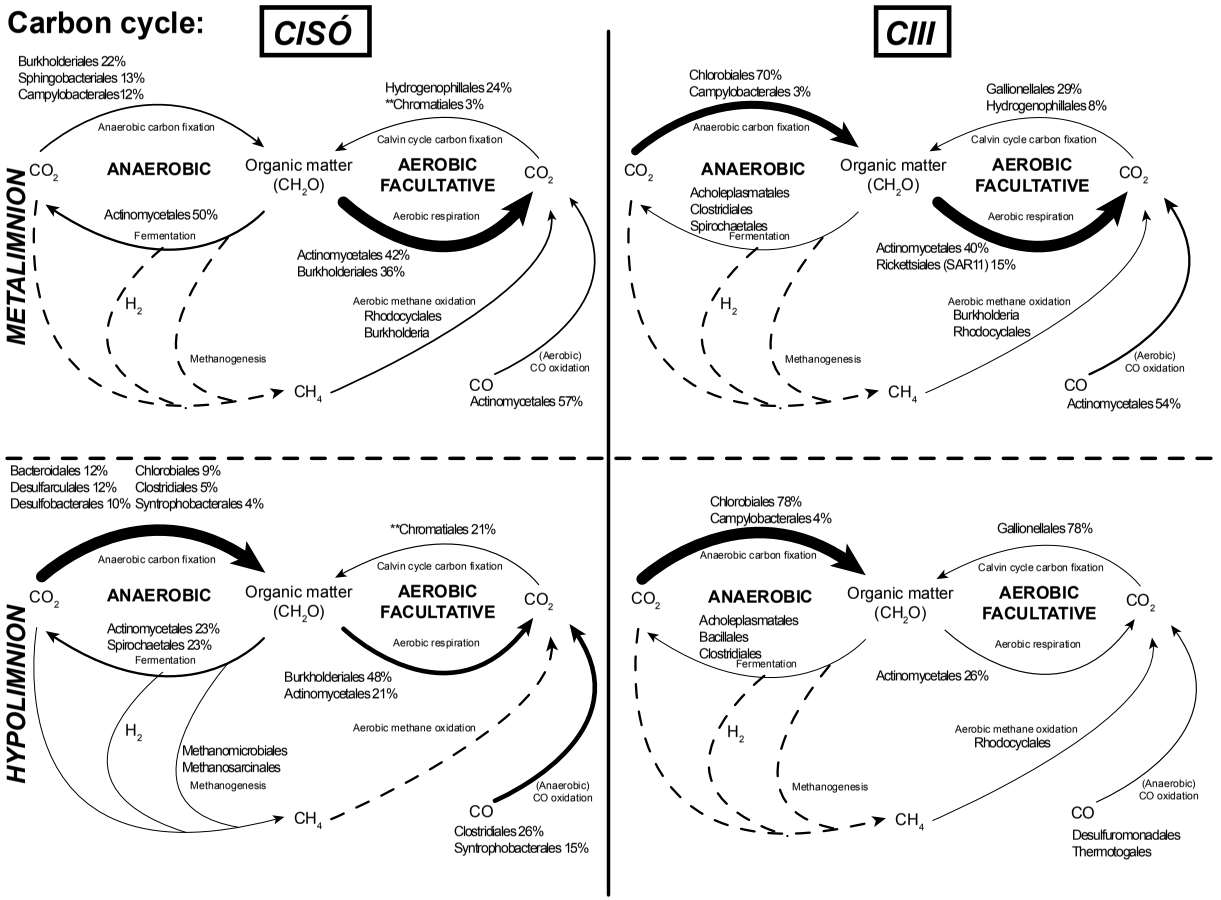

Figure 4.4: Genetic potential for several steps of the carbon cycle in Lake Cisó and Banyoles basin C-III using a combination of normalized marker genes. Arrows size proportional to the potential flux of the carbon pathways (100% value, see Supplementary Table A.C4.3). Dotted lines: not detected marked genes but putative presence of the pathway (see main text). Relative abundances for the main microbes potentially driving each conversion step are shown (only for those that contributed >1% of the marker genes mixture). ***Chromatiales*: anoxygenic phototrophy through the Calvin cycle.

Figure 4.5: Genetic potential for several steps of the nitrogen cycle in Lake Ciso and Banyoles basin C-III using a combination of normalized marker genes. Arrows size proportional to the potential flux of the nitrogen pathways (100% value, see Supplementary Table A.C4.3). Dotted lines: not detected marked genes but putative presence of the pathway (see main text). Relative abundances for the main microbes potentially driving each conversion step are shown (only for those that contributed >1% of the marker genes mixture). **Presence of AOA, AOB and NOB reads in the metagenomic pool.

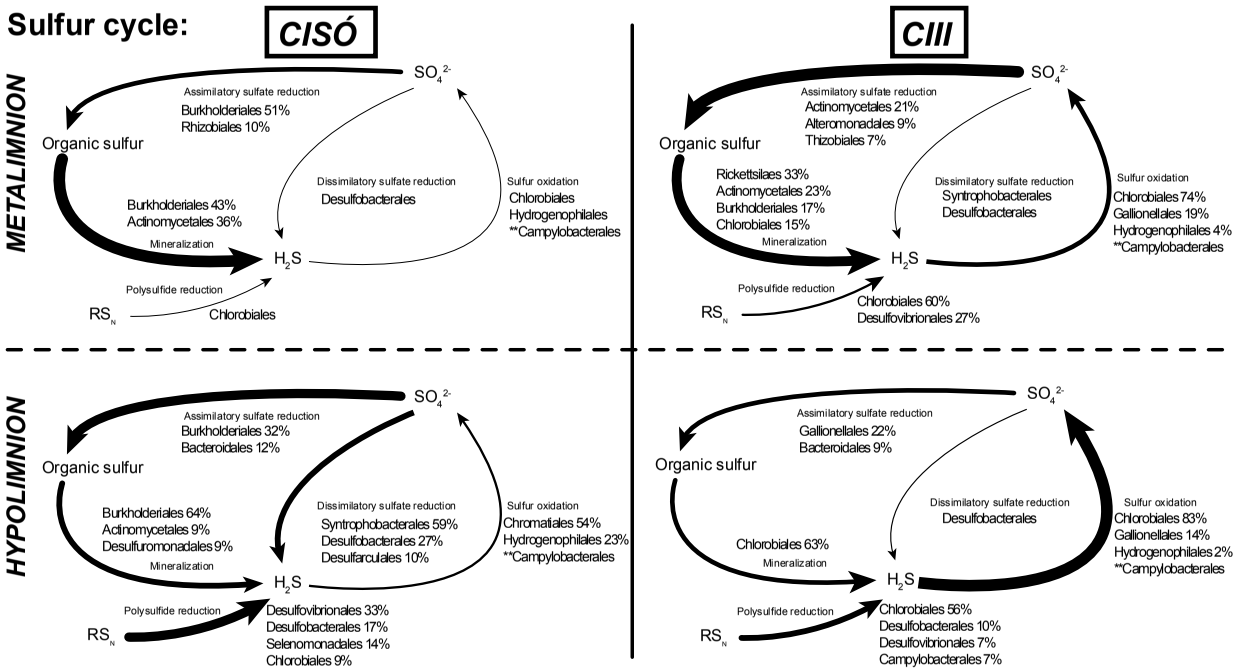

Figure 4.6: Genetic potential for several steps of the sulfur cycle in Lake Cisó and Banyoles basin C-III using a combination of normalized marker genes. Arrows size proportional to the potential flux of the sulfur pathways (100% value, see Supplementary Table A.C4.3). Relative abundances for the main microbes potentially driving each conversion step are shown (only for those that contributed >1% of the marker genes mixture). ***Campylobacteraceae* contributed through *sox* genes not reported in KEGG database.

Table 4.3: Carbon fixation cycles and main metabolic traits of the C-fixing microorganisms found in this study. *SRAO: sulfate-reducing ammonium oxidation. [a]Also known as reverse Krebs cycle, reverse tricarboxylic acid cycle (rTCA) and reverse citric acid cycle. [b]Also known as Wood–Ljungdahl pathway.

Taxa/ phylogeny	C-fixation pathway	Traits	Main genera identified in Lakes Cisó and CIII from the 16S rRNA gene present in the metagenomic pool
Gallionellales *Betaproteo-bacteria*	Calvin	Facultative Chemolithoautotroph Energy sources: Fe(II)/sulfide Denitrification	*Sideroxydans*
Hydrogeno-philales *Betaproteo-bacteria*	Calvin	Chemolithoautotroph Sulfide oxidation	
Campylo-bacterales *Epsilonpro-teobacteria*	Arnon[a]	Chemolithoautotroph Denitrification Sulfide oxidation	*Arcobacter, Sulfuricurvum, Sulfurimonas*
Chromatiales *Gammapro-teobacteria*	Calvin	Photolithoautotroph Anaerobic Tolerates oxygen	*Lamprocystis*
Chlorobiales *Chlorobi*	Arnon[a]	Photolithoautotroph Anaerobic (strict) N fixation	*Chlorobium luteolum*
Desulfo-bacterales *Deltaproteo-bacteria*	Arnon[a] Reductive acetil-CoA[b]	Heterotroph Sulfate reducers	*Desulfatiferula, Desulfobulbus, Desulfocapsa, Desulfosalsimonas*
Syntropho-bacterales *Deltaproteo-bacteria*	Arnon[a] Reductive acetil-CoA(?)[b]	Heterotroph Sulfate reducer/ sulfide oxidation SRAO*	*Desulfomonile*
Desulfuro-monadales *Deltaproteo-bacteria*	Reductive Acetil-CoA[b]	Nitrate dependent Fe(II) oxidation with production of ammonium (Weber et al., 2006)	

For the nitrogen cycle, most of the detected marker genes catalyzed N assimilation and mineralization (Supplementary Table A.C4.3, Fig. 4.5). Denitrification was observed in low abundance in all the cases (c. 3% of the nitrogen functional reads selected), and the main taxa involved were *Campylobacterales* (autotrophic *Sulfurimonas* and *Arcobacter*), *Oceanospirillales* (heterotrophs) and *Gallionellales* (autotrophic *Sideroxydans*). Conversely, the potential for nitrogen fixation (*nif* genes) was observed in all the cases, though in higher abundance under euxinia (18%±11%) than in the oxic-anoxic interfaces (4%±4%). The *nif* genes were most related to *Chlorobium* in Lake Banyoles, while in Lake Cisó were most similar to *Syntrophobacterales*. Under the most euxinic conditions, c. 6% of the total nitrogen marker genes examined were the anammox catalyzing enzyme hydrazine oxidoreductase, though these were associated with *Syntrophobacterales* instead of the planctomycetales found in oceanic anoxic zones. Both aerobic ammonia oxidation and nitrification marker genes had very low abundance, and only were properly detected in Lake Banyoles C-III hypolimnion (*amoC* gene 97% identical to *Nitrosospira multiformis*). However, metagenomic reads matching *Thaumarchaeota* (AOA), *Nitrosomonadales* and *Nitrosococcus* (AOB), and *Nitrospirae* NOB were detected in all lakes and water layers (Fig. 4.5, dotted lines), pointing out that the genetic potential to close the nitrogen cycle was there, but at very low abundance as compared to other pathways in the cycle.

Finally, in the S cycle (Supplementary Table A.C4.3, Fig. 4.6) the highest percentage of the reads matched assimilatory sulfate reduction (28%±9% of those targeted sulfur marker genes) and sulfur mineralization (35%±25%) mostly driven by the predominant heterotrophic organisms found in each water layer (*Actinomycetales* and *Burkholderiales*). Most sulfide oxidation genes likely originated from *Chlorobiales* in Lake Banyoles C-III, and *Chromatiales* in Lake Cisó, with further contributions from chemolithotrophs *Gallionellales*, *Hydrogenophilales*, and *Campylobacterales*. The potential for planktonic sulfate reduction was only observed in strong euxinia (Lake Cisó hypolimnion, 16% of targeted sulfur reads as compared to

1.4%±1% in the remaining samples), with reads likely originating from *Desulfobacterales* and most probably *Syntrophobacterales*, although members of this group may carry out both reductive and oxidative parts of the sulfur cycle. Interestingly, we observed a high richness of sulfate-reducing bacteria genera (Table 4.3) with the potential to degrade a wide variety of carbon compounds to help to maintain the high sulfide concentrations found in Lake Cisó.

While the metagenomic dataset does not contain transcriptome or proteome data, and thus only indicates potential function, we observed a direct linear relationship between relative abundance of dissimilatory sulfate reduction genes and *in situ* sulfide concentrations ($r= 0.998$, $p= 0.002$). Although this comparison should be carefully interpreted because the low number of samples compared, it suggests a close link between both the abundance of planktonic SRB genomes and sulfide production. We also observed significant direct linear relationships between the relative abundance of anaerobic carbon fixation genes from bacterial chemotrophs and denitrification ($r= 0.958$, $p= 0.042$) suggesting a close link between chemoautotrophy and the nitrogen cycle.

Discussion

Stratified planktonic environments with sharp chemical gradients and sulfide-rich bottom waters are valuable current windows on past Earth conditions. Anoxic and euxinic conditions were common but spatially and temporally heterogeneous in ancient oceans during Proterozoic (Lyons et al. 2014, Reinhard et al. 2013) and may have played an important role in mass extinctions during the Phanerozoic (Meyer and Kump 2008). The presence of marker pigments for photosynthetic sulfur bacteria (i.e. isorenieratene and okenone) have been often reported as evidence of euxinic conditions in ancient oceans (Damsté and Köster 1998, Brocks et al. 2005). These conditions are not common nowadays, although persistent euxinia can be found in deep silled basins such as the Black Sea, Baltic

Sea, and Cariaco Basin (Millero 1991, Stewart et al. 2007). Future climate change scenarios predict, however, an increasing of euxinia phenomena, mainly in coastal marine ecosystems (Diaz and Rosenberg 2008). The study of stratified sulfurous lakes has, therefore, an additional interest to predict biogeochemical functioning and microbial interactions in such future scenarios. In the present study, we explored the community composition and functional genes content along a gradient of redox conditions in a karstic sulfurous area. Continental systems are cheaper and easier to sample than marine basins, and a large variety of photo- and chemolithotrophs organisms, sulfide-oxidizing and sulfate-reducing bacteria, fermenters, denitrifying microbes, methanogens and methane oxidizers are expected to be found according to previous studies (e.g., Casamayor et al. 2000, Barberán and Casamayor 2011). The metabolisms harbored by these microorganisms have the potential to provide insights into the ecosystems operating in euxinic early stages of Earth. The strong euxinic conditions found in Lake Cisó may match biogeochemistry in ancient coastal areas, whereas basin C-III in Lake Banyoles may represent the transition from euxinic coastal areas to merely anoxic and rich Fe conditions in the ancient open ocean (Fig. 4.7).

The very low abundance of genes for nitrification, the minor presence of anammox genes, the high potential for nitrogen fixation and mineralization, and the potential for chemotrophic CO_2 fixation and CO oxidation all provide potential clues on the ancient oceanic anoxic zones functioning. The low abundance of ammonia oxidizers (AOA and AOB) agrees with the high ammonia accumulation in the anoxic bottom of the lakes, the lack of oxygen,and presence of potentially toxic sulfide. We observed, however, a higher gene abundance of AOB relative to AOA in the metagenomic pool that may have a geochemical link related to the abundance of Fe in these environments. AOA have a highly copper-dependent system for ammonia oxidation and electron transport (Walker et al. 2010), completely different from the iron-dependent system present in AOB. The tradeoff in Fe versus Cu rich ammonia oxidation enzymatic

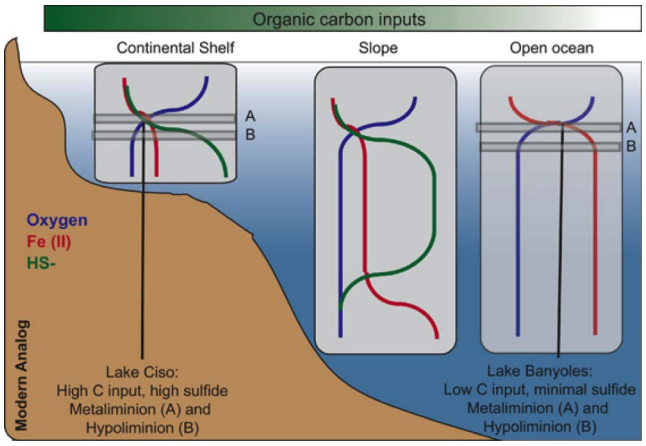

Figure 4.7: Lake Cisó and basin C-III of Lake Banyoles as modern analogues of anoxic conditions prevailing in the ancient ocean. The illustration shows the geochemical distributions of Fe, S, C, and O_2 in depth profiles and along different oceanic regimes (shelf, slope, open ocean) during the Proterozoic (Lyons et al. 2014). Lake Cisó would be closer to coastal and continental shelf areas whereas Banyoles C-III would be a more open ocean analog.

systems would suggest that AOA evolved relatively recently (<550 million years ago) and that the Proterozoic oceans, which would have been Fe rich, would have been AOB dominated. Interestingly, the evolutionary dynamics of the *amoA* genes cladogenesis events visualized using lineage through time plots, displays a different scenario for AOA and AOB, with AOB showing a more constant cladogenesis through the evolutionary time whereas AOA experienced two fast diversification events separated by a long steady-state period (Fernàndez-Guerra and Casamayor 2012).

The potential for nitrogen fixation and denitrification was detected in both autotrophs and heterotroph microbial lineages, suggesting a diverse range of potential overlaps between carbon and nitrogen cycling in the ancient ocean, and an active nitrogen cycle in anoxic systems. Our results show a potential major contribution to nitrogen fixation by *Chlorobiaceae* under euxinic conditions. *Chlorobiaceae* were also the major contributors to carbon fixation in

Banyoles C-III coupled to sulfide oxidation through the Arnon cycle. Therefore, the reported presence of *Chlorobiaceae* in the ancient ocean (Damsté and Köster 1998, Brocks et al. 2005) would have been of major relevance not only for the carbon cycle but also for the nitrogen cycle. *Campylobacterales* (*Epsilonproteobacteria*) accounted for a large percentage of the denitrification genes in the anaerobic layers of both lakes, but were taxonomically segregated (*Arcobacter* dominated in Cisó, *Sulfurimonas* was present in C-III). Both genera respire nitrate coupled to C fixation in the dark through the reverse TCA cycle (Burgin and Hamilton 2007, Grote et al. 2012, Labrenz et al. 2005), being potentially able to couple denitrification to sulfur oxidation (Ghosh and Dam 2009). The other important group involved in denitrification was the chemolithoautotrophic *Gallionellales* oxidizing sulfide or Fe^{2+} while respiring nitrate, and producing NH_4^+ or N_2. The presence of *Gallionellales* exclusively in C-III is probably due to their close relation with the iron cycle (Weber et al. 2006), and by the fact that an active Fe^{2+} cycle has been previously detected in Lake Banyoles (Garcia-Gil et al. 1990). The potential role of *Gallionellales* in ancient oceans with an active iron cycle is therefore of major interest.

The case of *Bacteroidales* also deserves to be mentioned. *Bacteroidales* have been typically considered aerobic or microaerophilic chemoorganoheterotrophic bacteria (Reichenbach 2006), and have been recurrently detected in the Banyoles area (Casamayor et al. 2000, Casamayor et al. 2002, Casamayor et al. 2012) and in marine environments (Fernández-Gomez et al. 2013). However, their role in anaerobic, sulfide-rich layers was not elucidated. Here, we assigned *Bacteroidales* as potentially catalyzing DNRA (dissimilatory nitrate reduction to ammonium), coupling the electron flow from organic matter to the reduction of nitrate. Thus, we would expect a potential gradient of distribution for anaerobic *Bacteroidales* in the ancient ocean being more abundant in the organic carbon and sulfide rich coastal zones (Fig. 4.7) than in the anoxic and more oligotrophic open ocean. We also noticed the low abundance of key processes in the anaerobic carbon cycle such as

CH_4 cycling, probably because in the presence of limiting levels of sulfate, methanogens are generally poor competitors with sulfate reducers in stratified natural environments (Raskin et al. 1996). Sulfate reduction normally occurs in fully anoxic sediments by SRB (Holmer and Storkholm 2001). However, as shown here, a water column with euxinic conditions and a high availability of organic carbon is also suitable for the growth of an important community of planktonic SRB.

Previous studies in Banyoles area measured unexpected high rates of dark carbon fixation at the oxic-anoxic interface and the hypolimnetic waters, accounting for 58% of total annual fixed carbon in Lake Cisó (Garcia-Cantizano et al. 2005). It was proposed that photosynthetic bacteria could be partly carrying out dark carbon incorporation *in situ* (Casamayor et al. 2008), and *Thiobacilli* may actively fix CO_2 at certain depths (Casamayor 2010). However the ecological factors modulating the process and the microbial populations performing dark carbon fixation are still not well understood (Casamayor et al. 2012). In the present investigation, we detected the potential for chemotrophic CO_2 fixation mainly through the reverse TCA cycle (K00174, K00175 and K00244 from *KEGG* Orthology) in *Bacteroidales, Campylobacterales* and *Desulfarculales*. In addition, other SRB such as *Desulfobacterales* may also participate through the anaerobic C_1-pathway (Wood-Ljungdahl pathway, K00194 and K00197) yielding formate assimilation and CO_2 fixation (Fuchs 2011, Hugler et al. 2003, Sun et al. 2010). Interestingly, the diversity of taxa potentially participating in carbon fixation in the dark was larger in Lake Cisó than in C-III, in agreement with *in situ* measurements carried out in former investigations (Casamayor 2010, Garcia-Cantizano et al. 2005). These findings would suggest an active carbon fixation in ancient euxinic oceans beyond the euphotic zone that certainly deserves further investigation.

Additionally, the oxidation of carbon monoxide (CO) generates ATP and CO_2 that may be further processed through one of the reductive CO_2 fixation pathways to be used as C source (King and

Weber 2007, Ragsdale 2004). Some studies indicate that organisms using CO as both energy and C source can be viewed as the extant survivors of early metabolic processes (Huber and Wächtershäuser 1997). In the hypoxic layers we found that the heterotrophic group of *Actinomycetales* accounted for most of CO monooxygenase genes in agreement with their mixotrophic lifestyle (Schmidt and Conrad 1993). More interestingly, in the anoxic depths of Lake Cisó we found that CO-oxidation genes were mainly related to SRB from *Deltaproteobacteria* group (*Geobacter* and delta proteobacterium NaphS2) and to *Firmicutes* (*Carboxidothermus hydrogenoformans, Moorella thermoacetica, Clostridium* spp.). This finding suggests that the fate of the reducing equivalents from CO-oxidation in anaerobic conditions could be coupled to sulfate-reduction (carried out by SRB) to produce sulfide, or to CO_2 reduction to produce acetate (SRB and Firmicutes) (King and Weber 2007, Roberts et al. 2004). To check whether CO oxidation could be coupled to CO_2 reduction to yield acetate (Ragsdale 2004, Roberts et al. 2004), we identified the phylogenetic affiliation of acetyl-CoA synthase genes (ACS, K14138), and found that *Desulfobacterales* and *Firmicutes* had the potential to use the Wood-Ljungdahl pathway to obtain energy and fix carbon from CO in the hypolimnion of Lake Cisó. However, although the CO-oxidizing genes were detected, we cannot assess their relevance in the lake or the ancient oceans because CO-oxidizing bacteria carry out a facultative mixotrophic metabolism (Gadkari et al. 1990).

Overall, the metagenomics approach unveiled the interrelationships between microbes and biogeochemical cycling in a comparative framework in two lakes that are modern analogues of ancient ocean conditions. These results may also help to develop new geochemical proxies to infer ancient ocean biology and chemistry. A major pitfall in our metagenomic approach is the reliance on the assumption that the genes come from a particular bacteria or archaea according to phylogentic annotation; lateral gene transfer would compromise the direct link of phylogeny to a metabolic pathway. In most of the cases we found the 16S rRNA gene counterpart present in the metagenomic data pool, giving additional

support to such links. Obvious next steps include an experimental quantification of the energy and matter fluxes involved in each of the metabolic pathways to get a complete picture on the tight coupling between microbes and biogeochemical cycling in euxinic ecosystems.

Acknowledgements

JC Auguet, M Llirós, F Gich, FM Lauro and JM Gasol are acknowledged for field and lab assistance and ancillary data. We sincerely appreciate insightful comments and suggestions from anonymous reviewers and the editor. This research was funded by Grants GOS-LAKES CGL2009-08523-E and DARKNESS CGL2012-32747 to EOC from the Spanish Office of Science (MINECO), from financial support by the Beyster Family Fund of the San Diego Foundation and the Life Technologies Foundation to the J. Craig Venter Institute, and the NASA Astrobiology Institute to CLD.

5

Speciation and ecological success in a natural population of green sulfur bacteria mediated by horizontal gene transfer[1,2]

Abstract

In a recent metagenomics study in the euxinic Lake Banyoles, a bloom of the green sulfur bacteria (GSB) *Chlorobium luteolum* was identified using metagenomic and 16S rRNA analysis. The bloom was detected in the boundary between the oxic and anoxic layers of the lake. Metagenomic assembly resulted in a bin of 41 contigs and a total size of 2.15 Mbp for the dominant population, which we named *Chl. luteolum* CIII. *Chl. luteolum* CIII is very similar (91.7% Average Nucleotide Identity (ANI) and 99.7% 16S rRNA identity) to its cultured counterpart *Chl. luteolum* DSM 273^{T}, which we used for a comparative analysis in order to determine genomic changes, e.g.,

[1] Llorens–Marès T, Z Liu, L Zeigler-Allen, DB Rusch, MT Craig, CL Dupont, DA Bryant and EO Casamayor. Manuscript submitted to ISME Journal.
[2] See supplementary material in Appendix A

horizontal gene transfer (HGT) that could explain the ecological success of CIII strain. Several differences in the potential for ferrous iron acquisition, ATP synthesis or gas vesicle formation were detected, but possibly, the most striking difference relates to pigment biosynthesis. *Chl. luteolum* DSM 273^T is a green-colored GSB that synthesizes bacteriochlorophyll (BChl) *c*, while *Chl. luteolum* CIII is a brown-colored GSB that synthesizes BChl *e*. We found that *Chl. luteolum* CIII had incorporated an 18-kbp cluster with the putative genes needed for BChl *e* biosynthesis and specific carotenoids that likely give *Chl. luteolum* CIII a photosynthetic advantage over other strains sharing the same niche. We also genomically characterized what we believe to be the first described GSB phage, which based on the metagenomic coverage, was likely in an active state of lytic infection. This phage may serve both to control the blooming population and as a vector for the observed HGT. This work links three closely related issues that are usually studied separately: HGT, ecological success and bloom control through phage infection.

Introduction

Green sulfur bacteria (GSB, *Chlorobiaceae*) form blooms, often of monoclonal nature, in the twilight zone of stratified lakes with euxinic (anoxic and sulfidic) bottom waters (Gregersen et al. 2009). GSB are anaerobic photoautotrophs that couple anoxic oxidation of sulfide and CO_2 fixation, and their specific contents in carotenoids and bacteriochlorophylls (BChl *c*, *d*, *e* and *a*) are ecological traits that dictate both their light-harvesting capacities and their potential ecological success (Montesinos et al. 1983, Van Gemerden and Mas 1995, Bryant et al. 2012). Usually brown-colored GSB (cells mostly containing BChl *e* and isorenieratene) bloom in deeper layers of stratified lakes, whereas green-colored GSB (cells with BChl *c* and chlorobactene as dominant pigments) are more abundant in anoxic water layers nearer the surface or underneath plates of purple sulfur bacteria (Montesinos et al. 1983). However, the genomic adaptations

of phototrophic sulfur bacterial blooms to particular environments is still unclear (Gregersen et al. 2009).

Horizontal gene transfer (HGT) is a major mechanism for bacterial innovation and adaptation to colonize new ecological niches and improve *in situ* performance, thus acting as a trigger for prokaryotic speciation (Ochman et al. 2000, Wiedenbeck and Cohan 2011). HGT may be driven by transformation (naturally incorporated environmental DNA), conjugation (i.e., genetic material acquired through plasmid exchange between cells), and transduction (through phage infection). Within *Chlorobiaceae*, *Chlorobaculum tepidum* TLS (formerly *Chlorobium tepidum* TLS), shows one of the genomes with the highest proportion of HGT (c. 24% of all genes, (Nakamura et al. 2004) probably related to the fact that this bacterium is naturally transformable (Ormerod 1988, Frigaard and Bryant 2001). Likely examples of transduction are also found in GSB; the *sox* cluster for thiosulfate utilization is a well-known example of lateral gene transfer in *Chlorobium phaeovibrioides* DSM 265 (Frigaard and Bryant 2008). However, phages infecting GSB have not been described so far (Frigaard and Bryant 2008).

Genome comparisons of closely related populations are important to identify the role of HGT in ecotype formation and ecological diversification (Cohan and Koeppel 2008). Metagenomic approaches can capture genomic differences in natural populations when pure cultures are difficult to obtain (Bhaya et al. 2007, Palenik et al. 2009, Klatt et al. 2011) and avoid the necessity to mimic the scale of natural ecosystems in laboratory experiments, which may discount the effect of potentially important variables for HGT (Aminov 2011). From an ecological perspective, the effect of HGT on the distribution and abundance of cyanobacteria of the genus *Prochlorococcus* and its ecotypes have been examined (Rocap et al. 2003, Martiny et al. 2009) and a comparative analysis of four *Pseudomonas putida* strains demonstrating that HGT played a key role in its adaptation process to each environmental niche (Wu et al. 2011). However, no studies have focused on the *in situ* context in which HGT explains the ecological success of a population and the

complex interplay between recombination and ecology in a natural population (Polz et al. 2013).

The reconstruction of microbial genomes directly from environmental DNA through metagenomics can be difficult (Luo et al. 2012). Initial studies have focused on simple communities, such as a low-complexity acid mine drainage microbial biofilm with 6 estimated species (Tyson et al. 2004). Other studies have used tools to help simplify the community, such as the use of enrichment cultures (Martin et al. 2006), sequencing multiple metagenomes of the same community (Albertsen et al. 2013) or a dual approach of single-cell sequencing with coassembly and binning of multiple metagenomes (Dupont et al. 2012). In the present study, we reconstructed the consensus genome of a natural blooming GSB population without previous culturing. This dominant population serves as a natural enrichment culture (Van Gemerden et al. 1985), from which a nearly complete genome was assembled and used to study ecosystem-specific adaptations. The presence of putative phage assemblies with homology to the consensus genome showed for the first time consistent evidence for virus-mediated horizontal gene transfer in a natural population of green sulfur bacteria.

Materials and methods

Environment and sample analysis

The bloom sample was collected from deep (24 m) euxinic waters of meromictic basin III (CIII) of karstic Lake Banyoles (NE Spain, 42 18'N, 21 45'E) on May 9, 2010. Brown-pigmented green sulfur bacteria massively and persistently bloom in C-III (Montesinos et al. 1983). Methods of sampling, environmental analysis, filtering, and DNA extraction were recently reported (Llorens-Mares et al. 2015). The size fraction 0.8-3 µm was targeted for assembly. In this sample we had measured high concentrations of BChl *e*, the characteristic pigment of brown-colored species of *Chlorobium* with a high relative abundance (>50%) of 16S rRNA gene closely matching (99.7%

identity) the green-colored species *Chlorobium luteolum* DSM 273^T (Llorens-Mares et al. 2015). Accordingly, the natural population from which we obtained the DNA for metagenomic sequencing and genome reconstruction was named *Chl. luteolum* CIII.

Metagenomics analyses

A total of 492,615 reads with 401-nt average read length were generated by shotgun metagenomics. Reads were assembled using two different software assemblers: Newbler Assembler (Roche) and CLC Assembly Cell (CLC bio), which produced 2,971 and 23,490 contigs, respectively. For each assembly we selected contigs > 3kb that were plotted against GC content and read depth (Supplementary Fig. A.C5.1). To assemble *Chl. luteolum* CIII specifically, we selected contigs with ~57% GC (equivalent to the 57.33% GC of *Chl. luteolum* DSM 273^T) and a read depth of ~29. Using these criteria, we selected 45 contigs from the Newbler assembly (average length, 47 kb, average read depth 29.9 ± 2.8, and mol% GC = 56.7%) and 75 contigs from the CLC assembly (average length 28 kb, average read depth 29.1 ± 3.2, and mol% GC = 56.7%). We then used phred/phrap/consed package (Ewing et al. 1998, Gordon et al. 1998, Gordon 2003) to combine these assemblies to produce a final assembly of 41 contigs totaling 2,152,917 bp with an average mol% GC = 56.73%.

Contigs were ordered and oriented according to the reference genome, *Chl. luteolum* DSM 273^T, and visualized for a synteny comparison using Genome Matcher (Ohtsubo et al. 2008). The genome encoded 2,057 open reading frames (ORFs) that were annotated with RAST (Aziz et al. 2008) with rigorous manual curation. We checked for genomic completeness by searching for a set of 110 universally occurring marker genes, very rarely duplicated, essential for cellular life, and believed to be very ancient (Dupont et al. 2012). All 110 of these genes were present in CIII genome, and all were present as single-copy genes.

We used DNAPlotter (Carver et al. 2009), for a visualization of different traits such as the global genome, the mol% GC, the GC

skew and all ORFs. For a visual comparison with the reference genome we used the Artemis Comparison Tool (ACT) (Rutherford et al. 2000, Carver et al. 2005, Carver et al. 2012). Perl scripts were run to obtain a list of the ORFs that were classified as orthologs with the reference genome using a whole-genome reciprocal BlastP analysis (Fuchsman and Rocap 2006, Moreno-Hagelsieb and Latimer 2008) in order to establish differences in protein coding between strains.

For a global comparison of similarity between genomes and to assess the Average Nucleotide Identity (ANI) of CIII genome with other sequenced GSB, we used JSpecies V1.2.1 (Richter and Rossello-Mora 2009). Hierarchical clustering analysis of the resulting all *vs*. all ANI similarity matrix obtained with JSpecies was performed in R (R Core Team 2014).

As a result of the assemblies with Newbler and CLC, we detected the presence of large contigs (>3 kb) with an unusually high read-depth (~79 to 325×; Supplementary Fig. A.C5.1). Based on their isolation from the cellular size fraction, these sequences were eventually assigned to a potential infecting phage population. We reassembled these contigs with the same procedure followed for *Chl. luteolum* CIII. A long contig (65 kb) with read depth 34 and mol% GC = 34.8 was also selected because the presence of genes coding for phage related proteins. We ended with five contigs designated as putatively phage-derived sequences. These contigs were annotated with the JCVI viral annotation pipeline (Lorenzi et al. 2011). One of the putative phage-derived contigs had similarity to a region of the *Chl. luteolum* CIII genome. This region was visualized for synteny using the R package genoPlotR (Guy et al. 2010).

16S rRNA phylogenetic analysis

A comprehensive phylogenetic tree of the 16S rRNA gene was generated with reference sequences from the phylum *Chlorobi*, from the assembled genome and from previous studies in the area (Figueras et al. 1997, Casamayor et al. 2000). Sequences were aligned with SINA aligner (Pruesse et al. 2012), and phylogenetically

compared by maximum likelihood with the general time-reversible model from RAxML v7.3.0 (Stamatakis 2006) using *Bacteroidetes fragilis* as outgroup.

BChl e phylogenetic analysis

Genes encoding proteins associated with BChl *e* biosynthesis (e.g., BchF3, BciD; Maresca 2007, Harada et al. 2013) and isorenieratene biosynthesis (CruB, Maresca et al. 2008b) were found on two different CIII contigs. We designed primers for each contig end in order to confirm by PCR amplification and DNA sequencing that the genes were contiguous and formed a cluster in one genomic locale in the natural population.

Only one gene, *bciD*, has conclusively been demonstrated to be involved in BChl *e* biosynthesis (Harada et al. 2013). This gene was previously annotated as encoding a protein of the radical S-adenosyl-L-methionine (RSAM) enzyme superfamily. Harada and coworkers showed that BciD is required for conversion of the C7 methyl group of BChlide *c* into the formyl group found in BChl *e*; however, the complete reaction mechanism remains unclear. The *bciD* gene is present in all brown-colored GSB with sequenced genomes (and is missing from the genomes of all green-colored GSB that synthesize BChl *c* or *d*). The *bciD* gene occurs in a cluster with other potential genes that may encode proteins with a role in BChl *e* biosynthesis: BchF3, a homolog of BchF (3-vinyl (bacterio)-chlorophyllide hydratase) and a putative dehydrogenase/oxidoreductase (SDR) (Maresca 2007). It has recently been suggested that a *bchQ* paralog, also present in all brown-colored GSB, could play a role in the synthesis of BChl *e* methylation homologs by adding methyl groups to the BChlide *e* at C-8^2 (Gomez Maqueo Chew et al. 2007, Thweatt and Bryant, unpublished results). Interestingly, the gene cluster also contains *cruB*, the γ-carotene cyclase that produces β–carotene, the precursor of isorenieratene, which is produced by almost all brown-colored GSB (Maresca 2007, Harada et al. 2013). Therefore, the concatenated protein sequences of these genes were used to

construct a maximum likelihood tree to assess the phylogenetic relationships of the Bchl *e* cluster inserted in strain *Chl. luteolum* CIII with the other sequenced brown-colored GSB species (*Chl. phaeobacteroides* DSM 266, *Chl. clathratiforme* DSM 5477, *Ptc. phaeum* CIB 2401, *Cba. limnaeum* DSM 1677 and *Ptc. phaeobacteroides* BS1). PartitionFinderProtein v1.0.1 (Lanfear et al. 2012) was used to determine the best substitution model for each partition, and RAxML v7.3.0 (Stamatakis 2006) was used to generate the maximum likelihood tree. We used as outgroup a combination of distantly related sequences for each of four concatenated proteins: SDR (short-chain dehydrogenase/reductase enzyme; AGA91907 from *Thioflavicoccus mobilis* 8321), CruB (ACF12554 from *Chloroherpeton thalassium* ATCC 35110), RSAM (radical *S*-adenosylmethionine protein; ACF01393 from *Rhodopseudomonas palustris* TIE-1) and BchF3 (ABB27675 from *Chlorobium chlorochromatii* CaD3). A visual syntenic analysis of the region containing the BChl *e* cluster in all sequenced genomes was performed using the R package genoPlotR (Guy et al. 2010).

FeoB, metallophospherase and vrl locus analyses

Both FeoB and metallophosphoesterase protein trees were generated as follows. Reference sequences were collected from the non-redundant NCBI database using BlastP and aligned using MUSCLE (Edgar 2004). Aligned sequences were cleaned with Gblocks (Castresana 2000), and a maximum likelihood tree for each protein alignment was generated using RAxML v7.3.0 (Stamatakis 2006). SyntTax (Oberto 2013) was used to explore the genomic context of FeoB in other *Chlorobium* spp. genomes and *vrl* locus in other genomes.

Results

Genome identification and 16S phylogenetic analyses

A hierarchical clustering analysis of the resulting all *vs*. all ANI values of *Chlorobi* genomes showed that the closest genome to Banyoles assembly was *Chl. luteolum* DSM 273^{T} with an ANI value of 91.7% (Fig. 5.1 and Supplementary Fig. A.C5.2). This was confirmed by a global syntenic visualization with the closest GSB sequenced genomes (Supplementary Fig. A.C5.3). The two genomic analyses indicated that *Chl. luteolum* CIII was closer to *Chl. luteolum* DSM 273^{T}, which together with *Chl. phaeovibrioides* DSM 265 formed a separate phylogenetic clade within the *Chlorobium* species.

The phylogenetic tree of the 16S rRNA sequences (Fig. 5.2) confirmed that the closest cultured relative was *Chl. luteolum* DSM 273^{T} (99.71% identity). We observed that the 16S rRNA sequence

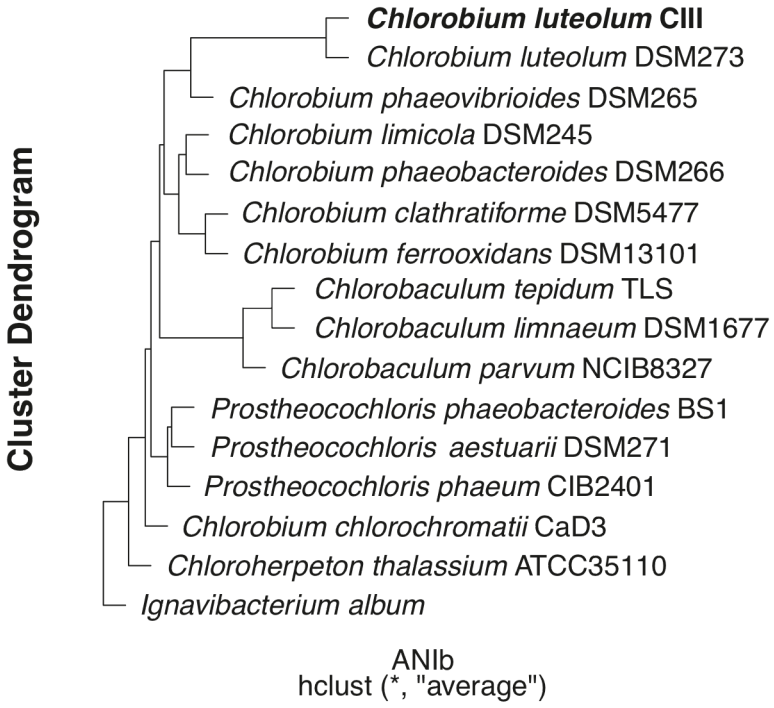

Figure 5.1: Hierarchical clustering analysis carried out on the ANI similarity matrix obtained from *Chlorobi* genomes with JSpecies software.

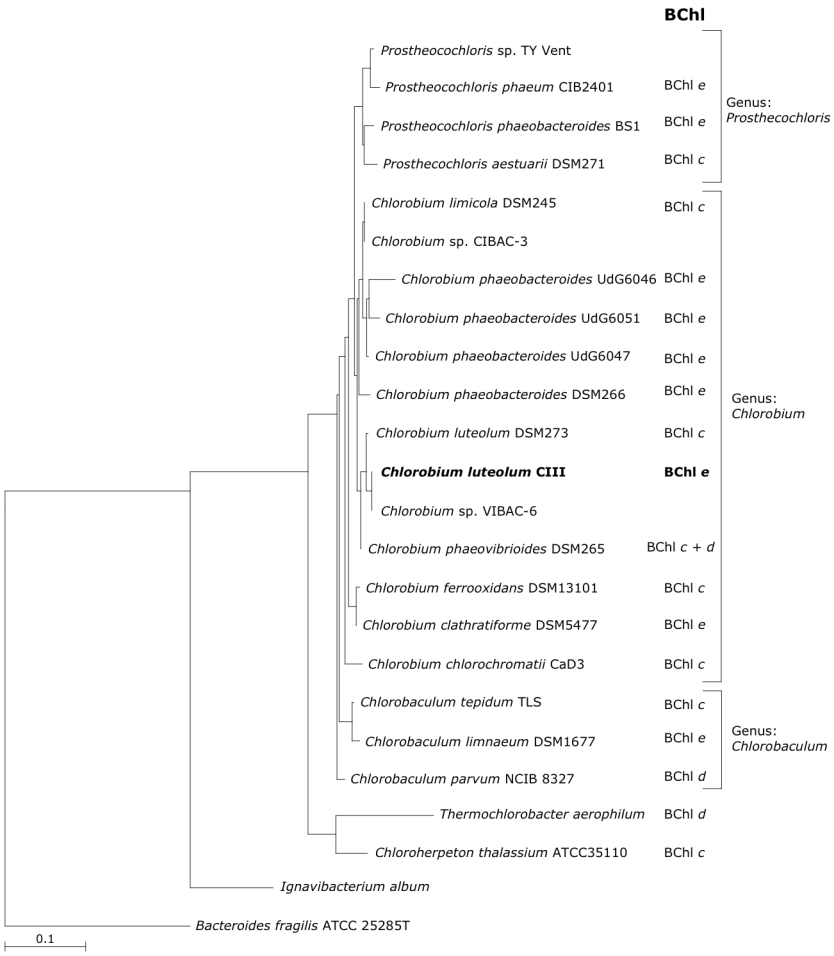

Figure 5.2: 16S rRNA RAxML phylogeny of *Chl. luteolum* CIII genome assembly with related species from the phylum *Chlorobi* and sequences from previous studies in Banyoles karstic area (UdG6046, UdG6047, UdG6051, VIBAC-6 and CIBAC-3). *Bacteroidetes fragilis* was used as the outgroup.

collected in 2010 was identical to VIBAC-6, which was collected from Lake Vilar in 1996 (Casamayor et al. 2000), a neighboring lake connected to Lake Banyoles. The tree topology slightly differed from other GSB trees (Imhoff 2003, Liu et al. 2012) because we used an alignment of 472 nucleotides in order to include the partial sequences CIBAC-3 and VIBAC-6 (Casamayor et al. 2000).

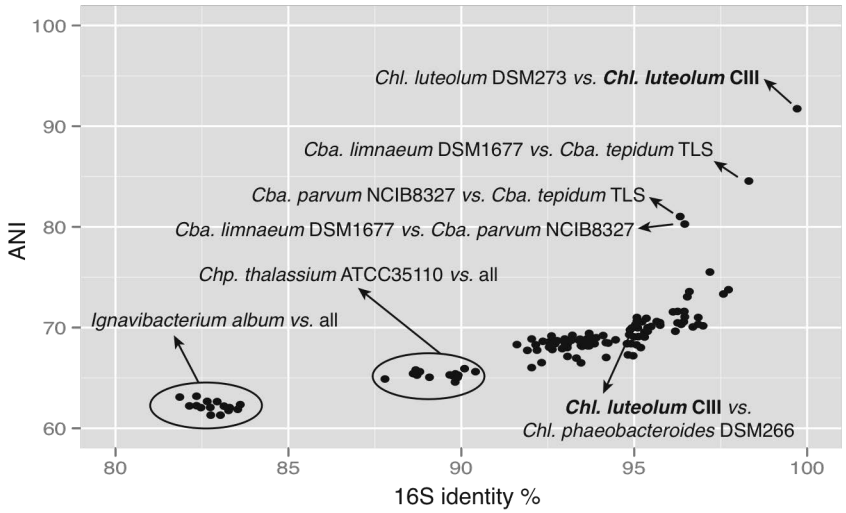

Figure 5.3: Plotted values of ANI versus 16S identity for *Chlorobi* genomes.

We plotted the 16S rRNA identity values *vs*. the ANI values for all genomes in order to establish the relationships among the 16S identities and whole genome similarities within the *Chlorobi* group (Fig. 5.3). Two genomes were distantly related in both terms: *Ignavibacterium album* and *Chloroherpeton thalassium* ATCC 35110. Most genomes fell within 66.0-73.7% ANI and 91.9-97.7% 16S identity. The three species of *Chlorobaculum* (i.e., *Cba. limnaeum* DSM 1677, *Cba. tepidum* TLS and *Cba. parvum* NCIB 8327) clustered together in the 16S rRNA phylogenetic tree (Fig. 5.2) and showed a ratio ANI:16S closer to 1:1 than other GSB but *Chl. luteolum* DSM 273^{T} *vs*. *Chl. luteolum* CIII (Fig. 5.3).

Key genetic events for the ecological success of strain CIII

Some clusters of genes were found to be missing from CIII as compared to DSM 273^{T} (Supplementary Table A.C5.1). For example, *Chl. luteolum* DSM 273^{T} has a gas vesicle gene cluster encoding eighteen proteins (YP374609 to YP374627), most of which have best hits to *Chl. clathratiforme* DSM 5477. More relevant was the

absence of an ATP synthase operon, which included the eight required genes (*atpA* (F_1), *atpD* (F_1), *atpG* (F_1), *atpH* (F_1), *atpC* (F_1), *atpE* (F_0), *atpB* (F_0) and *atpF* (F_0)) for the synthesis of the ATP synthase complex. We checked for the presence of additional ATP synthase genes, as they are essential for cell viability, and found them interspersed across the genome (both in DSM 273^T and CIII). Apparently the operon found in *Chl. luteolum* DSM 273^T and missing in CIII strain had homology with the Na^+-dependent F_1F_0-ATP synthase found in the halotolerant cyanobacterium *Aphanothece halophytica* (Soontharapirakkul et al. 2011), indicating that it could be related to salt tolerance, which should not be required in the freshwater Lake Banyoles.

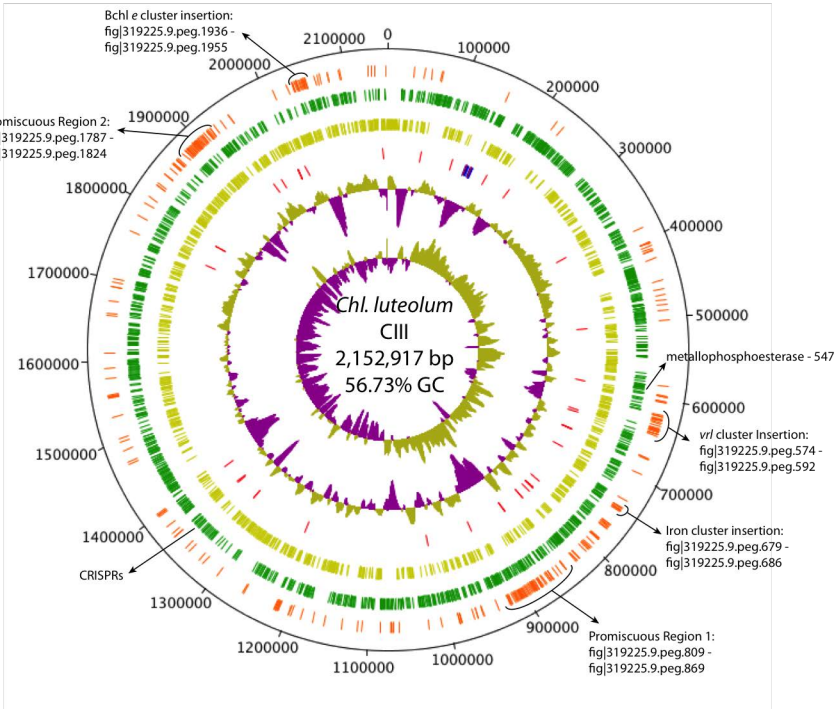

Figure 5.4: Circular map of *Chl. luteolum* CIII genome using DNAplotter. The first two circles starting from the center are GC-skew and G+C content. Baseline on the G+C plot represents de average value of 56.7%. The other four circles starting from G+C content are tRNA and rRNA (red and blue respectively), all reverse strand ORFs (light green), all forward strand ORFs (green) and all the ORFs more closely related to genes in organisms other than *Chl. luteolum* DSM 273^T (orange). Special features are indicated.

In contrast, 286 genes in the *Chl. luteolum* CIII genome were more closely related to genes in organisms other than *Chl. luteolum* DSM 273^T and thus might have been acquired by HGT (Fig. 5.4; Supplementary Table A.C5.2). Among them eight open reading frames (from 679 to 686) were detected in contig-51 with the same structure and best protein similarity scores (95-99%) to *Chl. phaeovibrioides* DSM 265 (Supplementary Table A.C5.2). The products of these genes were identified as two copies of FeoA, FeoB, flavodoxin, a ferritin-DPS family member, and three hypothetical proteins. A phylogenetic tree of the FeoB proteins showed that two different variants of FeoB are encoded in *Chlorobium* spp. genomes (Supplementary Fig. A.C5.4). The first form of the FeoB is predicted to be a protein of 712 aa, and it is present in most *Chlorobium* spp. genomes including *Chl. luteolum* DSM 273^T and *Chl. luteolum* CIII. The second form of FeoB is a protein of 790 aa with homologs only found in some GSB, including *Cba. tepidum* TLS, *Cba. parvum* NCIB 8327, *Chl. limicola* DSM 245, *Ptc. phaeobacteroides* BS1, *Chl. phaeobacteroides* DSM 266 and *Chl. phaeovibrioides* DSM 265 (Supplementary Fig. A.C5.5).

The region including ORFs 1936 to 1955 (Supplementary Table A.C5.2) showed greatest similarity (80-99%) with *Chl. phaeobacteroides* DSM 266 and *Chl. clathratiforme* DSM 5477 proteins. A closer inspection of this region allowed us to link it with BChl *e* and isorenieratene biosynthesis, which are mostly obligately linked processes (Maresca 2007). The region with the BChl *e* genes was initially split into two contigs: ORFs 1936 to 1944 at the end of contig31 and ORFs 1945 to 1955 in the beginning of contig41 (Supplementary Fig. A.C5.6). Due to the importance of this region in explaining the ecological role and the gain of the ability to synthesize BChl *e*, we decided to close this gap using PCR and DNA sequencing with the original high molecular weight DNA used for sequencing. The result was a 1312 nucleotide linking sequence, which contained a transposase of the IS4 family, with best hit with *Chl. phaeobacteroides* DSM 266 (YP_912276). The presence of this IS4 element, which occurs multiple times in the *Chl. luteolum* CIII,

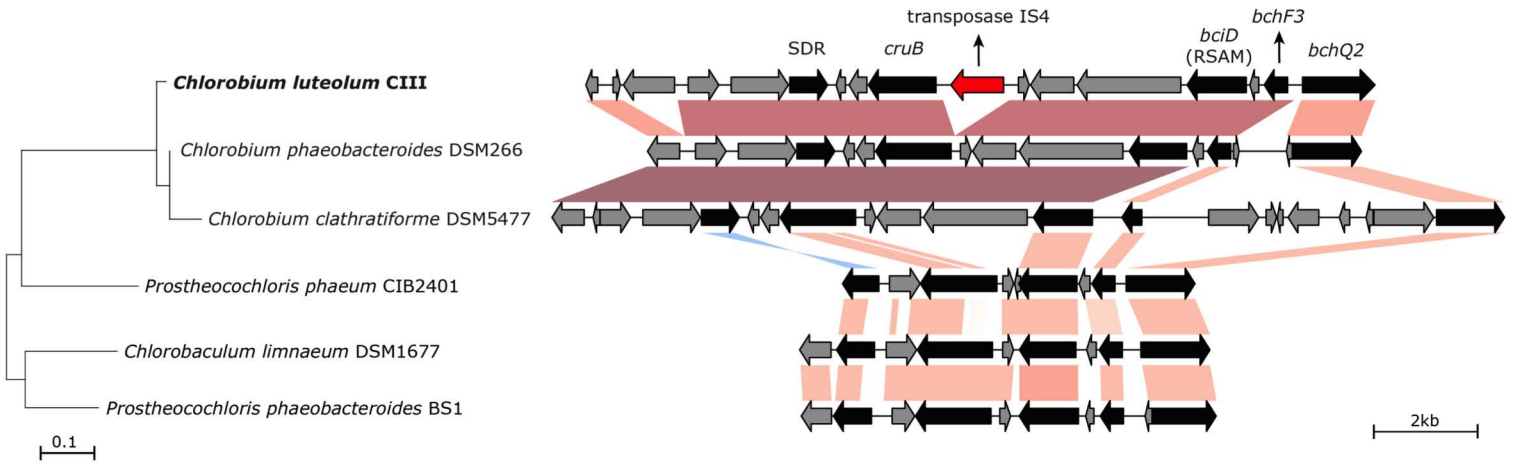

Figure 5.5: Maximum likelihood phylogeny with RAxML of five concatenated proteins (SDR, CruB, BciD (RSAM), BchF3 and BchQ2) found in all BChl e synthesizing genomes. A combination of distantly related sequences for each of the four concatenated genes were used as the outgroup. The genome synteny of the region is shown next to the phylogenetic tree. The bit score of the BLAST alignment is represented with shades of red (same orientation) and blue (inverse orientation).

explained why this gene cluster was initially split between two contigs.

The phylogenetic tree of the putative proteins involved in BChl *e* biosynthesis showed a high similarity between *Chl. clathratiforme* DSM 5477, *Chl. phaeobacteroides* DSM 266 and *Chl. luteolum* CIII (Fig. 5.5), respectively. A synteny analysis of the region showed that gene positions were always conserved (Fig. 5.5) with the exception of an inversion in the SDR gene, a putative dehydrogenase/ oxidoreductase. It also showed that *Chl. clathratiforme* DSM 5477, *Chl. phaeobacteroides* DSM 266 and *Chl. luteolum* CIII had additional genes in this cluster that apparently were not related to BChl *e* biosynthesis, possibly explaining a different phylogenetic history and also showing the genomic flexibility of this region. A detailed analysis of the transition in mol% GC across this cluster with *Chl. phaeobacteroides* DSM 266 (Supplementary Fig. A.C5.7), showed the same GC pattern in the incorporated region in contrast with the "outside" regions, which had the GC average of its respective genomes: 57% for *Chl. luteolum* CIII and 48% for *Chl. phaeobacteroides* DSM 266, suggesting HGT as the most probable mechanism for its incorporation in the genome.

Phage-related HGT

We detected the insertion of a cluster of six genes (ORFs 574 to 592 on contigs 44 and 20) not found in the genome of *Chl. luteolum* DSM 273^{T}, that had homologs with the virulence-related locus (*vrl* locus) of *Dichelobacter nodosus* (Haring et al. 1995). Specifically, we found *vrlJKLOPQ* in *Chl. luteolum* CIII, a cluster that has been found in highly dissimilar organisms, including *Acidothermus cellulolyticus*, *Thermoanaerobacter ethanolicus*, *Nitrosococcus mobilis* and *N. oceani* (Knaust et al. 2007). A synteny analysis of the region added *Desulfovibrio aespoeensis* Aspo2 and *Methanosalsum zhilinae* DSM 4017 to this list (Supplementary Fig. A.C5.8). The presence of phage-related proteins at the end of the region (Supplementary Fig. A.C5.8: ORFs 590 and 591), suggests the possible horizontal transfer of the cluster containing the *vrl* proteins.

A couple of genomic regions were characterized by multiple recombination events according to the comparison of *Chl. luteolum* CIII with *Chl. luteolum* DSM 273^T (Supplementary Fig. A.C5.9), and thus we named them "promiscuous regions." Most of the genes in these regions were found in different contigs and were classified as encoding hypothetical proteins. Not surprisingly, many of the genes found in these "promiscuous regions" were related to mobile elements (integrases, recombinases, transposases, among others), but some of them were also annotated as phage-related proteins. In addition to the phage-related proteins found in the genome, another genomic indicator of past phage infection was identified within the assembled *Chl. luteolum* CIII sequences; CRISPRs (Clustered Regularly Interspaced Short Palindromic Repeats), which are region(s) of a genome that contain multiple, short repeats with interspersed spacer DNA, acquired from past viral encounters (Westra et al. 2014). One CRISPR locus was identified that contains a direct repeat sequence of 32 bp and 12 spacer regions (Supplementary Fig. A.C5.10 and Supplementary Table A.C5.3). Although no spacer sequences were identified within the larger data, it suggests this bacterium uses a CRISPR/Cas-like mechanism to evade phage infection.

The "promiscuous regions", together with CRISPRs and the *vrl* locus, provided evidence for the ongoing association and genomic exchange between *Chl. luteolum* CIII and phages. Another interesting observation was that 36.9% of the non-hypothetical proteins with non-reciprocal BLAST hits to strain *Chl. luteolum* DSM 273^T (the theoretically acquired proteins) were related to mobile elements or phages (Fig. 5.6). This illustrates the plasticity of these genomes and the substantial gene flow that appears to be occurring, mostly between closely related genomes but also between phylogenetically distant organisms (e.g., the *vrl* locus). The taxonomic assignment of the proteins gained by *Chl. luteolum* CIII (Fig. 5.7) showed that 39% of these proteins had best hits with other GSB, but a striking 33% were most closely related to a large variety of species, with *Proteobacteria* being the taxon with the highest hits.

Putative GSB phage

To date phages infecting GSB have not been reported (Frigaard and Bryant 2008). However, the presence in the genome of both a large number of phage-related proteins and CRISPR repeats are strong arguments supporting the existence of such viruses. In the assembly analysis carried out in the present study, we found a set of large contigs (>3 kbp) with a very high read depth (Supplementary Fig. A.C5.2). We re-assembled these contigs following the same procedure used for *Chl. luteolum* CIII, and obtained 5 contigs (Supplementary Table A.C5.4) that were identified as putative bacteriophage (see below). Due to the procedures for isolation, i.e., plankton size fraction analyzed between 0.8 and 3 µm, these putative phages were likely to be infecting the GSB at the time of sampling, either through a lysogenic or lytic infection process. Putative phage contigs 2 and 4 could not be classified to any known bacteriophage and only encoded three phage-related genes. Based on homology of multiple ORFs to an N4-like phage, contig 1 was probably derived from a Podovirus. Finally, according to the GC content, read depth (Supplementary Table A.C5.4), and predicted host-acquired auxiliary metabolic genes (AMG), contigs 3 and 5 (Supplementary Table A.C5.5) are predicted to be derived from a putative lytic *Myoviridae* phage. The read depth of contigs 3 and 5 is ~6-fold higher (i.e.,

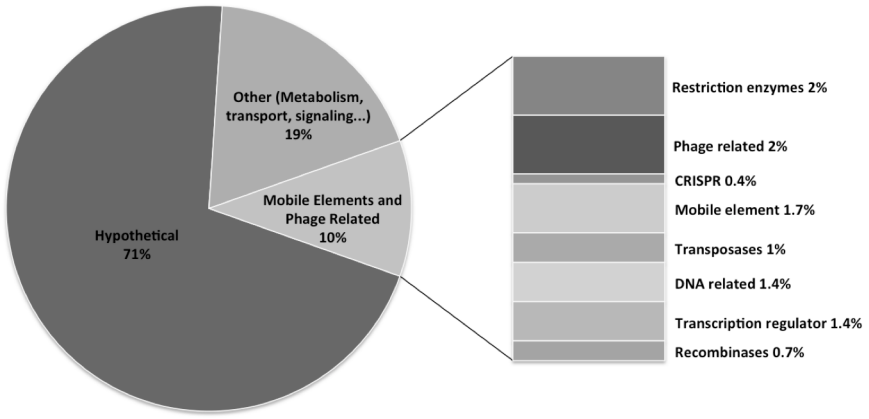

Figure 5.6: Plot with the percentage of non-reciprocal CIII ORFs with strain DSM 273^{T} assigned to different functional categories.

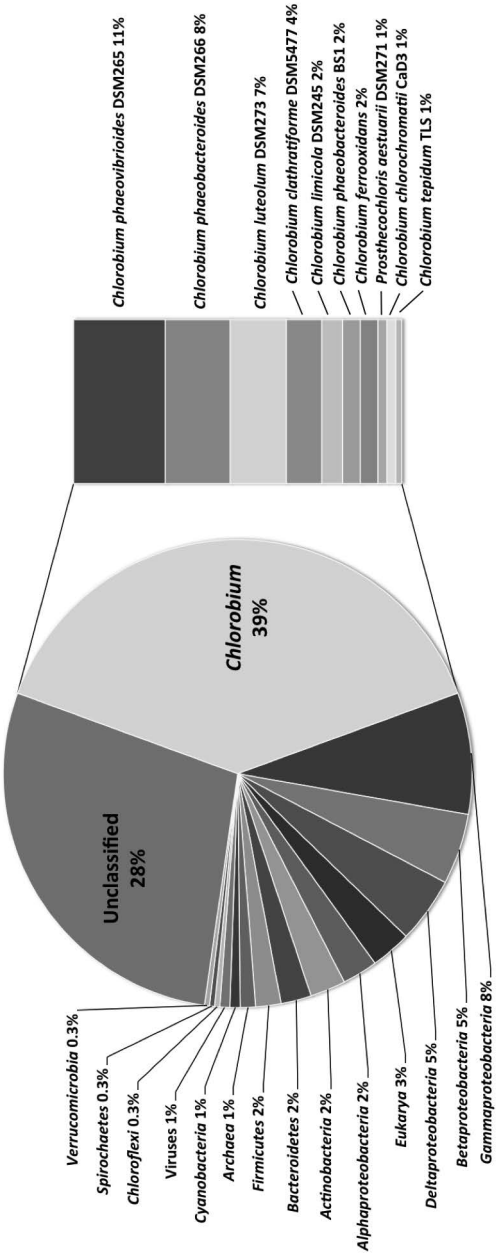

Figure 5.7: Plot with the taxonomic assignment of non-reciprocal CIII ORFs with strain DSM 273^{T}.

174×) than the average for *Chl. luteolum* CIII, which strongly suggests that this virus was involved in an active, lytic infection process. A phylogenetic reconstruction of the phage-conserved DNA polymerase provided further evidence that the predicted sequences form a distinctive lineage related to DNA polymerases found in other bacteriophage (Supplementary Fig. A.C5.11). The largest contig was 106 kb (contig 5), and its predicted proteins indicated a mixed homology to known bacteriophage (Supplementary Fig. A.C5.12); this is not unexpected because no phage has yet been described for GSB (Frigaard and Bryant 2008).

BlastN analysis of *Chl. luteolum* CIII *versus* the putative phage returned a high-identity region of 51 nucleotides next to the *vrl* locus in *Chl. luteolum* CIII that matched two separate parts of the putative phage (Fig. 5.8). One was 20 nt long with 100% identity, and the other was 33 nt long but contained two mismatches. The two regions were separated by 2169 nt, in which the coding sequence for a hypothetical protein from *Sinorhizobium* phage PBC5 (Contig5_11) was found (Fig. 5.8 and Supplementary Table A.C5.5). Interestingly, next to this similarity region, and as part of the *vrl* locus insertion, we found a bacteriophage P4 integrase (ORF 591) and a phage transcriptional regulator *alpA* (ORF 590). About 50 kb from this region, a putative AMG within a region of conserved phage genes was predicted to be a metallophosphoesterase, a Ser/Thr protein phosphatase (Supplementary Table A.C5.5; Contig5_33), with strong sequence homology with ORF 547 from *Chl. luteolum* CIII genome (Fig. 5.8). A phylogenetic tree of metallophosphoesterase sequences was constructed, and showed that the protein encoded on Contig5_33 was clearly derived from GSB, and also had close sequence homology with other phage metallophosphoesterases (Fig. 5.9). Together these data provide consistent evidence for phage/host interactions in GSB.

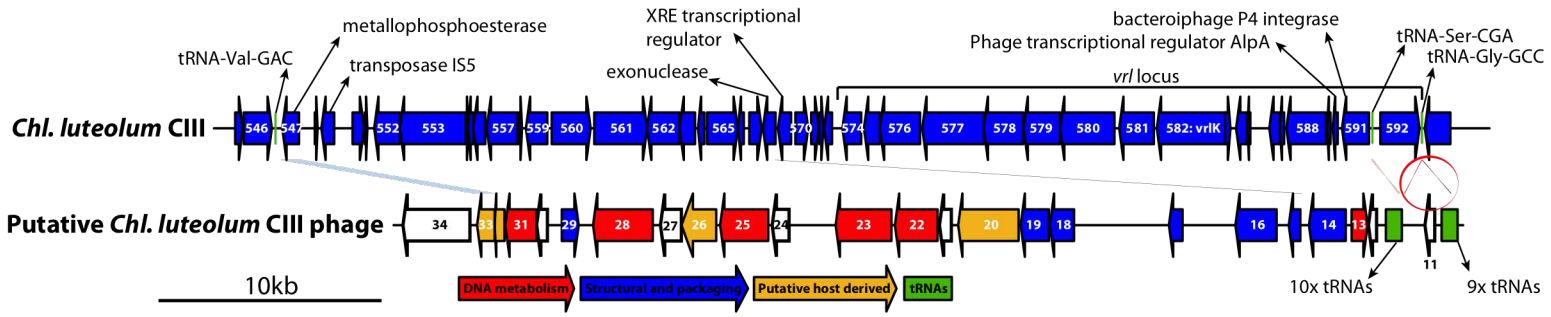

Figure 5.8: Syntenic analysis showing the relationship of the putative GSB phage with the *Chl. luteolum* CIII genome sequence. A blue shade indicates the homology region of the metallophosphoesterase gene. A red circle indicates the region with the 51 nucleotides identity region. The types of genes identified in the putative *Chl. luteolum* CIII phage are indicated in colors: DNA metabolism (red), structural and packaging (blue), putative host derived (yellow) and tRNAs (green). Special features on both sequences are indicated and described with arrows.

Discussion

HGT has been widely assumed to be a major mechanism for bacterial innovation in order to allow an organism to colonize new ecological niches or improve its performance in its current niche (Wiedenbeck and Cohan 2011). Many HGT studies on this subject are focused on the exchange of virulence-associated genes in human and animal pathogens (Franken et al. 2001, Saunders et al. 2005, Kienesberger et al. 2014), or antibiotic resistance genes that affect the multi-resistance problem (Summers 2006, Aminov 2010). A genome comparison with a closely related cultured counterpart helped us to determine the genes associated with the ecological

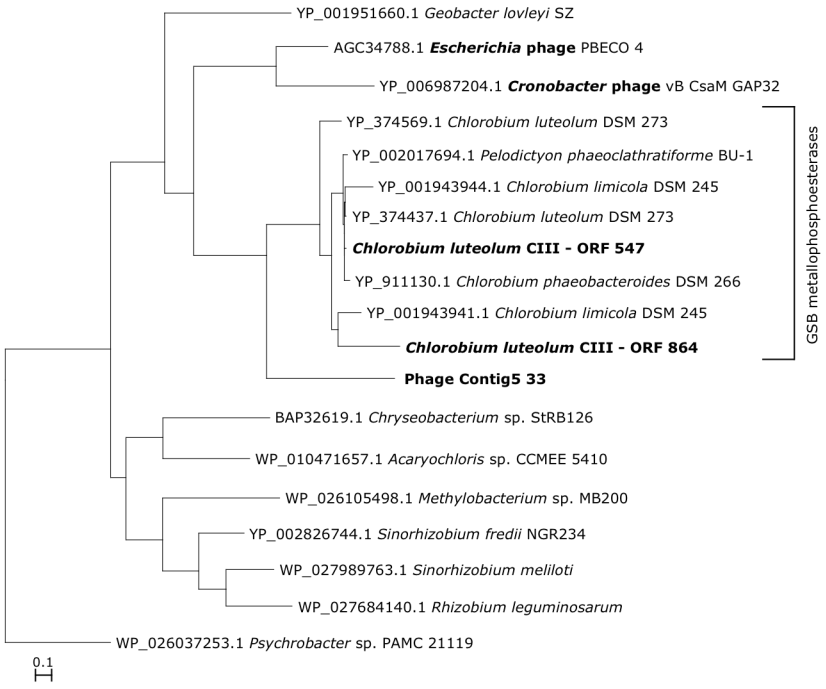

Figure 5.9: Maximum likelihood phylogeny with RAxML of metallophosphoesterase proteins. In bold the homologous metallophosphoesterases found in *Chl. luteolum* CIII and the putative associated phage shown in Fig. 5.8. A metallophosphoesterase from *Psychrobacter* sp. PAMC 21119 was used as the outgroup.

success of the strain blooming in Lake Banyoles basin CIII. The ecology and physiology of phototrophic sulfur bacteria in stratified lakes under euxinic conditions has been widely studied not only from an ecological point of view (Montesinos et al. 1983, Van Gemerden and Mas 1995, Borrego et al. 1999) but also from a genomic perspective (Tonolla et al. 2005, Frigaard and Bryant 2008, Habicht et al. 2011, Bryant et al. 2012). These previous findings provide this study with a consistent background to explore the role of HGT in the ecological success of a natural population, and possibly to understand the complex interplay between recombination and ecology in the environment (Polz et al. 2013). The genome reconstruction of a dominant GSB population, *Chl. luteolum* CIII, that has a closely related, cultivated counterpart with a fully sequenced genome, *Chl. luteolum* DSM 273^{T}, provided a unique opportunity to explore some of the genes that convey advantages to the natural population.

The Average Nucleotide Identity (ANI) between two genomes is used as a standard for the prokaryotic species definition (Richter and Rossello-Mora 2009), and an ANI above ~95-96% is considered to indicate that the compared strains belong to the same species. Interestingly, the two *Chl. luteolum* strains compared here exhibited 99.7% identity in 16S rRNA sequence and only 91.7% ANI. This could simply reflect time, indicating that the differences found between strains DSM 273^{T} and CIII are very recent and that the high degree of genetic exchange between these two *Chlorobi* populations is not yet reflected by their 16S rRNA sequences, but significantly captured through a whole-genome evaluation like ANI. This supports the idea that lateral exchange of genetic material within GSB occurs at a very high rate, as seen on a general study about HGT, in which *Cba. tepidum* TLS was the bacterium with the highest proportion of horizontally transferred genes in its genome (Nakamura et al. 2004), and that GSB are good candidates for HGT-guided evolution studies.

GSB are strict photoautotrophs that strongly depend on light availability and light harvesting for growth. In order to exploit the light wavelengths that reach the anoxic deep water layers where GSB

reside, these organisms synthesize specific carotenoids and specialized light-harvesting antenna organelles, chlorosomes, which are the most efficient light-harvesting structures known (Frigaard and Bryant 2006, Orf and Blankenship 2013). The type of BChl preferentially found in the chlorosome is one of the key factors that explain the ecological success of a strain within the water column (Montesinos et al. 1983, Van Gemerden and Mas 1995, Bryant et al. 2012).

Brown-pigmented blooms of GSB had already been detected in Lake Banyoles basin CIII in 1978 (Montesinos et al. 1983) and a sample taken in 1996 in the Banyoles area (VIBAC-6, Casamayor et al. 2000) possibly comes from the same population as that assembled in this study. On the other hand, strains UdG6047, UdG6046 and UdG6051 isolated from Banyoles (Figueras et al. 1997), were classified as *Chlorobium phaeobacteroides* because they were brown and contained BChl *e* and isorenieratene. Altogether, these findings show that pigments such as BChl *e* are not reliable phylogenetic markers, thus they should not be used for phylogenetic classification because they are not monophyletic traits (Maresca 2007). This can easily be shown to be the case, as a frameshift mutation in the *bchU* gene causes the mutant to produce BChl *d* instead of BChl *c* (Maresca et al. 2004) while a mutation in *bciD* causes cells to produce BChl *c* instead of BChl *e* (Harada et al. 2013). The presence of a transposase IS4 in the cluster of genes thought to mediate the synthesis of BChl *e* may partly explain the mobility of this region and may additionally be related to recent biological transformations, not only within a genome but also in horizontal transfer mechanisms (Ochman et al. 2000, De Palmenaer et al. 2008), which is the most reasonable explanation for the pigment-phylogeny incongruences.

The BChl *e* cluster acquired by *Chl. luteolum* CIII confers some advantages that are crucial from an ecological point of view. Firstly, the absorption peak of the BChl shifts from 746 nm in BChl *c* to 714 nm in BChl *e* (Harada et al. 2013) allowing it to cover a different range of wavelengths. However, more importantly, there is a

large increase in absorption in the blue near 520 nm, which overlaps strongly with those light wavelengths that penetrate most deeply in the water column. Furthermore, the BChl *e* cluster includes the *cruB* gene, which is responsible for the biosynthesis of b-carotene and thus enables the production of isorenieratene and b-isorenieratene, which are almost universally associated with organisms that synthesize BChl *e* (Maresca et al. 2008a). These carotenoids are important elements to broaden and increase the absorption of brown-colored species between 480 and 550 nm (Imhoff 1995) and expand the photo-adaptation range (Hirabayashi et al. 2004). These differences are of great significance in terms of competition in an ecological niche where light is one of the limiting factors (Van Gemerden and Mas 1995, Stomp et al. 2007).

Iron is an essential micronutrient for many life processes including photosynthesis, respiration and nitrogen fixation (Martin et al. 1994, Boyd et al. 2000, Dupont et al. 2006). GSB have numerous proteins with Fe/S clusters in the reaction centers, including high intracellular levels of ferredoxins and rubredoxins (Bryant et al. 2012), and are therefore highly dependent upon iron for growth. Among them, FeoAB proteins are used for the uptake of Fe^{2+} (Kammler et al. 1993), flavodoxin as a low-potential electron donor that replaces ferredoxin and is induced by iron limitation (LaRoche et al. 1996, Chauhan et al. 2011), and ferritin-DPS as an iron storage protein (Andrews et al. 2003). FeoAB catalyze the uptake of reduced ferrous iron, which predominates under low-oxygen conditions (Bhaya et al. 2007), and the genes for FeoAB have also been found in closely related populations of the same species (Bhaya et al. 2007, Klatt et al. 2011). Soluble Fe^{2+} is abundant in basin CIII (Garcia-Gil 1990), but the reaction with hydrogen sulfide reduces its biological availability and thus, the incorporation of an iron transport cluster for ferrous iron by lateral transfer might confer both a higher affinity to *Chl. luteolum* CIII strain, and higher iron storage capacity. In addition, the presence of a flavodoxin in the cluster might be helpful under iron limitation because flavodoxin replaces ferredoxin in many reactions, thus saving iron for reaction centers and cytochromes and

giving this strain a clear advantage in the competition with other microorganisms sharing the same environment.

There are many ways to explain all these genomic differences, and one of them is transduction, the process by which horizontal transfer of genetic material is accomplished through phage infection. Viruses have two main roles in microbial ecology. Firstly, they are the main "predators" for bacterial populations in environments where only a few grazers are present and low bacterial diversity is found, like the anoxic hypolimnion of stratified karst lakes (Pedros-Alio et al. 2000, Bettarel et al. 2004). In these conditions only phages or nutrient limitation are capable of controlling the blooming populations (Maranger et al. 1994, Deng and Hayes 2008, Riemann and Grossart 2008) that are typical for GSB or PSB in stratified lakes (Overmann 1997, Gregersen et al. 2009). Secondly, they can manipulate the environment by influencing the history and evolution of their hosts through transduction (Rohwer and Thurber 2009). At the present time, no phage capable of infecting a GSB has ever been isolated (Frigaard and Bryant 2008), but we describe here a phage sequence that could explain both HGT events and control of the dominant *Chl. luteolum* CIII strain. The presence of CRISPRs and the high proportion of mobile elements and phage-related proteins in the *Chl. luteolum* CIII genome provides strong evidence for previous phage infection, and a close relationship between GSB and phages. In this study, we observed the presence of phage-related contigs with very high read-depth, which directly points to the possibility of an ongoing lytic infection of the dominant *Chl. luteolum* CIII population.

Additional indirect evidences for a GSB–phage relationship are also provided for in our analyses. Metallophosphoesterases represent a functionally diverse superfamily of enzymes with two metal ions bound at the conserved active site (Lohse et al. 1995). Within metallophosphoesteraes, Ser/Thr protein phosphatases are important components of various regulatory mechanisms for metabolic processes through signal transduction by protein phosphorylation (Villafranca et al. 1996). This mechanism has recently been reported to be present and functional in prokaryotes

(Macek et al. 2008). Ser/Thr phosphatases have previously been identified in phages such as PBECO4 (Kim et al. 2013) or bacteriophage λ, suggesting they may mediate the dephosphorylation of certain proteins to allow more effective production of phage or regulate viral transcription (Cohen and Cohen 1989). Thus, the presence of a metallophosphoesterase in the phage sequence assembly, which has close phylogenetic identity to a gene associated with the putative host GSB, is robust evidence connecting this phage with *Chl. luteolum* CIII.

Further evidence linking our phage and GSB genomes is the similarity found in the region next to the insertion of the *vrl* locus, which has previously been related to virulence factors (Billington et al. 1999). However, a recent study (Knaust et al. 2007) demonstrated the expression of the *vrl* locus in *Desulfococcus multivorans* and a high degree of conservation of various *vrl* orthologs found in other sequenced genomes, suggesting that these genes could serve a yet-unknown function distinct from pathogenicity. Interestingly, proteins encoded by the *vrl* locus have best BlastP hits with distantly related organisms, suggesting that transfer of these genes might occur through a nonspecific bacterial virus (Chiura 1997, Fuhrman 1999), an idea that is consistent with observations in *D. nodosus*, for which it has also been speculated that virus-mediated gene transfer has occurred (Cheetham et al. 1995, Haring et al. 1995, Billington et al. 1999, Knaust et al. 2007). Finally, the phylogenetic reconstruction of the phage-conserved DNA polymerase showed an association with a distinct lineage of *Myoviridae*. Considering that no phage has yet been described for any GSB, it is not surprising that it would be difficult to associate this polymerase precisely with a specific virus.

Additional mechanisms that can drive HGT cannot be ruled out from our study. Bacterial lysis releases DNA to the environment and natural transformation is the uptake and incorporation of free DNA by any bacterium capable of acquiring exogenous DNA. GSB belonging to the genus *Chlorobaculum* are well known to be naturally transformable (Ormerod 1988, Frigaard and Bryant 2001, Harada et al. 2013), and thus transformation might be a mechanism that could

explain the incorporation of clusters of genes from closely related organisms sharing the same ecological niche, like the gene clusters for BChl *e* synthesis or iron transport from other GSB. Finally, conjugation is the transfer of genetic material between bacteria through cell-to-cell transfer and has been suggested to be a major mechanism responsible for HGT (Norman et al. 2009, Halary et al. 2010, Wozniak and Waldor 2010). A gene expression system by conjugative plasmid transfer has recently been tested in GSB (Azai et al. 2013); however, it is not likely to be a common natural mechanism in GSB. Among 18 GSB with sequenced genomes, only *Ptc. aestuarii* DSM 271^{T} was found to contain any plasmids, although the one plasmid it contained did harbor genes for the production of a conjugative apparatus (Bryant et al. 2012).

Overall, we were able to reconstruct the genome of an ecologically successful GSB population from an euxinic karstic lake. The availability of a closely related reference genome, *Chl. luteolum* DSM 273^{T}, was crucial for an exhaustive comparative analysis and for the detection of key genetic differences. The ecological implications of acquiring the genes for BChl *e* synthesis and Fe transport are substantial, and they could confer upon *Chl. luteolum* CIII a clear advantage over green-colored GSB in water-column positioning. Brown-colored GSB containing BChl *e* can harvest light efficiently at much greater depths in the water column than green-colored organisms synthesizing BChl *c* or BChl *d* (Maresca et al. 2004). We cannot infer the mechanism by which *Chl. luteolum* CIII lost the putative salt tolerance ATPase cluster but we suspect that these genes would be unnecessary in a freshwater lake ecosystem like Lake Banyoles. Because genomes are not available, we cannot clarify why the *Chlorobium phaeobacteroides* strains previously isolated from Lake Banyoles (Figueras et al. 1997), possibly were not successful populations *in situ*. The influence of phages in the environment is much larger than previously thought (Fuhrman 1999, Sharon et al. 2009a), and we describe here strong initial evidence for a putative phage that infects GSB, that could both control the blooming population and that could act as a HGT vector. It may now

be possible to confirm these ideas through laboratory experiments. The *vrl* locus points to a viral-related cluster with the potential to be transferred between distantly related organisms and deserves more investigation in order to determine its function, which will be necessary to understand its recurrent presence in distantly related genomes. Follow-up studies should be focused to reveal why GSB genomes are so flexible in terms of horizontal gene transfer and intensify the search for and research on GSB phages, to understand how they might be responsible for exerting biological control and genome flexibility on these ancient photoautotrophic microorganisms.

Acknowledgements

This research was funded by grant DARKNESS CGL2012-32747 from the Spanish Office of Science (MINECO) to EOC and by the Global Ocean Sampling Project supported by the Beyster Family Foundation Fund of the San Diego Foundation and the Life Technology Foundation (to JCVI). Work on BChl *e* biosynthesis and the genomics of GSB in the laboratory of D. A. B. was supported by the Division of Chemical Sciences, Geosciences, and Biosciences, Office of Basic Energy Sciences of the U.S. Department of Energy through Grant DE-FG02-94ER20137.

Part II: Oxic system with oligotrophic waters

6

Winter to spring changes in the slush bacterial community composition of a high-mountain lake (Lake Redon, Pyrenees)[1,2]

Abstract

Bacterial community composition was analyzed in the slush layers of snow-covered Lake Redon (2,240 m altitude, Limnological Observatory of the Pyrenees, LOOP, NE Spain) in winter and spring and compared with bacteria from the lake water column, using 16S rRNA gene clone libraries and CARD-FISH counts. The set of biological data was related to changes in bacterial production and to other relevant environmental variables measured *in situ*. In winter, up

[1] Original publication in Appendix B: Llorens-Marès T, JC Auguet, EO Casamayor (2012) Winter to spring changes in the slush bacterial community composition of a high mountain lake (Lake Redon, Pyrenees). *Environ Microbiol Reports* 4(1):50-56. *doi: 10.1111/j.1758-2229.2011.00278.x.*

[2] See supplementary material in Appendix A

to 70% of the 16S rRNA sequences found in the slush were closely related to planktonic bacteria from the water column beneath the ice. Conversely, during spring ablation, 50% of the sequences had >97% identity with bacteria from the cryosphere (i.e., globally distributed glaciers, snow, and ice) and may have originated from remote aerosol deposition. The transition winter to spring was characterized by consistent community changes switching from assemblages dominated by *Betaproteobacteria, Verrucomicrobia* and *Bacteroidetes* during snowpack growth to communities essentially dominated by the *Bacteroidetes* of classes *Cytophagia* and *Sphingobacteria.* This strong bacterial composition switch was associated with consistent increases in bacterial abundance and production, and decreasing bacterial diversity.

Introduction

Ice cover and snowpacks in high-altitude lakes play a pivotal role in the dynamic of the pelagic system by preventing turbulence and reducing the exchange of light, heat, gases, liquid and particles between the atmosphere and the water column (Catalan 1992, Wharton et al. 1993). The ice cover generally lasts 6 months or longer and is characterized by sandwich-like structures constituted by a superposition of snow, white ice and slush (i.e., a mixture of water and snow) layers on top of a sheet of black ice (Eppacher 1966, Adams and Allan 1987). Episodic events of flooding by lake water, melting and freezing drive dynamic changes in the physical structure and chemical characteristics of alpine ice covers (Catalan 1989, Psenner et al. 1999). Microbial activities and biomasses in the slush layers are far larger than in the water column, with a great variety and density of morphologies including short rods and cocci-like bacteria, filaments, flagellate protists (autotrophic and heterotrophic), and ciliates (Felip et al. 1995, Felip et al. 1999b).

While microbial communities from the remote cryospheres such as sea ice (Bowman et al. 1997, Brinkmeyer et al. 2003), polar

lakes (Priscu et al. 1999, Crump et al. 2003, Mosier et al. 2007) and glacier habitats (Zhang et al. 2008, Xiang et al. 2009, Zhang et al. 2009) have been extensively documented, those thriving in nearer non-permanent ice covered alpine lakes have remained poorly studied. Most of such studies have been mainly focused on eukaryotic microorganisms by traditional microscopy methods, as in the case of Lake Redon (Felip et al. 1995, Felip et al. 1999b, Felip et al. 2002), or in Lake Gossenköllessee, Tyrolean Alps, using general bacterial probes and FISH counts (Alfreider et al. 1996). In this work, we described the 16S rRNA gene composition of bacteria inhabiting the slush layers of an alpine lake, both in winter during growing of the snowpack, and in spring during the melting phase. Overall, bacterial composition and functioning in Lake Redon were closely related to other ice-related ecosystems on Earth suggesting that alpine areas are good models to improve the current understanding on the dynamics and functional role of cold adapted microorganisms facing climate variations.

Results and discussion

Samples were collected from different slush layers (see Fig. 6.1) and the lake water column (2 m depth beneath the ice sheet) of Lake Redon (Limnological Observatory of the Pyrenees, LOOP, NE Spain) both in winter during growth of the snowpack (March 20, 2009; 246 cm cover thickness), and in spring during the ablation phase (May 27, 2009; 70 cm cover thickness). One sample from a pool formed at the top of the snowpack in spring was also added to the study. The limnology of the lake and the different planktonic populations have been extensively studied for the last 25 years with traditional (Catalan et al. 2006), and recently with DNA-based (Hervas and Casamayor 2009) approaches. Water from the slush layer was pumped from small holes drilled in the cover (see more details in Felip et al. 1995). Bacterial community composition was analyzed by 16S rRNA gene clone libraries (Hervas and Casamayor 2009) and

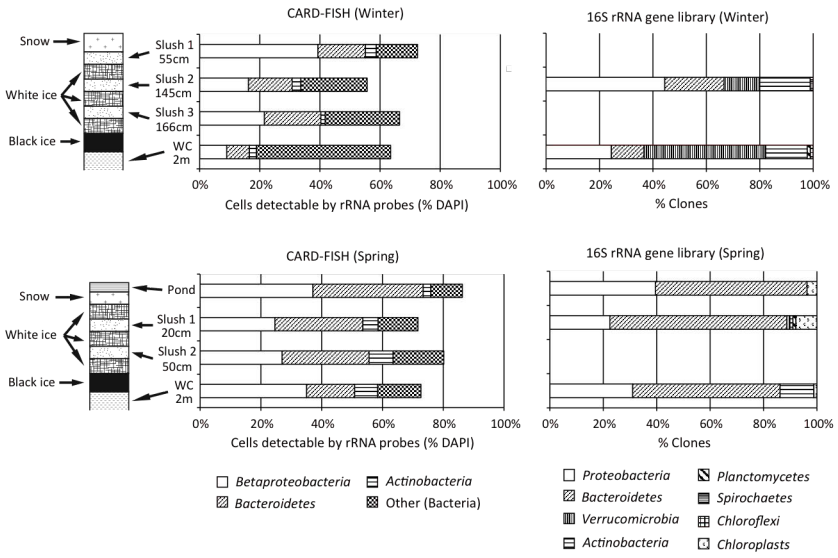

Figure 6.1: Bacterial community structure in Lake Redon after CARD-FISH counts and 16S rRNA gene clone libraries. Populations are represented by relative abundances of clones in different phylogenetic groups. The ice-cover during winter (March) was 246 cm thick and composed by three slush layers at 55cm, 145cm and 166cm from the surface, respectively. In spring (May) melting ponds were present on the ice-cover, which was only 70 cm thick and showed two slush layers at 20 cm and 50 cm from the surface. Water Column (WC) samples were collected 2 m depth from the black ice.

CARD-FISH counts (Medina-Sanchez et al. 2005). DNA extraction and cloning conditions were as previously reported (Dumestre et al. 2002, Ferrera et al. 2004) Overall, 437 sequences were analyzed (see accession numbers FR696618 to FR697054 in GenBank and Table 6.1 for more details), and environmental information for each sample made publicly available (accession numbers ERS016138-ERS016142 in GenBank). Bacterial activity was estimated by [3H]leucine incorporation according to the method described by Kirchman (1993) with slight modifications (Felip et al. 1995).

The highest concentrations of NO_3 and NH_4 were found in the top slush layer in winter, and in the water column in spring (Table 6.1). NO_2 concentrations were similar in the water columns (WC), but increased significantly in the slush layers in spring. Interestingly, the highest concentrations were found in the pond sample (1.04 µeq L^{-1}).

Table 6.1: Concentration of nitrogen compounds, total dissolved phosphorous (TDP), dissolved organic carbon (DOC), bacterial abundance (DAPI counts) and production (BP) in the set of samples analyzed, and diversity indicators obtained from clone libraries in slush (SL), water column (WC), and an ice-melting pond in Lake Redon. OTUs and diversity indices were calculated at 3% cut-off. Samples labelled in bold were selected for 16S rRNA gene clone libraries. nd: not determined.

	Layer	NO_3 (µeq L^{-1})	NH_4 (µeq L^{-1})	NO_2 (µeq L^{-1})	TDP (nmol L^{-1})	DOC (mg L^{-1})	DAPI ($\times 10^4$cells mL^{-1})	BP (pmol Leu $L^{-1}h^{-1}$)	Clone numbers	OTU (97%)	Coverage (%)	S_{Chao1}
Winter	SL 1	17	14.2	0.08	90	1.2	14.9	nd	Nd	nd	nd	nd
	SL 2	**7**	**2.4**	**0.05**	**94**	**0.6**	**9.9**	**4.2±0.2**	**90**	**50**	**68**	**81 ± 18**
	SL 3	7	3.4	0.05	68	0.6	16.5	nd	Nd	nd	nd	nd
	WC	**6**	**2.8**	**0.07**	**44**	**0.5**	**42.5**	**1.2±0.2**	**90**	**45**	**61**	**164 ± 93**
Spring	**POND**	**3**	**3.8**	**1.04**	**284**	**1.3**	**178.5**	**223.1±5.2**	**81**	**42**	**63**	**114 ± 53**
	SL 1	**4**	**3.5**	**0.38**	**180**	**0.8**	**86.5**	**276.3±11.0**	**89**	**18**	**88**	**73 ± nd**
	SL 2	4	3.2	0.28	123	0.6	76.1	nd	Nd	nd	nd	nd
	WC	**15**	**9.6**	**0.07**	**60**	**0.7**	**68.8**	**78.0±9.1**	**87**	**38**	**72**	**77 ± 29**

Total dissolved phosphorus (TDP) and dissolved organic carbon (DOC) showed the highest concentrations closer to the surface (Table 6.1) both in winter (top slush layers) and spring (pond). We did not observe temporal changes in DOC concentrations but TDP doubled in the spring, probably due to frequent Saharan dust depositions on this area (Hervas et al. 2009, Reche et al. 2009). All concentrations were within previously reported ranges in this area (Felip et al. 1995, Felip et al. 1999b).

Total DAPI counts and bacterial production values in slush layers were similar to those found by Alfreider et al. (1996) and tended to be higher than in the water column (WC), except for DAPI counts during winter (Table 6.1). Slush layers offer better conditions for bacterial growth than the WC because the ice grains matrix with nutrient-rich interstitial water, provides a better environment for bacterial activity, interaction between cells and substrate, and for the development of filamentous forms as previously discussed (Felip et al. 1995, Felip et al. 1999b). We observed that *Bacteroidetes* were particularly favored being twice as abundant in the slush layers than in the plankton as shown by CARD-FISH counts (Fig. 6.1). *Betaproteobacteria* cells were also found to be more abundant in the slush layers in winter. These results are in agreement with a previous CARD-FISH work carried out in Lake Gossenköllessee (Alfreider et al. 1996). As in this previous work, we also observed a shift towards bacteria that did not hybridize with any of the group-specific probes tested in the transition from the upper slush layer to the WC. Particularly in March, up to 70% of EUB338 positive cells did not hybridize with any of the group specific probes tested, and the sum of the cells hybridized with probes BET42a (for *Betaproteobacteria)*, HGC69a (for *Actinobacteria)* and CF319a (for *Bacteroidetes)* was particularly low. We could relate this fact to the abundance of *Verrucomicrobia* sequences in the WC (up to 46%, Fig. 6.1). Interestingly, bacterial production increased 72.2 ± 48.2 fold (Table 6.1) from winter to spring, and we observed significant increases in bacterial abundance (4.2 ± 2.6 fold, Table 6.1), mainly by *Bacteroidetes* (12 times more abundant in spring vs. winter),

Betaproteobacteria (nine times) and *Actinobacteria* (10 times) (Fig. 6.1). During the ablation phase, light availability increased promoting massive algae growth (Felip et al. 1999b), further fuelling most of the bacterial activity detected. Glaciers, which hold 75% of the freshwater on the planet, are largely autotrophic systems (Anesio et al. 2009), and polar sea ice has also shown a net autotrophic activity integrated over an entire season although polar seas melting will probably exacerbate bacterial respiration (Kaartokallio 2004). Ice-melting is therefore a major promoter of community transitions both in marine and in inland waters. Previous studies in Lake Redon (Pyrenees) and Lake Gossenköllesee (Tyrolean Alps) showed that temporal changes in eukaryotic assemblages were strongly affected by the physical transformation of the lake cover and the snowpack in the catchment (Felip et al. 1999b, Felip et al. 2002). After 16S rRNA gene analyses, we observed drastic changes in the slush bacterial community composition (Fig. 6.1) and a decrease in bacterial diversity from winter to spring (Table 6.1). The vulnerability of the cryosphere (i.e., cold ecosystems) to climate change and its potential large influence in the emission of greenhouse gases will certainly promote more research on the ecology of the microbial communities inhabiting these habitats.

All the sequences obtained in this work fell into eight bacterial phyla (Fig. 6.1 and Supplementary Fig. A.C6.1). Overall, *Bacteroidetes* was the most abundant (42% of all 16S rRNA gene sequences) and showed a marked winter to spring increase in abundance (17 ± 7 to 59 ± 6% respectively, Fig. 6.1); there was a clear phylogenetic segregation between the ice-growth phase in winter (mostly *Flavobacteria* and *Bacteroidia*) and the spring ablation period (mostly *Cytophagia* and *Sphingobacteria*) (Fig. 6.2 and Supplementary Fig. A.C6.1). *Bacteroidetes* are abundant in inland waters (Barberan and Casamayor 2010) and closely related to phytoplankton blooms, both using phytoplankton exudates during algal growth (Zeder et al. 2009) or complex DOM derived from senescent phytoplankton (Pinhassi et al. 2004, Teira et al. 2008). Algae were abundant in the spring sample as detected by

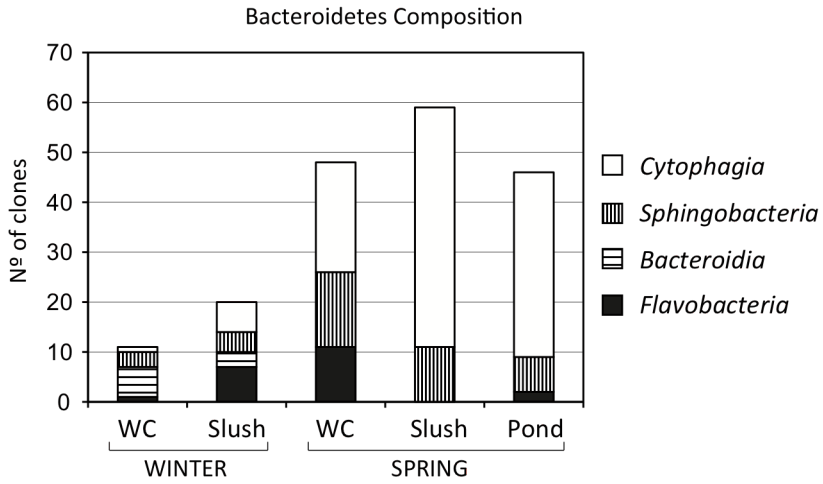

Figure 6.2: Relative abundance of the different Classes within the phylum *Bacteroidetes* represented by the number of clones found in each layer.

microscopic observations and the recovering of chloroplast sequences and probably *Bacteroidetes* were stimulated by the algal blooming. Indeed, *Bacteroidetes* is a very diverse chemoheterotrophic bacterial group with many aerobic members that can degrade biopolymers such as cellulose and chitin, and the high molecular mass fraction of the DOM (Kirchman 2002), at relatively low temperatures (Mary et al. 2006).

Proteobacteria were also very abundant in the clone libraries with 32% of the sequences, and 80% of them being *Betaproteobacteria*. Most of these sequences fell into four previously described freshwater clusters, Beta-I-II-III-IV (Glockner et al. 2000, Zwart et al. 2002, Hervas and Casamayor 2009), respectively, and in two new clusters essentially formed by sequences from the cryosphere (Supplementary Fig. A.C6.1). As for *Bacteroidetes*, we also observed winter-to-spring phylogenetic segregation within the *Betaproteobacteria*. The GSK16 subcluster containing sequences mainly from freshwater ultraoligotrophic cold environments, subglacial environments, and alpine and nival lakes was mainly detected in spring, whereas the *Rhodoferax* subcluster, a cosmopolitan freshwater group also very abundant in humic and eutrophic lakes

(Zwart et al. 2002, Simek et al. 2005), was mostly detected in winter. As mentioned elsewhere (Hervas and Casamayor 2009), these differences in temporal distributions suggest different ecologies or physiologies among closely related *Betaproteobacteria.*

Verrucomicrobia 16S rRNA sequences represented 12% of total clones, most of them only seen in winter. *Verrucomicrobia* have been found in cold environments such as Lake Vida, Antarctica (Mosier et al. 2007) or Lake Puma Yumco, Tibetan Plateau (Liu et al. 2009), but never at the relative abundances we found in the WC (42%) and slush (16%) of Lake Redon. Thus, alpine lakes might represent a suitable environment to further investigate this relatively unknown phylum (Sangwan et al. 2004). Finally, *Actinobacteria* (c. 10%), *Planctomycetes* (0.5%), *Spirochaetes* (0.5%) and *Chloroflexi* (0.2%) were also detected in the clone libraries.

Slush bacterial assemblages were very similar to the water column both in winter and spring (Fig. 6.3) and more than 70% of the 16S rRNA gene sequences during the snowpack growth phase had the closest match with sequences from lakes (Fig. 6.4). These results suggested initial colonization of the slush by bacteria from the same

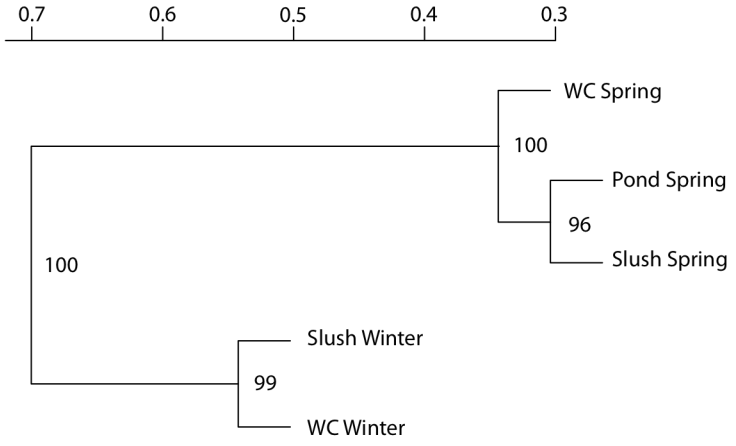

Figure 6.3: Hierarchical clustering analysis (UPGMA algorithm with Jackknife supporting values, 100 replicates) carried out on the five libraries constructed in this study. Distances between clusters are expressed in UniFrac units: a distance of 0 means that two environments are identical and a distance of 1 means that two environments contain mutually exclusive lineages.

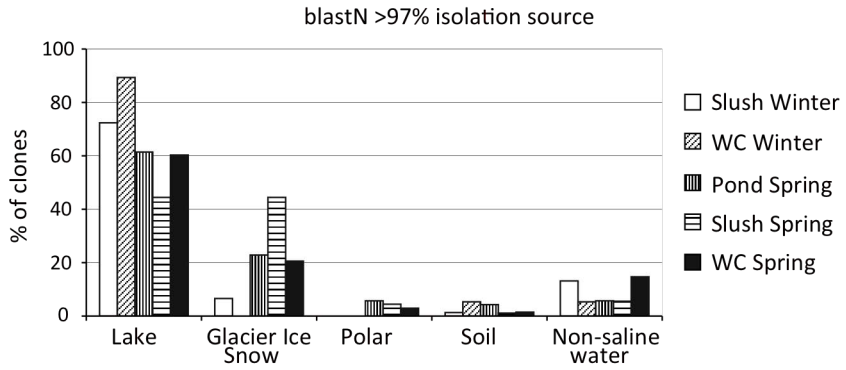

Figure 6.4: Isolation sources of the closest BLAST match found in GenBank for each of the samples analyzed. Only BLAST matches with more than 97% identity were considered.

lake water and are in agreement with previous phytoplankton studies where initial slush algae originated from the phytoplankton rich surface waters that flood the ice cover due to hydrostatic adjustment (Felip et al. 1995, Felip et al. 1999b). Conversely, during spring ablation, 50% of the 16S rRNA gene slush sequences had the highest identity with sequences from the cryosphere (i.e., globally distributed glaciers, ice, snow, and polar regions). A similar switch was previously described in the phytoplankton where non-planktonic species probably introduced by melting water coming from the snowpack were observed (Felip et al. 2002). Conversely, in spring the first meters of the lake water column were influenced by melting waters as more than 20% of planktonic 16S rRNA gene bacterial sequences were closely related to sequences from the cryosphere (Fig. 6.4).

Overall c. 90% of the slush sequences were closely related (>97% identity) to either cold freshwater lakes (66%) such as Lake Michigan (Mueller-Spitz et al. 2009), Crater Lake (Page et al. 2004) and Lake Fuchskuhle (Glockner et al. 2000) (See Supplementary Table A.C6.1 for details and Fig. 6.4) or to polar or glacial environments (23%) such as Puruogangri Ice Core (Zhang et al. 2008) or an Arctic sea-ice melt pond (Brinkmeyer et al. 2003). These data are in agreement with the idea that aquatic bacteria in high-

mountain regions are globally distributed (Zwart et al. 1998, Glockner et al. 2000, Liu et al. 2006, Sommaruga and Casamayor 2009) but only develop in cold and oligotrophic habitats as alpine lakes, glaciers, snow or polar environments. As previously discussed (Hervas et al. 2009, Hervas and Casamayor 2009), airborne dispersal is probably the mechanism that better explains the cosmopolitanism found in alpine areas. Despite their minor quantitative relevance in the whole cryosphere, these alpine areas are very convenient systems for surveying changes in microbial composition, dynamics, activity, and fate following environmental perturbations.

Acknowledgements

We are thankful to Centre de Recerca d'Alta Muntanya, Universitat de Barcelona, Vielha for laboratory facilities. L Camarero, M Felip, M Vila-Costa, X Triadó, and A Fernandez-Guerra are acknowledged for field and lab assistance and ancillary data. This research was supported by grants PIRENA CGL2009-13318 and GOS-LAKES CGL2009-08523-E to E.O.C., and CONSOLIDER grant GRACCIE CSD2007-00067 from the Spanish Office of Science and Innovation (MICINN). J.C.A. benefits from a Juan de la Cierva postdoctoral fellow (MICINN).

7

A metagenomics view on the microbial biogeochemical potential of an ultraoligotrophic high-mountain lake (Lake Redon, Pyrenees)[1]

Abstract

The biodiversity and potential functional role of a deep high-mountain lake was analyzed by microbial metagenomics. We explored three samples from two contrasted limnological situations: the surface slush during the ice melting phase, and the epilimnion and hypolimnion at the end of the stratification period. The slush sample was dominated by algae whereas bacteria dominated the planktonic samples. Diversity indices were higher in the hypolimnion and lower in the slush, where a bloom of *Chrysophyceae* dominated the community. Accordingly, most of the reads from the slush showed the potential for aerobic respiration and aerobic carbon fixation by

[1] See supplementary material in Appendix A

algae. In contrast, planktonic aerobic respiration was mainly dominated by heterotrophic *Burkholderiales* in the epilimnion and *Actinobacteria* and *Burkholderiales* in the hypolimnion. The potential for an active nitrogen cycle (nitrification, nitrite oxidation and nitrate reduction) was mainly found in the slush and hypolimnion. No genes for dissimilatory nitrate reduction to ammonium were detected and potential for methanogenesis, anaerobic ammonia oxidation and dissimilatory sulfur pathways were only detected in the hypolimnion. The microbial community of the lake seems to have adapted to P-limitation by the ability to uptake and utilize organic phosphorus. Overall, we evaluated the main processes shaping the biogeochemistry of Lake Redon and unveiled the presence of marker genes for key biogeochemical pathways, which may help to further study the response of alpine lakes to environmental changes.

Introduction

The study of biogeochemical processes in highly diluted alpine oligotrophic environments is a difficult task. High-altitude aquatic ecosystems experience extreme physical conditions like low temperatures, high UV radiation, ultraoligotrophic conditions and strong temporal dynamics driven by a long winter with the formation of an ice cover. They harbour lower concentrations of microbial biomass than other aquatic systems, which make it difficult to explore microbial activities and processes by classical *in situ* methods (Sommaruga 2001, Catalan et al. 2006). These conditions are very difficult and tedious to mimic in the laboratory, and therefore the culturability of microorganisms living under such extreme conditions is very low. Molecular ecology and metagenomics may help microbial ecologists to overcome these difficulties to properly explore ecological processes and microbial community composition in highly diluted waters (Alfreider et al. 1996, Llorens-Mares et al. 2012, Barberan and Casamayor 2014).

Physical properties, biogeochemical processes and primary production in high-mountain Lake Redon have been largely studied by traditional limnologists (Catalan 1988, Catalan et al. 1992, Camarero et al. 1999). Microbial activities (Felip et al. 1995) and eukaryotic microbial assemblages inhabiting Lake Redon were described by fluorescence and microscopic analysis (Felip et al. 1999a, Felip et al. 2002). However, there is still a lack of a mechanistic knowledge to understand how the environment shapes the bacterial community composition and the individual roles carried out within the carbon, nitrogen, sulfur and phosphorus cycles. Previous studies highlighted a prevalent role of the nitrogen cycle in high-mountain lakes (Catalan 1992, Catalan et al. 1994), where atmospheric depositions (i.e., rain and snow) act as main sources of nitrogen, phosphorus and iron (Camarero and Catalan 1993, Catalan et al. 1994, Reche et al. 2009). In addition, phosphorus limitation may play a prevalent role in microbial growth and phytoplankton composition and productivity (Catalan et al. 2006, Camarero and Catalan 2012). Unveiling the microbial communities potentially involved in the biogeochemical cycling will favour a better understanding on the ecological lake functioning and help the interpretation of past and future studies related with both climate change and remote sensing of environmental pollution (Catalan et al. 2002).

In the present study, we explored three different water layers of the deep glacial dimictic Lake Redon (central Pyrenees): the slush during the ice-covered period, and the epilimnion and hypolimnion during the stratified period before the autumn overturn. These three different situations were analyzed by metagenomics and *in silico* analysis for phylogenetic classification and identification of the main metabolic pathways. We hypothesized to find a limited dissimilatory sulfur cycle because of the presence of oxygen in the whole water column and a predominance of aerobic-related genes in all the samples with autotrophy dominating in the slush and epilimnion. We also expected an important presence of nitrogen- and phosphorus-

cycling genes in order to overcome the nutrient limitation inherent to such oligotrophic systems.

Materials and methods

Study site, samples collection and sequencing

Lake Redon is a high-altitude dimictic lake with mixing periods in spring and autumn. Located in the central Pyrenees (42º 38' 34" N, 0º 46' 13" E, altitude 2240m, maximum depth 73 m, surface 0.24km^2), it has been extensively studied by limnologists (Limnological Observatory of the Pyrenees, LOOP, NE Spain) for its extreme and dynamic conditions through the year and for being excellent sentinels and recorders of past and present environmental changes (Catalan et al. 2006). Due to its isolation, small catchment area and lack of vegetation, the lake is oligotrophic and atmospheric deposition is the main source of nitrogen and phosphorus (Camarero and Catalan 2012). The lake is usually covered by ice during 6 months of the year; this cover is characterized by sandwich-like structures constituted by a superposition of snow, white ice and slush (i.e., a mixture of water and snow) layers on top of a sheet of black ice (Eppacher 1966, Adams and Allan 1987). The slush layers have been largely studied in terms of structure and chemical composition (Catalan 1989), as well as microbial community and productivity (Felip et al. 1995, Llorens-Mares et al. 2012).

The lake was sampled in spring during the ablation phase (slush layer May 12, 2010) and in autumn (September 25, 2013) during the stratified period (2 m depth for epilimnion and 60 m for hypolimnion). The slush sample (25 L) was passed through a 30 µm nylon mesh and kept in the dark until further processing in the lab 2–4 hours later. Then, the sample was pre-filtered by 3.0 µm and the cells were collected on a 0.1 µm Supor 293 mm membrane disc filters (Pall Life Sciences, IL, USA), and stored in liquid nitrogen and further at -80ºC until DNA extraction (fraction analyzed 0.1 to 3.0 µm). Environmental DNA was obtained after enzymatic digestion and

phenol extraction in Tris-EDTA buffer, and 454 pyrosequencing analyses were carried out at the J Craig Venter Institute in Rockville, MD, USA as recently reported (Zeigler Allen et al. 2012). The planktonic samples (15L) were passed through a 30 µm nylon mesh and kept in the dark until further processing in the lab 2–4 hours later. The samples were pre-filtered by 5.0 µm and the plankton collected onto 0.2 µm polycarbonate membranes (47 mm diameter, Nucleopore, Whatman Ltd.) and stored at -20ºC in lysis buffer (40mM EDTA, 50mM Tris, pH 8.3, 0.75 M sucrose) until nucleic acid extraction (fraction analyzed 0.2 to 5.0 µm). For the genomic DNA extraction, the membranes were enzymatically digested with lysozyme, proteinase K and sodium dodecylsulfate incubation, followed by phenol-chloroform-isoamyl (25:24:1, v/v/v) extraction. Purification and concentration was carried out with Amicon® Ultra 4 Centrifugal Filter Units – 100000 NMWL (Millipore). Shotgun library generation (550 bp), DNA preparation and Illumina MiSeq (Illumina, San Diego, CA) sequencing with 2×250 bp configuration was performed at ASCIDEA (Barcelona, Spain).

DNA sequences analyses

Metagenomics sequences were quality filtered and annotated as recently reported (Llorens-Mares et al. 2015). Approximately four hundred thousand reads were recovered from the slush sample by 454 sequencing technology, and about ten million reads from the planktonic samples by Illumina. KEGG Orthologs (KO) annotation was used for functional analysis and KO counts were normalized according to the length of the read and the length of the target gene (Sharon et al. 2009b) in order to have comparable results from the different sequencing methodologies. The functional analyses focused in the genetic potential of the main biogeochemical cycles, i.e., carbon (C), nitrogen (N) and sulfur (S) cycling (Lauro et al. 2011, Llorens-Mares et al. 2015). In order to investigate the role of phosphate (P) incorporation and processing in phosphorus-limited conditions, we compiled the key genes for phosphorus cycling (Gifford et al. 2011, Vila-Costa et al. 2013) into the KO list for

functional analysis (Supplementary Table A.C7.1). We also evaluated the presence of a key gene for anoxygenic phototrophy *pufM* (K08929). Heatmap plots, diversity and statistical analyses were generated with R (R Core Team 2014).

Microbial community structure by 16S and 18S rRNA genes analysis

Extraction from the metagenome pool of the bacterial 16S and eukaryal 18S ribosomal RNA genes was based on hidden Markov models (HMMs) (Huang et al. 2009). The resulting 16S and 18S reads were quality trimmed using the SILVAngs pipeline (Quast et al. 2013) and classified using the SINA aligner (Pruesse et al. 2012) with release SILVA 119 using a minimum identity of 70% for 16S and 85% for 18S. The classification was based on a lowest common ancestor quorum of 70% on the best 10 matches. The 16S rRNA gene from chloroplasts and mitochondria were removed from subsequent analyses.

Results

Biogeochemical parameters

The lake was thermally stratified in autumn when the plankton samples were taken with a thermocline spanning from 11 to 26 m and a temperature gradient from 13 to 4ºC. The slush sample contained higher concentrations of ammonia, nitrate and phosphorus, possibly as a consequence of the heavy snowfall at the time of sampling (Table 7.1). The concentration of ammonia and nitrate were low in the plankton samples but higher in the hypolimnion compared to the epilimnion. Oxygen was present in the whole water column, with lower concentration in the hypolimnion (7.1 mg l^{-1}).

Table 7.1: Biogeochemical data for Lake Redón. Abbreviations: DOC, dissolved organic carbon; TDP, total dissolved phosphorus.

	Slush	Epilimnion	Hypolimnion
Depth (m)	0	2	60
Temperature (ºC)	0	13	4
Conductivity (µS cm^{-1})	8.2	9.6	10.1
Oxygen (mg l^{-1})	8.5	8.6	7.1
Light (% incident)	100	90	0
DOC (mg l^{-1})	0.55	0.3	0.2
pH	5.49	6.84	6.22
TDP (µM)	0.35	0.01	0.02
NH_4 (µM)	16.43	0.3	3.1
NO_2 (µM)	0.08	0.08	0.09
NO_3 (µM)	11.74	4.6	6.3
Bacterial abundance (x 10^5 cells ml^{-1})	8.6	5.2	8.8

Microbial community structure

At the time of sampling the slush sample was dominated by eukaryotes (>80% of the total rRNA reads) whereas prokaryotes dominated planktonic samples both in surface (93%) and in deep waters (95%) (Fig. 7.1 and Supplementary Table A.C7.2). Higher prokaryotic diversity was found in the hypolimnion (Table 7.2; Shannon-Weaver index H'=3.23) than in the slush (H'=2.40) and the epilimnion (H'=1.90). The highest eukaryotic diversity was also found in the hypolimnion (H'=2.59), followed by the epilimnion (H'=2.34) and the lowest diversity in the slush (H'=0.67). This result is in agreement with an algal bloom of *Chrysophyceae* (85% of 18S rRNA recovered reads and 73% of total rRNA reads) present in the slush layer in May. From these, c. 70% of the sequences were assigned to the uncultured *Chrysophyceae* group CCMP1899 and 20% to the chrysophyta genus *Hydrurus*. The second most abundant lineage in the slush was the fungi *Chytridiomycota* (5.5%). Sequences related to other protists such as *Ciliophora* (2.5%), *Basidiomycota* and

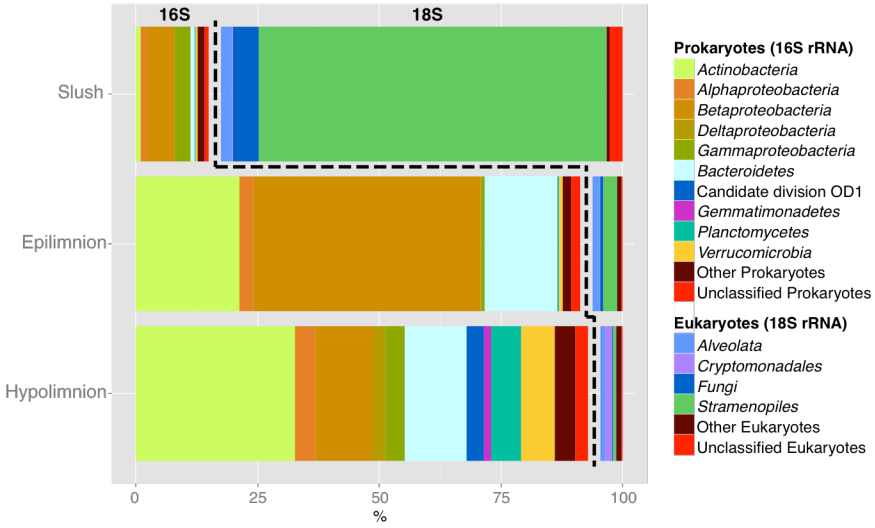

Figure 7.1: Global community structure (relative abundances at the Phylum level except for *Proteobacteria* at the Class level) of Lake Redon obtained from the 16S and 18S rRNA gene present in the metagenomic pool. See detailed information in supplementary Table A.C7.2.

Table 7.2: Metagenomic data.

	Slush	Epilimnion	Hypolimnion
Total number of reads	396197	10307742	11618730
Functionally assigned metagenomic reads as KO	33080 (8.3%)	1567195 (15.2%)	903012 (7.8%)
Reads of key genes in C, N, S and P cycles	836	46014	26358
16S rRNA genes in the metagenomic pool*	73	8838	8795
16S rRNA Shannon-Weaver index	2.40	1.90	3.23
18S rRNA genes in the metagenomic pool	402	598	433
18S rRNA Shannon-Weaver index	0.67	2.34	2.59

*Chloroplasts and mitochondria were discarded in this count.

Cercozoa were also found. The bacterial component represented only 15.4% of the microbial community present in the slush and was dominated by *Burkholderiales* (*Betaproteobacteria*, 34.2% of total 16S rRNA reads) followed by *Pseudomonadales* (*Gammaproteobacteria*, 17.8%) and in lower proportion *Clostridiales* (*Firmicutes*, 5.5%) and *Acidimicrobiales* (*Actinobacteria*, 4.1%). Archaeal ribosomal sequences were not detected.

In the epilimnion, the eukaryotic 18S rRNA gene pool was dominated by the algae *Chrysophyceae* (33%) mainly of the uncultured clusters LG07-07 (30% of total chrysophytes), P34.48 (14%), and E222 (11%), and of the order *Chromulinales* (16%). *Bicosoecida* (8% of total 18S rRNA gene reads) and the alveolates *Ciliphora* (16.1%) and *Dinoflagellata* (6%) were also present in the epilimnion. Up to 10.5% of the 18S rRNA gene reads were from fungi (mainly *Basidiomycota* and *Ascomycota*), and 6% were affiliated to the protist *Cercozoa*. Conversely, the hypolimnetic protists were dominated by *Cryptomonas* (30.5%), the alveolates *Protalveolata* (10.6%) and *Ciliophora* (8%), *Nucletmycea* (9%) and *Chrysophyceae* (9%, most of them of the uncultured P34.48 cluster and *Chromulinales*). We also observed substantial differences in the planktonic bacterial community composition between the epi- and hypolimnion. The 16S rRNA gene pool from the epilimnion was dominated by *Burkholderiales* (48.7%), *Frankiales* (19.1%) and *Flavobacteriales* (9.3%). Conversely, the bacterial assemblage from the hypolimnion was more evenly distributed and *Frankiales* dominated (24.5%), followed by *Burkholderiales* (7.9%), *Sphingobacteriales* (6.2%), *Flavobacteriales* (5.5%), *Planktomycetales* (4.4%), *Acidimicrobiales* (4.1%), Candidate Division OD1 (3.8%) and various verrucomicrobial lineages (7.5%). Nine hypolimnion sequences (0.1% of the total 16S rRNA gene reads) affiliated to the domain Archaea (*Euryarchaeotal* clade DHVEG-6).

Functional analysis

Metagenomic reads were functionally annotated through KO numbers (*e*-value 10^{-5}) and 15.2% of the reads from the epilimnion could be assigned to a KO, whereas only 8.3% and 7.8% for the slush and hypolimnion, respectively, matched KO. The functionally assigned reads were filtered to selectively identify marker genes related to C, N, S and P cycling (Supplementary Table A.C7.1). Aerobic respiration and aerobic carbon fixation (through Calvin Cycle) accounted for most of the reads from the slush sample, followed by assimilatory and mineralization pathways from the nitrogen and sulfur cycle (Supplementary Table A.C7.3). The epilimnion and hypolimnion were dominated by aerobic respiration as well as assimilation and mineralization of nitrogen and sulfur. CO oxidation was more abundant in the epilimnion than in the hypolimnion, whereas anaerobic C fixation followed the opposite tendency. Nitrate reduction and nitrite oxidation reads were mainly found in the slush, but also detected in the hypolimnion. No genes for ammonification (dissimilatory nitrate reduction to ammonium; DNRA) were detected in the dataset, while genes for methanogenesis, anammox-related and dissimilatory sulfur pathways were only detected in the hypolimnion. A functional hierarchical analysis of the C, N and S pathways (Fig. 7.2), showed that the slush was functionally different in comparison with the planktonic samples, which grouped together.

The relative abundances of the normalized counts for carbon- (Fig. 7.3), nitrogen- (Fig. 7.4) and sulfur-cycling (Fig. 7.5) genes were used as a proxy of the potential relevance of each biogeochemical cycle in each sample. The analyses showed a comparative overview on the geochemistry of the lake and unveiled the main microbial populations potentially behind of each biochemical step. The main pathway in all three samples was aerobic C respiration (51.9-65.5% of the marker genes for the C cycle). However, the phyla performing this process were very different in the slush, dominated by algae, and the planktonic communities, which were mainly dominated by heterotrophic *Burkholderiales* in the epilimnion and various orders of *Actinobacteria* and *Burkholderiales* in the hypolimnion. Carbon

fixation through the Calvin cycle was abundant in the slush sample by algae, and rare in the planktonic samples. Carbon monoxide (CO) oxidation marker genes were mainly found in the planktonic samples and related to heterotrophic bacteria (*Burholderiales*, *Rhizobiales* and *Rhodospirillales*). Anaerobic carbon fixation was mainly found in the hypolimnion mostly by *Burkholderiales* and *Rhizobiales* (probably anaplerotic through the reductive citric acid cycle/Arnon pathway).

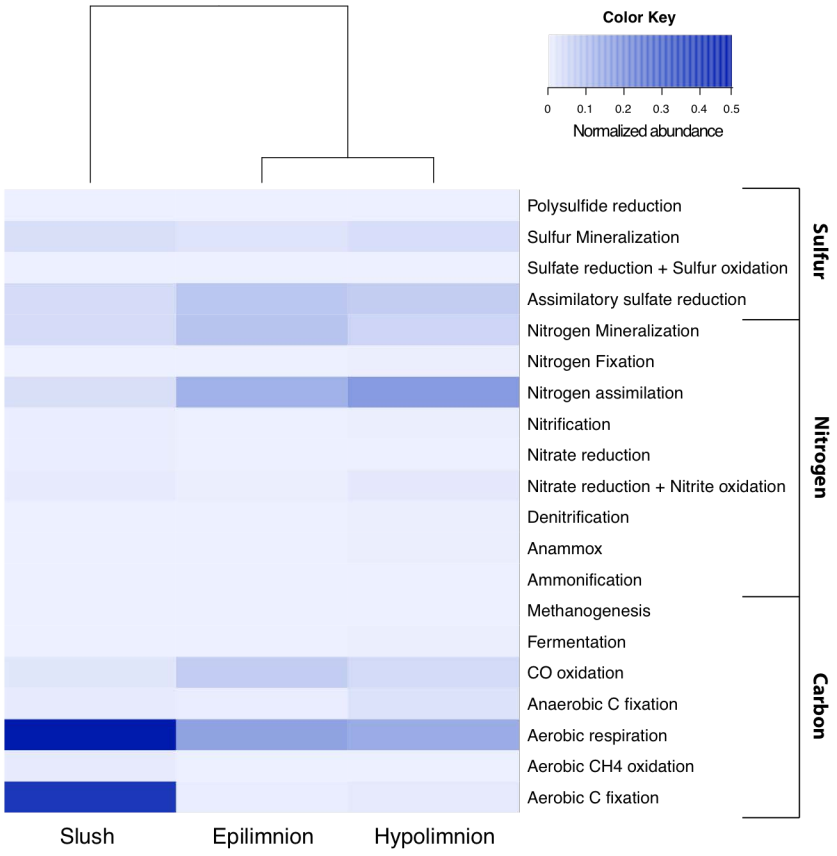

Figure 7.2: Heatmap plot and functional clustering of the selected KEGG Orthologs for the predicted ORFs from the metagenomic reads for Lake Redon.

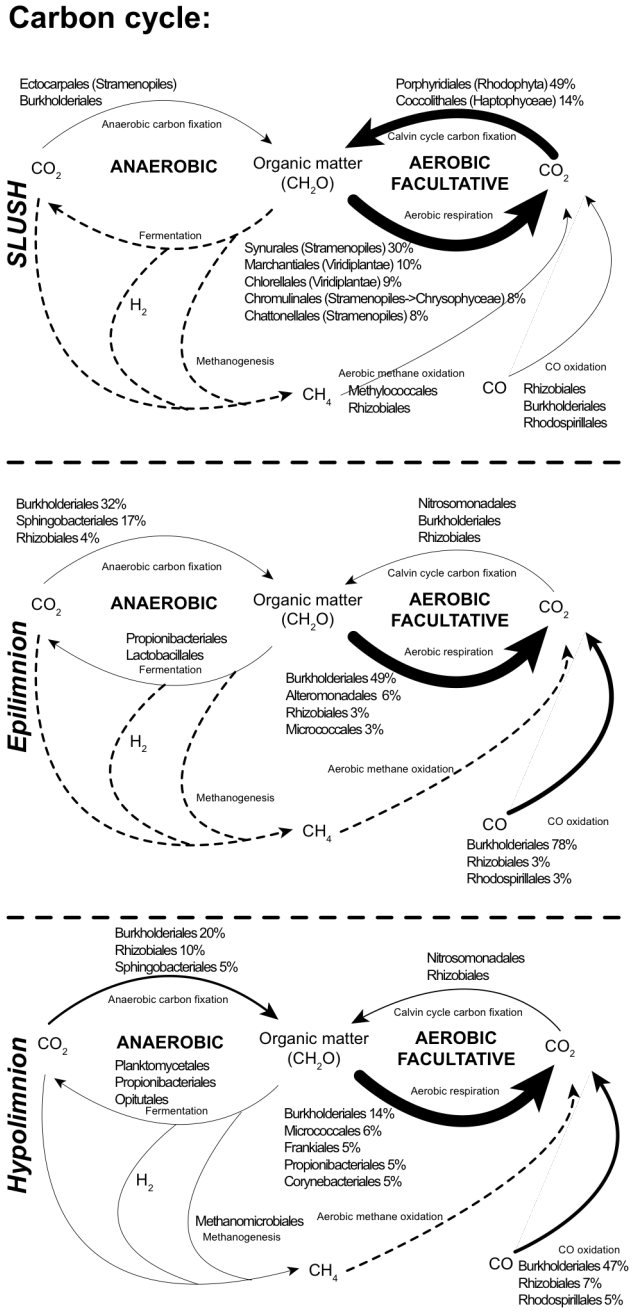

Figure 7.3: Genetic potential for several steps of the carbon cycle in Lake Redon using a combination of normalized marker genes. Arrows size proportional to the potential flux of the carbon pathways (100% value, see Supplementary Table A.C7.3). Dotted lines: not detected marker genes. Relative abundances for the main microbes potentially driving each conversion step are shown (only for those that contributed >1% of the marker genes mixture).

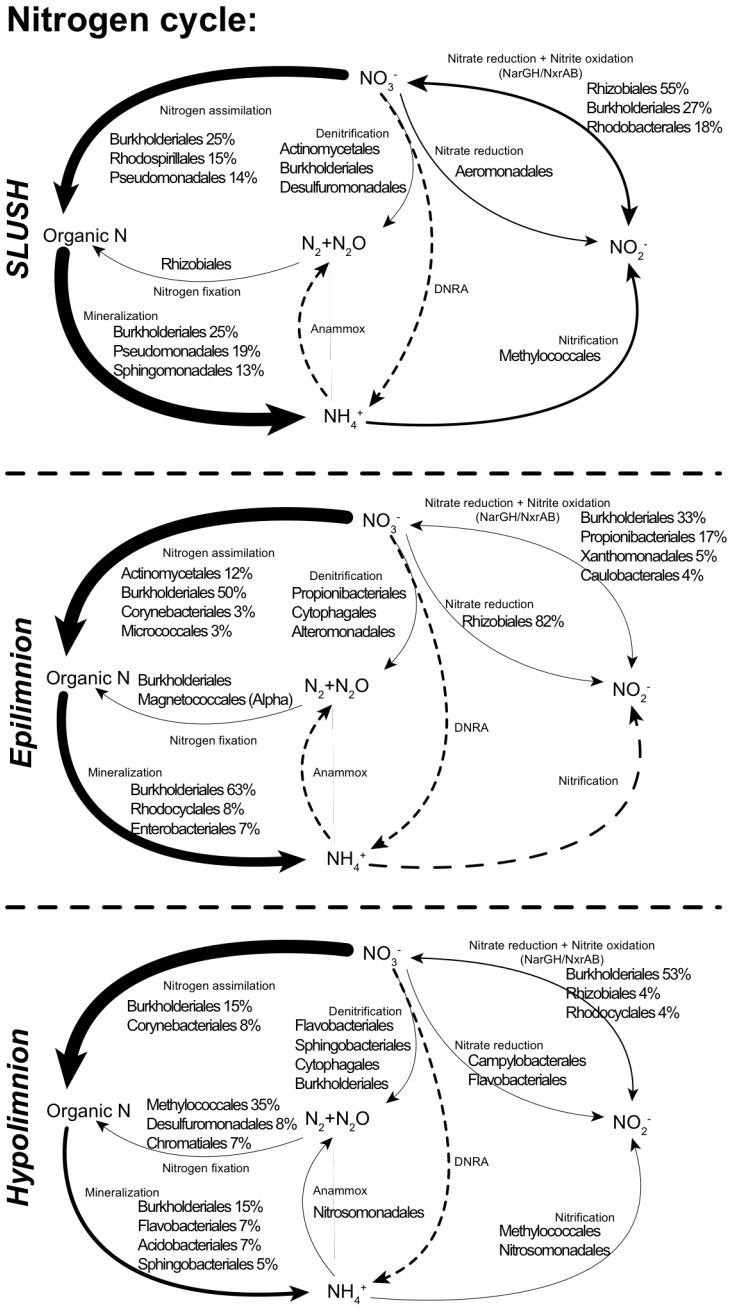

Figure 7.4: Genetic potential for several steps of the nitrogen cycle in Lake Redon using a combination of normalized marker genes. Arrows size proportional to the potential flux of the nitrogen pathways (100% value, see Supplementary Table A.C7.3). Dotted lines: not detected marker genes. Relative abundances for the main microbes potentially driving each conversion step are shown (only for those that contributed >1% of the marker genes mixture).

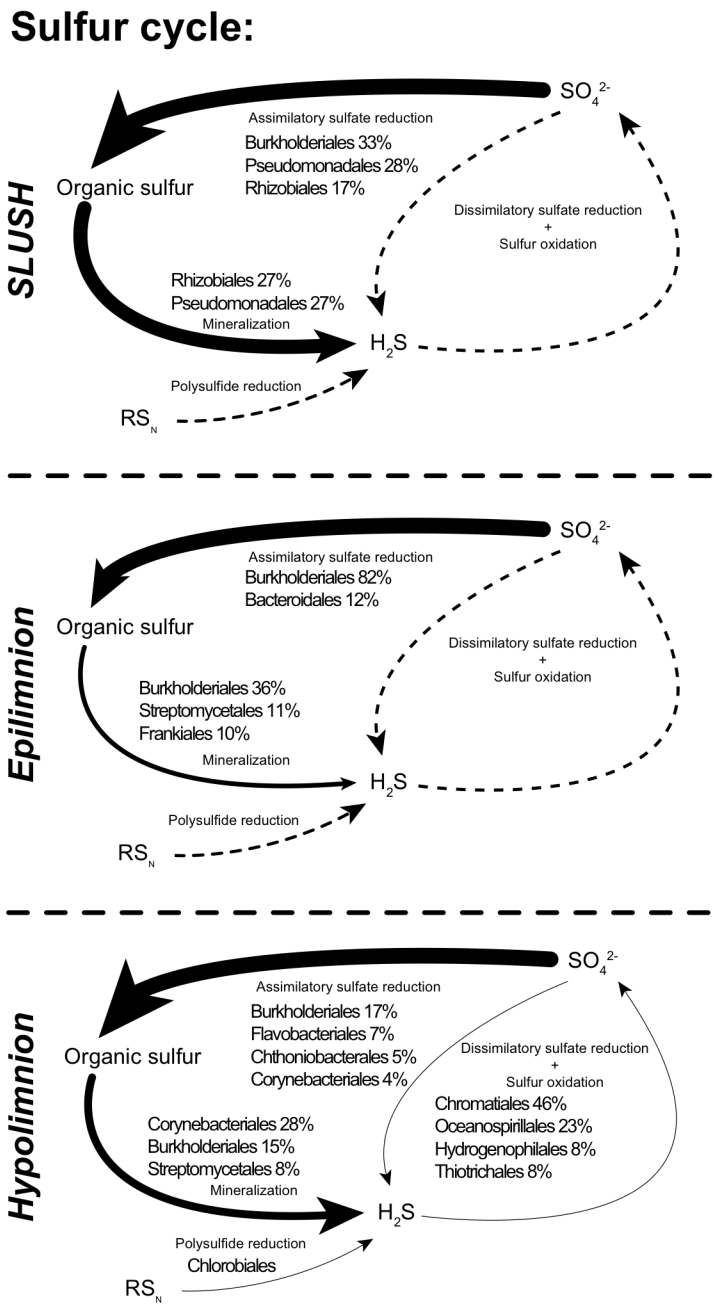

Figure 7.5: Genetic potential for several steps of the sulfur cycle in Lake Redon using a combination of normalized marker genes. Arrows size proportional to the potential flux of the sulfur pathways (100% value, see Supplementary Table A.C7.3). Dotted lines: not detected marker genes. Relative abundances for the main microbes potentially driving each conversion step are shown (only for those that contributed >1% of the marker genes mixture).

Most of the marker genes detected for the nitrogen cycle were related to assimilation and mineralization (Fig. 7.4 and Supplementary Table A.C7.3). The relative proportion of nitrogen assimilation reads increased from the slush to the hypolimnion (35.3-69%) whereas mineralization reads were abundant in the slush and epilimnion (c. 41%) and lower in the hypolimnion (20.3%). Both steps were mainly performed by diverse heterotrophic bacteria (*Betaproteobacteria*, *Alphaproteobacteria* and *Actinobacteria*). The *nap* genes for nitrate reduction were mainly detected in the slush by the facultative anaerobe *Aeromonadales*. On the other hand, the reversible nitrate reduction-nitrite oxidation pathway (through genes *nar*GH/*nxr*AB) was abundant in both the slush and the hypolimnion by *Rhizobiales* and *Burkholderiales*. Nitrification marker genes (for aerobic ammonia oxidation) had higher abundances in the slush, mainly from *Methylococcales*, and were also detected in the hypolimnion by *Methylococcales* and *Nitrosomonadales*. We also detected the presence of *Nitrosomonadales* in the 16S rRNA pool of the epilimnion showing the potential for nitrification in this layer (although below detection limits in the functional analysis). The potential for denitrification and nitrogen fixation (*nif* genes) was rare in the epilimnion but reached up to c. 1.5% in the slush and hypolimnion. Denitrification in the hypolimnion was mostly related to *Bacteroidetes* (*Flavobacteriales*, *Sphingobacteriales* and *Cytophagales*), and to *Actinomycetales*, *Burkholderiales* and *Desulfuromonadales* in the slush. Nitrogen fixation was mostly assigned to *Rhizobiales* in the slush community and to *Methylococcales* in the hypolimnion. Finally, the key gene for anammox was only detected in the hypolimnion matching *Nitrosomonadales*.

The sulfur cycle (Fig. 7.5 and Supplementary Table A.C7.3) was dominated by assimilatory and mineralization steps (>99% of total targeted sulfur reads), and we only detected in the hypolimnion marker genes for polysulfide reduction and the reversible *apr* and *dsr* genes for dissimilatory sulfate reduction and sulfur oxidation.

The P cycle was studied separately and compared with the abundances previously found in meso-eutrophic lakes from the Banyoles area where phosphorus has a higher availability (Fig. 7.6 and Supplementary Table A.C7.3). Five of the steps related to the phosphorus cycle were found to be significantly different in lake Redon compared to the abundances found in Banyoles area (p-value < 0.05, t-test). In the case of phosphate regulation and phosphonoacetate hydrolase, the relative abundances were

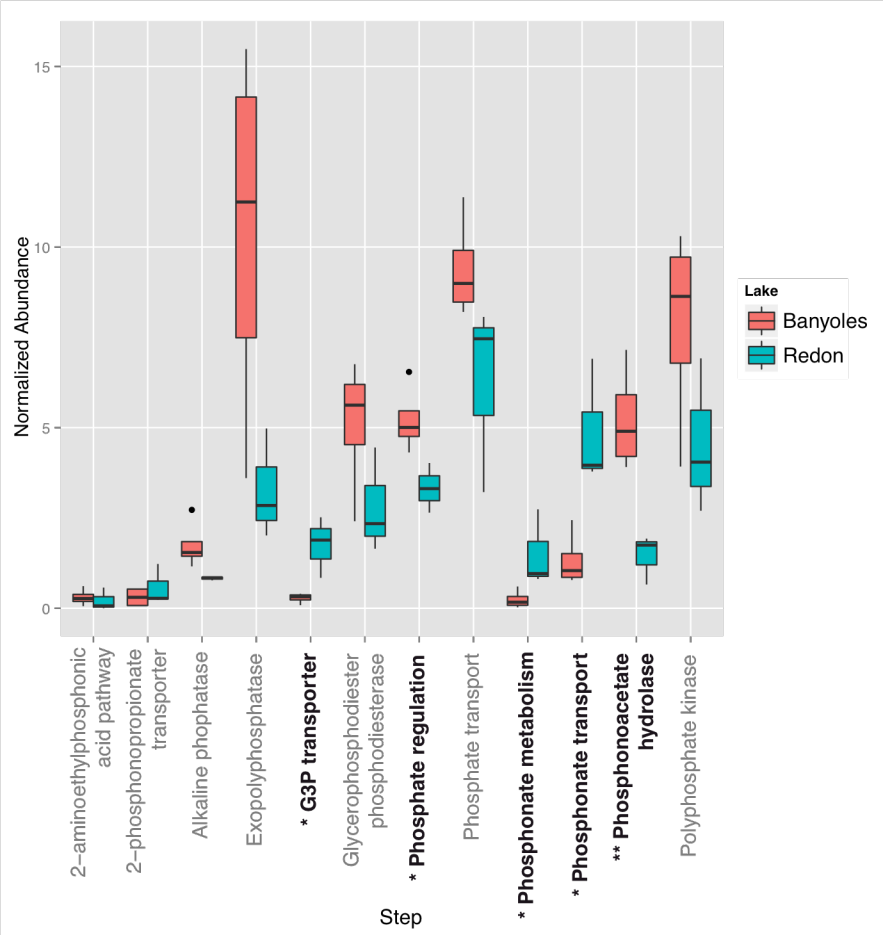

Figure 7.6: Boxplot showing differences in the genetic potential for several steps of the phosphorus cycle in Lake Redon (three samples: slush, epilimnion and hypolimnion) and Lake Banyoles area (four samples: two lakes metalimnion and hypolimnion) using a combination of normalized marker genes. Significant differences are labeled with one asterisk (p-value < 0.05, t-test) or two asterisks (p-value < 0.01, t-test).

significantly higher in Banyoles. In contrast, marker genes for the glycerol-3-phosphate (G3P) transporter, and phosphonate transport and metabolism were more abundant in Lake Redon. Phosphonate transport and metabolism in the slush were dominated by *Rhizobiales* (c. 50%) and *Burkholderiales* (c. 24%), and by *Burkholderiales* in the planktonic samples. The G3P transporter was mainly assigned to *Rhodobacterales* in the slush, and again to *Burkholderiales* but also *Rhizobiales* in the plankton.

Finally, the normalized abundance of the key gene for anoxygenic phototrophy (*pufM*) was also evaluated. Only one sequence of the slush metagenome was assigned to *pufM*, while *pufM* sequences from the epilimnion doubled those found in the hypolimnion and were mostly affiliated to *Rhodobacterales* (37% and 30% respectively) and *Rhizobiales* (14% and 21% respectively).

Discussion

Microbial eukaryotic community composition in Lake Redon

Initial studies on phytoplankton ecology and productivity of Lake Redon were carried out more than 25 years ago (Catalan et al. 1992). The microbial eukaryotic communities analysed by traditional microscopic observations were usually dominated by chrysophytes and cryptophytes in the ice and snow cover (Felip et al. 1995, Felip et al. 1999b), and chrysophytes and chlorophytes in the water column, with *Cryptophyta* being mostly associated with deep water layers (Felip et al. 1999a). According to these previous studies, the microbial assemblages of the slush are highly dynamic depending on the phase of the ice cover (Felip et al. 1995, Felip et al. 1999b). Recently DNA sequencing methods applied to the planktonic eukaryotic communities of 11 Pyrenean lakes, including Lake Redon, showed a high genetic richness and a significant dominance of *Chrysophyceae*, *Cryptophyta* and *Alveolata* (Llorens-Mares et al. 2012, Triado-Margarit and Casamayor 2012, Barberan and

Casamayor 2014). In the present work, we observed that a bloom of *Chrysophyceae*, potentially formed by different populations, dominated the microbial assemblage of the slush. Small autotrophic flagellated chrysophytes are usually found in the water column and slush samples of oligotrophic alpine lakes (Felip et al. 2002) and are considered to be adapted to extreme cold and nutrient limited environments (Kammerlander et al. 2015). The 18S rRNA gene dataset of the epilimnion was also dominated by *Chrysophyceae* but its relative abundance decreased in the hypolimnion, where *Cryptomonas* dominated the eukaryotic fraction. This tendency has also been detected previously by microscopic studies (Felip et al. 1999a), and the metagenomics data also agreed that cryptophytes were more abundant in the hypolimnion. Interestingly, the taxonomic affiliations within the *Chrysophyceae* showed that the slush was dominated by the uncultured group CCMP1899 and the genus *Hydrurus*, two clades that had been previously related to sea ice and snow (Harding et al. 2011, Majaneva et al. 2012, Garcia-Descalzo et al. 2013). In contrast, the plankton was dominated by various groups (LG07-07, *Chromulinales*, P34.48 and E222) different from those found in the slush and mostly reported from freshwater lakes (Richards et al. 2005, Triado-Margarit and Casamayor 2012), some of them potentially with a mixotrophic lifestyle (Felip et al. 1999a).

The fungi *Chytridiomycota* had been previously reported in high-elevation soils that depend on soil moisture from melting snowbanks (Freeman et al. 2009). These conditions are very similar to those found in the slush layer where we detected *Chytridiomycota* as the second most abundant eukaryotic phylum. In addition, *Chytridiomycota* have been recently reported in Pyrenean lakes and freshwater oligotrophic systems but are still poorly known (Monchy et al. 2011, Triado-Margarit and Casamayor 2012). Interestingly, in the epilimnion 10.5% of the 18S rRNA sequences were related to Fungi but mainly from the clades *Basidiomicota* and *Ascomycota*. These two fungal groups have been previously found in aquatic systems, also in high-altitude cold lakes (Libkind et al. 2009) and are efficient decomposers of organic matter.

Finally, *Bicosoecids*, a typical planktonic group in freshwater lakes that was below detection limits in a previous study carried out by PCR amplification, cloning and sequencing of the 18S rRNA gene in the same area in July 2008 (Triado-Margarit and Casamayor 2012), was found at relatively high abundances in the epilimnion (8%). This discrepancy suggests either a marked temporal dynamics for this small flagellate or a priming bias in the previous PCR study. Other important eukaryotic groups detected here, were in agreement with previous studies in remote high-mountain lakes (Triado-Margarit and Casamayor 2012, Kammerlander et al. 2015) like the alveolates *Ciliophora* (mostly in the epilimnion) and *Protalveolata* (the second most abundant phylum in the hypolimnion), or *Chlorophyta* and *Cercozoa* more evenly distributed in the water column.

Prokaryotic community structure in Lake Redon

Substantial differences were observed between the slush sample analyzed in a previous study in Lake Redon, March and May 2009 (Llorens-Mares et al. 2012) where it was dominated by *Bacteroidetes* and *Betaproteobacteria*. In May 2010, *Burkholderiales* (*Betaproteobacteria*) was the most abundant order followed by *Pseudomonadales* (*Gammaproteobacteria*) and *Bacteroidetes* were not among the most abundant populations. Other studies that reported the bacterial composition in slush assemblages of alpine lakes (Alfreider et al. 1996) or a glacier ice metagenome (Simon et al. 2009), showed higher presence of *Betaproteobacteria* and *Bacteroidetes* and a minor contribution of *Gammaproteobacteria*. However, most of the gammaproteobacterial sequences detected in the slush, affiliated with *Acinetobacter* sp. that has been previously related with dust depositions in Pyrenean lakes (Hervas et al. 2009, Hervas and Casamayor 2009). Three dust depositions were recorded in the five weeks prior to the sampling of the slush (http://www.calima.ws), which may explain the high abundance of *Acinetobacter*-like sequences found in this sample.

The epilimnion sample showed the typical bacterial composition of an oligotrophic freshwater system (Newton et al.

2011, Barberan and Casamayor 2014), with dominance of aerobic heterotrophs *Betaproteobacteria* (mainly *Burkholderiales* of the family *Comamonadaceae* and genus *Limnohabitans*), *Actinobacteria* (mainly *Frankiales*) and *Bacteroidetes* (mainly *Flavobacteriales* and *Sphingobacteriales*). Contrastingly, the hypolimnion harboured much more diversity than the epilimnion or the slush, and *Actinobacteria* was the most abundant phyla above *Bacteroidetes* and *Betaproteobacteria*. Different groups with contrasting metabolic strategies were detected in the hypolimnion, like *Planktomycetes*, which may perform anaerobic ammonium oxidation (Jetten et al. 2003) or *Verrucomicrobia*, which can efficiently respond to phosphorus availability in the hypolimnion (Lindstrom et al. 2004). Candidate division OD1 was also detected in the deep layer and it has been previously detected in boreal suboxic hypolimnion being directly related to anaerobic methane oxidation (Peura et al. 2012). In addition, the presence of other methylotrophic bacteria like *Methylophilales* (2.3%) and *Methylococcales* (2.4%) suggest that the methane cycle could be active in the sediment of Lake Redon, as previously reported in a small boreal polyhumic lake with a large anoxic hypolimnion (Taipale et al. 2011). However, there are not many studies unveiling the community composition and diversity of the hypolimnetic layers of freshwater systems. Here, we add support to the hypothesis that hypolimnia harbour more diversity than the epilimnion and that they contain poorly characterized bacteria that are more difficult to culture and study (Barberan and Casamayor 2011, Peura et al. 2012). Thus, it is important to explore these habitats in order to seek for novel microbial life and to feed databases with new metabolic potential (Barberan and Casamayor 2014).

The presence of diverse archaeal populations in freshwater habitats has been recently studied (Lliros et al. 2008, Auguet et al. 2010), and specially, the role of ammonia-oxidizing archaea (AOA) in the first step of nitrification, which may play a pivotal role in oligotrophic environments (Martens-Habbena et al. 2009, Auguet et al. 2011, Auguet et al. 2012). In turn, total abundances of archaea have always been minoritary (0-7%) among the prokaryotic

community of high-mountain lakes (Pernthaler et al. 1998, Auguet et al. 2012). Strong seasonality for archaeal communities have been previously reported (Murray et al. 1998, Pernthaler et al. 1998), and highly related to the dynamics of ammonium and nitrite concentrations (Auguet et al. 2011). Here, we only found 0.1% of archaeal sequences and exclusively in the hypolimnion that matched the enigmatic and heterogeneous Deep Sea Hydrothermal Vent Euryarchaeotic Group 6 (DHVEG-6). The DHVEG-6 clade was initially reported from deep-sea hydrothermal vents and related to the methane metabolism with the ability to grow in relatively oxidative environments (Nunoura et al. 2012). Members of this large group have also been detected in saline shallow lakes (Casamayor et al. 2013) but the lack of cultured representatives makes it a largely unknown microbial group.

Functional potential of the microbial communities inhabiting Lake Redon

In general, metagenomic studies usually assign 20-30% of the total sequences to KEGG Orthologs (Simon et al. 2009, Llorens-Mares et al. 2015). However, we could only annotate through KO up to 15% of the reads from the epilimnion, 8% for the slush, and 8% for the hypolimnion. These numbers are certainly below expectations and clearly show lack of information in databases probably related to the difficulty of culturing bacteria from these habitats that usually need very specific conditions to grow in the laboratory. But most importantly, it highlights that major microbiological efforts should be focused on these habitats in order to unveil some of the metabolisms present, and to improve the current understanding of the biogeochemical cycling under low redox conditions.

Aerobic respiration was the most important step detected within the carbon cycle for Lake Redon, as expected for a freshwater lake dominated by heterotrophic and autotrophic microorganisms. Carbon fixation through the Calvin cycle was remarkable in the slush sample in agreement with the bloom of *Chrysophyceae* identified by

18S rRNA gene taxonomy. However, the genes from the Calvin cycle where mainly annotated as taxonomically related to *Rhodophyta* and *Haptophyceae*. This incongruence is probably a consequence of the lack of available *Chrysophyceae* genomes in databases that lead to a misclassification after distantly matching the closest sequences available in databases. In turn, we observed a low presence of Calvin cycle genes in the epilimnion in agreement with previous studies that locate the deep chlorophyll maximum in Lake Redon at 25-35 meters depth (Catalan and Camarero 1991).

Another feature that could widen the strategies in order to obtain energy is the ability to use light as a complementary energy source through aerobic anoxygenic phototrophy (AAP) (Yurkov and Beatty 1998). The presence of AAP in marine habitats has been largely studied (Beja et al. 2002, Allgaier et al. 2003), but the relevance in freshwater habitats has been neglected until recently (Salka et al. 2011), and their role in oligotrophic habitats may be important as an alternative to reduce the requirements for organic substrates (Caliz and Casamayor 2014). In Lake Redon we detected the key gene for AAP (*pufM*) in the plankton and only one sequence was detected in the slush. Most of these sequences were related to either *Rhodobacterales* or *Rhizobiales*. However, this is probably a misidentification due to the lack of *Limnohabitans* genomes in databases, which were identified as the major contributors of *pufM* diversity in high-altitude lakes in the Pyrenees (Caliz and Casamayor 2014). Actually, 30% of the 16S rRNA sequences that were classified as *Burkholderiales* in the epilimnion were also assigned to *Limnohabitans*.

The current understanding of the global nitrogen cycle has been substantially extended over the last years, including new players and pathways mainly carried out by specialized microorganisms (Thamdrup 2012) that added new possibilities to nitrogen transformations *in situ*. Bulk measurements of the water chemistry in Lake Redon had indicated a nitrate increase near the bottom possibly from an active microbial nitrification using the ammonium released from the sediment (Catalan et al. 1992). Recent

studies on high-mountain lakes have evaluated the importance of ammonia-oxidizing archaea (AOA) in the nitrogen cycle, suggesting a pivotal role of archaea in nitrification (Martens-Habbena et al. 2009), especially in oligotrophic systems where the abundances of ammonia-oxidizing bacteria (AOB) by PCR amplification showed contradictory results (Auguet et al. 2012, Vila-Costa et al. 2014). Here, we only detected a very low abundance of archaea in the hypolimnion and the nitrification genes detected were all related to AOB (Fig. 7.4, *Nitrosomonadales* and *Methylococcales*). Previous studies on the temporal dynamics of AOA, showed that changes in AOA abundances were both very dynamic and narrowly allocated in the water column (Auguet et al. 2011, Restrepo-Ortiz et al. 2014), thus it is possible that we could not capture the importance of AOA at the time and depths of sampling. The lack of nitrification genes by both archaea and bacteria in the epilimnion may be related to both the photoinhibition at high light intensities (Guerrero and Jones 1996, Merbt et al. 2012, Small et al. 2013) and the lack of substrate. Interestingly, the potential for the second step of nitrification, nitrite oxidation, was detected in the three samples collected, but the lowest abundance was again found in the epilimnion. Genes for the additional process by which ammonia can be oxidized (anaerobic ammonia oxidation, anammox), were only detected at very low abundances in the hypolimnion by *Nitrosomonadales*, suggesting a minor contribution of the anammox process. Previous studies suggested that the ammonium produced in the sediment by microbial decomposition of the organic matter from early summer phytoplankton blooms was behind the active nitrification detected in summer-autumn (Catalan 1992, Catalan et al. 1992). Because we could just capture a small nitrifying community in the hypolimnion, most of this process is probably ocurring in the surface sediment. Another study (Auguet et al. 2011) also suggested that the dark slush layers in winter-spring could be hotspots for nitrification when algae did not develop yet and atmospheric depositions (i.e., rain or snow) were rich in ammonium. We could not detect archaeal sequences for AOA in the 16S rRNA gene pool from the slush sample (probably

both because of the radiation effect mostly on AOA (Merbt et al. 2012) and the competition with algae for reactive nitrogen), but we could detect the presence of genes for nitrification by *Methylococcales*, which indicates the potential for AOB nitrification in the ammonium rich slush layer.

For the sulfur cycle we did not expect to find the potential for dissimilatory sulfur utilization as the lake is mainly oxygenated during the whole year. However the presence of sulfate as a dominant anion in the lake (Camarero et al. 1999) possibly allows the presence of phyla with the potential to utilize as energy source the small amounts of sulfide probably produced in the sediment, and fuelled the presence of populations with the potential to use polysulfides and carry out sulfur oxidation.

Finally, most oligotrophic lakes are characterized by P limitation (Catalan et al. 2006, Camarero and Catalan 2012), which is a key element for bacterial growth. Thus, the microbial community living in P-limited environments must be adapted to these conditions. Most studies on the P cycle focused their attention in marine environments (Bjorkman and Karl 2003, Longnecker et al. 2010) and showed a bacterial prevalence to the utilization of inorganic phosphorus in front of dissolved organic phosphorus (DOP). However, recent studies showed the capability to incorporate and process DOP in the form of phosphonates by bacteria (Quinn et al. 2007, Martinez et al. 2010, Luo et al. 2011). Here, we compared the key genes for P cycling with a non-oligotrophic environment (two lakes in Banyoles karstic area; Llorens-Mares et al. 2015), and detected that genes for phosphonate transport, metabolism and G3P transporter were significantly more abundant in Lake Redon than Banyoles area. This is adding evidence that the microbial community of the oligotrophic Lake Redon have adapted to P-limitation by the ability to uptake and utilize phosphorus in organic forms that come from the decomposition of senescent phytoplankton blooms occurring in the lake. A previous metatranscriptomic study in a phosphorus limited mountain lake (Vila-Costa et al. 2013), showed a higher expression of phosphonate transport, metabolism and G3P

transporter during the night and it has also been suggested that the ability to metabolize phosphonates as a sole P source may explain the success of *Trichodesmium* in low-phosphate environments (Dyhrman et al. 2006, Dyhrman et al. 2007), which may explain the overrepresentation of such genes in Lake Redon.

Overall, we provided by microbial metagenomics a large repertory of marker genes, showing the biogeochemical potential of an ultraoligotrophic stratified lake. These results may help to better understand the biogeochemical drivers in these ecosystems and help to address further studies on the biology and chemistry of these lakes, which are considered very sensitive sentinels for environmental changes. The lack of cultured counterparts in the databases emerged as a major pitfall for a complete metagenomic analysis, highlighting the need of complementary microbiological and biochemical approaches to fully unveil the links between microbes and biogeochemical cycling in oligotrophic environments.

Acknowledgements

J Caliz, M Sala and X Triadó-Margarit are acknowledged for field and lab assistance and ancillary data. This research was funded by Grants GOS-LAKES CGL2009-08523-E and DARKNESS CGL2012-32747 to EOC from the Spanish Office of Science (MINECO) and from financial support by the Beyster Family Fund of the San Diego Foundation and the Life Technology Foundation to the J Craig Venter Institute.

General overview

8

General discussion

The main goal of this Thesis was to explore the links between biogeochemistry and microbial diversity using both the functional potential unveiled by metagenomics and the main nutrients cycling framework for a mechanistic approach to disentangle the complex whole-system ecology in stratified lakes. Two contrasted lacustrine habitats were explored, the euxinic waters of the Banyoles karstic system (BKS) and the oligotrophic oxygenated waters of Lake Redon (Pyrenees).

8.1 A comparative overview of the main bacterial players in the stratified aquatic ecosystems explored

The environmental context of the systems studied showed highly contrasting biogeochemical situations, both among lakes and within lakes (Table 8.1). Overall, Lake Cisó and Lake Banyoles basin C-III showed much lower oxygen concentration and higher organic carbon load than samples from Lake Redon. High accumulation of ammonia was detected in BKS, whereas only the surface slush in Lake Redon showed high ammonia values. Hypolimnetic layers of BKS always harboured higher concentrations of sulfides than the

Table 8.1: Biogeochemical data for Lake Cisó, Banyoles basin C-III and Lake Redon. Abbreviations: RD, Lake Redon; EL, epilimnion; HL, hypolimnion; ML, metalimnion; n.d., not determined; b.d.l., below detection limits; TOC, total organic carbon; DOC, dissolved organic carbon; TDP, total dissolved phosphorus.

	Cisó ML	Cisó HL	C-III ML	C-III HL	RD Slush	RD EL	RD HL
Oxygen (mg l^{-1})	0.10	0	0.25	0	8.5	8.6	7.1
TOC (mg l^{-1})	5	3	1.5	3	n.d.	n.d.	n.d.
DOC (mg l^{-1})	n.d.	n.d.	n.d.	n.d.	0.55	0.3	0.2
TDP (µM)	1.05	2.83	0.33	0.37	0.35	0.01	0.02
NH_4 (µM)	44.4	51.0	25.0	37.5	16.4	0.3	3.1
NO_2 (µM)	0.75	b.d.l.	0.21	0.00	0.08	0.08	0.09
NO_3 (µM)	2.2	1.4	6.2	0.5	11.7	4.6	6.3
H_2S (µM)	12.8	531.9	0.8	3.6	0	0	0
SO_4^{2-} (µM)	8327	n.d.	2602	3851	33	26	n.d.

respective metalimnions, with Lake Cisó hypolimnion presenting the highest euxinic conditions of the system. In turn, sulfate was detected in Lake Redon, but much higher concentrations were found in BKS, because of its karstic gypsum-rich nature.

A comparative analysis with all 16S rRNA metagenomic sequences (Fig. 8.1) showed that samples from BKS clustered together (hierarchical clustering at the Order level) and were significantly different from those in Lake Redon (BKS *vs*. Lake Redon ANOSIM R = 0.8333, p-value = 0.029), which also clustered together. The main drivers of these differences were *Campylobacterales*, *Chlorobiales* and *Desulfobacterales* that were significantly higher in BKS (p-value < 0.05, wilcox-test) and *Cytophagales*, *Planktomycetales* and *Pseudomonadales* that were significantly more abundant in Lake Redon (p-value < 0.05, Wilcoxon-test).

Betaproteobacteria and *Actinobacteria* are the most common lineages of bacteria in freshwater lakes (Newton et al. 2011). Overall, in our cases study *Betaproteobacteria* was the most abundant group

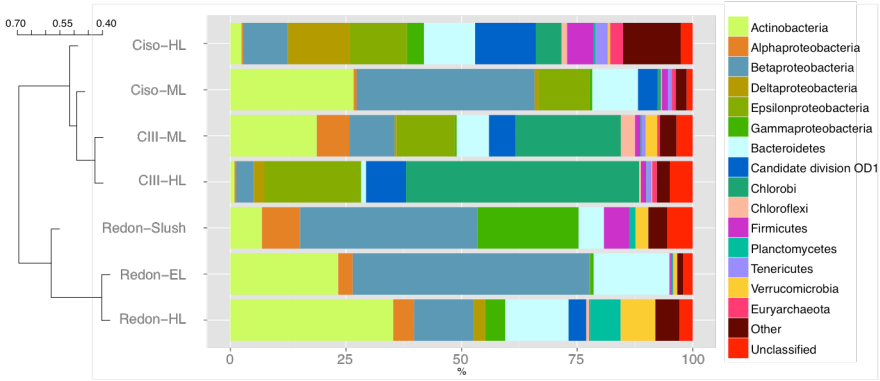

Figure 8.1: Prokaryotic community structure (relative abundances) of Banyoles Karstic Area (Lake Cisó and Lake Banyoles basin CIII) and Lake Redon obtained from the 16S rRNA gene present in the metagenomic pool. Hierarchical clustering based on Bray-Curtis dissimilarity matrices at the Order level. EL: Epilimnion; ML: Metalimnion; HL: Hypolimnion.

(23 ± 19%) followed by *Actinobacteria* (16 ± 13%). However, their dominance varied depending on the layer, with *Betaproteobacteria* being always higher in the presence of high oxygen (epilimnion and slush), whilst *Actinobacteria* dominated under lower oxygen concentrations like those found in BKS metalimnia or the hypolimnion of Lake Redon. *Bacteroidetes* is a very diverse chemoorganotrophic group with the potential to degrade complex biopolymers, which explains their important presence in both the eutrophic Lake Cisó and the oligotrophic Lake Redon where they can use either phytoplankton exudates during algal growth (Zeder et al. 2009) or complex dissolved organic matter (DOM) from senescent phytoplankton (Pinhassi et al. 2004, Teira et al. 2008). *Chlorobi* and *Epsilonproteobacteria* are not typical phyla found in oxygenated freshwater lakes and they were not found in Lake Redon. However, their abundances in BKS were very important, with GSB blooming in basin C-III of Lake Banyoles and *Epsilonproteobacteria* being consistently present in high abundances (>10%). Their importance is related to the oxidation of the abundant sulfide either through chemolithoautotrophy (*Epsilonproteobacteria*) or photolithoautotrophy (*Chlorobiales*).

In general, we observed that diversity was always higher in the hypolimnia than in the upper water masses. The relative abundances of Candidate Division OD1 in BKS (8 ± 4% all samples) and Lake Redon hypolimnia (4%), suggests an important role of this uncultured heterogeneous group in the biogeochemical cycling of stratified aquatic ecosystems. OD1 had been previously found in anoxic environments and may have the potential to be an obligate fermenter producing acetate, formate, lactate and ethanol as end products (Wrighton et al. 2012, Wrighton et al. 2014). Conversely, archaeal sequences were not abundant and mainly found in hypolimnetic waters, both in BKS (~3%; mostly methanogens) and Lake Redon (0.01%; Candidate division DHVEG-6). Previous studies analyzed and highlighted the role of archaea in oligotrophic environments, mainly ammonia-oxidizing archaea (AOA) (Auguet et al. 2011, Auguet et al. 2012, Restrepo-Ortiz et al. 2014), but also uncultured freshwater *Euryarchaeota* (Restrepo-Ortiz and Casamayor 2013). These studies also showed a strong seasonality of these AOA populations, which peaked in summer and were significantly related to the dynamics of ammonium and changes in the amount of atmospheric precipitation, which is the main source of nitrogen in remote mountain catchments (Catalan et al. 1994). Thus, we may have not captured the importance of archaea at the time of sampling (autumn) but they might be important depending on the biogeochemical dynamics of the lake.

8.2 Comparative analysis of the functional potential of the two contrasting ecosystems explored

The application of normalization procedures (Sharon et al. 2009b), permitted a comparison of the functional potential harboured in the different samples circumventing the different methodologies applied (Fig. 8.2). In contrast to taxonomic clustering (Fig. 8.1), functional clustering grouped together all planktonic samples, telling apart the slush as the most idiosyncratic sample as a consequence of an algal

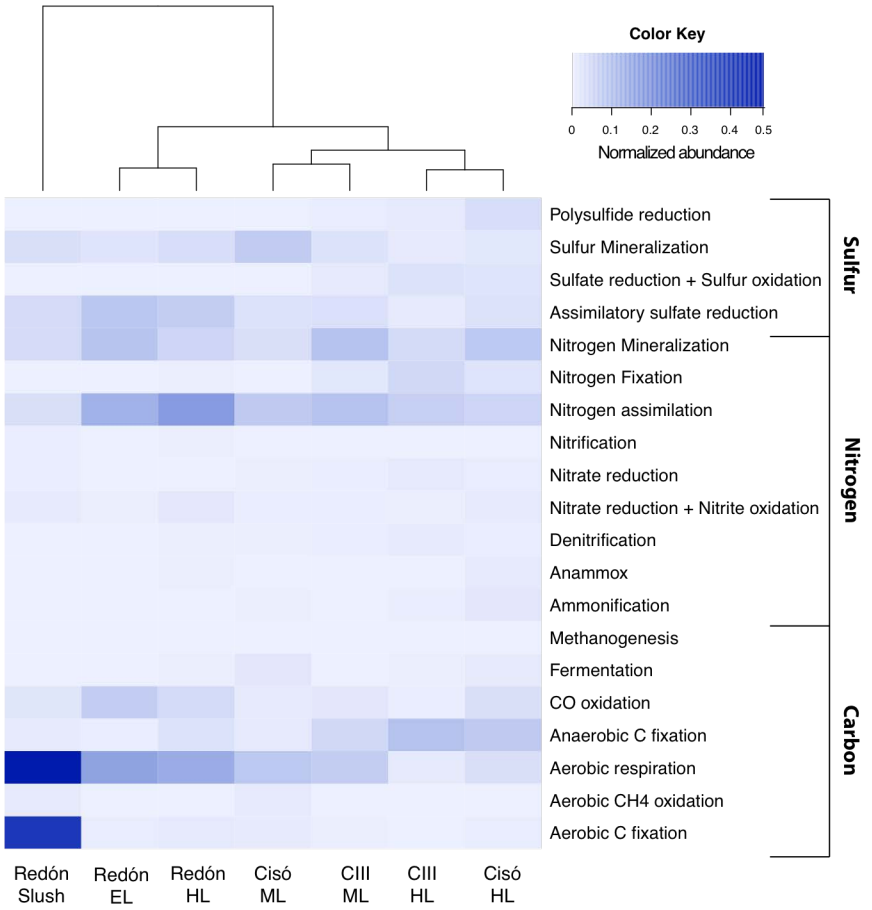

Figure 8.2: Heatmap plot and functional clustering of a selection of key KEGG Orthologs for the predicted open reading frames (ORFs) form the metagenomic reads of Banyoles Karstic Area (Lake Cisó and Lake Banyoles basin CIII) and Lake Redon. EL: Epilimnion; ML: Metalimnion; HL: Hypolimnion.

bloom and the predominance of aerobic C fixation and respiration. Both samples from Lake Redon clustered together, but the most interesting feature relied on the fact that BKS hypolimnia were functionally more similar each other than to metalimnia, in contrast to taxonomic clustering, which grouped the samples in agreement with sulfide concentrations, telling the most euxinic sample (Lake Cisó hypolimnion) apart (Chapter 4).

Using a comparative analysis merging the genetic potential for all the samples from BKS and Lake Redon, respectively, we carried

out an exercise to unveil which were the most important functions that described the characteristic biogeochemical cycling present in each system (Fig. 8.3).

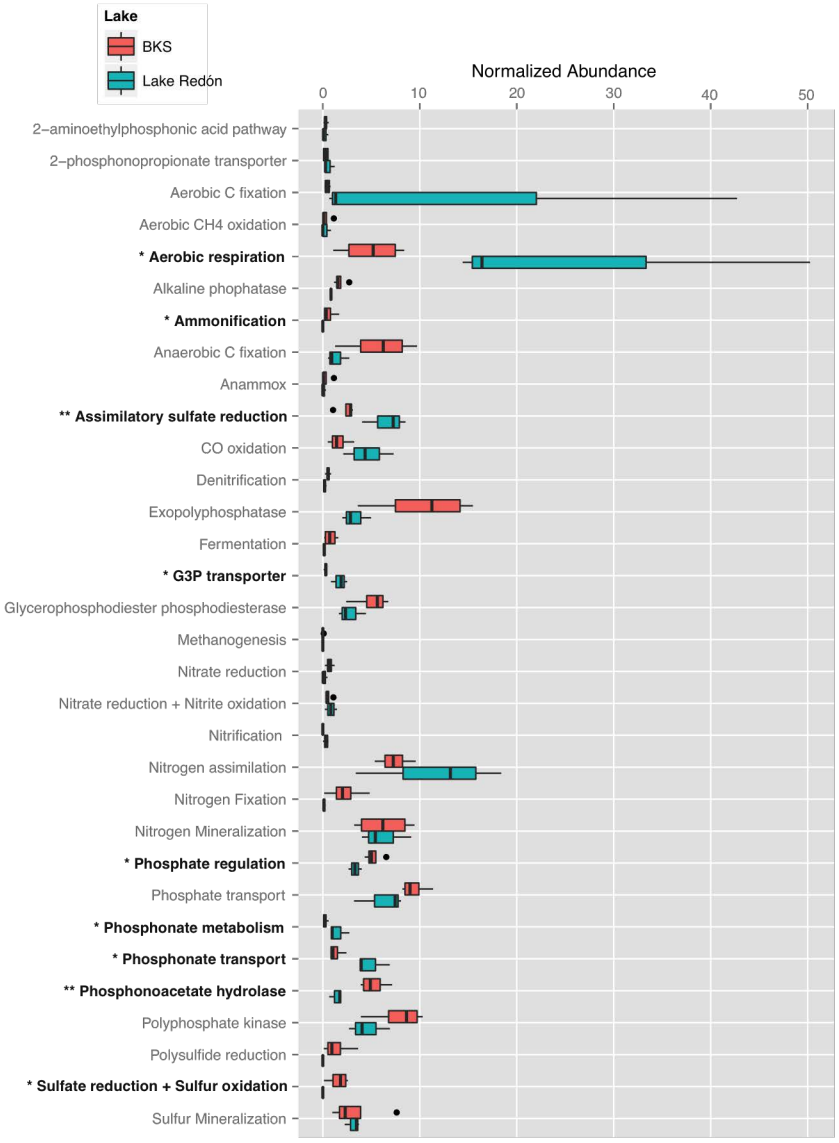

Figure 8.3: Heatmap plot and functional clustering of a selection of key KEGG Orthologs for the predicted open reading frames (ORFs) form the metagenomic reads of Banyoles karstic system (BKS: Lake Cisó and Lake Banyoles basin CIII) and Lake Redon. EL: Epilimnion; ML: Metalimnion; HL: Hypolimnion. Significant differences are labeled with one asterisk (p-value < 0.05, t-test) or two asterisks (p-value < 0.01, t-test).

For the carbon cycle, aerobic respiration was significantly higher in Lake Redon (p-value < 0.05, t-test), something that was expected for its mainly aerobic characteristics. The potential for aerobic C fixation through the Calvin cycle was also higher in Lake Redon as a consequence of the algal bloom in the slush sample. In contrast, anaerobic C fixation (both through phototrophic processes and chemotrophic processes) was, as expected, more abundant in BKS related to its sulfurous nature.

The nitrogen cycle only showed one significant difference (p-value < 0.05, t-test), the highest abundance of ammonification (Dissimilatory Nitrate Reduction to Ammonia; DNRA) in BKS. The first electron acceptor after oxygen is usually nitrate, thus the presence of DNRA potential in BKS where anoxia predominated, was expected. BKS usually show accumulation of ammonia in the hypolimnion, related to the lack of oxygen and presence of potentially toxic sulfide to ammonia oxidizers. In contrast, Lake Redon shows a higher potential for nitrification, mostly in the slush and hypolimnion. Finally, the potential for nitrogen assimilation was also higher in Lake Redon. Assimilatory pathways are those that lead to incorporation of a nutrient into organic (cellular) components. Possibly the ultraoligotrophic characteristics of Lake Redon force microbial populations to efficiently incorporate any nitrogen compound present in the environment and thus be overrepresented in the microbial metagenome.

For the sulfur cycle, assimilatory pathways were again significantly higher in Lake Redon than in BKS (p-value < 0.01, t-test). The vast availability of sulfur compounds in BKS probably makes it less important to incorporate essential sulfur into organic compounds, which turns into a vital necessity in Lake Redon. The potential for DNRA was detected in BKS but the sulfate-rich waters, makes it an appropriate environment for the development of sulfate-reducing bacteria and sulfide oxidizers. Consequently, in BKS the

genetic potential is higher for sulfate reduction and sulfur oxidation than for DNRA.

Finally, for the phosphorus cycle, G3P transporter, phosphonate metabolism and phosphonate transport were found to be significantly higher in Lake Redon (p-value < 0.05, t-test). The ultraoligotrophic nature of the lake and the phosphate limitation explain the higher proportion of pathways that led to efficiently incorporate and metabolize organic phosphorus (Chapter 7).

8.3 Potential and limitations of microbial metagenomics

We used two different metagenomic technologies in this PhD thesis: 454 pyrosequencing, producing a lower number (~300,000 reads / run) but longer reads (~400 bp) and Illumina, producing a larger number (~10 million reads / run) but shorter reads (~250 bp). Both protocols have been proved to be a good alternative to PCR-based 16S-tag sequencing for evaluate microbial structure and diversity (Logares et al. 2014). Bioinformatics filtering of the 16S sequences directly from the metagenomic reads avoids the use of PCR amplification and primer bias, which may result in changes of the *in situ* relative proportions. In general, a good agreement between methods is expected, but the use of 16S-tag sequencing and metagenomics in the same sample (Chapter 3 and 4), detected underestimation of *Epsilonproteobacteria* as a consequence of a mismatch in the reverse primer, thus confirming the advantages of using metagenomics to simultaneously explore both microbial biodiversity and functionality in a given ecosystem. However, the cost of metagenomics is still too high to be routinely used on a day-to-day basis for the simultaneous analysis of several tens of samples, and PCR-tag sequencing is a valid approach still for large comparisons of microbial communities at a reasonable cost.

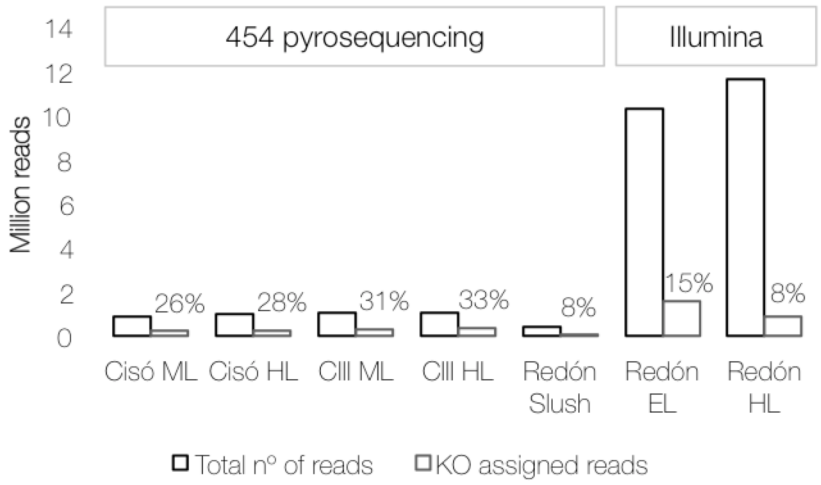

Figure 8.4: Plot showing the total number of reads for each metagenomics study and the percentage of functionally assigned reads by KEGG Orthology annotation. EL: Epilimnion; ML: Metalimnion; HL: Hypolimnion.

The massive application of metagenomics and whole-community sequencing, potentially could make available the entire genomic pool of a community. However, the whole annotation process lacks from a universal and comprehensible database in order to identify and contextualize all these sequences (Gilbert and Dupont 2011). A major pitfall during the annotation process is the low percentage of 'known' proteins. In this work, using the KEGG Orthology database we could only assign between 8 and 33% of the total reads (Fig. 8.4). As mentioned above, Illumina sequencing technology provides a much higher number of sequences than 454 sequencing, but the reads generated are shorter and only 8-15% of these reads could be annotated, which is common for other Illumina-based studies (Prakash and Taylor 2012). However, the slush sample by 454 sequencing, which typically yields 25% annotated reads (Simon et al. 2009, Lauro et al. 2011) also returned a low percentage of annotated reads (8%), suggesting that this special and undersampled environment may hide high levels of genomic novelty, possibly because no closely related representatives were found in the databases. The lack of cultured representatives and experimental

studies to confirm predicted functions are the main reason for this large pool of unknown proteins that we were not able to annotate and unveil their functions. The use of either experimental approaches (Reisch et al. 2008) or bioinformatic techniques (Abe et al. 2009, Jaroszewski et al. 2009) is currently of major interest to explore this unknown fraction of the metagenomic protein universe and to expand the potential and accuracy of metagenomics analyses.

Metagenomics can also be useful to obtain genomic information from uncultured organisms, especially in environmental samples of limited complexity. In this PhD thesis we used a natural blooming population of the uncultured green sulfur bacteria (GSB), *Chlorobium luteolum* CIII, to reconstruct its genome *in silico* (Chapter 5). The high similarity of *Chl*. *luteolum* CIII with a cultured counterpart, *Chl. luteolum* DSM273^{T} helped to carry out this reconstruction and added more insights on the debate of the prokaryote species definition (Doolittle and Zhaxybayeva 2009, Richter and Rossello-Mora 2009). The identification of key genomic differences through HGT events explained the ecological success of *Chl*. *luteolum* CIII. Altogether, we probably captured the first events in the ecological differentiation of a new species, with consistent genomic differences but still with high 16S rRNA gene identity (Shapiro et al. 2012). The genome reconstruction and the clues unveiled using bioinformatic analysis added evidences for a first putative GSB phage and for the key factors involved in speciation processes in prokaryotes and the importance of HGT in ecological success.

Overall, our analyses provided a new view on the well-known biogeochemical functioning of karstic and alpine lakes. In spite of the limitations of metagenomics and annotation, we used the previous knowledge on the ecology of the lakes to prove that metagenomics is a very accurate way to unveil the links between functional potential and microbial biodiversity of a given ecosystem. We also could identify some populations as potential key stone species of biogeochemical processes and this knowledge can be further used

to establish new hypothesis to be tested both through experimental approaches and matter and energy fluxes quantification. Finally, this PhD thesis also added some ideas in order to understand the functioning of ancient anoxic oceans, using euxinic lakes as modern analogs with different carbon inputs as proxies of different oceanic situations.

9

Conclusions

- The hypolimnia of Lakes Cisó, Vilar and Banyoles showed higher bacterial novelty than metalimnia with *Elusimicrobia* and *Chloroflexi* harbouring the highest number of novel 16S rRNA gene sequences.

- The potential for dark carbon fixation in these lakes was tentatively assigned to *Hydrogenophilales* (*Thiobacillus*-like) and *Gallionellales* (*Syderoxidans*-like) via the Calvin cycle, *Bacteroidales*, *Campylobacterales* and *Desulfarculales* through the Arnon cycle, and *Desulfobacterales* via the reductive acetil-CoA cycle.

- If the findings from sulfurous lakes are equivalent to ancient oceans (as in the case of green sulfur bacteria), then *Gallionellales* may have played an important role in the biogeochemistry of the iron cycle, a low contribution of nitrification and archaea was probably accounting for the nitrogen cycle, *Campylobacterales* may have acted as the main players of denitrification, and *Bacteroidales* may have been main players for dissimilatory nitrate reduction to ammonium mainly in organic carbon-rich zones.

- The acquisition of laterally transferred genes offering new functional alternatives, was key in order to explain the ecological success of the recurrent green sulfur bacteria bloom in Lake Banyoles basin CIII. The drivers for such horizontal gene transfer were potentially phages.

- In the slush of Lake Redon, the community composition shift from winter to spring was characterized by a decrease in bacterial diversity, dominance of *Bacteroidetes* and consistent increases in bacterial abundance and production.

- The potential for nitrification in Lake Redon was mainly found in the slush and hypolimnion by ammonia-oxidizing bacteria. Lower abundances of nitrification genes were found in the epilimnion.

- Planktonic microbial communities of Lake Redon showed a higher genomic potential for assimilatory pathways (nitrite, phosphate and sulfate) than those from the Banyoles area.

Bibliography

Bibliography

Abe, T., S. Kanaya, H. Uehara, and T. Ikemura. 2009. A novel bioinformatics strategy for function prediction of poorly-characterized protein genes obtained from metagenome analyses. DNA Res **16**:287-297.

Adams, W. P., and C. Allan. 1987. Aspects of the chemistry of ice, notably snow, on lakes. Pages 393–466 *in* H. G. Jones and W. J. Orville-Thomas, editors. Seasonal snowcovers: physics, chemistry, hydrology. Reidel Publishing Company, Dordrecht, The Netherlands.

Albertsen, M., P. Hugenholtz, A. Skarshewski, K. L. Nielsen, G. W. Tyson, and P. H. Nielsen. 2013. Genome sequences of rare, uncultured bacteria obtained by differential coverage binning of multiple metagenomes. Nature Biotechnology **31**:533-+.

Alfreider, A., J. Pernthaler, R. Amann, B. Sattler, F. O. Glockner, A. Wille, and R. Psenner. 1996. Community analysis of the bacterial assemblages in the winter cover and pelagic layers of a high mountain lake by in situ hybridization. Appl Environ Microbiol **62**:2138-2144.

Allgaier, M., H. Uphoff, A. Felske, and I. Wagner-Dobler. 2003. Aerobic anoxygenic photosynthesis in Roseobacter clade bacteria from diverse marine habitats. Appl Environ Microbiol **69**:5051-5059.

Aminov, R. I. 2010. A brief history of the antibiotic era: lessons learned and challenges for the future. Front Microbiol **1**.

Aminov, R. I. 2011. Horizontal gene exchange in environmental microbiota. Front Microbiol **2**.

Anbar, A. D. 2008. Oceans Elements and Evolution. Science **322**:1481-1483.

Andrews, S. C., A. K. Robinson, and F. Rodriguez-Quinones. 2003. Bacterial iron homeostasis. FEMS Microbiol Rev **27**:215-237.

Anesio, A. M., A. J. Hodson, A. Fritz, R. Psenner, and B. Sattler. 2009. High microbial activity on glaciers: importance to the global carbon cycle. Global Change Biology **15**:955-960.

Auguet, J. C., A. Barberan, and E. O. Casamayor. 2010. Global ecological patterns in uncultured Archaea. Isme Journal **4**:182-190.

Auguet, J. C., N. Nomokonova, L. Camarero, and E. O. Casamayor. 2011. Seasonal Changes of Freshwater Ammonia-Oxidizing Archaeal Assemblages and Nitrogen Species in Oligotrophic Alpine Lakes. Appl Environ Microbiol **77**:1937-1945.

Auguet, J. C., X. Triado-Margarit, N. Nomokonova, L. Camarero, and E. O. Casamayor. 2012. Vertical segregation and phylogenetic characterization of ammonia-oxidizing Archaea in a deep oligotrophic lake. Isme Journal **6**:1786-1797.

Azai, C., J. Harada, and H. Oh-oka. 2013. Gene Expression System in Green Sulfur Bacteria by Conjugative Plasmid Transfer. PLoS ONE **8**.

Aziz, R. K., D. Bartels, A. A. Best, M. DeJongh, T. Disz, R. A. Edwards, K. Formsma, S. Gerdes, E. M. Glass, M. Kubal, F. Meyer, G. J. Olsen, R. Olson, A. L. Osterman, R. A. Overbeek, L. K. McNeil, D. Paarmann, T. Paczian, B. Parrello, G. D. Pusch, C. Reich, R. Stevens, O. Vassieva, V. Vonstein, A. Wilke, and O. Zagnitko. 2008. The RAST Server: rapid annotations using subsystems technology. BMC Genomics **9**:75.

Bañeras, L., M. Ros-Ponsati, X. P. Cristina, J. L. Garcia-Gil, and C. M. Borrego. 2010. Phosphorus deficiency and kinetics of alkaline phosphatase in isolates and natural populations of phototrophic sulphur bacteria. FEMS Microbiol Ecol **73**:243-253.

Barberan, A., and E. O. Casamayor. 2010. Global phylogenetic community structure and beta-diversity patterns in surface bacterioplankton metacommunities. Aquatic Microbial Ecology **59**:1-10.

Barberan, A., and E. O. Casamayor. 2011. Euxinic Freshwater Hypolimnia Promote Bacterial Endemicity in Continental Areas. Microb Ecol **61**:465-472.

Barberan, A., and E. O. Casamayor. 2014. A phylogenetic perspective on species diversity, beta-diversity and biogeography for the microbial world. Mol Ecol **23**:5868-5876.

Bascompte, J., and R. V. Sole. 1995. Rethinking Complexity - Modeling Spatiotemporal Dynamics in Ecology. Trends in Ecology & Evolution **10**:361-366.

Beja, O., M. T. Suzuki, J. F. Heidelberg, W. C. Nelson, C. M. Preston, T. Hamada, J. A. Eisen, C. M. Fraser, and E. F. DeLong. 2002. Unsuspected diversity among marine aerobic anoxygenic phototrophs. Nature **415**:630-633.

Bettarel, Y., T. Sime-Ngando, C. Amblard, and J. Dolan. 2004. Viral activity in two contrasting lake ecosystems. Appl Environ Microbiol **70**:2941-2951.

Bhaya, D., A. R. Grossman, A. S. Steunou, N. Khuri, F. M. Cohan, N. Hamamura, M. C. Melendrez, M. M. Bateson, D. M. Ward, and J. F. Heidelberg. 2007. Population level functional diversity in a microbial community revealed by comparative genomic and metagenomic analyses. Isme Journal **1**:703-713.

Billington, S. J., A. S. Huggins, P. A. Johanesen, P. K. Crellin, J. K. Cheung, M. E. Katz, C. L. Wright, V. Haring, and J. I. Rood. 1999. Complete nucleotide

sequence of the 27-kilobase virulence related locus (vrl) of Dichelobacter nodosus: Evidence for extrachromosomal origin. Infection and Immunity **67**:1277-1286.

Bjorkman, K. M., and D. M. Karl. 2003. Bioavailability of dissolved organic phosphorus in the euphotic zone at station ALOHA, North Pacific Subtropical Gyre. Limnology and Oceanography **48**:1049-1057.

Borrego, C. M., L. Baneras, and J. Garcia-Gil. 1999. Temporal variability of Chlorobium phaeobacteroides antenna pigments in a meromictic karstic lake. Aquatic Microbial Ecology **17**:121-129.

Bowman, J. P., S. A. McCammon, M. V. Brown, D. S. Nichols, and T. A. McMeekin. 1997. Diversity and association of psychrophilic bacteria in Antarctic sea ice. Appl Environ Microbiol **63**:3068-3078.

Boyd, P. W., A. J. Watson, C. S. Law, E. R. Abraham, T. Trull, R. Murdoch, D. C. E. Bakker, A. R. Bowie, K. O. Buesseler, H. Chang, M. Charette, P. Croot, K. Downing, R. Frew, M. Gall, M. Hadfield, J. Hall, M. Harvey, G. Jameson, J. LaRoche, M. Liddicoat, R. Ling, M. T. Maldonado, R. M. McKay, S. Nodder, S. Pickmere, R. Pridmore, S. Rintoul, K. Safi, P. Sutton, R. Strzepek, K. Tanneberger, S. Turner, A. Waite, and J. Zeldis. 2000. A mesoscale phytoplankton bloom in the polar Southern Ocean stimulated by iron fertilization. Nature **407**:695-702.

Brinkmeyer, R., K. Knittel, J. Jurgens, H. Weyland, R. Amann, and E. Helmke. 2003. Diversity and structure of bacterial communities in arctic versus antarctic pack ice. Appl Environ Microbiol **69**:6610-6619.

Brock, T. D. 1966. Principles of Microbial Ecology. Prentice-Hall, Englewood Cliffs, New Jersey, USA.

Brocks, J. J., G. D. Love, R. E. Summons, A. H. Knoll, G. A. Logan, and S. A. Bowden. 2005. Biomarker evidence for green and purple sulphur bacteria in a stratified Palaeoproterozoic sea. Nature **437**:866-870.

Brown, C. T., L. A. Hug, B. C. Thomas, I. Sharon, C. J. Castelle, A. Singh, M. J. Wilkins, K. C. Wrighton, K. H. Williams, and J. F. Banfield. 2015. Unusual biology across a group comprising more than 15% of domain Bacteria. Nature **advance online publication**.

Bryant, D., Z. Liu, T. Li, F. Zhao, A. G. Costas, C. Klatt, D. Ward, N.-U. Frigaard, and J. Overmann. 2012. Comparative and Functional Genomics of Anoxygenic Green Bacteria from the Taxa Chlorobi, Chloroflexi, and Acidobacteria. Pages 47-102 *in* R. Burnap and W. Vermaas, editors. Functional Genomics and Evolution of Photosynthetic Systems. Springer Netherlands.

Burgin, A. J., and S. K. Hamilton. 2007. Have we overemphasized the role of denitrification in aquatic ecosystems? A review of nitrate removal pathways. Frontiers in Ecology and the Environment **5**:89-96.

Caliz, J., and E. O. Casamayor. 2014. Environmental controls and composition of anoxygenic photoheterotrophs in ultraoligotrophic high-altitude lakes (Central Pyrenees). Environ Microbiol Rep **6**:145-151.

Camacho, A., and E. Vicente. 1998. Carbon photoassimilation by sharply stratified phototrophic communities at the chemocline of Lake Arcas (Spain). FEMS Microbiol Ecol **25**:11-22.

Camarero, L., and J. Catalan. 1993. Chemistry of Bulk Precipitation in the Central and Eastern Pyrenees, Northeast Spain. Atmospheric Environment Part a-General Topics **27**:83-94.

Camarero, L., and J. Catalan. 2012. Atmospheric phosphorus deposition may cause lakes to revert from phosphorus limitation back to nitrogen limitation. Nat Commun **3**:1118.

Camarero, L., M. Felip, M. Ventura, F. Bartumeus, and J. Catalan. 1999. The relative importance of the planktonic food web in the carbon cycle of an oligotrophic mountain lake in a poorly vegetated catchment (Redó, Pyrenees). Journal of Limnology **58**:203-212.

Campbell, B. J., and S. C. Cary. 2004. Abundance of reverse tricarboxylic acid cycle genes in free-living microorganisms at deep-sea hydrothermal vents. Appl Environ Microbiol **70**:6282-6289.

Canfield, D. E., A. N. Glazer, and P. G. Falkowski. 2010. The evolution and future of Earth's nitrogen cycle. Science **330**:192-196.

Carini, P., A. E. White, E. O. Campbell, and S. J. Giovannoni. 2014. Methane production by phosphate-starved SAR11 chemoheterotrophic marine bacteria. Nat Commun **5**:4346.

Carver, T., S. R. Harris, M. Berriman, J. Parkhill, and J. A. McQuillan. 2012. Artemis: an integrated platform for visualization and analysis of high-throughput sequence-based experimental data. Bioinformatics **28**:464-469.

Carver, T., N. Thomson, A. Bleasby, M. Berriman, and J. Parkhill. 2009. DNAPlotter: circular and linear interactive genome visualization. Bioinformatics **25**:119-120.

Carver, T. J., K. M. Rutherford, M. Berriman, M. A. Rajandream, B. G. Barrell, and J. Parkhill. 2005. ACT: the Artemis Comparison Tool. Bioinformatics **21**:3422-3423.

Casamayor, E. O. 2010. Vertical distribution of planktonic autotrophic thiobacilli and dark CO2 fixation rates in lakes with oxygen-sulfide interfaces. Aquatic Microbial Ecology **59**:217-228.

Casamayor, E. O., I. Ferrera, X. Cristina, C. M. Borrego, and J. M. Gasol. 2007. Flow cytometric identification and enumeration of photosynthetic sulfur bacteria and potential for ecophysiological studies at the single-cell level. Environ Microbiol **9**:1969-1985.

Casamayor, E. O., J. Garcia-Cantizano, and C. Pedros-Alio. 2008. Carbon dioxide fixation in the dark by photosynthetic bacteria in sulfide-rich stratified lakes with oxic-anoxic interfaces. Limnology and Oceanography **53**:1193-1203.

Casamayor, E. O., M. Lliros, A. Picazo, A. Barberan, C. M. Borrego, and A. Camacho. 2012. Contribution of deep dark fixation processes to overall CO2 incorporation and large vertical changes of microbial populations in stratified karstic lakes. Aquatic Sciences **74**:61-75.

Casamayor, E. O., J. Mas, and C. Pedros-Alio. 2001a. In Situ Assessment on the Physiological State of Purple and Green Sulfur Bacteria through the Analyses of Pigment and 5S rRNA Content. Microb Ecol **42**:427-437.

Casamayor, E. O., G. Muyzer, and C. Pedros-Alio. 2001b. Composition and temporal dynamics of planktonic archaeal assemblages from anaerobic sulfurous environments studied by 16S rDNA denaturing gradient gel electrophoresis and sequencing. Aquatic Microbial Ecology **25**:237-246.

Casamayor, E. O., C. Pedros-Alio, G. Muyzer, and R. Amann. 2002. Microheterogeneity in 16S ribosomal DNA-defined bacterial populations from a stratified planktonic environment is related to temporal changes and to ecological adaptations. Appl Environ Microbiol **68**:1706-1714.

Casamayor, E. O., H. Schafer, L. Baneras, C. Pedros-Alio, and G. Muyzer. 2000. Identification of and spatio-temporal differences between microbial assemblages from two neighboring sulfurous lakes: Comparison by microscopy and denaturing gradient gel electrophoresis. Appl Environ Microbiol **66**:499-508.

Casamayor, E. O., X. Triado-Margarit, and C. Castaneda. 2013. Microbial biodiversity in saline shallow lakes of the Monegros Desert, Spain. FEMS Microbiol Ecol **85**:503-518.

Castresana, J. 2000. Selection of conserved blocks from multiple alignments for their use in phylogenetic analysis. Mol Biol Evol **17**:540-552.

Catalan, J. 1988. Physical properties of the environment relevant to the pelagic ecosystem of a deep high-mountain lake (Estany Redó, Central Pyrenees). Oecol. aquat **9**:89-123.

Catalan, J. 1989. The winter cover of a high-mountain mediterranean lake (Estany-Redo, Pyrenees). Water Resources Research **25**:519-527.

Catalan, J. 1992. Evolution of dissolved and particulate matter during the ice-covered period in a deep, high-mountain lake. Canadian Journal of Fisheries and Aquatic Sciences **49**:945-955.

Catalan, J., E. Ballesteros, L. Camarero, M. Felip, and E. Gacia. 1992. Limnology in the Pyrenean lakes. Limnetica **8**:27-38.

Catalan, J., and L. Camarero. 1991. Ergoclines and Biological Processes in High Mountain Lakes - Similarities between Summer Stratification and the Ice-Forming Periods in Lake Redo (Pyrenees). International Association of Theoretical and Applied Limnology - Proceedings, Vol 24, Pt 2 **24**:1011-1015.

Catalan, J., L. Camarero, M. Felip, S. Pla, M. Ventura, T. Buchaca, F. Bartumeus, G. de Mendoza, A. Miró, E. Casamayor, J. Sánchez-Medina, M. Bacardit, M. Altuna, M. Bartrons, and D. Díaz de Quijano. 2006. High mountain lakes: extreme habitats and witnesses of environmental changes. Limnetica **25**:551-584.

Catalan, J., L. Camarero, E. Gacia, E. Ballesteros, and M. Felip. 1994. Nitrogen in the Pyrenean lakes (Spain). Hydrobiologia **274**:17-27.

Catalan, J., S. Pla, M. Rieradevall, M. Felip, M. Ventura, T. Buchaca, L. Camarero, A. Brancelj, P. G. Appleby, A. Lami, A. Grytnes, A. Agusti-Panareda, and R. Thompson. 2002. Lake Redo ecosystem response to an increasing warming in the Pyrenees during the twentieth century. Journal of Paleolimnology **28**:129-145.

Chauhan, D., I. M. Folea, C. C. Jolley, R. Kouril, C. E. Lubner, S. Lin, D. Kolber, F. Wolfe-Simon, J. H. Golbeck, E. J. Boekema, and P. Fromme. 2011. A Novel Photosynthetic Strategy for Adaptation to Low-Iron Aquatic Environments. Biochemistry **50**:686-692.

Cheetham, B. F., D. B. Tattersall, G. A. Bloomfield, J. I. Rood, and M. E. Katz. 1995. Identification of a Gene Encoding a Bacteriophage-Related Integrase in a Vap Region of the Dichelobacter-Nodosus Genome. Gene **162**:53-58.

Chiura, H. X. 1997. Generalized gene transfer by virus-like particles from marine bacteria. Aquatic Microbial Ecology **13**:75-83.

Cohan, F. M., and A. F. Koeppel. 2008. The Origins of Ecological Diversity in Prokaryotes. Current Biology **18**:R1024-U1017.

Cohen, P. T., and P. Cohen. 1989. Discovery of a protein phosphatase activity encoded in the genome of bacteriophage lambda. Probable identity with open reading frame 221. Biochem J **260**:931-934.

Comeau, A. M., T. Harding, P. E. Galand, W. F. Vincent, and C. Lovejoy. 2012. Vertical distribution of microbial communities in a perennially stratified Arctic lake with saline, anoxic bottom waters. Scientific Reports **2**.

Crump, B. C., G. W. Kling, M. Bahr, and J. E. Hobbie. 2003. Bacterioplankton community shifts in an arctic lake correlate with seasonal changes in organic matter source. Appl Environ Microbiol **69**:2253-2268.

Damsté, J. S. S., and J. Köster. 1998. A euxinic southern North Atlantic Ocean during the Cenomanian/Turonian oceanic anoxic event. Earth and Planetary Science Letters **158**:165-173.

De Palmenaer, D., P. Siguier, and J. Mahillon. 2008. IS4 family goes genomic. BMC Evol Biol **8**:18.

del Campo, J., and R. Massana. 2011. Emerging Diversity within Chrysophytes, Choanoflagellates and Bicosoecids Based on Molecular Surveys. Protist **162**:435-448.

Deng, L., and P. K. Hayes. 2008. Evidence for cyanophages active against bloom-forming freshwater cyanobacteria. Freshwater Biology **53**:1240-1252.

Diaz, R. J., and R. Rosenberg. 2008. Spreading dead zones and consequences for marine ecosystems. Science **321**:926-929.

Doolittle, W. F., and O. Zhaxybayeva. 2009. On the origin of prokaryotic species. Genome Res **19**:744-756.

Dumestre, J. F., E. O. Casamayor, R. Massana, and C. Pedros-Alio. 2002. Changes in bacterial and archaeal assemblages in an equatorial river induced by the water eutrophication of Petit Saut dam reservoir (French Guiana). Aquatic Microbial Ecology **26**:209-221.

Dupont, C. L., J. Larsson, S. Yooseph, K. Ininbergs, J. Goll, J. Asplund-Samuelsson, J. P. McCrow, N. Celepli, L. Z. Allen, M. Ekman, A. J. Lucas, Å. Hagström, M. Thiagarajan, B. Brindefalk, A. R. Richter, A. F. Andersson, A. Tenney, D. Lundin, A. Tovchigrechko, J. A. A. Nylander, D. Brami, J. H. Badger, A. E. Allen, D. B. Rusch, J. Hoffman, E. Norrby, R. Friedman, J. Pinhassi, J. C. Venter, and B. Bergman. 2014. Functional Tradeoffs Underpin Salinity-Driven Divergence in Microbial Community Composition. PLoS ONE **9**:e89549.

Dupont, C. L., D. B. Rusch, S. Yooseph, M. J. Lombardo, R. A. Richter, R. Valas, M. Novotny, J. Yee-Greenbaum, J. D. Selengut, D. H. Haft, A. L. Halpern, R. S. Lasken, K. Nealson, R. Friedman, and J. C. Venter. 2012. Genomic insights to SAR86, an abundant and uncultivated marine bacterial lineage. Isme Journal **6**:1186-1199.

Dupont, C. L., S. Yang, B. Palenik, and P. E. Bourne. 2006. Modern proteomes contain putative imprints of ancient shifts in trace metal geochemistry. Proc Natl Acad Sci U S A **103**:17822-17827.

Dyhrman, S. T., J. W. Ammerman, and B. A. S. Van Mooy. 2007. Microbes and the Marine Phosphorus Cycle. Oceanography **20**:110-116.

Dyhrman, S. T., P. D. Chappell, S. T. Haley, J. W. Moffett, E. D. Orchard, J. B. Waterbury, and E. A. Webb. 2006. Phosphonate utilization by the globally important marine diazotroph Trichodesmium. Nature **439**:68-71.

Edgar, R. C. 2004. MUSCLE: multiple sequence alignment with high accuracy and high throughput. Nucleic Acids Res **32**:1792-1797.

Edgar, R. C. 2010. Search and clustering orders of magnitude faster than BLAST. Bioinformatics **26**:2460-2461.

Edgar, R. C., B. J. Haas, J. C. Clemente, C. Quince, and R. Knight. 2011. UCHIME improves sensitivity and speed of chimera detection. Bioinformatics **27**:2194-2200.

Ekau, W., H. Auel, H. O. Portner, and D. Gilbert. 2010. Impacts of hypoxia on the structure and processes in pelagic communities (zooplankton, macro-invertebrates and fish). Biogeosciences **7**:1669-1699.

Eppacher, T. 1966. Umweltfaktoren und Lebewelt im Pelagial des Gossenköllesees (Kühtai, Stubaier Alpen, 2.413 m). PhD thesis. University of Innsbruck.

Ewing, B., L. Hillier, M. C. Wendl, and P. Green. 1998. Base-calling of automated sequencer traces using phred. I. Accuracy assessment. Genome Res **8**:175-185.

Felip, M., F. Bartumeus, S. Halac, and J. Catalan. 1999a. Microbial plankton assemblages, composition and biomass, during two ice-free periods in a deep high mountain lake (Estany Redó, Pyrenees). Journal of Limnology **58**:10.

Felip, M., L. Camarero, and J. Catalan. 1999b. Temporal changes of microbial assemblages in the ice and snow cover of a high mountain lake. Limnology and Oceanography **44**:973-987.

Felip, M., B. Sattler, R. Psenner, and J. Catalan. 1995. Highly active microbial communities in the ice and snow cover of high mountain lakes. Appl Environ Microbiol **61**:2394-2401.

Felip, M., A. Wille, B. Sattler, and R. Psenner. 2002. Microbial communities in the winter cover and the water column of an alpine lake: system connectivity and uncoupling. Aquatic Microbial Ecology **29**:123-134.

Fernandez-Gomez, B., M. Richter, M. Schuler, J. Pinhassi, S. G. Acinas, J. M. Gonzalez, and C. Pedros-Alio. 2013. Ecology of marine Bacteroidetes: a comparative genomics approach. Isme Journal **7**:1026-1037.

Fernandez-Guerra, A., and E. O. Casamayor. 2012. Habitat-Associated Phylogenetic Community Patterns of Microbial Ammonia Oxidizers. PLoS ONE **7**.

Ferrera, I., R. Massana, E. O. Casamayor, V. Balague, O. Sanchez, C. Pedros-Alio, and J. Mas. 2004. High-diversity biofilm for the oxidation of sulfide-containing effluents. Applied Microbiology and Biotechnology **64**:726-734.

Figueras, J. B., L. J. Garcia-Gil, and C. A. Abella. 1997. Phylogeny of the genus Chlorobium based on 16S rDNA sequence. FEMS Microbiol Lett **152**:31-36.

Fillol, M., A. Sànchez-Melsió, F. Gich, and C. M. Borrego. 2015. Diversity of Miscellaneous Crenarchaeotic Group archaea in freshwater karstic lakes and their segregation between planktonic and sediment habitats.

Franken, C., G. Haase, C. Brandt, J. Weber-Heynemann, S. Martin, C. Lammler, A. Podbielski, R. Lutticken, and B. Spellerberg. 2001. Horizontal gene transfer and host specificity of beta-haemolytic streptococci: the role of a putative composite transposon containing scpB and lmb. Molecular Microbiology **41**:925-935.

Freeman, K. R., A. P. Martin, D. Karki, R. C. Lynch, M. S. Mitter, A. F. Meyer, J. E. Longcore, D. R. Simmons, and S. K. Schmidt. 2009. Evidence that chytrids dominate fungal communities in high-elevation soils. Proc Natl Acad Sci U S A **106**:18315-18320.

Frigaard, N.-U., and D. Bryant. 2008. Genomic Insights into the Sulfur Metabolism of Phototrophic Green Sulfur Bacteria. Pages 337-355 *in* R. Hell, C. Dahl, D. Knaff, and T. Leustek, editors. Sulfur Metabolism in Phototrophic Organisms. Springer Netherlands.

Frigaard, N.-U., and D. A. Bryant. 2006. Chlorosomes: antenna organelles in photosynthetic green bacteria. Pages 79-114 Complex intracellular structures in prokaryotes. Springer.

Frigaard, N. U., and D. A. Bryant. 2001. Chromosomal gene inactivation in the green sulfur bacterium Chlorobium tepidum by natural transformation. Appl Environ Microbiol **67**:2538-2544.

Fuchs, G. 2011. Alternative Pathways of Carbon Dioxide Fixation: Insights into the Early Evolution of Life? Pages 631-+ *in* S. Gottesman and C. S. Harwood, editors. Annual Review of Microbiology, Vol 65. Annual Reviews, Palo Alto.

Fuchsman, C. A., and G. Rocap. 2006. Whole-genome reciprocal BLAST analysis reveals that planctomycetes do not share an unusually large number of genes with Eukarya and Archaea. Appl Environ Microbiol **72**:6841-6844.

Fuhrman, J. A. 1999. Marine viruses and their biogeochemical and ecological effects. Nature **399**:541-548.

Fuhrman, J. A., M. S. Schwalbach, and U. Stingl. 2008. Proteorhodopsins: an array of physiological roles? Nat Rev Microbiol **6**:488-494.

Gadkari, D., K. Schricker, G. Acker, R. M. Kroppenstedt, and O. Meyer. 1990. Streptomyces thermoautotrophicus sp. nov., a Thermophilic CO- and H(2)-Oxidizing Obligate Chemolithoautotroph. Appl Environ Microbiol **56**:3727-3734.

Galloway, J. N., A. R. Townsend, J. W. Erisman, M. Bekunda, Z. Cai, J. R. Freney, L. A. Martinelli, S. P. Seitzinger, and M. A. Sutton. 2008. Transformation of the nitrogen cycle: recent trends, questions, and potential solutions. Science **320**:889-892.

Garcia-Cantizano, J., E. O. Casamayor, J. M. Gasol, R. Guerrero, and C. Pedros-Alio. 2005. Partitioning of CO2 incorporation among planktonic microbial guilds and estimation of in situ specific growth rates. Microb Ecol **50**:230-241.

Garcia-Descalzo, L., E. Garcia-Lopez, M. Postigo, F. Baquero, A. Alcazar, and C. Cid. 2013. Eukaryotic microorganisms in cold environments: examples from Pyrenean glaciers. Front Microbiol **4**:55.

Garcia-Gil, L. J. 1990. Phototrophic bacteria and iron cycle in Lake Banyoles. Autonomous University of Barcelona.

Garcia-Gil, L. J., and C. A. Abella. 1992. Population dynamics of phototrophic bacteria in three basins of Lake Banyoles (Spain). Pages 87-94 *in* V. Ilmavirta and R. Jones, editors. The Dynamics and Use of Lacustrine Ecosystems. Springer Netherlands.

Garcia-Gil, L. J., L. Salagenoher, J. V. Esteva, and C. A. Abella. 1990. Distribution of iron in lake Banyoles in relation to the ecology of purple and green sulur bacteria. Hydrobiologia **192**:259-270.

Ghosh, W., and B. Dam. 2009. Biochemistry and molecular biology of lithotrophic sulfur oxidation by taxonomically and ecologically diverse bacteria and archaea. FEMS Microbiol Rev **33**:999-1043.

Gich, F., J. Garcia-Gil, and J. Overmann. 2001. Previously unknown and phylogenetically diverse members of the green nonsulfur bacteria are indigenous to freshwater lakes. Archives of Microbiology **177**:1-10.

Gies, E. A., K. M. Konwar, J. T. Beatty, and S. J. Hallam. 2014. Illuminating Microbial Dark Matter in Meromictic Sakinaw Lake. Appl Environ Microbiol **80**:6807-6818.

Gifford, S. M., S. Sharma, J. M. Rinta-Kanto, and M. A. Moran. 2011. Quantitative analysis of a deeply sequenced marine microbial metatranscriptome. ISME J **5**:461-472.

Gilbert, J. A., and C. L. Dupont. 2011. Microbial metagenomics: beyond the genome. Ann Rev Mar Sci **3**:347-371.

Glockner, F. O., E. Zaichikov, N. Belkova, L. Denissova, J. Pernthaler, A. Pernthaler, and R. Amann. 2000. Comparative 16S rRNA analysis of lake bacterioplankton reveals globally distributed phylogenetic clusters including an abundant group of actinobacteria. Appl Environ Microbiol **66**:5053-5065.

Goll, J., D. B. Rusch, D. M. Tanenbaum, M. Thiagarajan, K. Li, B. A. Methe, and S. Yooseph. 2010. METAREP: JCVI metagenomics reports--an open source tool for high-performance comparative metagenomics. Bioinformatics **26**:2631-2632.

Gomez Maqueo Chew, A., N. U. Frigaard, and D. A. Bryant. 2007. Bacteriochlorophyllide c C-8(2) and C-12(1) methyltransferases are essential for adaptation to low light in Chlorobaculum tepidum. Journal of Bacteriology **189**:6176-6184.

Gordon, D. 2003. Viewing and editing assembled sequences using Consed. Curr Protoc Bioinformatics **Chapter 11**:Unit11 12.

Gordon, D., C. Abajian, and P. Green. 1998. Consed: a graphical tool for sequence finishing. Genome Res **8**:195-202.

Gregersen, L. H., D. A. Bryant, and N. U. Frigaard. 2011. Mechanisms and evolution of oxidative sulfur metabolism in green sulfur bacteria. Front Microbiol **2**:116.

Gregersen, L. H., K. S. Habicht, S. Peduzzi, M. Tonolla, D. E. Canfield, M. Miller, R. P. Cox, and N. U. Frigaard. 2009. Dominance of a clonal green sulfur bacterial population in a stratified lake. FEMS Microbiol Ecol **70**:30-41.

Grote, J., G. Jost, M. Labrenz, G. J. Herndl, and K. Juergens. 2008. Epsilonproteobacteria Represent the Major Portion of Chemoautotrophic Bacteria in Sulfidic Waters of Pelagic Redoxclines of the Baltic and Black Seas. Appl Environ Microbiol **74**:7546-7551.

Grote, J., T. Schott, C. G. Bruckner, F. O. Glockner, G. Jost, H. Teeling, M. Labrenz, and K. Jurgens. 2012. Genome and physiology of a model Epsilonproteobacterium responsible for sulfide detoxification in marine oxygen depletion zones. Proc Natl Acad Sci U S A **109**:506-510.

Guerrero, M. A., and R. D. Jones. 1996. Photoinhibition of marine nitrifying bacteria. I. Wavelength-dependent response. Marine ecology progress series. Oldendorf **141**:183-192.

Guerrero, R., E. Montesinos, I. Esteve, and C. Abella. 1980. Physiological Adaptation and Growth of Purple and Green Sulfur Bacteria in a Meromictic Lake (Vila) as Compared to a Holomictic Lake (Siso). Pages 161-171 *in* M. Dokulil, H. Metz, and D. Jewson, editors. Shallow Lakes Contributions to their Limnology. Springer Netherlands.

Guerrero, R., E. Montesinos, C. Pedros-Alio, I. Esteve, J. Mas, H. Van Gemerden, P. A. G. Hofman, and J. F. Bakker. 1985. Phototrophic sulfur bacteria in two Spanish lakes: vertical distribution and limiting factors. Limnology and Oceanography **30**:919-931.

Guy, L., J. R. Kultima, and S. G. Andersson. 2010. genoPlotR: comparative gene and genome visualization in R. Bioinformatics **26**:2334-2335.

Habicht, K. S., M. Miller, R. P. Cox, N. U. Frigaard, M. Tonolla, S. Peduzzi, L. G. Falkenby, and J. S. Andersen. 2011. Comparative proteomics and activity of a green sulfur bacterium through the water column of Lake Cadagno, Switzerland. Environ Microbiol **13**:203-215.

Halary, S., J. W. Leigh, B. Cheaib, P. Lopez, and E. Bapteste. 2010. Network analyses structure genetic diversity in independent genetic worlds. Proc Natl Acad Sci U S A **107**:127-132.

Harada, J., T. Mizoguchi, S. Satoh, Y. Tsukatani, M. Yokono, M. Noguchi, A. Tanaka, and H. Tamiaki. 2013. Specific Gene bciD for C7-Methyl Oxidation in Bacteriochlorophyll e Biosynthesis of Brown-Colored Green Sulfur Bacteria. PLoS ONE **8**.

Harding, T., A. D. Jungblut, C. Lovejoy, and W. F. Vincent. 2011. Microbes in High Arctic Snow and Implications for the Cold Biosphere. Appl Environ Microbiol **77**:3234-3243.

Haring, V., S. J. Billington, C. L. Wright, A. S. Huggins, M. E. Katz, and J. I. Rood. 1995. Delineation of the Virulence-Related Locus (Vrl) of Dichelobacter-Nodosus. Microbiology-Uk **141**:2081-2089.

Herlemann, D. P. R., O. Geissinger, and A. Brune. 2007. The termite group I phylum is highly diverse and widespread in the environment. Appl Environ Microbiol **73**:6682-6685.

Herlemann, D. P. R., O. Geissinger, W. Ikeda-Ohtsubo, V. Kunin, H. Sun, A. Lapidus, P. Hugenholtz, and A. Brune. 2009. Genomic Analysis of "Elusimicrobium minutum," the First Cultivated Representative of the Phylum "Elusimicrobia" (Formerly Termite Group 1). Appl Environ Microbiol **75**:2841-2849.

Hervas, A., L. Camarero, I. Reche, and E. O. Casamayor. 2009. Viability and potential for immigration of airborne bacteria from Africa that reach high mountain lakes in Europe. Environ Microbiol **11**:1612-1623.

Hervas, A., and E. O. Casamayor. 2009. High similarity between bacterioneuston and airborne bacterial community compositions in a high mountain lake area. FEMS Microbiol Ecol **67**:219-228.

Hirabayashi, H., T. Ishii, S. Takaichi, K. Inoue, and K. Uehara. 2004. The role of carotenoids in the photoadaptation of the brown-colored sulfur bacterium Chlorobium phaeobacteroides. Photochem Photobiol **79**:280-285.

Holmer, M., and P. Storkholm. 2001. Sulphate reduction and sulphur cycling in lake sediments: a review. Freshwater Biology **46**:431-451.

Huang, Y., P. Gilna, and W. Li. 2009. Identification of ribosomal RNA genes in metagenomic fragments. Bioinformatics **25**:1338-1340.

Huber, C., and G. Wachtershauser. 1997. Activated acetic acid by carbon fixation on (Fe,Ni)S under primordial conditions. Science **276**:245-247.

Hugler, M., H. Huber, K. O. Stetter, and G. Fuchs. 2003. Autotrophic CO2 fixation pathways in archaea (Crenarchaeota). Arch Microbiol **179**:160-173.

Imhoff, J. 1995. Taxonomy and Physiology of Phototrophic Purple Bacteria and Green Sulfur Bacteria. Pages 1-15 *in* R. Blankenship, M. Madigan, and C. Bauer, editors. Anoxygenic Photosynthetic Bacteria. Springer Netherlands.

Imhoff, J. F. 2003. Phylogenetic taxonomy of the family Chlorobiaceae on the basis of 16S rRNA and fmo (Fenna-Matthews-Olson protein) gene sequences. Int J Syst Evol Microbiol **53**:941-951.

Jaroszewski, L., Z. Li, S. S. Krishna, C. Bakolitsa, J. Wooley, A. M. Deacon, I. A. Wilson, and A. Godzik. 2009. Exploration of uncharted regions of the protein universe. PLoS Biol **7**:e1000205.

Jetten, M. S. M., O. Sliekers, M. Kuypers, T. Dalsgaard, L. van Niftrik, I. Cirpus, K. van de Pas-Schoonen, G. Lavik, B. Thamdrup, D. Le Paslier, H. J. M. Op den Camp, S. Hulth, L. P. Nielsen, W. Abma, K. Third, P. Engstrom, J. G. Kuenen, B. B. Jorgensen, D. E. Canfield, J. S. S. Damste, N. P. Revsbech, J. Fuerst, J. Weissenbach, M. Wagner, I. Schmidt, M. Schmid, and M. Strous. 2003. Anaerobic ammonium oxidation by marine and freshwater planctomycete-like bacteria. Applied Microbiology and Biotechnology **63**:107-114.

Kaartokallio, H. 2004. Food web components, and physical and chemical properties of Baltic Sea ice. Marine Ecology-Progress Series **273**:49-63.

Kammerlander, B., H.-W. Breiner, S. Filker, R. Sommaruga, B. Sonntag, and T. Stoeck. 2015. High diversity of protistan plankton communities in remote high mountain lakes in the European Alps and the Himalayan mountains.

Kammler, M., C. Schon, and K. Hantke. 1993. Characterization of the Ferrous Iron Uptake System of Escherichia-Coli. Journal of Bacteriology **175**:6212-6219.

Kasting, J. F., and J. L. Siefert. 2002. Life and the evolution of Earth's atmosphere. Science **296**:1066-1068.

Kienesberger, S., H. Sprenger, S. Wolfgruber, B. Halwachs, G. G. Thallinger, G. I. Perez-Perez, M. J. Blaser, E. L. Zechner, and G. Gorkiewicz. 2014. Comparative Genome Analysis of Campylobacter fetus Subspecies Revealed Horizontally Acquired Genetic Elements Important for Virulence and Niche Specificity. PLoS ONE **9**.

Kim, M. S., S. S. Hong, K. Park, and H. Myung. 2013. Genomic analysis of bacteriophage PBECO4 infecting Escherichia coli O157:H7. Arch Virol **158**:2399-2403.

King, G. M., and C. F. Weber. 2007. Distribution, diversity and ecology of aerobic CO-oxidizing bacteria. Nat Rev Microbiol **5**:107-118.

Kirchman, D. L. 1993. Leucine incorporation as a measure of biomass production by heterotrophic bacteria. Pages 509-512 *in* P. F. Kemp, B. F. Sherr, E. B. Sherr, and J. J. Cole, editors. Handbook of Methods in Aquatic Microbial Ecology. Lewis Publishers, Boca Raton, FL, USA.

Kirchman, D. L. 2002. The ecology of Cytophaga-Flavobacteria in aquatic environments. FEMS Microbiol Ecol **39**:91-100.

Klatt, C. G., J. M. Wood, D. B. Rusch, M. M. Bateson, N. Hamamura, J. F. Heidelberg, A. R. Grossman, D. Bhaya, F. M. Cohan, M. Kuhl, D. A. Bryant, and D. M. Ward. 2011. Community ecology of hot spring cyanobacterial mats: predominant populations and their functional potential. Isme Journal **5**:1262-1278.

Klepac-Ceraj, V., C. A. Hayes, W. P. Gilhooly, T. W. Lyons, R. Kolter, and A. Pearson. 2012. Microbial diversity under extreme euxinia: Mahoney Lake, Canada. Geobiology **10**:223-235.

Knaust, F., M. Kube, R. Reinhardt, and R. Rabus. 2007. Analyses of the vrl gene cluster in Desulfococcus multivorans: Homologous to the virulence-associated locus of the ovine footrot pathogen Dichelobacter nodosus strain A198. Journal of Molecular Microbiology and Biotechnology **13**:156-164.

Kunin, V., A. Copeland, A. Lapidus, K. Mavromatis, and P. Hugenholtz. 2008. A bioinformatician's guide to metagenomics. Microbiol Mol Biol Rev **72**:557-578, Table of Contents.

Labrenz, M., G. Jost, C. Pohl, S. Beckmann, W. Martens-Habbena, and K. Jurgens. 2005. Impact of different in vitro electron donor/acceptor conditions

on potential chemolithoautotrophic communities from marine pelagic redoxclines. Appl Environ Microbiol **71**:6664-6672.

Lam, P., and M. M. Kuypers. 2011. Microbial nitrogen cycling processes in oxygen minimum zones. Ann Rev Mar Sci **3**:317-345.

Lane, D. J., B. Pace, G. J. Olsen, D. A. Stahl, M. L. Sogin, and N. R. Pace. 1985. Rapid determination of 16S ribosomal RNA sequences for phylogenetic analyses. Proc Natl Acad Sci U S A **82**:6955-6959.

Lanfear, R., B. Calcott, S. Y. Ho, and S. Guindon. 2012. Partitionfinder: combined selection of partitioning schemes and substitution models for phylogenetic analyses. Mol Biol Evol **29**:1695-1701.

LaRoche, J., P. W. Boyd, R. M. L. McKay, and R. J. Geider. 1996. Flavodoxin as an in situ marker for iron stress in phytoplankton. Nature **382**:802-805.

Lauro, F. M., M. Z. DeMaere, S. Yau, M. V. Brown, C. Ng, D. Wilkins, M. J. Raftery, J. A. Gibson, C. Andrews-Pfannkoch, M. Lewis, J. M. Hoffman, T. Thomas, and R. Cavicchioli. 2011. An integrative study of a meromictic lake ecosystem in Antarctica. ISME J **5**:879-895.

Lehours, A. C., P. Evans, C. Bardot, K. Joblin, and F. Gerard. 2007. Phylogenetic diversity of archaea and bacteria in the anoxic zone of a meromictic lake (Lake Pavin, France). Appl Environ Microbiol **73**:2016-2019.

Li, W. Z., and A. Godzik. 2006. Cd-hit: a fast program for clustering and comparing large sets of protein or nucleotide sequences. Bioinformatics **22**:1658-1659.

Libkind, D., M. Moline, J. P. Sampaio, and M. van Broock. 2009. Yeasts from high-altitude lakes: influence of UV radiation. FEMS Microbiol Ecol **69**:353-362.

Lindstrom, E. S., K. Vrede, and E. Leskinen. 2004. Response of a member of the Verrucomicrobia, among the dominating bacteria in a hypolimnion, to increased phosphorus availability. Journal of Plankton Research **26**:241-246.

Liu, Y., T. Yao, N. Jiao, S. Kang, Y. Zeng, and S. Huang. 2006. Microbial community structure in moraine lakes and glacial meltwaters, Mount Everest. FEMS Microbiol Lett **265**:98-105.

Liu, Y. Q., T. D. Yao, L. P. Zhu, N. Z. Jiao, X. B. Liu, Y. H. Zeng, and H. C. Jiang. 2009. Bacterial Diversity of Freshwater Alpine Lake Puma Yumco on the Tibetan Plateau. Geomicrobiology Journal **26**:131-145.

Liu, Z., C. G. Klatt, M. Ludwig, D. B. Rusch, S. I. Jensen, M. Kuhl, D. M. Ward, and D. A. Bryant. 2012. 'Candidatus Thermochlorobacter aerophilum:' an aerobic chlorophotoheterotrophic member of the phylum Chlorobi defined by metagenomics and metatranscriptomics. ISME J **6**:1869-1882.

Lliros, M., L. Alonso-Saez, F. Gich, A. Plasencia, O. Auguet, E. O. Casamayor, and C. M. Borrego. 2011. Active bacteria and archaea cells fixing bicarbonate in the dark along the water column of a stratified eutrophic lagoon. FEMS Microbiol Ecol **77**:370-384.

Lliros, M., E. O. Casamayor, and C. Borrego. 2008. High archaeal richness in the water column of a freshwater sulfurous karstic lake along an interannual study. FEMS Microbiol Ecol **66**:331-342.

Llorens-Mares, T., J. C. Auguet, and E. O. Casamayor. 2012. Winter to spring changes in the slush bacterial community composition of a high-mountain lake (Lake Redon, Pyrenees). Environ Microbiol Rep **4**:50-56.

Llorens-Mares, T., S. Yooseph, J. Goll, J. Hoffman, M. Vila-Costa, C. M. Borrego, C. L. Dupont, and E. O. Casamayor. 2015. Connecting biodiversity and potential functional role in modern euxinic environments by microbial metagenomics. ISME J **9**:1648-1661.

Logares, R., S. Sunagawa, G. Salazar, F. M. Cornejo-Castillo, I. Ferrera, H. Sarmento, P. Hingamp, H. Ogata, C. de Vargas, G. Lima-Mendez, J. Raes, J. Poulain, O. Jaillon, P. Wincker, S. Kandels-Lewis, E. Karsenti, P. Bork, and S. G. Acinas. 2014. Metagenomic 16S rDNA Illumina tags are a powerful alternative to amplicon sequencing to explore diversity and structure of microbial communities. Environ Microbiol **16**:2659-2671.

Lohse, D. L., J. M. Denu, and J. E. Dixon. 1995. Insights derived from the structures of the Ser/Thr phosphatases calcineurin and protein phosphatase 1. Structure **3**:987-990.

Longnecker, K., M. W. Lomas, and B. A. S. Van Mooy. 2010. Abundance and diversity of heterotrophic bacterial cells assimilating phosphate in the subtropical North Atlantic Ocean. Environ Microbiol **12**:2773-2782.

Lorenzi, H. A., J. Hoover, J. Inman, T. Safford, S. Murphy, L. Kagan, and S. J. Williamson. 2011. TheViral MetaGenome Annotation Pipeline (VMGAP): An automated tool for the functional annotation of viral Metagenomic shotgun sequencing data. Stand Genomic Sci **4**:418-429.

Luo, C. W., D. Tsementzi, N. C. Kyrpides, and K. T. Konstantinidis. 2012. Individual genome assembly from complex community short-read metagenomic datasets. Isme Journal **6**:898-901.

Luo, H. W., H. M. Zhang, R. A. Long, and R. Benner. 2011. Depth distributions of alkaline phosphatase and phosphonate utilization genes in the North Pacific Subtropical Gyre. Aquatic Microbial Ecology **62**:61-69.

Lynch, M. D. J., and J. D. Neufeld. 2015. Ecology and exploration of the rare biosphere. Nature Reviews Microbiology **13**:217-229.

Lyons, T. W., C. T. Reinhard, and N. J. Planavsky. 2014. The rise of oxygen in Earth's early ocean and atmosphere. Nature **506**:307-315.

Macek, B., F. Gnad, B. Soufi, C. Kumar, J. V. Olsen, I. Mijakovic, and M. Mann. 2008. Phosphoproteome analysis of E. coli reveals evolutionary conservation of bacterial Ser/Thr/Tyr phosphorylation. Mol Cell Proteomics **7**:299-307.

Madigan, M. T. 2012. Brock biology of microorganisms. Benjamin Cummings, San Francisco.

Majaneva, M., J. M. Rintala, M. Piisila, D. P. Fewer, and J. Blomster. 2012. Comparison of wintertime eukaryotic community from sea ice and open water in the Baltic Sea, based on sequencing of the 18S rRNA gene. Polar Biology **35**:875-889.

Maranger, R., D. F. Bird, and S. K. Juniper. 1994. Viral and Bacterial Dynamics in Arctic Sea-Ice during the Spring Algal Bloom near Resolute, Nwt, Canada. Marine Ecology Progress Series **111**:121-127.

Maresca, J. A. 2007. The genetic basis for pigment variation among green sulfur bacteria. The Pennsylvania State University, University Park.

Maresca, J. A., A. Gomez Maqueo Chew, M. R. Ponsati, N. U. Frigaard, J. G. Ormerod, and D. A. Bryant. 2004. The bchU gene of Chlorobium tepidum encodes the c-20 methyltransferase in bacteriochlorophyll c biosynthesis. Journal of Bacteriology **186**:2558-2566.

Maresca, J. A., J. E. Graham, and D. A. Bryant. 2008a. The biochemical basis for structural diversity in the carotenoids of chlorophototrophic bacteria. Photosynth Res **97**:121-140.

Maresca, J. A., S. P. Romberger, and D. A. Bryant. 2008b. Isorenieratene biosynthesis in green sulfur bacteria requires the cooperative actions of two carotenoid cyclases. Journal of Bacteriology **190**:6384-6391.

Martens-Habbena, W., P. M. Berube, H. Urakawa, J. R. de la Torre, and D. A. Stahl. 2009. Ammonia oxidation kinetics determine niche separation of nitrifying Archaea and Bacteria. Nature **461**:976-U234.

Martin, H. G., N. Ivanova, V. Kunin, F. Warnecke, K. W. Barry, A. C. McHardy, C. Yeates, S. M. He, A. A. Salamov, E. Szeto, E. Dalin, N. H. Putnam, H. J. Shapiro, J. L. Pangilinan, I. Rigoutsos, N. C. Kyrpides, L. L. Blackall, K. D. McMahon, and P. Hugenholtz. 2006. Metagenomic analysis of two enhanced biological phosphorus removal (EBPR) sludge communities. Nature Biotechnology **24**:1263-1269.

Martin, J. H., K. H. Coale, K. S. Johnson, S. E. Fitzwater, R. M. Gordon, S. J. Tanner, C. N. Hunter, V. A. Elrod, J. L. Nowicki, T. L. Coley, R. T. Barber, S. Lindley, A. J. Watson, K. Vanscoy, C. S. Law, M. I. Liddicoat, R. Ling, T.

Stanton, J. Stockel, C. Collins, A. Anderson, R. Bidigare, M. Ondrusek, M. Latasa, F. J. Millero, K. Lee, W. Yao, J. Z. Zhang, G. Friederich, C. Sakamoto, F. Chavez, K. Buck, Z. Kolber, R. Greene, P. Falkowski, S. W. Chisholm, F. Hoge, R. Swift, J. Yungel, S. Turner, P. Nightingale, A. Hatton, P. Liss, and N. W. Tindale. 1994. Testing the Iron Hypothesis in Ecosystems of the Equatorial Pacific-Ocean. Nature **371**:123-129.

Martinez, A., G. W. Tyson, and E. F. DeLong. 2010. Widespread known and novel phosphonate utilization pathways in marine bacteria revealed by functional screening and metagenomic analyses. Environ Microbiol **12**:222-238.

Martiny, A. C., M. L. Coleman, and S. W. Chisholm. 2006. Phosphate acquisition genes in Prochlorococcus ecotypes: evidence for genome-wide adaptation. Proc Natl Acad Sci U S A **103**:12552-12557.

Martiny, A. C., Y. Huang, and W. Z. Li. 2009. Occurrence of phosphate acquisition genes in Prochlorococcus cells from different ocean regions. Environ Microbiol **11**:1340-1347.

Mary, I., D. G. Cummings, I. C. Biegala, P. H. Burkill, S. D. Archer, and M. V. Zubkov. 2006. Seasonal dynamics of bacterioplankton community structure at a coastal station in the western English Channel. Aquatic Microbial Ecology **42**:119-126.

Medina-Sanchez, J. M., M. Felip, and E. O. Casamayor. 2005. Catalyzed reported deposition-fluorescence in situ hybridization protocol to evaluate phagotrophy in mixotrophic protists. Appl Environ Microbiol **71**:7321-7326.

Merbt, S. N., D. A. Stahl, E. O. Casamayor, E. Marti, G. W. Nicol, and J. I. Prosser. 2012. Differential photoinhibition of bacterial and archaeal ammonia oxidation. FEMS Microbiol Lett **327**:41-46.

Meyer, K. M., and L. R. Kump. 2008. Oceanic euxinia in Earth history: Causes and consequences. Pages 251-288 Annual Review of Earth and Planetary Sciences.

Millero, F. J. 1991. The oxidation of H2S in Framvaren fjord. Limnology and Oceanography **36**:1006-1014.

Monchy, S., G. Sanciu, M. Jobard, S. Rasconi, M. Gerphagnon, M. Chabe, A. Cian, D. Meloni, N. Niquil, U. Christaki, E. Viscogliosi, and T. Sime-Ngando. 2011. Exploring and quantifying fungal diversity in freshwater lake ecosystems using rDNA cloning/sequencing and SSU tag pyrosequencing. Environ Microbiol **13**:1433-1453.

Montesinos, E., R. Guerrero, C. Abella, and I. Esteve. 1983. Ecology and Physiology of the Competition for Light between Chlorobium-Limicola and

Chlorobium-Phaeobacteroides in Natural Habitats. Appl Environ Microbiol **46**:1007-1016.

Moreno-Hagelsieb, G., and K. Latimer. 2008. Choosing BLAST options for better detection of orthologs as reciprocal best hits. Bioinformatics **24**:319-324.

Mosier, A. C., A. E. Murray, and C. H. Fritsen. 2007. Microbiota within the perennial ice cover of Lake Vida, Antarctica. FEMS Microbiol Ecol **59**:274-288.

Mueller-Spitz, S. R., G. W. Goetz, and S. L. McLellan. 2009. Temporal and spatial variability in nearshore bacterioplankton communities of Lake Michigan. FEMS Microbiol Ecol **67**:511-522.

Mullis, K. B., and F. A. Faloona. 1987. Specific synthesis of DNA in vitro via a polymerase-catalyzed chain reaction. Methods Enzymol **155**:335-350.

Murray, A. E., C. M. Preston, R. Massana, L. T. Taylor, A. Blakis, K. Wu, and E. F. DeLong. 1998. Seasonal and spatial variability of bacterial and archaeal assemblages in the coastal waters near Anvers Island, Antarctica. Appl Environ Microbiol **64**:2585-2595.

Nakamura, Y., T. Itoh, H. Matsuda, and T. Gojobori. 2004. Biased biological functions of horizontally transferred genes in prokaryotic genomes. Nat Genet **36**:760-766.

Newton, R. J., S. E. Jones, A. Eiler, K. D. McMahon, and S. Bertilsson. 2011. A Guide to the Natural History of Freshwater Lake Bacteria. Microbiology and Molecular Biology Reviews **75**:14-49.

Norman, A., L. H. Hansen, and S. J. Sorensen. 2009. Conjugative plasmids: vessels of the communal gene pool. Philosophical Transactions of the Royal Society B-Biological Sciences **364**:2275-2289.

Nunoura, T., Y. Takaki, H. Kazama, M. Hirai, J. Ashi, H. Imachi, and K. Takai. 2012. Microbial Diversity in Deep-sea Methane Seep Sediments Presented by SSU rRNA Gene Tag Sequencing. Microbes and Environments **27**:382-390.

O'Malley, M. A. 2008. 'Everything is everywhere: but the environment selects': ubiquitous distribution and ecological determinism in microbial biogeography. Stud Hist Philos Biol Biomed Sci **39**:314-325.

O'Malley, M. A., and J. Dupre. 2007. Size doesn't matter: towards a more inclusive philosophy of biology. Biology & Philosophy **22**:155-191.

Oberto, J. 2013. SyntTax: a web server linking synteny to prokaryotic taxonomy. BMC Bioinformatics **14**:4.

Ochman, H., J. G. Lawrence, and E. A. Groisman. 2000. Lateral gene transfer and the nature of bacterial innovation. Nature **405**:299-304.

Ohtsubo, Y., W. Ikeda-Ohtsubo, Y. Nagata, and M. Tsuda. 2008. GenomeMatcher: a graphical user interface for DNA sequence comparison. BMC Bioinformatics **9**:376.

Orf, G. S., and R. E. Blankenship. 2013. Chlorosome antenna complexes from green photosynthetic bacteria. Photosynth Res **116**:315-331.

Ormerod, J. G. 1988. Natural Genetic Transformation in Chlorobium. Pages 315-319 *in* J. M. Olson, J. G. Ormerod, J. Amesz, E. Stackebrandt, and H. G. Trüper, editors. Green Photosynthetic Bacteria. Springer US.

Overmann, J. 1997. Mahoney Lake: A Case Study of the Ecological Significance of Phototrophic Sulfur Bacteria. Pages 251-288 *in* J. G. Jones, editor. Advances in Microbial Ecology. Springer US.

Page, K. A., S. A. Connon, and S. J. Giovannoni. 2004. Representative freshwater bacterioplankton isolated from Crater Lake, Oregon. Appl Environ Microbiol **70**:6542-6550.

Palenik, B., Q. Ren, V. Tai, and I. T. Paulsen. 2009. Coastal Synechococcus metagenome reveals major roles for horizontal gene transfer and plasmids in population diversity. Environ Microbiol **11**:349-359.

Pedros-Alio, C., J. I. Calderon-Paz, and J. M. Gasol. 2000. Comparative analysis shows that bacterivory, not viral lysis, controls the abundance of heterotrophic prokaryotic plankton. FEMS Microbiol Ecol **32**:157-165.

Pedros-Alio, C., and R. Guerrero. 1993. Microbial ecology in Lake Ciso. Advances in Microbial Ecology **13**:155-209.

Pernthaler, J., F. O. Glockner, S. Unterholzner, A. Alfreider, R. Psenner, and R. Amann. 1998. Seasonal community and population dynamics of pelagic bacteria and archaea in a high mountain lake. Appl Environ Microbiol **64**:4299-4306.

Peura, S., A. Eiler, S. Bertilsson, H. Nykanen, M. Tiirola, and R. I. Jones. 2012. Distinct and diverse anaerobic bacterial communities in boreal lakes dominated by candidate division OD1. Isme Journal **6**:1640-1652.

Pinhassi, J., M. M. Sala, H. Havskum, F. Peters, O. Guadayol, A. Malits, and C. Marrase. 2004. Changes in bacterioplankton composition under different phytoplankton regimens. Appl Environ Microbiol **70**:6753-6766.

Polz, M. F., E. J. Alm, and W. P. Hanage. 2013. Horizontal gene transfer and the evolution of bacterial and archaeal population structure. Trends in Genetics **29**:170-175.

Prakash, T., and T. D. Taylor. 2012. Functional assignment of metagenomic data: challenges and applications. Brief Bioinform **13**:711-727.

Priscu, J. C., E. E. Adams, W. B. Lyons, M. A. Voytek, D. W. Mogk, R. L. Brown, C. P. McKay, C. D. Takacs, K. A. Welch, C. F. Wolf, J. D. Kirshtein, and R. Avci. 1999. Geomicrobiology of subglacial ice above Lake Vostok, Antarctica. Science **286**:2141-2144.

Prosser, J. I. 2012. Ecosystem processes and interactions in a morass of diversity. FEMS Microbiol Ecol **81**:507-519.

Prosser, J. I., and G. W. Nicol. 2008. Relative contributions of archaea and bacteria to aerobic ammonia oxidation in the environment. Environ Microbiol **10**:2931-2941.

Pruesse, E., J. Peplies, and F. O. Glockner. 2012. SINA: accurate high throughput multiple sequence alignment of ribosomal RNA genes. Bioinformatics.

Psenner, R., B. Sattler, A. Wille, C. H. Fritsen, J. C. Priscu, M. Felip, and J. Catalan. 1999. Lake ice microbial communities in alpine and antarctic lakes. Pages 17–31 *in* S. F. Margesin R, editor. Cold adapted organisms. Springer-Verlag, Heidelberg.

Quast, C., E. Pruesse, P. Yilmaz, J. Gerken, T. Schweer, P. Yarza, J. Peplies, and F. O. Glockner. 2013. The SILVA ribosomal RNA gene database project: improved data processing and web-based tools. Nucleic Acids Res **41**:D590-596.

Quinn, J. P., A. N. Kulakova, N. A. Cooley, and J. W. McGrath. 2007. New ways to break an old bond: the bacterial carbon-phosphorus hydrolases and their role in biogeochemical phosphorus cycling. Environ Microbiol **9**:2392-2400.

R Core Team. 2014. R: A Language and Environment for Statistical Computing. R Foundation for Statistical Computing, Vienna, Austria.

Ragsdale, S. W. 2004. Life with carbon monoxide. Crit Rev Biochem Mol Biol **39**:165-195.

Raskin, L., B. E. Rittmann, and D. A. Stahl. 1996. Competition and coexistence of sulfate-reducing and methanogenic populations in anaerobic biofilms. Appl Environ Microbiol **62**:3847-3857.

Reche, I., E. Ortega-Retuerta, O. Romera, E. Pulido-Villena, R. Morales-Baquero, and E. O. Casamayor. 2009. Effect of Saharan dust inputs on bacterial activity and community composition in Mediterranean lakes and reservoirs. Limnology and Oceanography **54**:869-879.

Reichenbach, H. 2006. The order Cytophagales. Pages 549–590 *in* Dworkin M, Falkow S, Rosenberg E, Schleifer K-H, and Stackebrandt E, editors. Prokaryotes. Springer, Berlin.

Reinhard, C. T., N. J. Planavsky, L. J. Robbins, C. A. Partin, B. C. Gill, S. V. Lalonde, A. Bekker, K. O. Konhauser, and T. W. Lyons. 2013. Proterozoic

ocean redox and biogeochemical stasis. Proc Natl Acad Sci U S A **110**:5357-5362.

Reisch, C. R., M. A. Moran, and W. B. Whitman. 2008. Dimethylsulfoniopropionate-dependent demethylase (DmdA) from Pelagibacter ubique and Silicibacter pomeroyi. Journal of Bacteriology **190**:8018-8024.

Restrepo-Ortiz, C. X., J. C. Auguet, and E. O. Casamayor. 2014. Targeting spatiotemporal dynamics of planktonic SAGMGC-1 and segregation of ammonia-oxidizing thaumarchaeota ecotypes by newly designed primers and quantitative polymerase chain reaction. Environ Microbiol **16**:689-700.

Restrepo-Ortiz, C. X., and E. O. Casamayor. 2013. Environmental distribution of two widespread uncultured freshwater Euryarchaeota clades unveiled by specific primers and quantitative PCR. Environ Microbiol Rep **5**:861-867.

Reysenbach, A. L., and E. Shock. 2002. Merging genomes with geochemistry in hydrothermal ecosystems. Science **296**:1077-1082.

Richards, T. A., A. A. Vepritskiy, D. E. Gouliamova, and S. A. Nierzwicki-Bauer. 2005. The molecular diversity of freshwater picoeukaryotes from an oligotrophic lake reveals diverse, distinctive and globally dispersed lineages. Environ Microbiol **7**:1413-1425.

Richter, M., and R. Rossello-Mora. 2009. Shifting the genomic gold standard for the prokaryotic species definition. Proc Natl Acad Sci U S A **106**:19126-19131.

Riemann, L., and H. P. Grossart. 2008. Elevated lytic phage production as a consequence of particle colonization by a marine Flavobacterium (Cellulophaga sp.). Microb Ecol **56**:505-512.

Rikmann, E., I. Zekker, M. Tomingas, T. Tenno, A. Menert, L. Loorits, and T. Tenno. 2012. Sulfate-reducing anaerobic ammonium oxidation as a potential treatment method for high nitrogen-content wastewater. Biodegradation **23**:509-524.

Rinke, C., P. Schwientek, A. Sczyrba, N. N. Ivanova, I. J. Anderson, J. F. Cheng, A. Darling, S. Malfatti, B. K. Swan, E. A. Gies, J. A. Dodsworth, B. P. Hedlund, G. Tsiamis, S. M. Sievert, W. T. Liu, J. A. Eisen, S. J. Hallam, N. C. Kyrpides, R. Stepanauskas, E. M. Rubin, P. Hugenholtz, and T. Woyke. 2013. Insights into the phylogeny and coding potential of microbial dark matter. Nature **499**:431-437.

Roberts, G. P., H. Youn, and R. L. Kerby. 2004. CO-sensing mechanisms. Microbiol Mol Biol Rev **68**:453-473, table of contents.

Rocap, G., F. W. Larimer, J. Lamerdin, S. Malfatti, P. Chain, N. A. Ahlgren, A. Arellano, M. Coleman, L. Hauser, W. R. Hess, Z. I. Johnson, M. Land, D.

Lindell, A. F. Post, W. Regala, M. Shah, S. L. Shaw, C. Steglich, M. B. Sullivan, C. S. Ting, A. Tolonen, E. A. Webb, E. R. Zinser, and S. W. Chisholm. 2003. Genome divergence in two Prochlorococcus ecotypes reflects oceanic niche differentiation. Nature **424**:1042-1047.

Rohwer, F., and R. V. Thurber. 2009. Viruses manipulate the marine environment. Nature **459**:207-212.

Rusch, D. B., A. L. Halpern, G. Sutton, K. B. Heidelberg, S. Williamson, S. Yooseph, D. Y. Wu, J. A. Eisen, J. M. Hoffman, K. Remington, K. Beeson, B. Tran, H. Smith, H. Baden-Tillson, C. Stewart, J. Thorpe, J. Freeman, C. Andrews-Pfannkoch, J. E. Venter, K. Li, S. Kravitz, J. F. Heidelberg, T. Utterback, Y. H. Rogers, L. I. Falcon, V. Souza, G. Bonilla-Rosso, L. E. Eguiarte, D. M. Karl, S. Sathyendranath, T. Platt, E. Bermingham, V. Gallardo, G. Tamayo-Castillo, M. R. Ferrari, R. L. Strausberg, K. Nealson, R. Friedman, M. Frazier, and J. C. Venter. 2007. The Sorcerer II Global Ocean Sampling expedition: Northwest Atlantic through Eastern Tropical Pacific. PLoS Biol **5**:398-431.

Rutherford, K., J. Parkhill, J. Crook, T. Horsnell, P. Rice, M. A. Rajandream, and B. Barrell. 2000. Artemis: sequence visualization and annotation. Bioinformatics **16**:944-945.

Salka, I., Z. Cuperova, M. Masin, M. Koblizek, and H. P. Grossart. 2011. Rhodoferax-related pufM gene cluster dominates the aerobic anoxygenic phototrophic communities in German freshwater lakes. Environ Microbiol **13**:2865-2875.

Sangwan, P., X. L. Chen, P. Hugenholtz, and P. H. Janssen. 2004. Chthoniobacter flavus gen. nov., sp nov., the first pure-culture representative of subdivision two, Spartobacteria classis nov., of the phylum Verrucomicrobia. Appl Environ Microbiol **70**:5875-5881.

Saunders, N. J., P. Boonmee, J. F. Peden, and S. A. Jarvis. 2005. Inter-species horizontal transfer resulting in core-genome and niche-adaptive variation within Helicobacter pylori. BMC Genomics **6**.

Schloss, P. D., S. L. Westcott, T. Ryabin, J. R. Hall, M. Hartmann, E. B. Hollister, R. A. Lesniewski, B. B. Oakley, D. H. Parks, C. J. Robinson, J. W. Sahl, B. Stres, G. G. Thallinger, D. J. Van Horn, and C. F. Weber. 2009. Introducing mothur: open-source, platform-independent, community-supported software for describing and comparing microbial communities. Appl Environ Microbiol **75**:7537-7541.

Schmetterer, G., A. Valladares, D. Pils, S. Steinbach, M. Pacher, A. M. Muro-Pastor, E. Flores, and A. Herrero. 2001. The coxBAC operon encodes a cytochrome c oxidase required for heterotrophic growth in the cyanobacterium

Anabaena variabilis strain ATCC 29413. Journal of Bacteriology **183**:6429-6434.

Schmidt, U., and R. Conrad. 1993. Hydrogen, carbon-monoxide, and methane dynamics in Lake Constance. Limnology and Oceanography **38**:1214-1226.

Severmann, S., and A. D. Anbar. 2009. Reconstructing Paleoredox Conditions through a Multitracer Approach: The Key to the Past Is the Present. Elements **5**:359-364.

Shade, A., S. E. Jones, and K. D. McMahon. 2008. The influence of habitat heterogeneity on freshwater bacterial community composition and dynamics. Environ Microbiol **10**:1057-1067.

Shapiro, B. J., J. Friedman, O. X. Cordero, S. P. Preheim, S. C. Timberlake, G. Szabo, M. F. Polz, and E. J. Alm. 2012. Population Genomics of Early Events in the Ecological Differentiation of Bacteria. Science **336**:48-51.

Sharon, I., A. Alperovitch, F. Rohwer, M. Haynes, F. Glaser, N. Atamna-Ismaeel, R. Y. Pinter, F. Partensky, E. V. Koonin, Y. I. Wolf, N. Nelson, and O. Beja. 2009a. Photosystem I gene cassettes are present in marine virus genomes. Nature **461**:258-262.

Sharon, I., A. Pati, V. M. Markowitz, and R. Y. Pinter. 2009b. A Statistical Framework for the Functional Analysis of Metagenomes. Pages 496-511 *in* S. Batzoglou, editor. Research in Computational Molecular Biology, Proceedings. Springer, Berlin, Heildelberg, Germany.

Simek, K., K. Hornak, J. Jezbera, M. Masin, J. Nedoma, J. M. Gasol, and M. Schauer. 2005. Influence of top-down and bottom-up manipulations on the R-BT065 subcluster of beta-proteobacteria, an abundant group in bacterioplankton of a freshwater reservoir. Appl Environ Microbiol **71**:2381-2390.

Simon, C., A. Wiezer, A. W. Strittmatter, and R. Daniel. 2009. Phylogenetic diversity and metabolic potential revealed in a glacier ice metagenome. Appl Environ Microbiol **75**:7519-7526.

Small, G. E., G. S. Bullerjahn, R. W. Sterner, B. F. N. Beall, S. Brovold, J. C. Finlay, R. M. L. McKay, and M. Mukherjee. 2013. Rates and controls of nitrification in a large oligotrophic lake. Limnology and Oceanography **58**:276-286.

Sommaruga, R. 2001. The role of solar UV radiation in the ecology of alpine lakes. J Photochem Photobiol B **62**:35-42.

Sommaruga, R., and E. O. Casamayor. 2009. Bacterial 'cosmopolitanism' and importance of local environmental factors for community composition in remote high-altitude lakes. Freshwater Biology **54**:994-1005.

Soontharapirakkul, K., W. Promden, N. Yamada, H. Kageyama, A. Incharoensakdi, A. Iwamoto-Kihara, and T. Takabe. 2011. Halotolerant cyanobacterium Aphanothece halophytica contains an Na+-dependent F1F0-ATP synthase with a potential role in salt-stress tolerance. J Biol Chem **286**:10169-10176.

Spang, A., J. H. Saw, S. L. Jorgensen, K. Zaremba-Niedzwiedzka, J. Martijn, A. E. Lind, R. van Eijk, C. Schleper, L. Guy, and T. J. G. Ettema. 2015. Complex archaea that bridge the gap between prokaryotes and eukaryotes. Nature **521**:173-179.

Stamatakis, A. 2006. RAxML-VI-HPC: maximum likelihood-based phylogenetic analyses with thousands of taxa and mixed models. Bioinformatics **22**:2688-2690.

Stewart, K., S. Kassakian, M. Krynytzky, D. DiJulio, and J. Murray. 2007. Oxic, suboxic, and anoxic conditions in the Black Sea. Pages 1-21 *in* V. Yanko-Hombach, A. Gilbert, N. Panin, and P. Dolukhanov, editors. The Black Sea Flood Question: Changes in Coastline, Climate, and Human Settlement. Springer Netherlands.

Stomp, M., J. Huisman, L. J. Stal, and H. C. Matthijs. 2007. Colorful niches of phototrophic microorganisms shaped by vibrations of the water molecule. ISME J **1**:271-282.

Summers, A. O. 2006. Genetic linkage and horizontal gene transfer, the roots of the antibiotic multi-resistance problem. Animal Biotechnology **17**:125-135.

Sun, H., S. Spring, A. Lapidus, K. Davenport, T. G. Del Rio, H. Tice, M. Nolan, A. Copeland, J. F. Cheng, S. Lucas, R. Tapia, L. Goodwin, S. Pitluck, N. Ivanova, I. Pagani, K. Mavromatis, G. Ovchinnikova, A. Pati, A. Chen, K. Palaniappan, L. Hauser, Y. J. Chang, C. D. Jeffries, J. C. Detter, C. Han, M. Rohde, E. Brambilla, M. Goker, T. Woyke, J. Bristow, J. A. Eisen, V. Markowitz, P. Hugenholtz, N. C. Kyrpides, H. P. Klenk, and M. Land. 2010. Complete genome sequence of Desulfarculus baarsii type strain (2st14(T)). Stand Genomic Sci **3**:276-284.

Sun, S. L., J. Chen, W. Z. Li, I. Altintas, A. Lin, S. Peltier, K. Stocks, E. E. Allen, M. Ellisman, J. Grethe, and J. Wooley. 2011. Community cyberinfrastructure for Advanced Microbial Ecology Research and Analysis: the CAMERA resource. Nucleic Acids Res **39**:D546-D551.

Taipale, S., P. Kankaala, M. W. Hahn, R. I. Jones, and M. Tiirola. 2011. Methane-oxidizing and photoautotrophic bacteria are major producers in a humic lake with a large anoxic hypolimnion. Aquatic Microbial Ecology **64**:81-95.

Takai, K., B. J. Campbell, S. C. Cary, M. Suzuki, H. Oida, T. Nunoura, H. Hirayama, S. Nakagawa, Y. Suzuki, F. Inagaki, and K. Horikoshi. 2005. Enzymatic and genetic characterization of carbon and energy metabolisms by

deep-sea hydrothermal chemolithoautotrophic isolates of Epsilonproteobacteria. Appl Environ Microbiol **71**:7310-7320.

Tamames, J., J. J. Abellan, M. Pignatelli, A. Camacho, and A. Moya. 2010. Environmental distribution of prokaryotic taxa. BMC Microbiol **10**.

Tanenbaum, D. M., J. Goll, S. Murphy, P. Kumar, N. Zafar, M. Thiagarajan, R. Madupu, T. Davidsen, L. Kagan, S. Kravitz, D. B. Rusch, and S. Yooseph. 2010. The JCVI standard operating procedure for annotating prokaryotic metagenomic shotgun sequencing data. Stand Genomic Sci **2**:229-237.

Teira, E., J. M. Gasol, M. Aranguren-Gassis, A. Fernandez, J. Gonzalez, I. Lekunberri, and X. A. Alvarez-Salgado. 2008. Linkages between bacterioplankton community composition, heterotrophic carbon cycling and environmental conditions in a highly dynamic coastal ecosystem. Environ Microbiol **10**:906-917.

Thamdrup, B. 2012. New pathways and processes in the global nitrogen cycle. Annual Review of Ecology, Evolution, and Systematics **43**:407-428.

Thomas, T., J. Gilbert, and F. Meyer. 2012. Metagenomics - a guide from sampling to data analysis. Microb Inform Exp **2**:3.

Tonolla, M., R. Peduzzi, and D. Hahn. 2005. Long-term population dynamics of phototrophic sulfur bacteria in the chemocline of Lake Cadagno, Switzerland. Appl Environ Microbiol **71**:3544-3550.

Tonolla, M., S. Peduzzi, A. Demarta, R. Peduzzi, and D. Hahn. 2004. Phototropic sulfur and sulfate-reducing bacteria in the chemocline of meromictic Lake Cadagno, Switzerland. 2004 **63**:10.

Treusch, A. H., S. Leininger, A. Kletzin, S. C. Schuster, H. P. Klenk, and C. Schleper. 2005. Novel genes for nitrite reductase and Amo-related proteins indicate a role of uncultivated mesophilic crenarchaeota in nitrogen cycling. Environ Microbiol **7**:1985-1995.

Triado-Margarit, X., and E. O. Casamayor. 2012. Genetic diversity of planktonic eukaryotes in high mountain lakes (Central Pyrenees, Spain). Environ Microbiol **14**:2445-2456.

Triado-Margarit, X., and E. O. Casamayor. 2013. High genetic diversity and novelty in planktonic protists inhabiting inland and coastal high salinity water bodies. FEMS Microbiol Ecol **85**:27-36.

Trüper, H. G., and H. G. Schlegel. 1964. Sulphur Metabolism in Thiorhodaceae .1. Quantitative Measurements on Growing Cells of Chromatium Okenii. Antonie Van Leeuwenhoek Journal of Microbiology and Serology **30**:225-&.

Tyson, G. W., J. Chapman, P. Hugenholtz, E. E. Allen, R. J. Ram, P. M. Richardson, V. V. Solovyev, E. M. Rubin, D. S. Rokhsar, and J. F. Banfield.

2004. Community structure and metabolism through reconstruction of microbial genomes from the environment. Nature **428**:37-43.

Van de Peer, Y., S. Chapelle, and R. De Wachter. 1996. A quantitative map of nucleotide substitution rates in bacterial rRNA. Nucleic Acids Res **24**:3381-3391.

Van Gemerden, H., and J. Mas. 1995. Ecology of Phototrophic Sulfur Bacteria. Pages 49-85 *in* R. Blankenship, M. Madigan, and C. Bauer, editors. Anoxygenic Photosynthetic Bacteria. Springer Netherlands.

Van Gemerden, H., E. Montesinos, J. Mas, and R. Guerrero. 1985. Diel Cycle of Metabolism of Phototrophic Purple Sulfur Bacteria in Lake Ciso (Spain). Limnology and Oceanography **30**:932-943.

Vaquer-Sunyer, R., and C. M. Duarte. 2008. Thresholds of hypoxia for marine biodiversity. Proc Natl Acad Sci U S A **105**:15452-15457.

Vila, X., and C. A. Abella. 1994. Effects of light quality on the physiology and the ecology of planktonic green sulfur bacteria in lakes. Photosynth Res **41**:53-65.

Vila-Costa, M., M. Bartrons, J. Catalan, and E. O. Casamayor. 2014. Nitrogen-cycling genes in epilithic biofilms of oligotrophic high-altitude lakes (Central Pyrenees, Spain). Microb Ecol **68**:60-69.

Vila-Costa, M., S. Sharma, M. A. Moran, and E. O. Casamayor. 2013. Diel gene expression profiles of a phosphorus limited mountain lake using metatranscriptomics. Environ Microbiol **15**:1190-1203.

Villafranca, J. E., C. R. Kissinger, and H. E. Parge. 1996. Protein serine/threonine phosphatases. Curr Opin Biotechnol **7**:397-402.

Walker, C. B., J. R. de la Torre, M. G. Klotz, H. Urakawa, N. Pinel, D. J. Arp, C. Brochier-Armanet, P. S. G. Chain, P. P. Chan, A. Gollabgir, J. Hemp, M. Hugler, E. A. Karr, M. Konneke, M. Shin, T. J. Lawton, T. Lowe, W. Martens-Habbena, L. A. Sayavedra-Soto, D. Lang, S. M. Sievert, A. C. Rosenzweig, G. Manning, and D. A. Stahl. 2010. Nitrosopumilus maritimus genome reveals unique mechanisms for nitrification and autotrophy in globally distributed marine crenarchaea. Proc Natl Acad Sci U S A **107**:8818-8823.

Weber, K. A., L. A. Achenbach, and J. D. Coates. 2006. Microorganisms pumping iron: anaerobic microbial iron oxidation and reduction. Nature Reviews Microbiology **4**:752-764.

Westra, E. R., A. Buckling, and P. C. Fineran. 2014. CRISPR-Cas systems: beyond adaptive immunity. Nat Rev Microbiol **12**:317-326.

Wharton, R. A., W. B. Lyons, and D. J. D. Marais. 1993. Stable isotopic biogeochemistry of carbon and nitrogen in a perennially ice-covered Antartic lake. Chemical Geology **107**:159-172.

Wiedenbeck, J., and F. M. Cohan. 2011. Origins of bacterial diversity through horizontal genetic transfer and adaptation to new ecological niches. FEMS Microbiol Rev **35**:957-976.

Woese, C. R., and G. E. Fox. 1977. Phylogenetic structure of the prokaryotic domain: the primary kingdoms. Proc Natl Acad Sci U S A **74**:5088-5090.

Woese, C. R., O. Kandler, and M. L. Wheelis. 1990. Towards a natural system of organisms: proposal for the domains Archaea, Bacteria, and Eucarya. Proc Natl Acad Sci U S A **87**:4576-4579.

Wozniak, R. A. F., and M. K. Waldor. 2010. Integrative and conjugative elements: mosaic mobile genetic elements enabling dynamic lateral gene flow. Nature Reviews Microbiology **8**:552-563.

Wright, J. J., K. M. Konwar, and S. J. Hallam. 2012. Microbial ecology of expanding oxygen minimum zones. Nature Reviews Microbiology **10**:381-394.

Wrighton, K. C., C. J. Castelle, M. J. Wilkins, L. A. Hug, I. Sharon, B. C. Thomas, K. M. Handley, S. W. Mullin, C. D. Nicora, A. Singh, M. S. Lipton, P. E. Long, K. H. Williams, and J. F. Banfield. 2014. Metabolic interdependencies between phylogenetically novel fermenters and respiratory organisms in an unconfined aquifer. Isme Journal **8**:1452-1463.

Wrighton, K. C., B. C. Thomas, I. Sharon, C. S. Miller, C. J. Castelle, N. C. VerBerkmoes, M. J. Wilkins, R. L. Hettich, M. S. Lipton, K. H. Williams, P. E. Long, and J. F. Banfield. 2012. Fermentation, Hydrogen, and Sulfur Metabolism in Multiple Uncultivated Bacterial Phyla. Science **337**:1661-1665.

Wu, X. A., S. Monchy, S. Taghavi, W. Zhu, J. Ramos, and D. van der Lelie. 2011. Comparative genomics and functional analysis of niche-specific adaptation in Pseudomonas putida. FEMS Microbiol Rev **35**:299-323.

Xiang, S. R., T. C. Shang, Y. Chen, Z. F. Jing, and T. D. Yao. 2009. Dominant Bacteria and Biomass in the Kuytun 51 Glacier. Appl Environ Microbiol **75**:7287-7290.

Yooseph, S., G. Sutton, D. B. Rusch, A. L. Halpern, S. J. Williamson, K. Remington, J. A. Eisen, K. B. Heidelberg, G. Manning, W. Z. Li, L. Jaroszewski, P. Cieplak, C. S. Miller, H. Y. Li, S. T. Mashiyama, M. P. Joachimiak, C. van Belle, J. M. Chandonia, D. A. Soergel, Y. F. Zhai, K. Natarajan, S. Lee, B. J. Raphael, V. Bafna, R. Friedman, S. E. Brenner, A. Godzik, D. Eisenberg, J. E. Dixon, S. S. Taylor, R. L. Strausberg, M. Frazier, and J. C. Venter. 2007. The Sorcerer II Global Ocean Sampling expedition: Expanding the universe of protein families. PLoS Biol **5**:432-466.

Yurkov, V. V., and J. T. Beatty. 1998. Aerobic anoxygenic phototrophic bacteria. Microbiol Mol Biol Rev **62**:695-724.

Zeder, M., S. Peter, T. Shabarova, and J. Pernthaler. 2009. A small population of planktonic Flavobacteria with disproportionally high growth during the spring phytoplankton bloom in a prealpine lake. Environ Microbiol **11**:2676-2686.

Zeigler Allen, L., E. E. Allen, J. H. Badger, J. P. McCrow, I. T. Paulsen, L. D. Elbourne, M. Thiagarajan, D. B. Rusch, K. H. Nealson, S. J. Williamson, J. C. Venter, and A. E. Allen. 2012. Influence of nutrients and currents on the genomic composition of microbes across an upwelling mosaic. ISME J **6**:1403-1414.

Zhang, X. F., T. D. Yao, L. D. Tian, S. J. Xu, and L. Z. An. 2008. Phylogenetic and physiological diversity of bacteria isolated from Puruogangri ice core. Microb Ecol **55**:476-488.

Zhang, X. J., X. J. Ma, N. L. Wang, and T. D. Yao. 2009. New subgroup of Bacteroidetes and diverse microorganisms in Tibetan plateau glacial ice provide a biological record of environmental conditions. FEMS Microbiol Ecol **67**:21-29.

Zwart, G., B. C. Crump, M. Agterveld, F. Hagen, and S. K. Han. 2002. Typical freshwater bacteria: an analysis of available 16S rRNA gene sequences from plankton of lakes and rivers. Aquatic Microbial Ecology **28**:141-155.

Zwart, G., W. D. Hiorns, B. A. Methe, M. P. Van Agterveld, R. Huismans, S. C. Nold, J. P. Zehr, and H. J. Laanbroek. 1998. Nearly identical 16S rRNA sequences recovered from lakes in North America and Europe indicate the existence of clades of globally distributed freshwater bacteria. Systematic and Applied Microbiology **21**:546-556.

Appendix A

Figure A.C3.1: Phylogenetic placement for the most novel (< 92 % identity to previously reported sequences) 16S rRNA gene sequences found in the amplicons mixture for of lakes Cisó, Vilar and Banyoles basin C-III. Partial sequences (mean length 250bp) were inserted in the original consensus ARB tree (www.arb-home.de) keeping the overall tree topology by using the parsimony interactive tool.

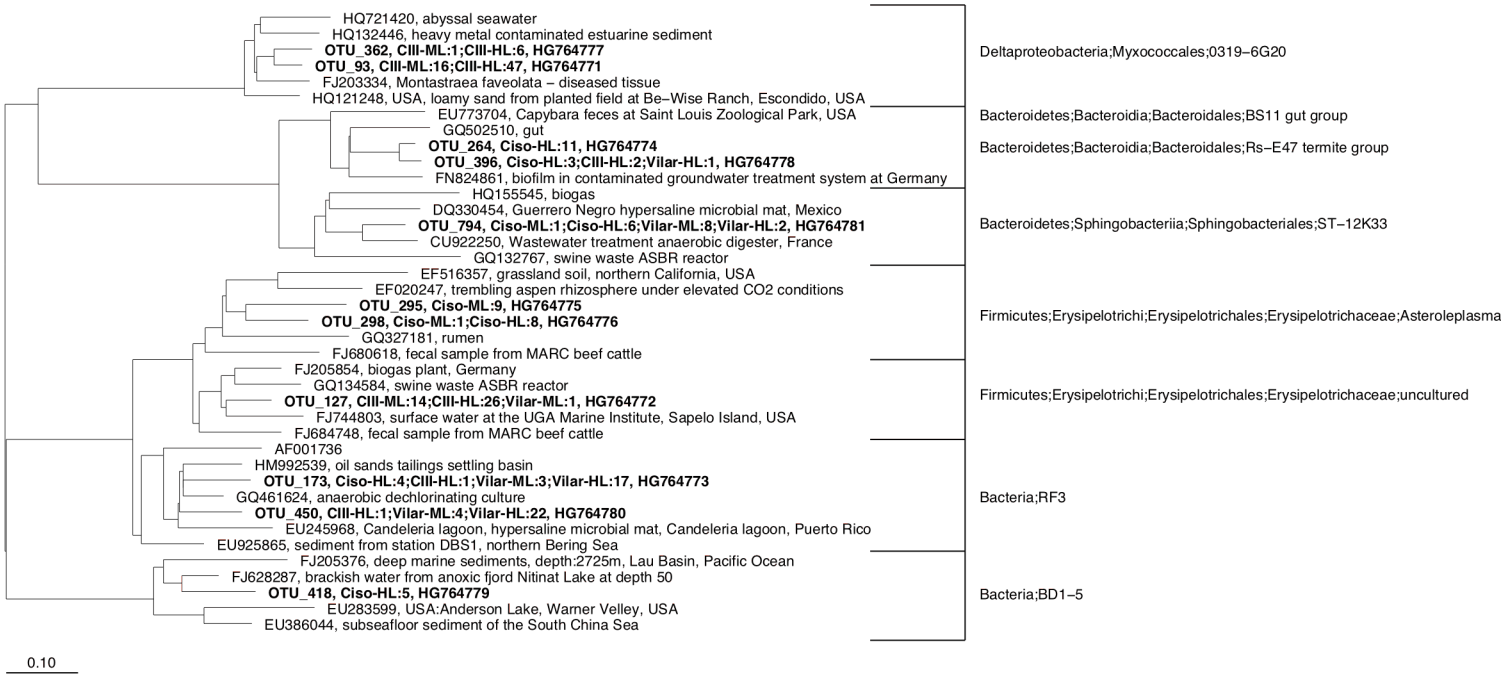

Table A.C3.1: Specific taxonomic composition (Order level) of Bacteria (% relative abundance) surveyed by PCR-amplified 16S rRNA gene and 454-tag sequencing for Banyoles basin C-III, Lake Vilar, and Lake Cisó. ML: Metalimnion. HL: Hypolimnion.

Phylum/Class	Order	Cisó-ML	Cisó-HL	CIII-ML	CIII-HL	Vilar-ML	Vilar-HL
Acidobacteria	Other	0.0	0.7	0.0	0.0	0.0	0.0
Actinobacteria	Acidimicrobiales	2.8	0.0	8.3	0.0	2.8	2.7
	Frankiales	14.2	1.3	21.0	2.3	15.7	24.2
	Micrococcales	21.3	3.7	0.0	0.0	3.2	1.7
	Other	1.8	0.2	1.6	0.5	2.3	2.6
Alphaproteo-bacteria	Rickettsiales (SAR11)	0.0	0.0	15.7	0.0	18.5	20.5
	Other	1.2	0.5	0.5	0.4	1.4	1.1
Bacteroidetes	Bacteroidales	0.0	3.8	0.0	0.0	1.7	5.3
	Flavobacteriales	4.4	0.0	3.5	0.0	12.0	1.4
	Sphingobacteriales	4.0	9.3	5.8	1.0	4.9	3.0
	Other	4.2	4.1	0.6	1.3	2.4	4.4
Betaproteo-bacteria	Burkholderiales	31.8	15.5	4.2	1.2	7.0	4.5
	Hydrogenophilales	0.0	0.0	0.0	0.0	3.2	2.4
	Methylophilales	3.7	0.0	1.4	0.0	2.2	1.9
	Gallionellales	0.0	0.0	2.4	8.2	0.0	0.0
	Rhodocyclales	0.0	0.0	0.0	0.0	3.9	5.2
	Other	0.4	0.5	0.4	1.9	1.0	0.2
Chlorobi	Chlorobiales	1.1	3.7	23.7	67.6	0.0	0.0
	Other	0.0	0.0	0.2	0.7	0.1	0.1
Chloroflexi	Anaerolineales	0.0	2.0	0.0	0.0	0.0	0.0
	Other	0.2	0.9	1.3	0.9	0.6	1.5
Cyanobacteria	Cyanobacteria	1.7	0.5	0.0	0.4	6.2	0.0
	Synechococcus	0.0	0.0	1.1	0.0	0.0	0.0
	Other	0.0	0.0	1.9	0.3	0.0	0.0
Deltaproteo-bacteria	Desulfobacterales	0.0	4.5	0.0	1.1	0.0	1.0
	Desulfuromonadales	0.0	0.0	0.0	1.1	0.0	0.0
	Myxococcales	0.0	0.0	0.0	0.0	1.1	0.0
	Syntrophobacterales	0.0	16.0	0.0	1.2	0.0	0.0
	Other	1.3	2.7	1.4	0.2	0.3	0.8
Epsilonproteo-bacteria	Campylobacterales	2.3	0.0	0.8	2.1	0.0	0.0
	Other	0.0	0.3	0.0	0.0	0.0	0.0
Firmicutes	Clostridiales	0.0	4.5	0.0	0.0	0.0	1.1
	Erysipelotrichales	0.0	2.3	0.0	1.2	2.7	3.1
	Other	0.6	0.0	0.8	0.4	0.2	0.0
Gammaproteo-bacteria	Aeromonadales	0.0	0.0	0.0	0.0	0.1	0.0
	Chromatiales	1.6	12.2	0.0	0.0	1.0	0.0
	Methylococcales	0.0	0.0	0.0	0.0	1.5	0.0
	Pseudomonadales	0.0	0.0	0.0	0.0	0.0	3.6
	Other	0.1	0.2	0.3	0.3	1.2	1.3
Spirochaetes	Spirochaetales	0.0	3.2	0.0	0.0	0.0	1.7
	Other	0.3	0.0	0.0	0.4	0.0	0.0
Tenericutes	Acholeplasmatales	0.0	3.0	0.0	0.0	0.0	0.0
	Other	0.0	0.0	0.0	0.9	0.0	0.0
Verrucomicrobia	Other	0.0	0.0	0.0	0.0	1.3	0.6
Other	Other	0.3	0.9	1.3	0.6	0.4	0.6
Unclassified	Unclassified	0.7	3.4	1.8	4.0	1.1	3.3

Table A.C3.2: Detailed information on the OTUs placed in the highest novelty plot area with mean abundances >0.01% (Fig. 3.4).

OTU	Cisó ML	Cisó HL	CIII ML	CIII HL	Vilar ML	Vilar HL	Layer >80%	Abundance	CCM	CEM	Closest Match	Classification
OTU_532	0	4	0	0	0	0	Hypolimnion	0.1-0.01	92.31	96.13	96.13	Acidobacteria Holophagae Holophagales Holophagaceae
OTU_416	0	5	0	0	0	0	Hypolimnion	0.1-0.01	84.53	93.41	93.41	Alphaproteobacteria Rickettsiales Candidatus
OTU_219	0	16	0	0	0	0	Hypolimnion	0.1-0.01	86.41	94.62	94.62	Alphaproteobacteria Rhodospirillales Rhodospirillaceae Thalassospira
OTU_398	0	9	0	0	0	0	Hypolimnion	0.1-0.01	87.86	91.4	91.4	Bacteroidetes Sphingobacteria Sphingobacteriales
OTU_283	0	10	0	0	0	0	Hypolimnion	0.1-0.01	88.1	91.86	91.86	Bacteroidetes Sphingobacteria Sphingobacteriales
OTU_522	0	4	0	0	0	0	Hypolimnion	0.1-0.01	86.96	94.07	94.07	Bacteroidetes Bacteroidia Bacteroidales Rikenellaceae
OTU_412	0	5	0	0	0	0	Hypolimnion	0.1-0.01	89.59	94.95	94.95	Bacteroidetes Sphingobacteria Sphingobacteriales WCHB1-69

Table A.C3.2: *Continued*

OTU	Cisó ML	Cisó HL	CIII ML	CIII HL	Vilar ML	Vilar HL	Layer >80%	Abundance	CCM	CEM	Closest Match	Classification
OTU_634	0	2	1	0	1	8	Hypolimnion	0.1-0.01	95.05	95.46	95.46	Bacteroidetes Bacteroidia Bacteroidales Porphyromonadaceae
OTU_200	0	12	0	0	0	6	Hypolimnion	0.1-0.01	86.28	96.34	96.34	Bacteroidetes Bacteroidia Bacteroidales FTLpost3
OTU_647	0	7	0	0	0	0	Hypolimnion	0.1-0.01	88.73	96.74	96.74	Bacteroidetes Bacteroidia Bacteroidales Rikenellaceae
OTU_491	0	0	0	4	0	0	Hypolimnion	0.1-0.01	93.67	96.04	96.04	Unresolved Betaproteobacteria
OTU_939	0	0	0	0	0	3	Hypolimnion	0.1-0.01	93.09	96.05	96.05	Betaproteobacteria Rhodocyclales Rhodocyclaceae uncultured
OTU_443	0	5	0	0	0	0	Hypolimnion	0.1-0.01	92.57	92.88	92.88	Unresolved Chloroflexi
OTU_182	0	11	1	4	0	0	Hypolimnion	0.1-0.01	86.35	94.85	94.85	Chloroflexi Anaerolineae Anaerolineales Anaerolineaceae
OTU_414	0	7	0	0	0	0	Hypolimnion	0.1-0.01	89.51	96.9	96.9	Chloroflexi Anaerolineae Anaerolineales Anaerolineaceae

Table A.C3.2: *Continued*

OTU	Cisó ML	Cisó HL	CIII ML	CIII HL	Vilar ML	Vilar HL	Layer >80%	Abundance	CCM	CEM	Closest Match	Classification
OTU_170	0	26	0	0	0	0	Hypolimnion	0.1-0.01	81.5	91.91	91.91	Deltaproteobacteria Myxococcales 0319-6G20
OTU_321	0	5	0	0	0	0	Hypolimnion	0.1-0.01	90.19	92.51	92.51	Deltaproteobacteria Desulfobacterales Desulfobacteraceae uncultured
OTU_330	1	6	0	0	0	0	Hypolimnion	0.1-0.01	92.64	93.32	93.32	Deltaproteobacteria Syntrophobacterales Syntrophaceae Desulfomonile
OTU_497	0	4	0	0	0	0	Hypolimnion	0.1-0.01	86.96	95.67	95.67	Deltaproteobacteria Sva0485
OTU_289	0	7	0	2	0	0	Hypolimnion	0.1-0.01	85.91	96.41	96.41	Deltaproteobacteria Myxococcales 0319-6G20
OTU_415	0	5	0	0	0	0	Hypolimnion	0.1-0.01	96.89	96.89	96.89	Deltaproteobacteria Desulfuromonadales Geobacteraceae Geobacter
OTU_469	0	0	0	4	0	0	Hypolimnion	0.1-0.01	86.59	95.9	95.9	Elusimicrobia
OTU_183	0	21	0	0	0	0	Hypolimnion	0.1-0.01	89.75	92.24	92.24	Firmicutes Clostridia Clostridiales Veillonellaceae

Table A.C3.2: *Continued*

OTU	Cisó ML	Cisó HL	CIII ML	CIII HL	Vilar ML	Vilar HL	Layer >80%	Abundance	CCM	CEM	Closest Match	Classification
OTU_245	1	12	0	0	0	0	Hypolimnion	0.1-0.01	83.81	93.03	93.03	Firmicutes Clostridia Clostridiales
OTU_638	0	1	0	0	0	2	Hypolimnion	0.1-0.01	90.84	96.95	96.95	Firmicutes Clostridia Clostridiales Ruminococcaceae
OTU_521	0	1	0	3	0	1	Hypolimnion	0.1-0.01	93.92	96.96	96.96	Firmicutes Clostridia Clostridiales Clostridiaceae
OTU_434	1	4	0	0	0	0	Hypolimnion	0.1-0.01	87.74	93.91	93.91	Spirochaetes Spirochaetales Spirochaetaceae
OTU_262	0	11	0	0	0	0	Hypolimnion	0.1-0.01	89.14	95.39	95.39	Spirochaetes Spirochaetales Spirochaetaceae
OTU_215	0	0	0	1	0	15	Hypolimnion	0.1-0.01	94.48	95.67	95.67	Spirochaetes Spirochaetales Spirochaetaceae
OTU_168	0	4	1	7	0	14	Hypolimnion	0.1-0.01	94.7	96.26	96.26	Spirochaetes Spirochaetales Spirochaetaceae
OTU_603	0	0	0	1	0	2	Hypolimnion	0.1-0.01	79.78	87.63	87.63	Unclassified
OTU_533	0	0	0	0	0	4	Hypolimnion	0.1-0.01	77.78	89.13	89.13	Unclassified
OTU_550	0	0	0	0	0	3	Hypolimnion	0.1-0.01	82.18	92.41	92.41	Unclassified
OTU_460	0	4	0	0	0	0	Hypolimnion	0.1-0.01	77.53	92.6	92.6	Unclassified

Table A.C3.2: *Continued*

OTU	Cisó ML	Cisó HL	CIII ML	CIII HL	Vilar ML	Vilar HL	Layer >80%	Abundance	CCM	CEM	Closest Match	Classification
OTU_489	0	4	0	0	0	0	Hypolimnion	0.1-0.01	80.61	92.75	92.75	Unclassified
OTU_374	0	0	1	5	0	0	Hypolimnion	0.1-0.01	78.28	93.45	93.45	Unclassified
OTU_208	0	1	3	3	2	16	Hypolimnion	0.1-0.01	80.58	94.23	94.23	Unclassified
OTU_164	0	5	1	3	1	18	Hypolimnion	0.1-0.01	88.92	94.32	94.32	Unclassified
OTU_475	0	0	0	0	0	4	Hypolimnion	0.1-0.01	86.33	94.37	94.37	Unclassified
OTU_296	0	9	0	0	0	0	Hypolimnion	0.1-0.01	79.55	94.7	94.7	Unclassified
OTU_602	0	1	0	0	0	2	Hypolimnion	0.1-0.01	78.46	94.8	94.8	Unclassified
OTU_339	0	7	1	5	1	9	Hypolimnion	0.1-0.01	82.93	95.71	95.71	Unclassified
OTU_304	0	9	0	0	0	0	Hypolimnion	0.1-0.01	84.71	96.12	96.12	Unclassified
OTU_418	0	5	0	0	0	0	Hypolimnion	0.1-0.01	75.45	88.43	88.43	Unclassified
OTU_173	0	4	0	1	3	17	Hypolimnion	0.1-0.01	84.38	92.13	92.13	Unclassified
OTU_362	0	0	1	6	0	0	Hypolimnion	0.1-0.01	84.39	89.54	89.54	Unclassified
OTU_298	1	8	0	0	0	0	Hypolimnion	0.1-0.01	84.94	86.04	86.04	Unclassified
OTU_396	0	3	0	2	0	1	Hypolimnion	0.1-0.01	86.03	88.33	88.33	Unclassified
OTU_264	0	11	0	0	0	0	Hypolimnion	0.1-0.01	86.59	88.81	88.81	Unclassified
OTU_123	1	51	0	0	0	0	Hypolimnion	1-0.1	90.67	92.75	92.75	Deltaproteobacteria Desulfobacterales Desulfobacteraceae uncultured
OTU_71	4	145	1	11	0	0	Hypolimnion	1-0.1	92.51	94.65	94.65	Firmicutes Clostridia Clostridiales Family
OTU_159	23	264	0	0	0	0	Hypolimnion	1-0.1	96.4	96.4	96.4	Gammaproteobacteria Chromatiales Chromatiaceae
OTU_450	0	0	0	1	4	22	Hypolimnion	1-0.1	83.64	91.46	91.46	Unclassified

Table A.C3.2: *Continued*

OTU	Cisó ML	Cisó HL	CIII ML	CIII HL	Vilar ML	Vilar HL	Layer >80%	Abundance	CCM	CEM	Closest Match	Classification
OTU_614	0	0	7	0	1	1	Metalimnion	0.1-0.01	90.94	96.99	96.99	Actinobacteria Acidimicrobiia Acidimicrobiales Acidimicrobiaceae
OTU_945	0	0	5	0	1	0	Metalimnion	0.1-0.01	90.91	95.96	95.96	Bacteroidetes Sphingobacteria Sphingobacteriales Chitinophagaceae
OTU_958	0	0	0	0	8	0	Metalimnion	0.1-0.01	93.14	96.41	96.41	Bacteroidetes Flavobacteria Flavobacteriales Cryomorphaceae
OTU_302	0	0	0	0	7	1	Metalimnion	0.1-0.01	92.56	96.92	96.92	Bacteroidetes Flavobacteria Flavobacteriales Cryomorphaceae
OTU_546	3	0	0	0	0	0	Metalimnion	0.1-0.01	81.84	91.93	91.93	Betaproteobacteria Nitrosomonadales Nitrosomonadaceae uncultured
OTU_385	0	0	0	0	5	1	Metalimnion	0.1-0.01	90.17	91.89	91.89	Gammaproteobacteria Chromatiales Ectothiorhodospiraceae Thioalkalispira

Table A.C3.2: *Continued*

OTU	Cisó ML	Cisó HL	CIII ML	CIII HL	Vilar ML	Vilar HL	Layer >80%	Abundance	CCM	CEM	Closest Match	Classification
OTU_199	0	0	1	2	15	0	Metalimnion	0.1-0.01	96.57	95.64	96.57	Gammaproteobacteria Chromatiales Chromatiaceae Thiocystis
OTU_594	3	0	0	0	0	0	Metalimnion	0.1-0.01	86.6	89.72	89.72	Unclassified
OTU_295	9	0	0	0	0	0	Metalimnion	0.1-0.01	80.73	82.57	82.57	Unclassified
OTU_727	0	0	0	0	33	0	Metalimnion	1-0.1	92.88	96.57	96.57	Bacteroidetes Flavobacteria Flavobacteriales Cryomorphaceae
OTU_103	0	0	0	0	53	4	Metalimnion	1-0.1	85.09	93.02	93.02	Deltaproteobacteria Myxococcales 0319-6G20

Figure A.C4.1: Comparison of the phylogenetic composition (phylum level) for the metagenomics reads found in each size fraction (3, 0.8, and 0.1 μm). Very similar composition was observed among the differents fractions.

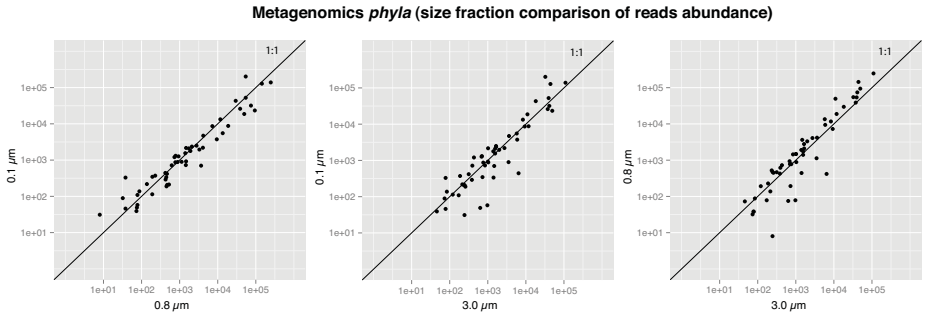

Figure A.C4.2: Vertical distributions of ammonium, nitrate and nitrite in Lake Banyoles basin C-III.

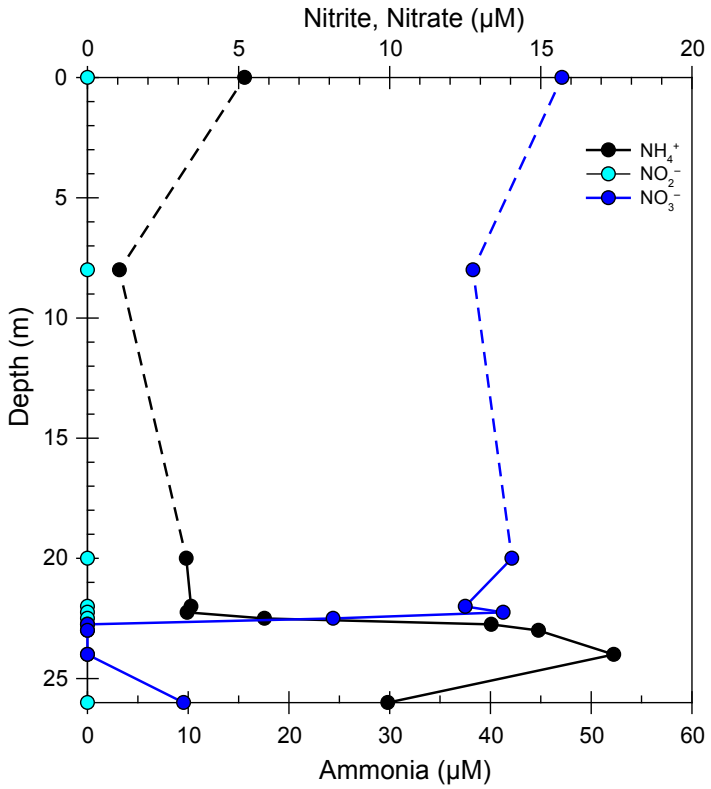

Figure A.C4.3: Relative abundance of archaea metagenomics reads mostly related to methanogens, with a few representatives within Thermococci, Thermoplasmata, Archaeoglobi, and Haloarchaea (100% in X axis is total euryarchaeota reads per sample).

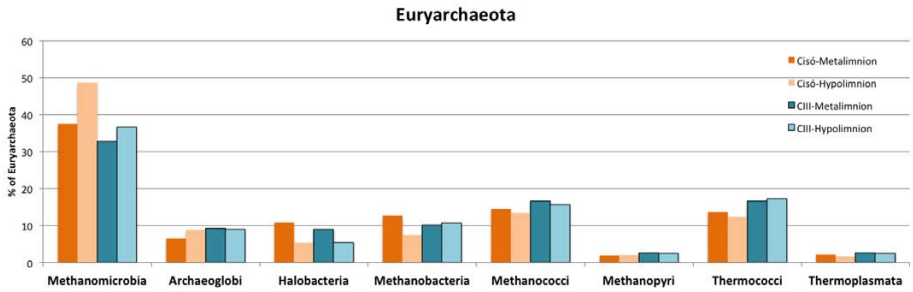

Figure A.C4.4: Housekeeping genes clustering of the metagenomes analyzed for Lake Cisó and Lake Banyoles basin C-III.

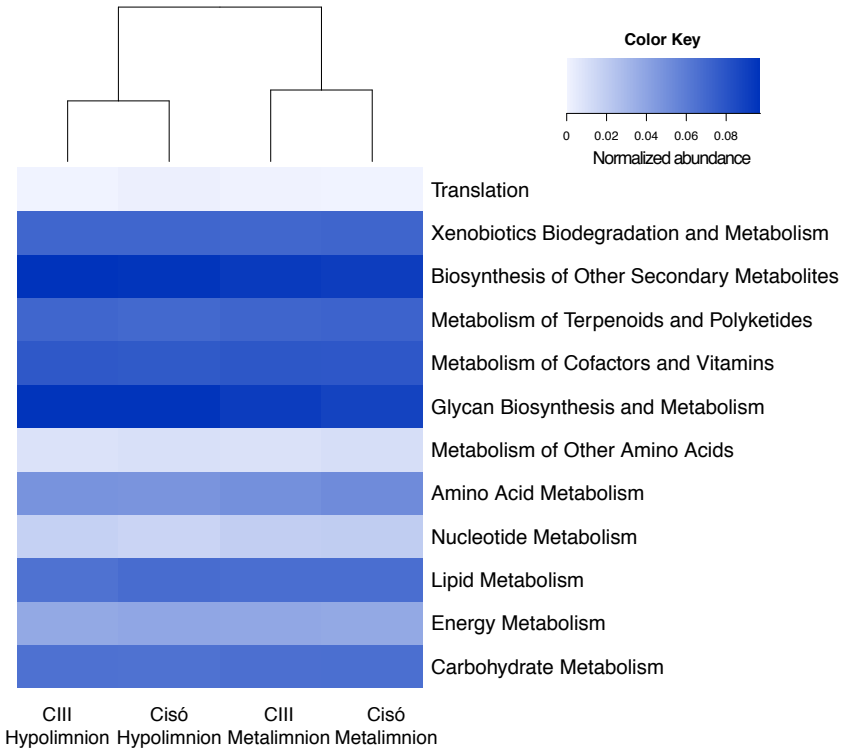

Table A.C4.1: Detailed list of the marker genes used in the present work for the carbon, nitrogen and sulfur cycles in for Banyoles basin C-III and Lake Cisó.

Cycle	Step	KEGG	Gene
CARBON	Aerobic C fixation*(Calvin cycle) (K00855+K01602)/2	K00855	phosphoribulokinase
		K01602	RuBisCO small chain
	Aerobic CH4 oxidation	K08684	methane monooxygenase
	Aerobic respiration (K02256+K02262)/2 +(K02274+K02276)/2	K02256	cytochrome c oxidase subunit I (coxI)
		K02262	cytochrome c oxidase subunit III (coxIII)
		K02274	cytochrome c oxidase subunit I (coxA)
		K02276	cytochrome c oxidase subunit III (coxC)
	Anaerobic C fixation (Arnon:K00174,K00175, K00244,K01648. Reductive Acetil-CoA: K00194,K00197) (K00174+K00175+K00244 +K01648)/4+(K00194 +K00197)/2	K00174	2-oxoglutarate:ferredoxin oxidoreductase subunit alpha
		K00175	2-oxoglutarate:ferredoxin oxidoreductase subunit beta
		K00244	frdA; fumarate reductase flavoprotein subunit
		K01648	adenosinetriphosphate (ATP) citrate lyase
		K00194	CO dehydrogenase subunit delta
		K00197	CO dehydrogenase subunit gamma
	CO oxidation (K03518+K03519+K03520) /3	K03518	CO dehydrogenase small subunit (coxS)
		K03519	cutM, coxM; carbon-monoxide dehydrogenase medium subunit
		K03520	cutL, coxL; carbon-monoxide dehydrogenase large subunit
	Fermentation	K00016	L-lactate dehydrogenase
	Methanogenesis (K00400+K00401)/2	K00400	coenzyme M methyl reductase beta subunit (mcrB)
		K00401	methyl coenzyme M reductase system, component A2
NITROGEN	Ammonification K05904+K03385	K03385	formate-dependent nitrite reductase periplasmic cytochrome c552 (nrfA)
		K05904	cytochrome c nitrite reductase (nrfA)
	Anammox (SRAO)	K10535	hydroxylamine oxidoreductase/hydrazine oxidoreducatse (hao/hzo)
	Denitrification (K02305+K04561+K00376) /3	K00376	nitrous oxide reductase (nosZ)
		K02305	nitric-oxide reductase (norC)
		K04561	nitric-oxide reductase (norB)
	Nitrate reduction + Nitrite oxidation (K00370+K00371)/2	K00370	nitrate reductase alpha & nitrite oxidoreductase (narG/nxrA)
		K00371	nitrate reductase beta & nitrite oxidoreductase (narH/nxrB)

Table A.C4.1: *Continued*

Cycle	Step	KEGG	Gene
NITROGEN	Nitrate reduction (K02567+K02568)/2	K02567	periplasmic nitrate reductase (napA)
		K02568	cytochrome c-type protein (napB)
	Nitrification (K10944+K10945+K10946) /3	K10944	ammonia monooxygenase subunit A (amoA)
		K10945	ammonia monooxygenase subunit B (amoB)
		K10946	ammonia monooxygenase subunit C (amoC)
	Nitrogen assimilation (K00360+K00367+K01915 +K00265+K00284)/3	K00265	glutamate synthase (NADPH/NADH) large chain (gltB)
		K00284	glutamate synthase (ferredoxin-dependent) (gltS)
		K00360	assimilatory nitrate reductase
		K00367	assimilatory nitrate reductase
		K01915	glutamine synthetase (glnA)
	Nitrogen Fixation (K00531+K02586+K02588 +K02591)/4	K00531	nitrogenase
		K02586	nitrogenase molybdenum-iron protein alpha chain (nifD)
		K02588	nitrogenase iron protein (nifH)
		K02591	nitrogenase molybdenum-iron protein beta chain (nifK)
	Nitrogen Mineralization K00260+K00261+K00262	K00260	glutamate dehydrogenase
		K00261	glutamate dehydrogenase
		K00262	glutamate dehydrogenase
SULFUR	Assimilatory sulfate reduction (K00860+K00956+K00957) /3	K00860	adenylylsulfate kinase (cysC)
		K00956	sulfate adenylyltransferase subunit 1 (cysN)
		K00957	sulfate adenylyltransferase subunit 2 (cysD)
	Dissimilatory sulfate reduction and sulfide oxidation** (K00394+K00395+K11180) /3	K00394	adenylylsulfate reductase subunit A (aprA)
		K00395	adenylylsulfate reductase subunit B (aprB)
		K11180	sulfite reductase (dsrA)
	Sulfur Mineralization K00456+K01011	K00456	cysteine dioxygenase
		K01011	3-mercaptopyruvate sulfurtransferase
	Polysulfide reduction	K08352	polysulfide reductase chain A (psrA)

*: *Chromatiales*: anoxygenic phototrophy through the Calvin cycle.
**: As marker genes K00394, K00395, K11180 can operate in both an oxidative and a reductive way. They were assigned to the sulfate reduction or sulfide oxidation step if they had a best match within KEGG to an ortholog from a sulfate-reducing or sulfur-oxidizing clade.

Table A.C4.2: Specific taxonomic composition (Order level) of Bacteria and Archaea (% relative abundance) according to the 16S rRNA gene present in the metagenomic pool for Lake Cisó and Lake Banyoles basin C-III. ML: Metalimnion. HL: Hypolimnion.

Phylum	Order	Ciso-ML	Ciso-HL	CIII-ML	CIII-HL	*average*
Chlorobi	Chlorobiales	0.65	5.36	22.46	50.44	19.73
Epsilonproteobacteria	Campylobacterales	10.97	12.46	12.61	20.84	14.22
Betaproteobacteria	Burkholderiales	35.27	9.52	3.91	0.51	12.30
OD1	OD1	4.30	13.15	5.80	8.64	7.97
Actinobacteria	Frankiales	7.96	0.35	11.74	0.64	5.17
Bacteroidetes	Sphingobacteriales	4.52	7.09	4.49	0.25	4.09
Actinobacteria	Micrococcales	13.12	1.38	0.14	0.00	3.66
Unclassified	Unclassified	1.29	2.60	3.48	4.96	3.08
Actinobacteria	Acidimicrobiales	2.58	0.00	5.36	0.00	1.99
Bacteroidetes	Flavobacteriales	4.95	0.52	2.17	0.00	1.91
Deltaproteobacteria	Syntrophobacterales	0.22	7.27	0.00	0.13	1.90
Alphaproteobacteria	SAR11	0.00	0.00	6.67	0.13	1.70
Betaproteobacteria	Nitrosomonadales	0.00	0.00	2.75	2.54	1.32
Firmicutes	Clostridiales	0.86	2.94	0.58	0.25	1.16
OP3	OP3	0.65	2.42	0.87	0.51	1.11
Euryarchaeota	Halobacteriales	0.86	1.90	0.58	1.02	1.09
Betaproteobacteria	Methylophilales	2.15	0.00	1.59	0.13	0.97
Deltaproteobacteria	Desulfobacterales	0.22	3.11	0.14	0.25	0.93
Gammaproteobacteria	Chromatiales	0.22	3.46	0.00	0.00	0.92
Actinobacteria	Unresolved Actinobacteria	1.72	0.00	1.45	0.25	0.86
OP11	OP11	0.22	2.08	0.29	0.64	0.80
Firmicutes	Erysipelotrichales	0.43	1.38	0.43	0.76	0.75
Tenericutes	Acholeplasmatales	0.65	1.90	0.00	0.13	0.67
Tenericutes	NB1-n	0.22	0.69	0.87	0.89	0.67
Betaproteobacteria	Unresolved Betaproteobacteria	0.65	0.17	1.16	0.38	0.59
Chloroflexi	SL56 marine group	0.00	0.00	2.32	0.00	0.58
Verrucomicrobia	vadinHA64	0.00	0.00	2.32	0.00	0.58
Deltaproteobacteria	Myxococcales	0.00	0.87	0.00	1.27	0.53
Chloroflexi	Anaerolineales	0.22	1.21	0.29	0.38	0.52
BD1-5	BD1-5	0.22	1.56	0.14	0.13	0.51
Firmicutes	Selenomonadales	0.00	1.38	0.14	0.13	0.41
Bacteroidetes	Unresolved Bacteroidetes	0.00	0.87	0.14	0.64	0.41
Bacteroidetes	Bacteroidales	0.22	1.21	0.00	0.13	0.39
Bacteroidetes	Other Bacteroidetes	0.00	1.38	0.14	0.00	0.38
Lentisphaerae	RFP12	0.00	1.38	0.00	0.00	0.35
Spirochaetae	Spirochaetales	0.22	1.04	0.00	0.13	0.35
Cyanobacteria	Chloroplast	0.43	0.35	0.43	0.00	0.30
Cyanobacteria	Synechococcus	0.00	0.17	1.01	0.00	0.30
Actinobacteria	PeM15	1.08	0.00	0.00	0.00	0.27
Deltaproteobacteria	Bdellovibrionales	0.43	0.35	0.14	0.00	0.23
SR1	SR1	0.22	0.52	0.00	0.00	0.18
Deltaproteobacteria	Unresolved Deltaproteobacteria	0.00	0.69	0.00	0.00	0.17
NPL-UPA2	NPL-UPA2	0.22	0.17	0.00	0.25	0.16
Betaproteobacteria	Rhodocyclales	0.22	0.00	0.29	0.13	0.16
Deltaproteobacteria	Desulfarculales	0.00	0.35	0.00	0.25	0.15
Elusimicrobia	Elusimicrobia	0.00	0.00	0.14	0.38	0.13

Table A.C4.2: *Continued*

Phylum	Order	Ciso-ML	Ciso-HL	CIII-ML	CIII-HL	*average*
Actinobacteria	Gaiellales	0.00	0.52	0.00	0.00	0.13
Lentisphaerae	Unresolved Lentisphaerae	0.00	0.52	0.00	0.00	0.13
Verrucomicrobia	Chthoniobacterales	0.00	0.52	0.00	0.00	0.13
TM7	TM7	0.00	0.52	0.00	0.00	0.13
Euryarchaeota	Methanomicrobiales	0.00	0.52	0.00	0.00	0.13
Gammaproteobacteria	Legionellales	0.22	0.17	0.00	0.13	0.13
Deltaproteobacteria	Sva0485	0.00	0.35	0.14	0.00	0.12
OP8	OP8	0.00	0.35	0.14	0.00	0.12
Chlorobi	Ignavibacteriales	0.00	0.17	0.29	0.00	0.12
Fibrobacteres	Fibrobacteria	0.00	0.17	0.14	0.13	0.11
Chloroflexi	Unresolved Chloroflexi	0.00	0.00	0.43	0.00	0.11
Alphaproteobacteria	Rhodobacterales	0.43	0.00	0.00	0.00	0.11
Lentisphaerae	WCHB1-41	0.00	0.17	0.00	0.25	0.11
Alphaproteobacteria	Rhizobiales	0.22	0.17	0.00	0.00	0.10
Deltaproteobacteria	Desulfuromonadales	0.00	0.00	0.00	0.38	0.10
Planctomycetes	Phycisphaerae	0.00	0.35	0.00	0.00	0.09
Betaproteobacteria	Hydrogenophilales	0.22	0.00	0.00	0.13	0.09
Lentisphaerae	Victivallales	0.00	0.17	0.14	0.00	0.08
Planctomycetes	Planctomycetales	0.00	0.17	0.14	0.00	0.08
Fusobacteria	Fusobacteriales	0.00	0.17	0.00	0.13	0.08
Alphaproteobacteria	Unresolved Alphaproteobacteria	0.00	0.00	0.29	0.00	0.07
Gammaproteobacteria	Pseudomonadales	0.00	0.00	0.29	0.00	0.07
Gemmatimonadetes	Gemmatimonadales	0.00	0.00	0.14	0.13	0.07
Planctomycetes	vadinHA49	0.00	0.00	0.14	0.13	0.07
Actinobacteria	Propionibacteriales	0.22	0.00	0.00	0.00	0.05
Gammaproteobacteria	Thiotrichales	0.22	0.00	0.00	0.00	0.05
Bacteroidetes	Cytophagales	0.22	0.00	0.00	0.00	0.05
TM6	TM6	0.22	0.00	0.00	0.00	0.05
Acidobacteria	Unresolved Acidobacteria	0.00	0.17	0.00	0.00	0.04
Actinobacteria	Corynebacteriales	0.00	0.17	0.00	0.00	0.04
Alphaproteobacteria	Rickettsiales	0.00	0.17	0.00	0.00	0.04
Deltaproteobacteria	43F-1404R	0.00	0.17	0.00	0.00	0.04
Deltaproteobacteria	Desulfovibrionales	0.00	0.17	0.00	0.00	0.04
Cyanobacteria	Gastranaerophilales	0.00	0.17	0.00	0.00	0.04
BRC1	BRC3	0.00	0.17	0.00	0.00	0.04
TA06	TA08	0.00	0.17	0.00	0.00	0.04
Euryarchaeota	Methanobacteriales	0.00	0.17	0.00	0.00	0.04
Euryarchaeota	Thermoplasmatales	0.00	0.17	0.00	0.00	0.04
Alphaproteobacteria	Caulobacterales	0.00	0.00	0.14	0.00	0.04
Gammaproteobacteria	Xanthomonadales	0.00	0.00	0.14	0.00	0.04
Verrucomicrobia	Opitutales	0.00	0.00	0.14	0.00	0.04
WS6	WS8	0.00	0.00	0.14	0.00	0.04
Alphaproteobacteria	Rhodospirillales	0.00	0.00	0.00	0.13	0.03
Alphaproteobacteria	Sphingomonadales	0.00	0.00	0.00	0.13	0.03
Lentisphaerae	MSBL3	0.00	0.00	0.00	0.13	0.03
Verrucomicrobia	OPB35	0.00	0.00	0.00	0.13	0.03

Table A.C4.3: Relative abundance of marker genes related to carbon, nitrogen and sulfur cycling as a proxy of the potential in situ relevance of the metabolic pathways. ML: Metalimnion. HL: Hypolimnion.

Cycle	Process	Cisó-ML %	Cisó-HL %	CIII-ML %	CIII-HL %
CARBON	Aerobic C fixation	5.6	3.9	2.0	1.6
	Aerobic CH4 oxidation	7.9	0.0	0.8	0.5
	Aerobic respiration	58.5	20.2	50.5	9.0
	Anaerobic C fixation	8.8	48.0	33.7	82.0
	CO oxidation	8.0	20.3	12.0	4.3
	Fermentation	11.2	7.0	1.0	2.5
	Methanogenesis	0.0	0.6	0.0	0.0
NITROGEN	Ammonification	1.7	8.1	0.5	2.6
	Anammox (SRAO)	0.0	5.5	0.3	0.3
	Denitrification	1.8	2.7	2.3	4.6
	Nitrate reduction + Nitrite oxidation (NarGH/NxrAB)	3.5	5.2	1.8	1.5
	Nitrate reduction	1.8	3.6	2.6	6.5
	Nitrification	0.0	0.0	0.0	0.0
	Nitrogen assimilation	63.6	25.5	42.5	36.1
	Nitrogen Fixation	1.1	10.7	8.1	25.8
	Nitrogen Mineralization	26.5	38.8	41.9	22.6
SULFUR	Assimilatory sulfate reduction	26.5	26.9	39.9	18.1
	Sulfur Mineralization	71.5	18.2	34.1	16.8
	Sulfur oxidation	0.4	5.6	16.6	41.8
	Dissimilatory sulfate reduction	0.7	15.6	0.9	2.7
	Polysilfide reduction	1.0	33.8	8.5	20.6

Figure A.C5.1: Plotted values of GC content versus read depth for each contig over 3kb from Newbler and CLC assemblies. Green dots show the sequences related to the blooming organism and selected for subsequent analysis. Red dots show the sequences related to the putative infecting phage.

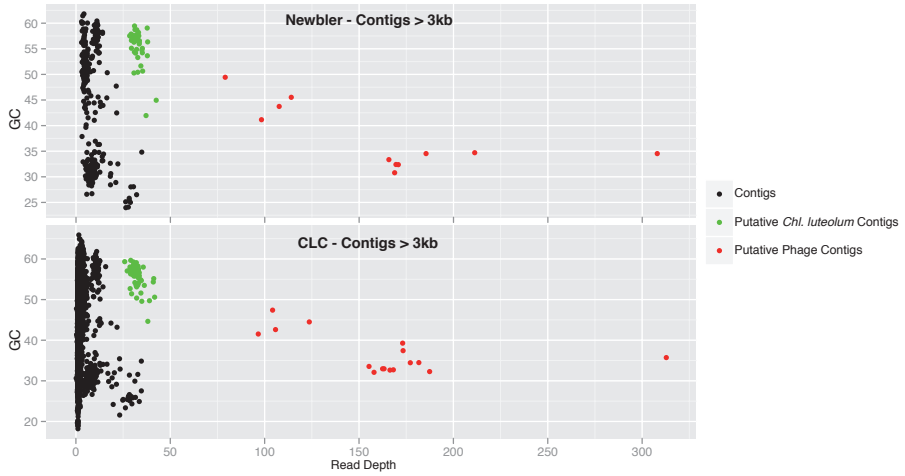

Figure A.C5.2: ACT view of the reference genome *Chl. luteolum* DSM 273^{T} (represented at the top) and the assembled genome of *Chl. luteolum* CIII (represented at the bottom). Red stripes show the regions with BLAST matches.

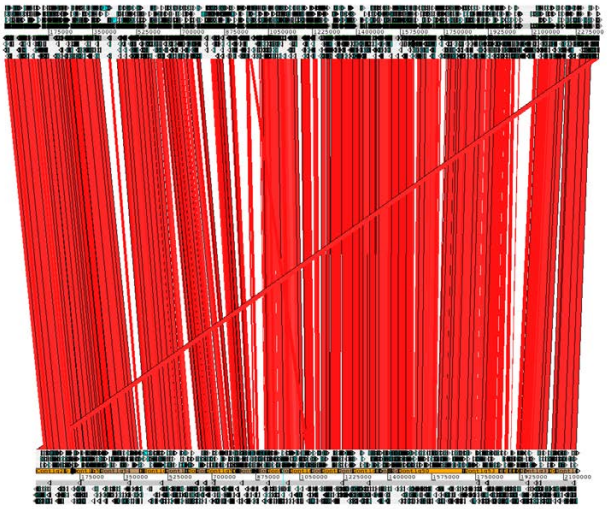

Figure A.C5.3: Whole genome alignments of *Chlorobi* genomes: a) *I. album*, b) *Chp. thalassium* ATCC 35110, c) *Chl. chlorochromatii* CaD3, d) *Ptc. phaeum* CIB 2401, e) *Ptc. aestuarii* DSM 271, f) *Ptc. phaeobacteroides* BS1, g) *Cba. parvum* NCIB 8327, h) *Cba. limnaeum* DSM 1677, i) *Cba. tepidum* TLS, j) *Chl. ferrooxidans* DSM 13101, k) *Chl. clathratiforme* DSM 5477, l) *Chl. phaeobacteroides* DSM 266, m) *Chl. limicola* DSM 245, n) *Chl. phaeovibrioides* DSM 265, o) *Chl. luteoulm* DSM 273^{T}, p) *Chl. luteolum* CIII. The dots show the conserved regions after BLAST analysis of each sequence versus the others. The green square marks both strains of *Chl. luteolum* whilst the orange square marks the three strains within the genus *Chlorobaculum*.

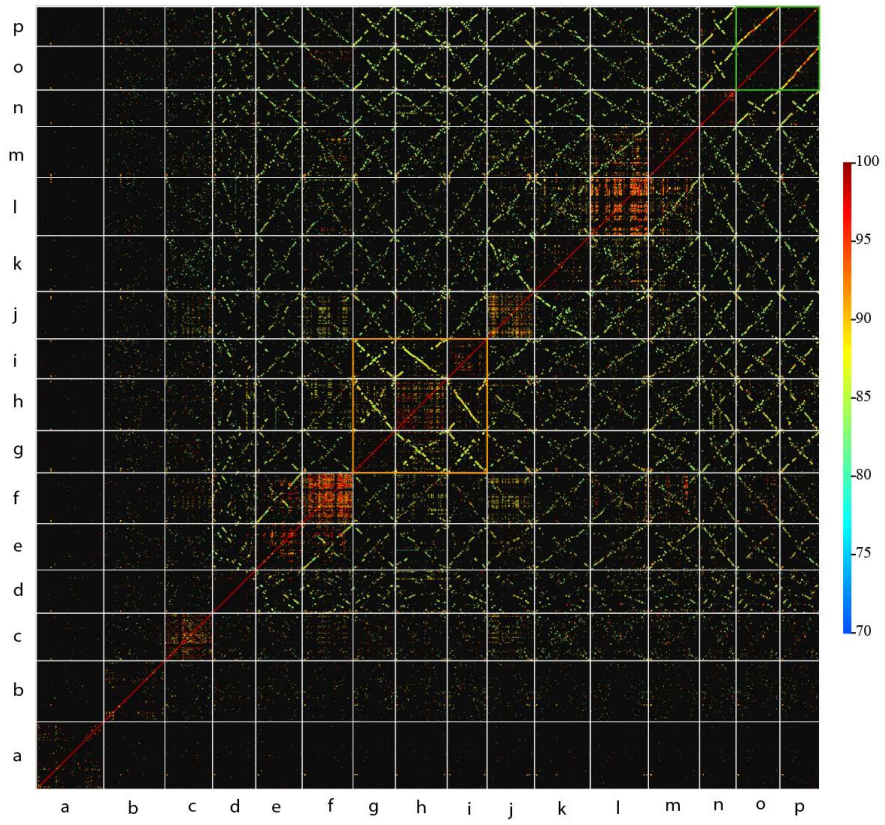

Figure A.C5.4: Maximum likelihood phylogeny with RAxML of the FeoB (Ferrous iron transport protein B). The red squares mark the two cluster forming each FeoB form in GSB. FeoB sequences related to *Chl. luteolum* sp. are in bold.

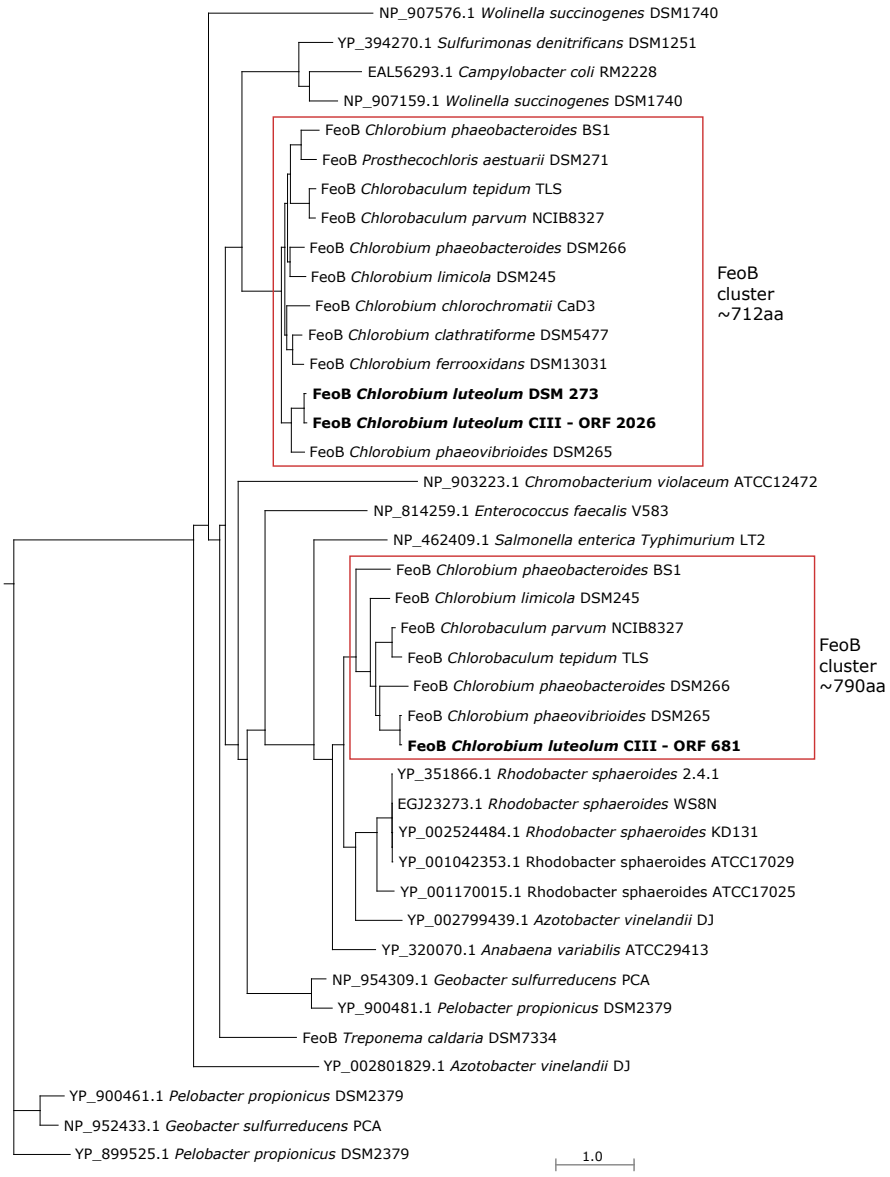

Figure A.C5.5: Syntenic analysis of the FeoB protein (form 790aa) within GSB using SyntTax (Oberto 2013).

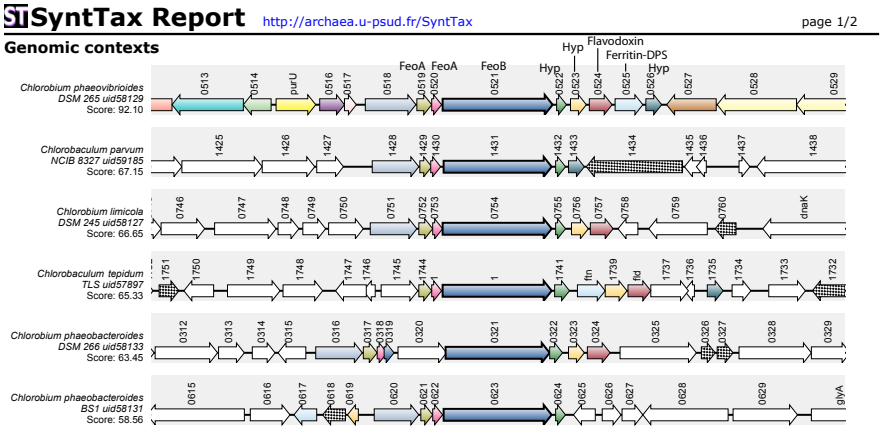

Figure A.C5.6: ACT view of the region with the insertion of the BChl *e* cluster in the assembled genome of *Chl. luteolum* CIII (represented at the bottom) in comparison with the reference genome *Chl. luteolum* DSM 273^{T} (represented at the top). Red stripes show the regions with BLAST matches. The inserted region covers from ~2032800 to ~2052600 of *Chl. luteolum* CIII.

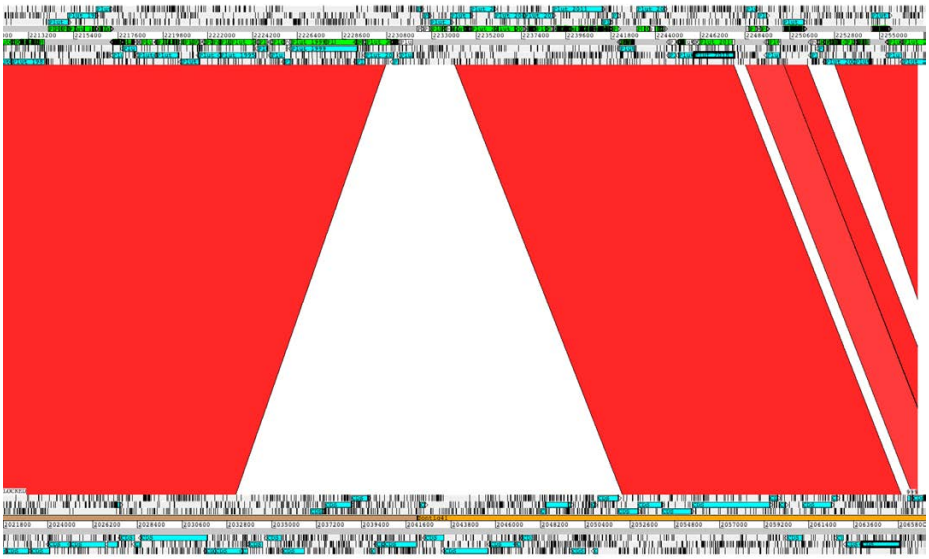

Figure A.C5.7: GC content plot of the region of the BChl *e* cluster in *Chl. luteolum* CIII (Contigs 31 and 41), with dots in black and red respectively, versus *Chl. phaeobacteroides* DSM266, with dots in blue. The squared dots show the position of each of the five proteins proposed for BChl *e* synthesis. The vertical red dots show the exact region that we propose to be inserted in *Chl. luteolum* CIII.

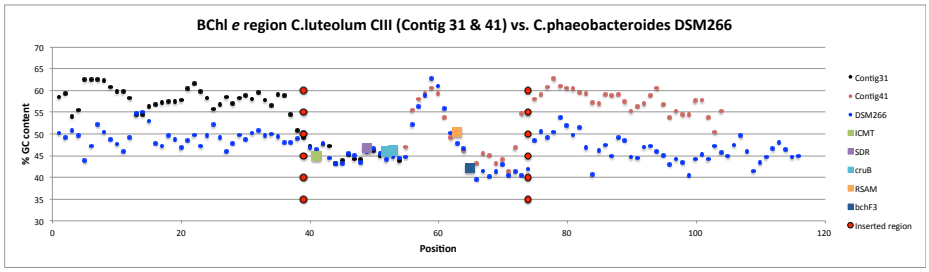

Figure A.C5.8: Syntenic analysis of ORFs 575 (*vrlQ*) to 584 (*vrlJ*) from *Chl. luteolum* CIII showing the relationships with the closest relatives of the *vrl* cluster.

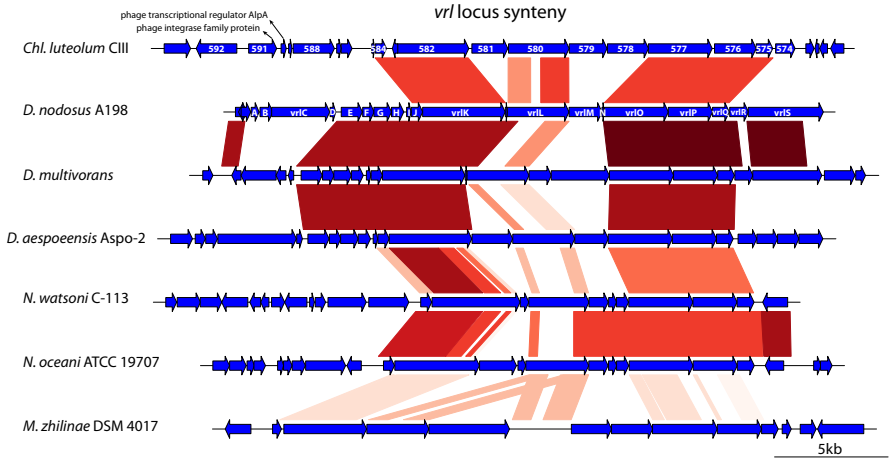

Figure A.C5.9: ACT view of the promiscuous regions found in the assembled genome of *Chl. luteolum* CIII (represented at the bottom) in comparison with the reference genome *Chl. luteolum* DSM 273^{T} (represented at the top). Red stripes show the regions with BLAST matches.

Promiscuous Region 1

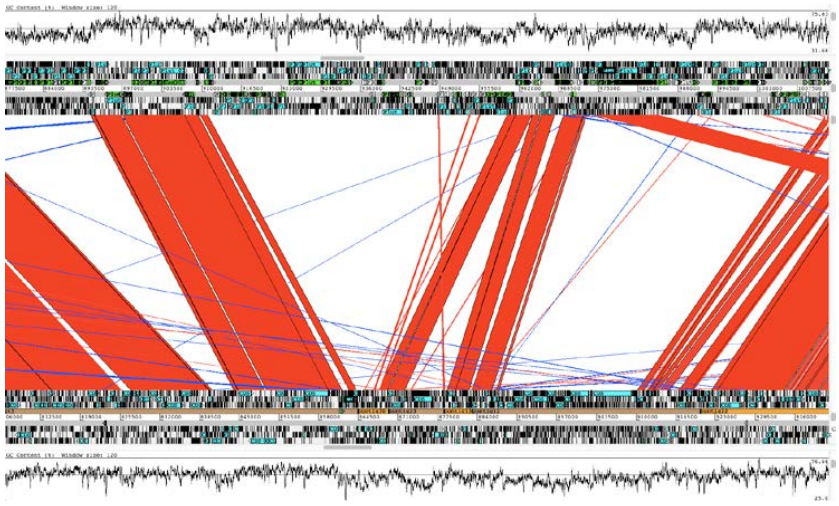

Promiscuous Region 2

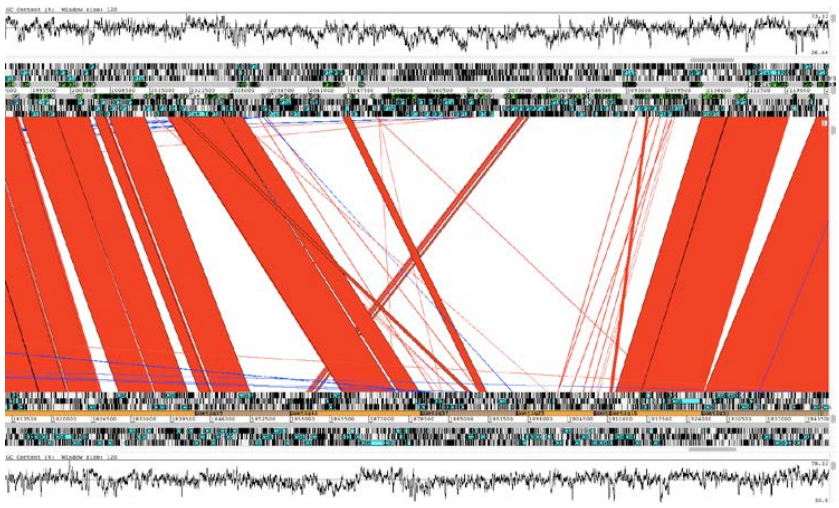

Figure A.C5.10: CRISPR region found in *Chl. luteolum* CIII genome.

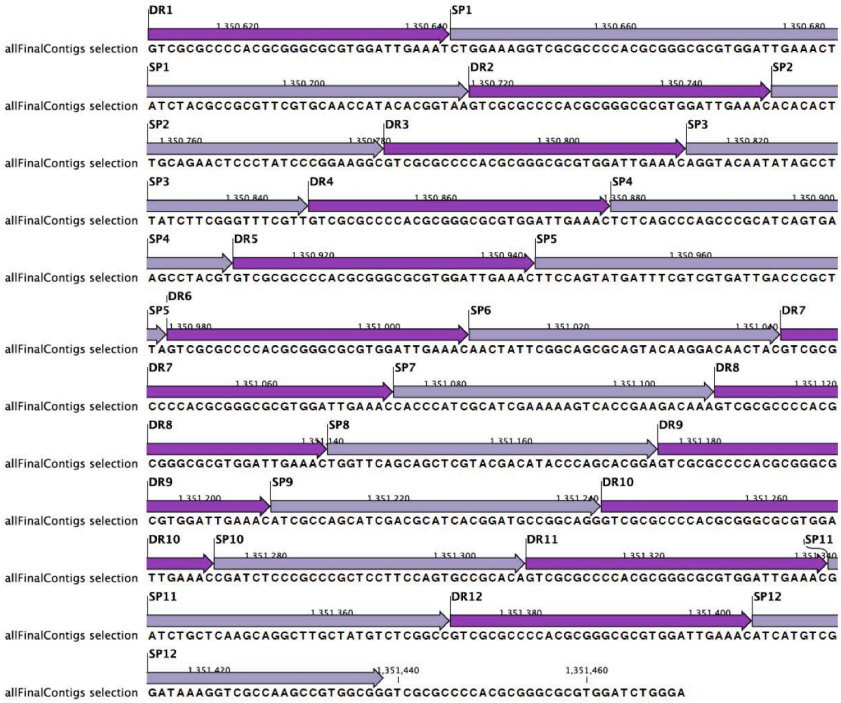

Figure A.C5.11: Phylogenetic reconstruction of the Contig5 putative phage conserved DNA polymerase protein.

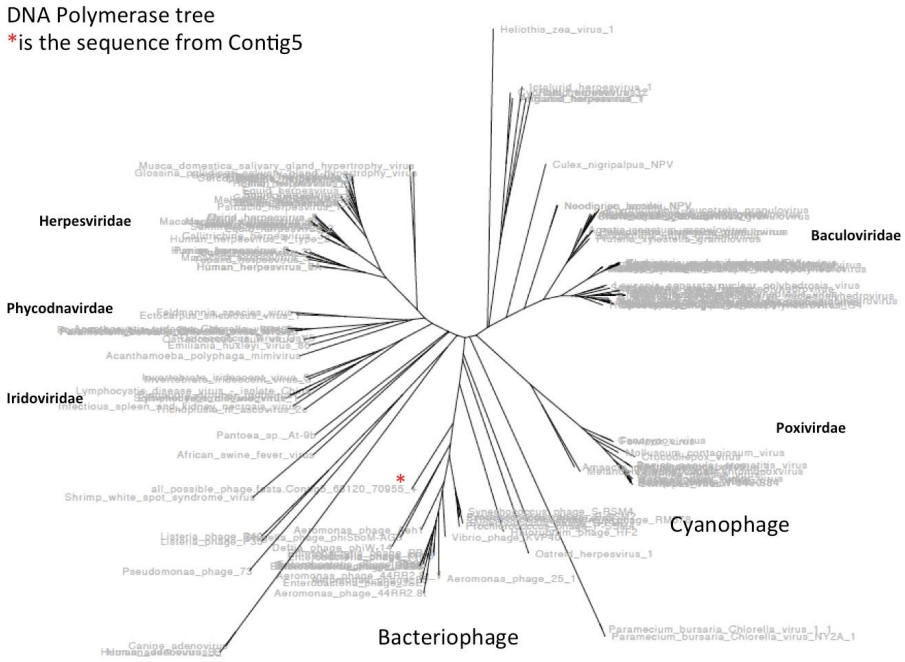

Figure A.C5.12: Contig5 putative phage homology annotation map.

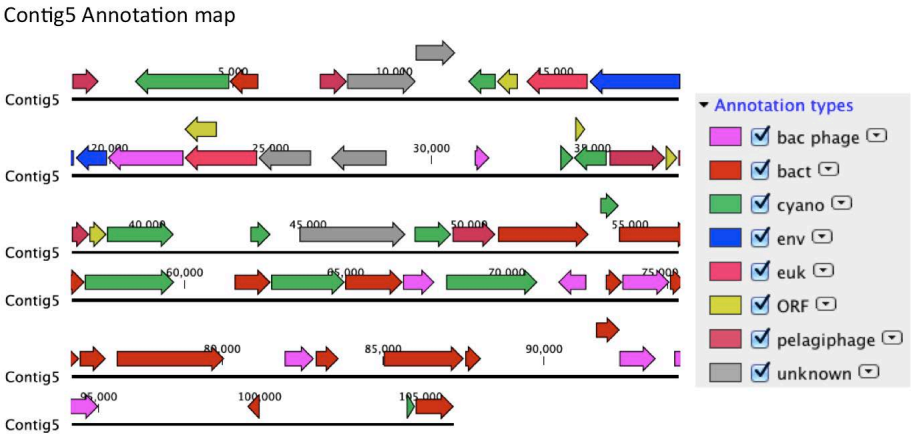

Table A.C5.1: List of proteins not found in *Chl. luteolum* CIII but present in *Chl. luteolum* DSM 273. In bold proteins commented in the text.

Chl. luteolum DSM 273 protein	Protein Length	Identity (%)	Coverage (%)	Protein BLAST First Hit
YP_373947.1	570	87.59	100	ribonuclease [Chlorobium phaeovibrioides DSM 265]
YP_373984.1	87	40	54	hypothetical protein Clim_0040 [Chlorobium limicola DSM 245]
YP_374035.1	562	62.99	100	sulfatase [Chlorobium phaeobacteroides DSM 266]
YP_374298.1	6678	96	74	putative outer membrane adhesin like protein [Chlorobium phaeovibrioides DSM 265]
YP_374299.1	609	71.72	98	outer membrane efflux protein [Chlorobium phaeovibrioides DSM 265]
YP_374301.1	274	67.18	95	hypothetical protein Cvib_0427 [Chlorobium phaeovibrioides DSM 265]
YP_374302.1	457	66.23	99	hypothetical protein Cvib_0428 [Chlorobium phaeovibrioides DSM 265]
YP_374303.1	474	71.98	98	peptidase M50 [Chlorobium phaeovibrioides DSM 265]
YP_374304.1	205	59.51	100	peptidase M50 [Chlorobium phaeovibrioides DSM 265]
YP_374395.1	310	90	100	glycosyl transferase family protein [Chlorobium phaeovibrioides DSM 265]
YP_374440.1	278	94.96	100	hypothetical protein Cvib_1738 [Chlorobium phaeovibrioides DSM 265]
YP_374441.1	256	98.44	100	hypothetical protein Cvib_1737 [Chlorobium phaeovibrioides DSM 265]
YP_374461.1	378	73.45	94	extracellular solute-binding protein [Chlorobium phaeovibrioides DSM 265]
YP_374484.1	64	81.25	75	hypothetical protein Cvib_0599 [Chlorobium phaeovibrioides DSM 265]
YP_374532.1	111	80.91	99	hypothetical protein Clim_0656 [Chlorobium limicola DSM 245]
YP_374533.1	94	81.91	100	hypothetical protein Cphamn1_1311 [Chlorobium phaeobacteroides BS1]
YP_374566.1	99	97.98	100	transposase IS3/IS911 family protein [Chlorobium phaeovibrioides DSM 265]
YP_374567.1	144	96.99	92	hypothetical protein Cvib_1140 [Chlorobium phaeovibrioides DSM 265]
YP_374568.1	164	69.81	65	hypothetical protein Cphamn1_0714 [Chlorobium phaeobacteroides BS1]
YP_374569.1	262	-	-	Hypothetical protein (without blast)
YP_374572.1	495	75.15	100	RNA-directed DNA polymerase [Prosthecochloris aestuarii DSM 271]
YP_374573.1	246	80.59	96	peptidase A24A
YP_374574.1	313	84.03	100	type II secretion system protein [Chlorobium phaeovibrioides DSM 265]
YP_374575.1	322	81.37	100	type II secretion system protein [Chlorobium phaeovibrioides DSM 265]
YP_374576.1	479	83.92	100	type II secretion system protein E [Chlorobium phaeovibrioides DSM 265]
YP_374577.1	381	83.46	100	Flp pilus assembly protein ATPase CpaE-like protein [Chlorobium phaeovibrioides DSM 265]
YP_374578.1	356	88.2	100	hypothetical protein Cvib_0567 [Chlorobium phaeovibrioides DSM 265]
YP_374579.1	140	79.17	100	TadE family protein [Chlorobium phaeovibrioides DSM 265]
YP_374580.1	461	84.82	100	type II and III secretion system protein [Chlorobium phaeovibrioides DSM 265]
YP_374581.1	262	87.79	100	SAF domain-containing protein [Chlorobium phaeovibrioides DSM 265]
YP_374595.1	282	38.1	45	Sel1 domain-containing protein [Candidatus Odyssella thessalonicensis]
YP_374596.1	213	-	-	Hypothetical protein (without blast)
YP_374597.1	4661	47.83	83	hypothetical protein Sden_0384 [Shewanella denitrificans OS217]
YP_374598.1	85	50	80	hypothetical protein [Brachyspira innocens]
YP_374599.1	260	28.8	70	sporulation initiation inhibitor protein soj [Enterococcus dispar]
YP_374600.1	572	58.46	95	type I secretion system ATPase [Prosthecochloris aestuarii DSM 271]
YP_374601.1	563	60.51	98	type I secretion system ATPase [Prosthecochloris aestuarii DSM 271]
YP_374602.1	393	64.95	94	secretion protein HlyD family protein [Prosthecochloris aestuarii DSM 271]
YP_374603.1	443	43.79	96	TolC family type I secretion outer membrane protein [Prosthecochloris aestuarii DSM 271]
YP_374604.1	169	-	-	Hypothetical protein (without blast)
YP_374605.1	101	-	-	Hypothetical protein (without blast)
YP_374606.1	60	71.43	58	gas vesicle protein [Oscillatoria acuminata PCC 6304]
YP_374607.1	68	-	-	Hypothetical protein (without blast)
YP_374608.1	105	-	-	Hypothetical protein (without blast)
YP_374609.1	**68**	**98.53**	**100**	**gas vesicle synthesis protein GvpA [Pelodictyon phaeoclathratiforme BU-1]**
YP_374610.1	**68**	**98.53**	**100**	**gas vesicle synthesis protein GvpA [Pelodictyon phaeoclathratiforme BU-1]**
YP_374611.1	**201**	**40.44**	**91**	**hypothetical protein Ppha_1817 [Pelodictyon phaeoclathratiforme BU-1]**
YP_374612.1	**387**	**39.9**	**98**	**hypothetical protein Ppha_1816 [Pelodictyon phaeoclathratiforme BU-1]**
YP_374613.1	**299**	**85.23**	**99**	**gas vesicle protein GvpN [Pelodictyon phaeoclathratiforme BU-1]**
YP_374614.1	**105**	**40.59**	**96**	**hypothetical protein Ppha_1814 [Pelodictyon phaeoclathratiforme BU-1]**
YP_374615.1	**97**	**81.44**	**100**	**gas vesicle protein GvpA [Pelodictyon phaeoclathratiforme BU-1]**
YP_374616.1	**183**	**57.87**	**97**	**hypothetical protein [Polaribacter]**
YP_374617.1	**314**	**52.41**	**99**	**ATPase [Polaribacter franzmannii]**
YP_374618.1	**718**	**75.56**	**99**	**ATPase AAA [Pelodictyon phaeoclathratiforme BU-1]**
YP_374620.1	**260**	**63.08**	**100**	**gas vesicle synthesis GvpLGvpF [Pelodictyon phaeoclathratiforme BU-1]**
YP_374621.1	**259**	**64.14**	**97**	**gas vesicle synthesis GvpLGvpF [Pelodictyon phaeoclathratiforme BU-1]**
YP_374622.1	**64**	**57.81**	**100**	**Gas vesicle G [Pelodictyon phaeoclathratiforme BU-1]**
YP_374623.1	**90**	**60.92**	**97**	**hypothetical protein Ppha_1805 [Pelodictyon phaeoclathratiforme BU-1]**
YP_374624.1	**262**	**34.62**	**99**	**hypothetical protein [Polaribacter franzmannii]**
YP_374625.1	**69**	**72.41**	**84**	**gas vesicle protein GvpA [Pelodictyon phaeoclathratiforme BU-1]**
YP_374626.1	**245**	**25.7**	**99**	**gas vesicle synthesis GvpLGvpF [Pelodictyon phaeoclathratiforme BU-1]**
YP_374627.1	**116**	**71.05**	**98**	**gas vesicle protein K [Pelodictyon phaeoclathratiforme BU-1]**
YP_374636.1	138	70.59	99	hypothetical protein Ppha_1968 [Pelodictyon phaeoclathratiforme BU-1]
YP_374652.1	330	43.62	90	type 11 methyltransferase [Chlorobium phaeovibrioides DSM 265]
YP_374656.1	96	40.48	44	hypothetical protein [Thermoplasmatales archaeon A-plasma]
YP_374677.1	119	82.35	100	hypothetical protein Cvib_1079 [Chlorobium phaeovibrioides DSM 265]
YP_374678.1	123	73.04	93	hypothetical protein Cvib_1077 [Chlorobium phaeovibrioides DSM 265]
YP_374679.1	191	76.22	86	hypothetical protein Cvib_1076 [Chlorobium phaeovibrioides DSM 265]
YP_374680.1	763	69.99	100	lipopolysaccharide biosynthesis protein [Chlorobium phaeovibrioides DSM 265]
YP_374681.1	450	61.11	100	sugar transferase [Chlorobium phaeovibrioides DSM 265]
YP_374682.1	402	67.4	91	DegT/DnrJ/EryC1/StrS aminotransferase [Pseudomonas fulva 12-X]
YP_374683.1	506	53.88	94	O-antigen transporter [Desulfotalea psychrophila LSv54]
YP_374684.1	232	50.43	100	hypothetical protein [Rhizobium leguminosarum]

Table A.C5.1: *Continued*

Chl. luteolum DSM 273 protein	Protein Length	Identity (%)	Coverage (%)	Protein BLAST First Hit
YP_374685.1	329	37.93	97	hypothetical protein AZKH_0360 [Azoarcus sp. KH32C]
YP_374686.1	333	43.5	98	glycosyl transferase family protein [Acidithiobacillus ferrooxidans ATCC 23270]
YP_374687.1	353	36.06	93	hydroxyneurosporene-O-methyltransferase [Synechococcus sp. PCC 6312]
YP_374688.1	397	47.1	100	group 1 glycosyl transferase [Thermodesulfobacterium geofontis OPF15]
YP_374689.1	427	28.64	95	hypothetical protein [Pseudomonas luteola]
YP_374690.1	361	52.77	95	group 1 glycosyl transferase [Nitratifractor salsuginis DSM 16511]
YP_374691.1	371	45	97	group 1 glycosyl transferase [Chlorobium phaeovibrioides DSM 265]
YP_374692.1	338	62.24	100	radical SAM domain-containing protein [Chlorobium phaeovibrioides DSM 265]
YP_374693.1	321	45.37	97	hypothetical protein [Agarivorans albus]
YP_374706.1	248	80.65	100	type 11 methyltransferase [Desulfovibrio africanus str. Walvis Bay]
YP_374707.1	240	-	-	Hypothetical protein (without blast)
YP_374708.1	315	68.99	100	type II secretion system protein [Pelodictyon phaeoclathratiforme BU-1]
YP_374709.1	322	60.87	100	type II secretion system protein [Chlorobium phaeovibrioides DSM 265]
YP_374710.1	472	77.97	99	type II secretion system protein E [Chlorobaculum parvum NCIB 8327]
YP_374711.1	381	71.39	100	Flp pilus assembly protein ATPase CpaE-like protein [Pelodictyon phaeoclathratiforme BU-1]
YP_374712.1	349	-	-	Hypothetical protein (without blast)
YP_374713.1	156	53.64	95	TadE family protein [Chlorobium phaeovibrioides DSM 265]
YP_374714.1	486	66.46	100	type II and III secretion system protein [Chlorobium phaeovibrioides DSM 265]
YP_374715.1	266	-	-	Hypothetical protein (without blast)
YP_374716.1	60	58.82	85	hypothetical protein CT0438 [Chlorobium tepidum TLS]
YP_374717.1	100	36.14	68	hypothetical protein [Actinomyces neuii]
YP_374718.1	429	61.59	99	amino acid permease-associated protein [Prosthecochloris aestuarii DSM 271]
YP_374719.1	305	69.4	88	AraC family transcripiotnal regulator [Pelodictyon phaeoclathratiforme BU-1]
YP_374720.1	371	55.36	93	RND family efflux transporter MFP subunit [Chlorobium phaeovibrioides DSM 265]
YP_374721.1	1070	84.54	99	hydrophobe/amphiphile efflux-1 (HAE1) family protein [Chlorobium phaeovibrioides DSM 265]
YP_374722.1	476	63.27	99	NodT family RND efflux system outer membrane lipoprotein [Pelodictyon phaeoclathratiforme BU-1]
YP_374723.1	266	76.32	100	oxidoreductase FAD/NAD(P)-binding subunit [Chlorobium phaeovibrioides DSM 265]
YP_374724.1	76	60.32	83	hypothetical protein Clim_1374 [Chlorobium limicola DSM 245]
YP_374725.1	371	70.94	91	cytochrome-c peroxidase [Prosthecochloris aestuarii DSM 271]
YP_374726.1	191	69.71	91	hypothetical protein Cvib_0736 [Chlorobium phaeovibrioides DSM 265]
YP_374727.1	101	40	53	conserved hypothetical protein [Talaromyces stipitatus ATCC 10500]
YP_374728.1	98	29.63	83	DEAD/DEAH box helicase [Flavobacteriaceae bacterium HQM9]
YP_374729.1	267	31.53	79	uncharacterized protein [Eubacterium dolichum CAG:375]
YP_374730.1	164	30.77	48	hypothetical protein [Caulobacter sp. AP07]
YP_374731.1	68	37.5	79	hypothetical protein Mlg_1310 [Alkalilimnicola ehrlichii MLHE-1]
YP_374732.1	215	48.45	90	N-acetylmuramoyl-L-alanine amidase [Marinilabilia salmonicolor]
YP_374733.1	151	48.84	57	hypothetical protein [Janthinobacterium sp. CG3]
YP_374735.1	191	70.68	100	hypothetical protein Cvib_0066 [Chlorobium phaeovibrioides DSM 265]
YP_374736.1	167	80.84	100	membrane-flanked domain-containing protein [Chlorobium phaeovibrioides DSM 265]
YP_374737.1	331	64.74	94	ADP-ribosylation/crystallin J1 [Chlorobium phaeovibrioides DSM 265]
YP_374738.1	116	77.78	93	XRE family transcriptional regulator [Pelodictyon phaeoclathratiforme BU-1]
YP_374739.1	190	50.55	96	vir region protein-like protein [Chlorobium ferrooxidans]
YP_374740.1	430	34.39	99	hypothetical protein [Thioalkalivibrio sp. ALgr3]
YP_374741.1	144	56.03	81	hypothetical protein [Thauera sp. 28]
YP_374742.1	87	63.22	100	XRE family transcriptional regulator [Thioalkalivibrio thiocyanoxidans]
YP_374743.1	107	74.76	96	XRE family transcriptional regulator [Pelodictyon phaeoclathratiforme BU-1]
YP_374744.1	113	70.37	96	hypothetical protein [Chlorobium ferrooxidans]
YP_374745.1	138	35.48	44	n-ethylammeline chlorohydrolase [Sutterella wadsworthensis CAG:135]
YP_374746.1	193	58.38	96	hypothetical protein [Chlorobium ferrooxidans]
YP_374747.1	261	49.01	97	hypothetical protein HYPDE_35033 [Hyphomicrobium denitrificans 1NES1]
YP_374748.1	783	47.34	99	hypothetical protein Gura_4117 [Geobacter uraniireducens Rf4]
YP_374749.1	606	43.61	99	hypothetical protein [Marinobacter lipolyticus]
YP_374757.1	698	-	-	Hypothetical protein (without blast)
YP_374758.1	162	65.98	59	KilA
YP_374760.1	129	49.21	98	hypothetical protein Cag_1618 [Chlorobium chlorochromatii CaD3]
YP_374762.1	198	85.13	98	resolvase [Prosthecochloris aestuarii DSM 271]
YP_374763.1	237	53.51	78	hypothetical protein Cphamn1_0562 [Chlorobium phaeobacteroides BS1]
YP_374764.1	342	-	-	Hypothetical protein (without blast)
YP_374765.1	643	-	-	Hypothetical protein (without blast)
YP_374766.1	260	-	-	Hypothetical protein (without blast)
YP_374767.1	990	-	-	Hypothetical protein (without blast)
YP_374768.1	508	56.2	99	polar amino acid ABC transporter inner membrane protein [Geobacter lovleyi SZ]
YP_374769.1	363	70.08	99	ABC transporter [Geobacter lovleyi SZ]
YP_374770.1	112	-	-	Hypothetical protein (without blast)
YP_374773.1	314	40.69	98	hypothetical protein Cphamn1_2329 [Chlorobium phaeobacteroides BS1]
YP_374774.1	722	23.33	71	conserved membrane hypothetical protein [Microcystis sp. T1-4]
YP_374776.1	78	-	-	Hypothetical protein (without blast)
YP_374777.1	278	51.83	69	Reverse transcriptase (RNA-dependent DNA polymerase) [Thiorhodovibrio sp. 970]
YP_374778.1	483	66.39	99	radical SAM domain-containing protein [Prosthecochloris aestuarii DSM 271]
YP_374779.1	372	33.57	97	NHPM bacteriocin system secretion protein [Haliscomenobacter hydrossis DSM 1100]
YP_374780.1	517	96.4	21	hypothetical protein Cphamn1_2332 [Chlorobium phaeobacteroides BS1]
YP_374781.1	724	98.76	100	ABC transporter-like protein [Chlorobium phaeobacteroides BS1]
YP_374782.1	741	97.98	100	ABC transporter-like protein [Chlorobium phaeobacteroides BS1]

Table A.C5.1: *Continued*

Chl. luteolum DSM 273 protein	Protein Length	Identity (%)	Coverage (%)	Protein BLAST First Hit
YP_374783.1	331	96.37	100	hypothetical protein Cphamn1_2329 [Chlorobium phaeobacteroides BS1]
YP_374784.1	86	-	-	Hypothetical protein (without blast)
YP_374785.1	471	43.71	98	SagB-type dehydrogenase domain-containing protein [Microcoleus sp. PCC 7113]
YP_374786.1	329	43.75	75	hypothetical protein SCE1572_24675 [Sorangium cellulosum So0157-2]
YP_374787.1	749	42.75	100	hypothetical protein [Oscillatoria sp. PCC 10802]
YP_374788.1	114	41.57	78	nitrile hydratase [Azospirillum amazonense]
YP_374789.1	116	-	-	Hypothetical protein (without blast)
YP_374790.1	79	-	-	Hypothetical protein (without blast)
YP_374791.1	339	29.64	82	hypothetical protein [Oscillatoria formosa]
YP_374792.1	94	-	-	Hypothetical protein (without blast)
YP_374793.1	118	-	-	Hypothetical protein (without blast)
YP_374794.1	68	-	-	Hypothetical protein (without blast)
YP_374795.1	94	-	-	Hypothetical protein (without blast)
YP_374798.1	137	50.41	88	response regulator receiver protein [Prosthecochloris aestuarii DSM 271]
YP_374799.1	738	50.55	98	multi-sensor signal transduction histidine kinase [Prosthecochloris aestuarii DSM 271]
YP_374805.1	109	-	-	Hypothetical protein (without blast)
YP_374864.1	214	52.22	95	thiamine monophosphate synthase [Chlorobium phaeovibrioides DSM 265]
YP_374885.1	96	78.95	99	plasmid stabilization system [Chlorobium phaeobacteroides BS1]
YP_374931.1	388	-	-	Hypothetical protein (without blast)
YP_374932.1	1099	-	-	Hypothetical protein (without blast)
YP_374933.1	376	-	-	Hypothetical protein (without blast)
YP_374934.1	588	35.69	93	hypothetical protein [Glaciecola punicea]
YP_374935.1	255	39.76	97	hypothetical protein [Chlorobium ferrooxidans]
YP_374936.1	964	-	-	Hypothetical protein (without blast)
YP_374945.1	143	-	-	Hypothetical protein (without blast)
YP_374968.1	**468**	**80.31**	**97**	**F0F1 ATP synthase subunit beta [Chlorobaculum parvum NCIB 8327]**
YP_374969.1	**129**	**63.57**	**100**	**ATP synthase F0F1 subunit epsilon [Chlorobium tepidum TLS]**
YP_374970.1	**106**	**54.46**	**95**	**F0F1-ATPase subunit [Prosthecochloris aestuarii DSM 271]**
YP_374971.1	**101**	**45.26**	**94**	**F1/F0 ATPase**
YP_374972.1	**223**	**74.89**	**100**	**F0F1 ATP synthase subunit A [Chlorobaculum parvum NCIB 8327]**
YP_374973.1	**93**	**75.27**	**100**	**alternate F1F0 ATPase F0 subunit C [Chlorobaculum parvum NCIB 8327]**
YP_374974.1	**264**	**44.84**	**94**	**alternate F1F0 ATPase F0 subunit B [Prosthecochloris aestuarii DSM 271]**
YP_374975.1	**511**	**71.31**	**97**	**F0F1 ATP synthase subunit alpha [Chlorobaculum parvum NCIB 8327]**
YP_374976.1	303	53.82	96	hypothetical protein [Zavarzinella formosa]
YP_374981.1	91	57.5	88	prevent-host-death protein [Rhizobium giardinii]
YP_374998.1	684	42.76	99	multi-sensor signal transduction histidine kinase [Pelodictyon phaeoclathratiforme BU-1]
YP_374999.1	101	38.57	66	hypothetical protein [Chlorobium ferrooxidans]
YP_375000.1	167	38	60	hypothetical protein [Chlorobium ferrooxidans]
YP_375001.1	283	37.7	89	hypothetical protein [Chlorobium ferrooxidans]
YP_375002.1	277	42.32	96	phosphate binding protein [Chlorobium phaeobacteroides BS1]
YP_375003.1	633	31.65	97	integral membrane sensor signal transduction histidine kinase [Chlorobium phaeovibrioides DSM 265]
YP_375004.1	241	-	-	Hypothetical protein (without blast)
YP_375005.1	203	-	-	Hypothetical protein (without blast)
YP_375006.1	118	-	-	Hypothetical protein (without blast)
YP_375007.1	203	-	-	Hypothetical protein (without blast)
YP_375008.1	218	47.59	75	hypothetical protein Cvib_0849 [Chlorobium phaeovibrioides DSM 265]
YP_375030.1	245	75.32	94	ABC transporter [Chlorobium ferrooxidans]
YP_375046.1	222	79.91	96	cob(II)yrinic acid a
YP_375077.1	164	31.88	37	hypothetical protein [Chlorobium ferrooxidans]
YP_375086.1	81	62.96	100	hypothetical protein [Chlorobium ferrooxidans]
YP_375090.1	476	63.95	80	hypothetical protein Cvib_0772 [Chlorobium phaeovibrioides DSM 265]
YP_375132.1	356	66.11	99	Protein of unknown function [Flavobacterium psychrophilum JIP02/86]
YP_375164.1	153	64.8	82	NUDIX hydrolase [Chlorobium ferrooxidans]
YP_375185.1	97	43.55	64	hypothetical protein Cvib_1030 [Chlorobium phaeovibrioides DSM 265]
YP_375205.1	259	38.58	99	predicted protein [Populus trichocarpa]
YP_375206.1	128	54	94	hypothetical protein [Selenomonas sp. CM52]
YP_375207.1	146	44.53	83	hypothetical protein PST_3752 [Pseudomonas stutzeri A1501]
YP_375237.1	247	82.89	92	ABC transporter-like protein [Pelodictyon phaeoclathratiforme BU-1]
YP_375261.1	183	41.72	83	PAS domain-containing protein [Nostoc sp. PCC 7524]
YP_375348.1	362	82.87	100	hydrogenase (NiFe) small subunit (hydA):Twin-arginine translocation pathway signal [Chlorobium ferrooxidans]
YP_375349.1	572	88.99	100	nickel-dependent hydrogenase large subunit [Pelodictyon phaeoclathratiforme BU-1]
YP_375350.1	227	80.62	100	Ni/Fe-hydrogenase
YP_375351.1	158	70.25	100	hydrogenase maturation protease [Pelodictyon phaeoclathratiforme BU-1]
YP_375352.1	226	60.47	95	cobalt transport protein CbiM [Ammonifex degensii KC4]
YP_375353.1	111	48.48	89	cobalamin biosynthesis protein [Dictyoglomus thermophilum H-6-12]
YP_375354.1	283	35.69	91	cobalt ABC transporter permease [Desulfitobacterium metallireducens]
YP_375355.1	269	51.33	96	hypothetical protein [Nocardioides sp. Iso805N]
YP_375356.1	347	77.52	100	hydrogenase [Chlorobium ferrooxidans]
YP_375357.1	362	83.43	100	hydrogenase expression/formation protein HypD [Pelodictyon phaeoclathratiforme BU-1]
YP_375358.1	90	73.86	97	hydrogenase assembly chaperone HypC/HupF [Chlorobium phaeobacteroides DSM 266]
YP_375359.1	719	62.06	99	(NiFe) hydrogenase maturation protein HypF [Pelodictyon phaeoclathratiforme BU-1]
YP_375360.1	268	74.63	99	hydrogenase nickel incorporation protein HypB [Chlorobium ferrooxidans]
YP_375361.1	117	70.09	100	hydrogenase nickel incorporation protein HypA [Pelodictyon phaeoclathratiforme BU-1]

Table A.C5.1: *Continued*

Chl. luteolum DSM 273 protein	Protein Length	Identity (%)	Coverage (%)	Protein BLAST First Hit
YP_375406.1	465	99.57	100	hypothetical protein Cphamn1_0372 [Chlorobium phaeobacteroides BS1]
YP_375438.1	131	46.09	95	cytochrome c [Chlorobium phaeovibrioides DSM 265]
YP_375439.1	639	45.93	96	receptor [Chlorobium tepidum TLS]
YP_375441.1	267	53.14	89	molybdenum ABC transporter
YP_375442.1	226	70.09	95	Fis family transcriptional regulator [Chlorobium phaeobacteroides DSM 266]
YP_375447.1	118	27.27	72	hypothetical protein EMIHUDRAFT_230279 [Emiliania huxleyi CCMP1516]
YP_375448.1	383	80.11	98	cystathionine gamma-synthase [Pelodictyon phaeoclathratiforme BU-1]
YP_375450.1	214	63.64	98	LuxR family transcriptional regulator [Chlorobium ferrooxidans]
YP_375451.1	317	82.33	100	cysteine synthase A [Pelodictyon phaeoclathratiforme BU-1]
YP_375452.1	335	76.35	99	sulfate transporter subunit [Chlorobium ferrooxidans]
YP_375453.1	277	77.26	100	sulfate/thiosulfate transporter subunit [Chlorobium ferrooxidans]
YP_375454.1	289	71.83	97	sulfate ABC transporter permease [Chlorobium ferrooxidans]
YP_375455.1	357	75.35	100	sulfate ABC transporter [Chlorobium ferrooxidans]
YP_375456.1	599	71.95	100	adenylylsulfate kinase [Chlorobium ferrooxidans]
YP_375457.1	293	79.52	100	sulfate adenylyltransferase [Chlorobium ferrooxidans]
YP_375458.1	250	67.26	90	phosphoadenosine phosphosulfate reductase [Chlorobium ferrooxidans]
YP_375459.1	319	53	89	sulfite reductase subunit beta [Chlorobium ferrooxidans]
YP_375465.1	622	63.56	97	protein-disulfide reductase [Chlorobium ferrooxidans]
YP_375466.1	306	61.69	96	thiamine biosynthesis protein ApbE [Chlorobium ferrooxidans]
YP_375467.1	417	52.73	97	hypothetical protein [Chlorobium ferrooxidans]
YP_375468.1	76	54.17	92	putative lipoprotein [Shewanella sp. ANA-3]
YP_375469.1	194	60.9	80	thiol:disulfide interchange protein DsbE [Chlorobium tepidum TLS]
YP_375549.1	244	37.5	28	PREDICTED: zinc finger protein 184-like [Monodelphis domestica]
YP_375561.1	237	77.63	96	hypothetical protein Cvib_1450 [Chlorobium phaeovibrioides DSM 265]
YP_375608.1	142	51.49	94	TOBE domain-containing protein [Chlorobium limicola DSM 245]
YP_375609.1	299	68.51	97	ABC transporter [Chlorobium phaeobacteroides DSM 266]
YP_375692.1	254	55.56	92	methyltransferase FkbM [Polaromonas sp. CF318]
YP_375702.1	180	46.2	87	hypothetical protein [Bacillus methanolicus]
YP_375718.1	242	66.86	71	hypothetical protein CT2253 [Chlorobium tepidum TLS]
YP_375719.1	614	44.89	60	hypothetical protein DaAHT2_2022 [Desulfurivibrio alkaliphilus AHT2]
YP_375720.1	627	49.59	98	hypothetical protein Nit79A3_2002 [Nitrosomonas sp. Is79A3]
YP_375721.1	448	-	-	Hypothetical protein (without blast)
YP_375722.1	311	30.12	52	hypothetical protein [Rhodopseudomonas sp. B29]
YP_375723.1	197	72.96	99	conserved hypothetical protein [Thiomonas arsenitoxydans]
YP_375724.1	109	40.57	97	hypothetical protein [Pseudomonas]
YP_375725.1	163	54.55	27	hypothetical protein [Clostridium botulinum]
YP_375726.1	526	69.01	99	integrase catalytic subunit [Chlorobium phaeobacteroides DSM 266]
YP_375727.1	246	80.08	100	IstB ATP binding domain-containing protein [Chlorobium phaeobacteroides DSM 266]
YP_375728.1	217	-	-	Hypothetical protein (without blast)
YP_375731.1	286	-	-	Hypothetical protein (without blast)
YP_375732.1	115	98.26	100	hypothetical protein Cvib_0656 [Chlorobium phaeovibrioides DSM 265]
YP_375733.1	112	61.54	93	hypothetical protein Cag_1308 [Chlorobium chlorochromatii CaD3]
YP_375734.1	111	97.3	100	XRE family transcriptional regulator [Chlorobium phaeovibrioides DSM 265]
YP_375735.1	100	30.49	69	1-O-acylceramide synthase precursor
YP_375738.1	309	52.27	99	UDP-glucose 4-epimerase [Herminiimonas arsenicoxydans]
YP_375739.1	253	52.24	97	hypothetical protein Tbd_1874 [Thiobacillus denitrificans ATCC 25259]
YP_375740.1	391	50.87	88	glycosyl transferase [Rhizobium sp. CF142]
YP_375741.1	317	55.41	96	UDP-glucose epimerase [Rhizobium leguminosarum bv. viciae 3841]
YP_375742.1	282	61.73	98	SAM-dependent methyltransferase [Rhizobium sp. CF142]
YP_375743.1	189	55.56	100	branched-chain amino acid transport system substrate-binding protein [Bradyrhizobium sp. DFCI-1]
YP_375744.1	276	54.58	99	biopolymer transporter TolQ [Bradyrhizobium sp. DFCI-1]
YP_375745.1	313	42.66	89	hypothetical protein Syn7502_03249 [Synechococcus sp. PCC 7502]
YP_375746.1	618	50.64	99	hypothetical protein [Methyloversatilis universalis]
YP_375747.1	274	48.06	94	glycosyl transferase family protein [Polynucleobacter necessarius subsp. asymbioticus QLW-P1DMWA-1]
YP_375748.1	415	26.13	93	hypothetical protein Ajs_3024 [Acidovorax sp. JS42]
YP_375750.1	465	99.57	100	hypothetical protein Cphamn1_0372 [Chlorobium phaeobacteroides BS1]
YP_375751.1	205	86.41	90	hypothetical protein Cvib_0639 [Chlorobium phaeovibrioides DSM 265]
YP_375752.1	226	39.25	94	hypothetical protein [Methylophilus methylotrophus]
YP_375753.1	405	53.32	100	hypothetical protein [Pseudomonas stutzeri]
YP_375756.1	251	39.46	87	hypothetical protein Cag_1263 [Chlorobium chlorochromatii CaD3]
YP_375757.1	595	46.26	99	hypothetical protein [Thioalkalivibrio sp. AKL17]
YP_375758.1	213	57.42	98	hypothetical protein [Methylococcus capsulatus]
YP_375759.1	436	47.42	98	polysaccharide biosynthesis protein [Thioalkalivibrio sp. ALRh]
YP_375760.1	97	51.14	91	hypothetical protein [Methylocystis rosea]
YP_375761.1	348	30.29	96	hypothetical protein [Janthinobacterium sp. CG3]
YP_375762.1	241	53.33	93	hypothetical protein [uncultured Thiohalocapsa sp. PB-PSB1]
YP_375763.1	181	50	98	hypothetical protein NE1883 [Nitrosomonas europaea ATCC 19718]
YP_375764.1	408	58.23	99	hypothetical protein NAL212_1260 [Nitrosomonas sp. AL212]
YP_375765.1	48	50.98	100	hypothetical protein Cphamn1_1966 [Chlorobium phaeobacteroides BS1]
YP_375766.1	91	50	93	prevent-host-death protein [Pseudomonas pelagia]
YP_375767.1	139	76.98	100	PilT domain-containing protein [Chlorobium phaeobacteroides DSM 266]
YP_375768.1	79	78.48	100	hypothetical protein Cphamn1_1965 [Chlorobium phaeobacteroides BS1]
YP_375769.1	136	93.38	100	putative transcriptional regulator [Chlorobium phaeovibrioides DSM 265]

Table A.C5.1: *Continued*

Chl. luteolum DSM 273 protein	Protein Length	Identity (%)	Coverage (%)	Protein BLAST First Hit
YP_375770.1	246	83.33	100	hypothetical protein Cvib_0610 [Chlorobium phaeovibrioides DSM 265]
YP_375771.1	272	99.63	100	hypothetical protein Cvib_0609 [Chlorobium phaeovibrioides DSM 265]
YP_375772.1	93	69.23	42	hypothetical protein NE1822 [Nitrosomonas europaea ATCC 19718]
YP_375773.1	271	68.91	99	hypothetical protein NE1821 [Nitrosomonas europaea ATCC 19718]
YP_375777.1	362	60.93	95	glycosyl transferase family protein [Chlorobium phaeovibrioides DSM 265]
YP_375779.1	343	90.38	100	lipopolysaccharide biosynthesis protein [Chlorobium phaeovibrioides DSM 265]
YP_375781.1	120	89.61	64	XRE family transcriptional regulator [Chlorobium phaeovibrioides DSM 265]
YP_375782.1	182	94.51	100	PA-phosphatase-like phosphoesterase [Chlorobium phaeovibrioides DSM 265]
YP_375783.1	390	89.43	95	XRE family transcriptional regulator [Chlorobium phaeovibrioides DSM 265]
YP_375792.1	152	75.66	100	mobile mystery protein A [Chlorobium limicola DSM 245]
YP_375793.1	395	64.89	99	filamentation induced by cAMP protein fic [Pelodictyon phaeoclathratiforme BU-1]
YP_375794.1	107	83.52	85	XRE family transcriptional regulator [Chlorobium phaeobacteroides DSM 266]
YP_375795.1	101	63.53	80	hypothetical protein Ppha_0790 [Pelodictyon phaeoclathratiforme BU-1]
YP_375805.1	100	57.14	35	ATP-dependent helicase [Desulfovibrio magneticus RS-1]
YP_375812.1	81	-	-	Hypothetical protein (without blast)
YP_375890.1	75	78.67	100	chlorosome envelope protein B [Chlorobium limicola DSM 245]
YP_375895.1	462	58.04	92	multi-sensor hybrid histidine kinase [Pelodictyon phaeoclathratiforme BU-1]
YP_375908.1	103	50.94	51	cytochrome C biogenesis protein CycH [Joostella marina]
YP_375909.1	88	51.67	67	Death-on-curing protein [Pasteurella multocida]
YP_375948.1	417	52.87	99	hypothetical protein Ppha_2822 [Pelodictyon phaeoclathratiforme BU-1]

Table A.C5.2: List of proteins present en Chl. Luteolum CIII but absent in Chl luteolum DSM 273. In bold proteins commented in the text.

Chl. luteolum CIII protein	Contig	Protein Length	Identity (%)	Coverage (%)	Protein BLAST First Hit	Comments
fig|319225.9.peg.32	Contig26	39	-	-	Hypothetical protein (without blast)	
fig|319225.9.peg.42	Contig26	41	-	-	Hypothetical protein (without blast)	
fig|319225.9.peg.50	Contig26	53	36	81	ALS operon regulatory protein [Patulibacter americanus]	
fig|319225.9.peg.60	Contig26	306	84	94	hypothetical protein Cvib_0032 [Chlorobium phaeovibrioides DSM 265]	
fig|319225.9.peg.136	Contig52	39	-	-	Hypothetical protein (without blast)	
fig|319225.9.peg.214	Contig52	265	94	100	50S ribosomal protein L2 [Pelodictyon phaeoclathratiforme BU-1]	
fig|319225.9.peg.234	Contig52	39	100	100	50S ribosomal protein L36 [Chlorobium phaeovibrioides DSM 265]	
fig|319225.9.peg.376	Contig54	82	29	99	hypothetical protein CRE_13618 [Caenorhabditis remanei]	
fig|319225.9.peg.396	Contig54	39	52	66	hypothetical protein conserved [Cyanidioschyzon merolae strain 10D]	
fig|319225.9.peg.397	Contig54	83	49	90	addiction module antitoxin [Pelobacter propionicus DSM 2379]	
fig|319225.9.peg.398	Contig54	57	46	66	CopG family transcriptional regulator [Chlorobium phaeobacteroides BS1]	
fig|319225.9.peg.399	Contig54	41	-	-	Hypothetical protein (without blast)	
fig|319225.9.peg.403	Contig54	118	32	74	1-(5-phosphoribosyl)-5-[(5-phosphoribosylamino)methylideneamino] imidazole-4-carboxamide isomerase [Escherichia coli]	
fig|319225.9.peg.405	Contig8	76	57	100	TPR repeat-containing protein [Chlorobium luteolum DSM 273]	
fig|319225.9.peg.407	Contig8	112	45	39	hypothetical protein ROP_36070 [Rhodococcus opacus B4]	
fig|319225.9.peg.408	Contig8	299	-	-	Hypothetical protein (without blast)	
fig|319225.9.peg.413	Contig21-32	753	62	62	outer membrane adhesin-like protein [Cellulophaga algicola DSM 14237]	
fig|319225.9.peg.420	Contig32	66	32	88	PREDICTED: mitochondrial dynamic protein MID49 [Ceratotherium simum simum]	
fig|319225.9.peg.427	Contig32	60	-	-	Hypothetical protein (without blast)	
fig|319225.9.peg.433	Contig32	58	45	95	hypothetical protein Paes_1821 [Prosthecochloris aestuarii DSM 271]	
fig|319225.9.peg.439	Contig32	42	-	-	Hypothetical protein (without blast)	
fig|319225.9.peg.447	Contig32	49	44	81	small nuclear ribonucleoprotein [Paracoccidioides sp. 'lutzii' Pb01]	
fig|319225.9.peg.455	Contig32	47	-	-	Hypothetical protein (without blast)	
fig|319225.9.peg.468	Contig32	43	-	-	Hypothetical protein (without blast)	
fig|319225.9.peg.541	Contig48	49	-	-	Hypothetical protein (without blast)	
fig|319225.9.peg.549	Contig48	202	83	87	transposase IS5 family [Chlorobium phaeobacteroides BS1]	
fig|319225.9.peg.550	Contig48	182	63	97	hypothetical protein Ppha_0792 [Pelodictyon phaeoclathratiforme BU-1]	
fig|319225.9.peg.551	Contig48	42	-	-	Hypothetical protein (without blast)	
fig|319225.9.peg.554	Contig44	39	-	-	Hypothetical protein (without blast)	
fig|319225.9.peg.555	Contig44	84	100	94	hypothetical protein Plut_0516 [Chlorobium luteolum DSM 273]	
fig|319225.9.peg.558	Contig44	48	-	-	Hypothetical protein (without blast)	
fig|319225.9.peg.574	**Contig44**	**294**	**67**	**98**	**hypothetical protein [Methylohaloblus crimeensis]**	**vrl cluster**
fig|319225.9.peg.575	**Contig44**	**250**	**84**	**100**	**hypothetical protein DNO_0175 [Dichelobacter nodosus VCS1703A]**	**vrl cluster-vrlQ**
fig|319225.9.peg.576	**Contig44**	**630**	**88**	**100**	**PglZ domain protein [Desulfococcus multivorans]**	**vrl cluster-vrlP**
fig|319225.9.peg.577	**Contig44**	**965**	**91**	**99**	**SNF2-related protein [Desulfococcus multivorans]**	**vrl cluster-vrlO**
fig|319225.9.peg.578	**Contig44**	**621**	**61**	**99**	**UvrD/REP helicase [Methanosalsum zhilinae DSM 4017]**	**vrl cluster**
fig|319225.9.peg.579	**Contig44**	**572**	**55**	**99**	**ATP-dependent endonuclease [Methanosalsum zhilinae DSM 4017]**	**vrl cluster**
fig|319225.9.peg.580	**Contig44**	**258**	**97**	**99**	**hypothetical protein Noc_0059 [Nitrosococcus oceani ATCC 19707]**	**vrl cluster-vrlL**
fig|319225.9.peg.581	**Contig44**	**544**	**60**	**99**	**transcriptional regulator [Alcanivorax hongdengensis]**	**vrl cluster**
fig|319225.9.peg.582	**Contig44-20**	**1085**	**91**	**100**	**virulence associated protein [Thiobacillus denitrificans]**	**vrl cluster-vrlK**
fig|319225.9.peg.583	**Contig20**	**82**	**-**	**-**	**Hypothetical protein (without blast)**	**vrl cluster**
fig|319225.9.peg.584	**Contig20**	**172**	**73**	**99**	**hypothetical protein [Pseudomonas aeruginosa]**	**vrl cluster-vrlJ**
fig|319225.9.peg.585	**Contig20**	**45**	**62**	**89**	**restriction endonuclease [Firmicutes bacterium CAG:176]**	**vrl cluster**
fig|319225.9.peg.586	**Contig20**	**166**	**29**	**74**	**putative uncharacterized protein [Ruminococcus sp. CAG:353]**	**vrl cluster**
fig|319225.9.peg.587	**Contig20**	**68**	**45**	**90**	**hypothetical protein Deba_0112 [Desulfarculus baarsii DSM 2075]**	**vrl cluster**
fig|319225.9.peg.588	**Contig20**	**623**	**77**	**96**	**hypothetical protein Cpha266_2066 [Chlorobium phaeobacteroides DSM 266]**	**vrl cluster**
fig|319225.9.peg.589	**Contig20**	**52**	**-**	**-**	**Hypothetical protein (without blast)**	**vrl cluster**
fig|319225.9.peg.590	**Contig20**	**79**	**66**	**83**	**phage transcriptional regulator AlpA [Chlorobium phaeobacteroides DSM 266]**	**vrl cluster**
fig|319225.9.peg.591	**Contig20**	**423**	**83**	**95**	**phage integrase family protein [Chlorobium phaeobacteroides DSM 266]**	**vrl cluster**
fig|319225.9.peg.592	**Contig20**	**614**	**44**	**99**	**Crp family transcriptional regulator [Halothece sp. PCC 7418]**	**vrl cluster**
fig|319225.9.peg.615	Contig20	40	56	82	hypothetical protein Cvib_0599 [Chlorobium phaeovibrioides DSM 265]	
fig|319225.9.peg.616	Contig20	65	100	100	hypothetical protein Plut_0557 [Chlorobium luteolum DSM 273]	
fig|319225.9.peg.617	Contig20	43	41	76	hypothetical protein [Hydrocarboniphaga effusa]	
fig|319225.9.peg.636	Contig51	73	53	42	prop expression regulator [Dickeya zeae]	
fig|319225.9.peg.668	Contig51	54	37	92	hypothetical protein [Streptomyces clavuligerus]	
fig|319225.9.peg.679	**Contig51**	**109**	**99**	**100**	**FeoA family protein [Chlorobium phaeovibrioides DSM 265]**	**Iron cluster**
fig|319225.9.peg.680	**Contig51**	**76**	**96**	**100**	**FeoA family protein [Chlorobium phaeovibrioides DSM 265]**	**Iron cluster**
fig|319225.9.peg.681	**Contig51**	**796**	**97**	**100**	**ferrous iron transport protein B [Chlorobium phaeovibrioides DSM 265]**	**Iron cluster**
fig|319225.9.peg.682	**Contig51**	**95**	**96**	**81**	**hypothetical protein Cvib_0522 [Chlorobium phaeovibrioides DSM 265]**	**Iron cluster**
fig|319225.9.peg.683	**Contig51**	**105**	**98**	**100**	**hypothetical protein Cvib_0523 [Chlorobium phaeovibrioides DSM 265]**	**Iron cluster**
fig|319225.9.peg.684	**Contig51**	**169**	**98**	**100**	**flavodoxin [Chlorobium phaeovibrioides DSM 265]**	**Iron cluster**
fig|319225.9.peg.685	**Contig51**	**201**	**98**	**100**	**Ferritin Dps family protein [Chlorobium phaeovibrioides DSM 265]**	**Iron cluster**
fig|319225.9.peg.686	**Contig51**	**118**	**95**	**100**	**hypothetical protein Cvib_0526 [Chlorobium phaeovibrioides DSM 265]**	**Iron cluster**
fig|319225.9.peg.705	Contig51	56	48	49	hypothetical protein Paes_0777 [Prosthecochloris aestuarii DSM 271]	
fig|319225.9.peg.706	Contig51	62	28	74	hypothetical protein [Nitritalea halalkaliphila]	
fig|319225.9.peg.708	Contig51	48	87	81	N-6 DNA methylase [Desulfococcus multivorans]	
fig|319225.9.peg.709	Contig51	52	39	94	hypothetical protein [Streptosporangium roseum DSM 43021]	
fig|319225.9.peg.710	Contig51	167	62	68	type I restriction-modification system subunit M [Dehalogenimonas lykanthroporepellens BL-DC-9]	
fig|319225.9.peg.712	Contig51	64	-	-	Hypothetical protein (without blast)	
fig|319225.9.peg.715	Contig51	45	67	82	hypothetical protein Cag_1199 [Chlorobium chlorochromatii CaD3]	
fig|319225.9.peg.729	Contig51	83	29	63	ABC transporter [Treponema succinifaciens DSM 2489]	
fig|319225.9.peg.730	Contig51	39	48	82	hypothetical protein [Metascardovia criceti]	
fig|319225.9.peg.732	Contig51	75	-	-	Hypothetical protein (without blast)	
fig|319225.9.peg.733	Contig51	45	71	55	hypothetical protein Plut_0699 [Chlorobium luteolum DSM 273]	
fig|319225.9.peg.734	Contig51	60	41	88	hypothetical protein Plut_0706 [Chlorobium luteolum DSM 273]	
fig|319225.9.peg.739	Contig51	51	86	56	RND family efflux transporter [Chlorobium luteolum DSM 273]	
fig|319225.9.peg.744	Contig51	53	-	-	Hypothetical protein (without blast)	
fig|319225.9.peg.746	Contig43	63	92	61	imidazoleglycerol-phosphate dehydratase [Chlorobium luteolum DSM 273]	
fig|319225.9.peg.747	Contig43	79	-	-	Hypothetical protein (without blast)	
fig|319225.9.peg.752	Contig43	48	-	-	Hypothetical protein (without blast)	

Table A.C5.2: *Continued*

Chl. luteolum CIII protein	Contig	Protein Length	Identity (%)	Coverage (%)	Protein BLAST First Hit	Comments
fig|319225.9.peg.753	Contig43	53	63	88	hypothetical protein Cphamn1_1271 [Chlorobium phaeobacteroides BS1]	
fig|319225.9.peg.757	Contig43	46	-	-	Hypothetical protein (without blast)	
fig|319225.9.peg.769	Contig43	86	68	67	5'-3'-deoxyribonucleotidase [Gordonia rhizosphera]	
fig|319225.9.peg.770	Contig43	50	66	96	5'-3'-deoxyribonucleotidase [Eudoraea adriatica]	
fig|319225.9.peg.771	Contig43	40	-	-	Hypothetical protein (without blast)	
fig|319225.9.peg.776	Contig43	425	65	89	hypothetical protein [Desulfobacter postgatei]	
fig|319225.9.peg.777	Contig43	50	98	82	hypothetical protein Plut_0742 [Chlorobium luteolum DSM 273]	
fig|319225.9.peg.794	Contig43	59	-	-	Hypothetical protein (without blast)	
fig|319225.9.peg.795	Contig43	196	-	-	Hypothetical protein (without blast)	
fig|319225.9.peg.796	Contig43	201	65	24	hypothetical protein EhV359 [Emiliania huxleyi virus 86]	
fig|319225.9.peg.801	Contig43	42	-	-	Hypothetical protein (without blast)	
fig|319225.9.peg.806	Contig43	47	-	-	Hypothetical protein (without blast)	
fig|319225.9.peg.809	**Contig43**	**47**	**80**	**100**	**phage integrase family protein [Chlorobium phaeobacteroides DSM 266]**	**Promiscuous region 1**
fig|319225.9.peg.810	**Contig43**	**79**	**69**	**99**	**phage integrase family protein [Chlorobium phaeobacteroides DSM 266]**	**Promiscuous region 1**
fig|319225.9.peg.811	**Contig43**	**423**	**78**	**98**	**phage resistance protein [Cupriavidus sp. HPC(L)]**	**Promiscuous region 1**
fig|319225.9.peg.813	**Contig30**	**58**	**45**	**89**	**hypothetical protein Cpha266_1600 [Chlorobium phaeobacteroides DSM 266]**	**Promiscuous region 1**
fig|319225.9.peg.814	**Contig30**	**78**	**35**	**66**	**KLTH0G08822p [Lachancea thermotolerans]**	**Promiscuous region 1**
fig|319225.9.peg.815	**Contig30**	**202**	**42**	**98**	**outer surface protein [Chlorobium tepidum TLS]**	**Promiscuous region 1**
fig|319225.9.peg.819	**Contig23**	**144**	**97**	**100**	**hypothetical protein Cvib_0100 [Chlorobium phaeovibrioides DSM 265]**	**Promiscuous region 1**
fig|319225.9.peg.820	**Contig23**	**39**	**76**	**55**	**XRE family plasmid maintenance system antidote protein [Chlorobium phaeobacteroides DSM 266]**	**Promiscuous region 1**
fig|319225.9.peg.822	**Contig23**	**406**	**87**	**100**	**hypothetical protein Cvib_1663 [Chlorobium phaeovibrioides DSM 265]**	**Promiscuous region 1**
fig|319225.9.peg.823	**Contig13**	**46**	**-**	**-**	**Hypothetical protein (without blast)**	**Promiscuous region 1**
fig|319225.9.peg.824	**Contig13**	**39**	**-**	**-**	**Hypothetical protein (without blast)**	**Promiscuous region 1**
fig|319225.9.peg.825	**Contig13**	**39**	**-**	**-**	**Hypothetical protein (without blast)**	**Promiscuous region 1**
fig|319225.9.peg.830	**Contig13**	**38**	**-**	**-**	**Hypothetical protein (without blast)**	**Promiscuous region 1**
fig|319225.9.peg.831	**Contig13-12**	**174**	**91**	**100**	**PAS/PAC sensor hybrid histidine kinase [Chlorobium luteolum DSM 273]**	**Promiscuous region 1**
fig|319225.9.peg.833	**Contig12**	**42**	**-**	**-**	**Hypothetical protein (without blast)**	**Promiscuous region 1**
fig|319225.9.peg.834	**Contig12**	**77**	**82**	**100**	**transposase IS4 family protein [Pelodictyon phaeoclathratiforme BU-1]**	**Promiscuous region 1**
fig|319225.9.peg.836	**Contig12**	**81**	**61**	**51**	**hypothetical protein [Chlorobium ferrooxidans]**	**Promiscuous region 1**
fig|319225.9.peg.837	**Contig12**	**47**	**64**	**98**	**CopG/Arc/MetJ family addiction module antidote protein [Chlorobium limicola DSM 245]**	**Promiscuous region 1**
fig|319225.9.peg.838	**Contig12**	**100**	**86**	**100**	**plasmid stabilization system [Chlorobium limicola DSM 245]**	**Promiscuous region 1**
fig|319225.9.peg.839	**Contig12**	**165**	**92**	**92**	**invertase/recombinase like protein [Chlorobium luteolum DSM 273]**	**Promiscuous region 1**
fig|319225.9.peg.840	**Contig12**	**219**	**38**	**97**	**KfrA protein [Xanthomonas axonopodis]**	**Promiscuous region 1**
fig|319225.9.peg.841	**Contig12**	**44**	**40**	**100**	**hypothetical protein [Nitrosococcus oceani]**	**Promiscuous region 1**
fig|319225.9.peg.842	**Contig12**	**401**	**90**	**99**	**type I restriction-modification system M subunit [Desulfarculus baarsii DSM 2075]**	**Promiscuous region 1**
fig|319225.9.peg.843	**Contig12**	**508**	**47**	**99**	**ATP-dependent DNA helicase [Methanosarcina acetivorans C2A]**	**Promiscuous region 1**
fig|319225.9.peg.844	**Contig12**	**511**	**85**	**100**	**DNA methyltransferase [Alcanivorax pacificus]**	**Promiscuous region 1**
fig|319225.9.peg.845	**Contig12**	**777**	**30**	**99**	**Hypothetical protein XCAW_s00004 [Xanthomonas citri subsp. citri Aw12879]**	**Promiscuous region 1**
fig|319225.9.peg.846	**Contig12**	**399**	**72**	**100**	**restriction modification system DNA specificity domain-containing protein [Desulfarculus baarsii DSM 2075]**	**Promiscuous region 1**
fig|319225.9.peg.847	**Contig12**	**494**	**71**	**99**	**hypothetical protein Acife_0670 [Acidithiobacillus ferrivorans SS3]**	**Promiscuous region 1**
fig|319225.9.peg.848	**Contig12**	**317**	**57**	**95**	**hypothetical protein Acife_0671 [Acidithiobacillus ferrivorans SS3]**	**Promiscuous region 1**
fig|319225.9.peg.849	**Contig12**	**993**	**85**	**99**	**HsdR family type I site-specific deoxyribonuclease [Desulfovibrio alaskensis G20]**	**Promiscuous region 1**
fig|319225.9.peg.850	**Contig12**	**2092**	**73**	**100**	**hypothetical protein BN69_1887 [Methylocystis sp. SC2]**	**Promiscuous region 1**
fig|319225.9.peg.851	**Contig12**	**102**	**49**	**82**	**hypothetical protein [Methylocystis parvus]**	**Promiscuous region 1**
fig|319225.9.peg.853	**Contig12**	**40**	**-**	**-**	**Hypothetical protein (without blast)**	**Promiscuous region 1**
fig|319225.9.peg.854	**Contig12**	**49**	**77**	**100**	**hypothetical protein [Pedosphaera parvula]**	**Promiscuous region 1**
fig|319225.9.peg.856	**Contig12**	**50**	**53**	**86**	**hypothetical protein Clim_0913 [Chlorobium limicola DSM 245]**	**Promiscuous region 1**
fig|319225.9.peg.858	**Contig12**	**49**	**-**	**-**	**Hypothetical protein (without blast)**	**Promiscuous region 1**
fig|319225.9.peg.861	**Contig12**	**323**	**66**	**100**	**sodium:calcium antiporter [Desulfovibrio longus]**	**Promiscuous region 1**
fig|319225.9.peg.864	**Contig12**	**270**	**65**	**97**	**Ser/Thr protein phosphatase [Chlorobium luteolum DSM 273]**	**Promiscuous region 1**
fig|319225.9.peg.865	**Contig12**	**43**	**54**	**62**	**acetolactate synthase putative [alpha proteobacterium BAL199]**	**Promiscuous region 1**
fig|319225.9.peg.867	**Contig22**	**169**	**66**	**99**	**hypothetical protein Ppha_0792 [Pelodictyon phaeoclathratiforme BU-1]**	**Promiscuous region 1**
fig|319225.9.peg.868	**Contig22**	**279**	**65**	**98**	**hypothetical protein [Thiothrix flexilis]**	**Promiscuous region 1**
fig|319225.9.peg.869	**Contig22**	**51**	**-**	**-**	**Hypothetical protein (without blast)**	**Promiscuous region 1**
fig|319225.9.peg.887	Contig22	38	57	62	Patatin [Oscillatoria nigro-viridis PCC 7112]	
fig|319225.9.peg.908	Contig22	90	31	88	hypothetical protein [Commensalibacter intestini]	
fig|319225.9.peg.910	Contig22	46	50	80	transcription factor putative [Ricinus communis]	
fig|319225.9.peg.916	Contig22	194	62	97	abortive phage resistance protein-like protein [Desulfovibrio alaskensis G20]	
fig|319225.9.peg.917	Contig22	446	72	98	abortive phage resistance protein [Nitrosomonas europaea ATCC 19718]	
fig|319225.9.peg.920	Contig22	38	-	-	Hypothetical protein (without blast)	
fig|319225.9.peg.934	Contig29	208	87	51	thiamine monophosphate synthase [Chlorobium luteolum DSM 273]	
fig|319225.9.peg.936	Contig29	64	-	-	Hypothetical protein (without blast)	
fig|319225.9.peg.937	Contig29	40	-	-	Hypothetical protein (without blast)	
fig|319225.9.peg.973	Contig46	63	43	77	hypothetical protein [Kaistia granuli]	
fig|319225.9.peg.1001	Contig46	43	-	-	Hypothetical protein (without blast)	
fig|319225.9.peg.1006	Contig46	160	95	100	hypothetical protein Cvib_0886 [Chlorobium phaeovibrioides DSM 265]	
fig|319225.9.peg.1007	Contig46	1189	95	100	hypothetical protein Cvib_0885 [Chlorobium phaeovibrioides DSM 265]	
fig|319225.9.peg.1040	Contig36	39	-	-	Hypothetical protein (without blast)	
fig|319225.9.peg.1045	Contig36	47	-	-	Hypothetical protein (without blast)	
fig|319225.9.peg.1062	Contig36	82	37	88	hypothetical protein Plut_1094 [Chlorobium luteolum DSM 273]	
fig|319225.9.peg.1099	Contig18	256	60	97	hypothetical protein Cvib_0813 [Chlorobium phaeovibrioides DSM 265]	
fig|319225.9.peg.1112	Contig18	39	-	-	Hypothetical protein (without blast)	
fig|319225.9.peg.1126	Contig18	112	56	88	hypothetical protein [Chlorobium ferrooxidans]	
fig|319225.9.peg.1130	Contig18	41	53	75	transposase-like [Chlorobium luteolum DSM 273]	
fig|319225.9.peg.1131	Contig18	38	-	-	Hypothetical protein (without blast)	
fig|319225.9.peg.1142	Contig11	92	-	-	Hypothetical protein (without blast)	
fig|319225.9.peg.1143	Contig11	38	-	-	Hypothetical protein (without blast)	
fig|319225.9.peg.1144	Contig11	261	55	100	hypothetical protein Cag_0645 [Chlorobium chlorochromatii CaD3]	
fig|319225.9.peg.1146	Contig11	214	45	88	hypothetical protein Cphamn1_1562 [Chlorobium phaeobacteroides BS1]	

Table A.C5.2: *Continued*

Chl. luteolum CIII protein	Contig	Protein Length	Identity (%)	Coverage (%)	Protein BLAST First Hit	Comments
fig|319225.9.peg.1147	Contig11	117	45	85	hypothetical protein Paes_0870 [Prosthecochloris aestuarii DSM 271]	
fig|319225.9.peg.1148	Contig11	237	51	95	two component transcriptional regulator [Chlorobium luteolum DSM 273]	
fig|319225.9.peg.1149	Contig11	305	35	99	integral membrane sensor signal transduction histidine kinase [Chlorobium phaeovibrioides DSM 265]	
fig|319225.9.peg.1150	Contig11	74	-	-	Hypothetical protein (without blast)	
fig|319225.9.peg.1194	Contig11	39	61	82	hypothetical protein Ppha_2587 [Pelodictyon phaeoclathratiforme BU-1]	
fig|319225.9.peg.1197	Contig11	39	-	-	Hypothetical protein (without blast)	
fig|319225.9.peg.1230	Contig28	49	-	-	Hypothetical protein (without blast)	
fig|319225.9.peg.1247	Contig28	54	-	-	Hypothetical protein (without blast)	
fig|319225.9.peg.1252	Contig28	538	61	95	PAS/PAC sensor hybrid histidine kinase [Chlorobium phaeovibrioides DSM 265]	
fig|319225.9.peg.1265	Contig28	56	72	96	hypothetical protein Cpha266_1437 [Chlorobium phaeobacteroides DSM 266]	
fig|319225.9.peg.1270	Contig28	49	-	-	Hypothetical protein (without blast)	
fig|319225.9.peg.1286	Contig45	38	-	-	Hypothetical protein (without blast)	
fig|319225.9.peg.1287	Contig45	44	48	77	PREDICTED: Fanconi anemia group B protein [Geospiza fortis]	
fig|319225.9.peg.1292	Contig45	209	51	99	DNA polymerase III subunits gamma and tau [Chlorobium phaeovibrioides DSM 265]	
fig|319225.9.peg.1304	Contig45	46	-	-	Hypothetical protein (without blast)	
fig|319225.9.peg.1318	Contig45	40	52	69	gDSL-like protein [Bacteroides sp. CAG:443]	
fig|319225.9.peg.1321	Contig45	47	-	-	Hypothetical protein (without blast)	
fig|319225.9.peg.1322	Contig45	52	63	90	hypothetical protein Clim_1106 [Chlorobium limicola DSM 245]	
fig|319225.9.peg.1325	Contig45	38	66	68	hypothetical protein BAD_1022 [Bifidobacterium adolescentis ATCC 15703]	
fig|319225.9.peg.1389	Contig50	42	64	85	hypothetical protein [Chlorobium ferrooxidans]	
fig|319225.9.peg.1392	Contig50	57	-	-	Hypothetical protein (without blast)	
fig|319225.9.peg.1407	Contig50	71	35	64	hypothetical protein [Acinetobacter]	
fig|319225.9.peg.1419	Contig50	53	42	83	hypothetical protein HICON_13940 [Haemophilus influenzae F3047]	
fig|319225.9.peg.1424	Contig50	71	-	-	Hypothetical protein (without blast)	
fig|319225.9.peg.1449	Contig50	64	39	75	hypothetical protein SUFG_00015 [Sulfitobacter phage pCB2047-B]	
fig|319225.9.peg.1470	Contig50	873	74	99	DNA mismatch repair protein MutS [Chlorobium ferrooxidans]	
fig|319225.9.peg.1471	Contig50	39	-	-	Hypothetical protein (without blast)	
fig|319225.9.peg.1473	Contig50	50	-	-	Hypothetical protein (without blast)	
fig|319225.9.peg.1494	Contig50	54	40	91	Sensory box histidine kinase [Cystobacter fuscus]	
fig|319225.9.peg.1506	Contig50	42	63	66	molybdenum ABC transporter periplasmic-binding protein [Chlorobium luteolum DSM 273]	
fig|319225.9.peg.1527	Contig50	71	37	93	hypothetical protein Ppha_0736 [Pelodictyon phaeoclathratiforme BU-1]	
fig|319225.9.peg.1569	Contig50	50	-	-	Hypothetical protein (without blast)	
fig|319225.9.peg.1573	Contig50	44	-	-	Hypothetical protein (without blast)	
fig|319225.9.peg.1584	Contig50	69	64	32	hypothetical protein CT1651 [Chlorobium tepidum TLS]	
fig|319225.9.peg.1600	Contig50	39	47	89	hypothetical protein PGTG_17879 [Puccinia graminis f. sp. tritici CRL 75-36-700-3]	
fig|319225.9.peg.1601	Contig50	144	82	100	hypothetical protein Cvib_1441 [Chlorobium phaeovibrioides DSM 265]	
fig|319225.9.peg.1608	Contig50	40	44	92	hypothetical protein [Selenomonas sp. FOBRC9]	
fig|319225.9.peg.1612	Contig19	38	47	86	hydroxydechloroatrazine ethylaminohydrolase [Pseudomonas mendocina]	
fig|319225.9.peg.1669	Contig53	79	-	-	Hypothetical protein (without blast)	
fig|319225.9.peg.1689	Contig53	41	-	-	Hypothetical protein (without blast)	
fig|319225.9.peg.1706	Contig53	40	74	95	hypothetical protein Ppha_0428 [Pelodictyon phaeoclathratiforme BU-1]	
fig|319225.9.peg.1715	Contig53	38	-	-	Hypothetical protein (without blast)	
fig|319225.9.peg.1734	Contig53	72	70	77	hypothetical protein Cvib_1564 [Chlorobium phaeovibrioides DSM 265]	
fig|319225.9.peg.1735	Contig53	40	-	-	Hypothetical protein (without blast)	
fig|319225.9.peg.1738	Contig53	328	48	77	hypothetical protein Plut_0559 [Chlorobium luteolum DSM 273]	
fig|319225.9.peg.1750	Contig53	292	40	100	hypothetical protein [Dysgonomonas gadei]	
fig|319225.9.peg.1751	Contig53-15	299	39	94	hypothetical protein [Dysgonomonas gadei]	
fig|319225.9.peg.1760	Contig15	204	54	91	type 11 methyltransferase [Allochromatium vinosum DSM 180]	
fig|319225.9.peg.1764	Contig15	168	27	73	membrane protein [Escherichia]	
fig|319225.9.peg.1765	Contig15-42	47	-	-	Hypothetical protein (without blast)	
fig|319225.9.peg.1766	Contig42	594	61	98	ABC transporter-like protein [Chlorobium phaeovibrioides DSM 265]	
fig|319225.9.peg.1769	Contig42	44	-	-	Hypothetical protein (without blast)	
fig|319225.9.peg.1770	Contig42	149	99	99	transposase [Chlorobium phaeobacteroides BS1]	
fig|319225.9.peg.1771	Contig42	208	98	99	transposase [Chlorobium phaeobacteroides BS1]	
fig|319225.9.peg.1772	Contig42	422	33	77	acyltransferase [Pseudomonas syringae]	
fig|319225.9.peg.1773	Contig42	126	-	-	Hypothetical protein (without blast)	
fig|319225.9.peg.1780	Contig42	44	51	81	hypothetical protein [Chlorobium ferrooxidans]	
fig|319225.9.peg.1787	**Contig42**	**90**	**87**	**53**	**putative transcriptional regulator [Chlorobium phaeovibrioides DSM 265]**	**Promiscuous region 2**
fig|319225.9.peg.1789	**Contig37**	**38**	**78**	**100**	**hypothetical protein Ppha_0599 [Pelodictyon phaeoclathratiforme BU-1]**	**Promiscuous region 2**
fig|319225.9.peg.1790	**Contig37**	**163**	**56**	**85**	**transcriptional regulator [Chlorobium chlorochromatii CaD3]**	**Promiscuous region 2**
fig|319225.9.peg.1791	**Contig37**	**217**	**56**	**99**	**hypothetical protein Mmol_0746 [Methylotenera mobilis JLW8]**	**Promiscuous region 2**
fig|319225.9.peg.1792	**Contig37**	**70**	**52**	**45**	**ATP-dependent helicase [Desulfovibrio magneticus RS-1]**	**Promiscuous region 2**
fig|319225.9.peg.1793	**Contig37**	**53**	**100**	**100**	**XRE family transcriptional regulator [Chlorobium phaeovibrioides DSM 265]**	**Promiscuous region 2**
fig|319225.9.peg.1794	**Contig37**	**108**	**100**	**100**	**hypothetical protein Cvib_0661 [Chlorobium phaeovibrioides DSM 265]**	**Promiscuous region 2**
fig|319225.9.peg.1795	**Contig37**	**284**	**98**	**100**	**HipA domain-containing protein [Chlorobium phaeovibrioides DSM 265]**	**Promiscuous region 2**
fig|319225.9.peg.1796	**Contig37**	**127**	**100**	**100**	**hypothetical protein Cvib_0659 [Chlorobium phaeovibrioides DSM 265]**	**Promiscuous region 2**
fig|319225.9.peg.1797	**Contig37**	**211**	**99**	**100**	**hypothetical protein Cvib_0658 [Chlorobium phaeovibrioides DSM 265]**	**Promiscuous region 2**
fig|319225.9.peg.1798	**Contig37**	**359**	**65**	**97**	**Appr-1-p processing domain-containing protein [Dickeya zeae Ech1591]**	**Promiscuous region 2**
fig|319225.9.peg.1799	**Contig37**	**151**	**61**	**100**	**hypothetical protein [Hydrogenophaga sp. PBC]**	**Promiscuous region 2**
fig|319225.9.peg.1800	**Contig37**	**67**	**-**	**-**	**Hypothetical protein (without blast)**	**Promiscuous region 2**
fig|319225.9.peg.1803	**Contig37**	**47**	**-**	**-**	**Hypothetical protein (without blast)**	**Promiscuous region 2**
fig|319225.9.peg.1804	**Contig37**	**46**	**82**	**100**	**hypothetical protein [Ralstonia pickettii]**	**Promiscuous region 2**
fig|319225.9.peg.1805	**Contig37**	**442**	**82**	**100**	**site-specific integrase/recombinase [Janthinobacterium sp. Marseille]**	**Promiscuous region 2**
fig|319225.9.peg.1806	**Contig37**	**38**	**84**	**100**	**resolvase family prophage LambdaMc01 [Lautropia mirabilis]**	**Promiscuous region 2**
fig|319225.9.peg.1807	**Contig37**	**85**	**77**	**96**	**hypothetical protein [Brachymonas chironomi]**	**Promiscuous region 2**
fig|319225.9.peg.1808	**Contig37**	**52**	**-**	**-**	**Hypothetical protein (without blast)**	**Promiscuous region 2**
fig|319225.9.peg.1809	**Contig25**	**470**	**62**	**99**	**Mannose-1-phosphate guanylyltransferase/mannose-6-phosphate isomerase [Lariibacter hongkongensis HLHK9]**	**Promiscuous region 2**
fig|319225.9.peg.1810	**Contig25**	**105**	**75**	**100**	**hypothetical protein [Limnohabitans sp. Rim47]**	**Promiscuous region 2**
fig|319225.9.peg.1811	**Contig25**	**204**	**51**	**90**	**hypothetical protein [Cupriavidus sp. UYPR2.512]**	**Promiscuous region 2**

Table A.C5.2: *Continued*

Chl. luteolum CIII protein	Contig	Protein Length	Identity (%)	Coverage (%)	Protein BLAST First Hit	Comments
fig|319225.9.peg.1812	**Contig25**	**358**	**54**	**95**	**transposase IS116/IS110/IS902 [Comamonas testosteroni CNB-2]**	**Promiscuous region 2**
fig|319225.9.peg.1813	**Contig25**	**41**	**74**	**95**	**Exclnuclease ABC C subunit domain protein partial [Methylosinus trichosporium]**	**Promiscuous region 2**
fig|319225.9.peg.1814	**Contig25**	**157**	**98**	**100**	**hypothetical protein Cvib_0613 [Chlorobium phaeovibrioides DSM 265]**	**Promiscuous region 2**
fig|319225.9.peg.1818	**Contig25**	**325**	**50**	**98**	**glycosyl transferase family protein [Chlorobium limicola DSM 245]**	**Promiscuous region 2**
fig|319225.9.peg.1819	**Contig25**	**46**	**39**	**62**	**NADH dehydrogenase subunit C [Methylophaga aminisulfidivorans]**	**Promiscuous region 2**
fig|319225.9.peg.1821	**Contig25**	**157**	**68**	**71**	**hypothetical protein Plut_1888 [Chlorobium luteolum DSM 273]**	**Promiscuous region 2**
fig|319225.9.peg.1822	**Contig25-14**	**252**	**63**	**53**	**lipopolysaccharide biosynthesis protein [Chlorobium phaeovibrioides DSM 265]**	**Promiscuous region 2**
fig|319225.9.peg.1824	**Contig10**	**173**	**87**	**95**	**hypothetical protein Plut_1885 [Chlorobium luteolum DSM 273]**	**Promiscuous region 2**
fig|319225.9.peg.1827	Contig10	53	46	67	molybdopterin oxidoreductase [Burkholderia phymatum STM815]	
fig|319225.9.peg.1828	Contig10	38	-	-	Hypothetical protein (without blast)	
fig|319225.9.peg.1830	Contig10	44	-	-	Hypothetical protein (without blast)	
fig|319225.9.peg.1831	Contig10	51	-	-	Hypothetical protein (without blast)	
fig|319225.9.peg.1834	Contig10	38	-	-	Hypothetical protein (without blast)	
fig|319225.9.peg.1837	Contig10	74	42	73	hypothetical protein B5T_03156 [Alcanivorax dieselolei B5]	
fig|319225.9.peg.1838	Contig10	50	83	59	transposase IS4 family protein [Chlorobium limicola DSM 245]	
fig|319225.9.peg.1841	Contig31	76	83	97	AsnC family transcriptional regulator [Chlorobium ferrooxidans]	
fig|319225.9.peg.1851	Contig31	50	36	90	iron transporter FeoB [Sphingomonas melonis]	
fig|319225.9.peg.1860	Contig31	77	34	62	hypothetical protein Ppha_0977 [Pelodictyon phaeoclathratiforme BU-1]	
fig|319225.9.peg.1861	Contig31	62	-	-	Hypothetical protein (without blast)	
fig|319225.9.peg.1913	Contig31	41	-	-	Hypothetical protein (without blast)	
fig|319225.9.peg.1929	Contig31	40	-	-	Hypothetical protein (without blast)	
fig|319225.9.peg.1936	**Contig31**	**207**	**92**	**100**	**alpha/beta hydrolase [Chlorobium phaeobacteroides DSM 266]**	**BChl *e* cluster**
fig|319225.9.peg.1937	**Contig31**	**219**	**96**	**99**	**isoprenylcysteine carboxyl methyltransferase [Pelodictyon phaeoclathratiforme BU-1]**	**BChl *e* cluster**
fig|319225.9.peg.1938	**Contig31**	**348**	**84**	**100**	**transposase and inactivated derivatives [Chlorobium phaeobacteroides DSM 266]**	**BChl *e* cluster**
fig|319225.9.peg.1940	**Contig31**	**427**	**96**	**100**	**coenzyme F420 hydrogenase/dehydrogenase subunit beta [Chlorobium phaeobacteroides DSM 266]**	**BChl *e* cluster**
fig|319225.9.peg.1941	**Contig31**	**258**	**93**	**100**	**short-chain dehydrogenase/reductase SDR [Pelodictyon phaeoclathratiforme BU-1]**	**BChl *e* cluster-SDR**
fig|319225.9.peg.1942	**Contig31**	**55**	**93**	**100**	**hypothetical protein Cpha266_0190 [Chlorobium phaeobacteroides DSM 266]**	**BChl *e* cluster**
fig|319225.9.peg.1943	**Contig31**	**122**	**87**	**100**	**hypothetical protein Ppha_2742 [Pelodictyon phaeoclathratiforme BU-1]**	**BChl *e* cluster**
fig|319225.9.peg.1944	**Contig31**	**514**	**95**	**100**	**hypothetical protein Cpha266_0192 [Chlorobium phaeobacteroides DSM 266]**	**BChl *e* cluster-cruB**
fig|319225.9.peg.1946	**Contig41**	**294**	**95**	**100**	**aldolase [Chlorobium phaeobacteroides DSM 266]**	**BChl *e* cluster**
fig|319225.9.peg.1947	**Contig41**	**706**	**97**	**100**	**short chain dehydrogenase [Chlorobium phaeobacteroides DSM 266]**	**BChl *e* cluster**
fig|319225.9.peg.1948	**Contig41**	**402**	**99**	**100**	**hypothetical protein Cpha266_0196 [Chlorobium phaeobacteroides DSM 266]**	**BChl *e* cluster-bciD (RSAM)**
fig|319225.9.peg.1949	**Contig41**	**60**	**80**	**100**	**hypothetical protein Cpha266_0197 [Chlorobium phaeobacteroides DSM 266]**	**BChl *e* cluster**
fig|319225.9.peg.1950	**Contig41**	**159**	**93**	**100**	**2-oxoglutarate synthase subunit 2-oxoacid-ferredoxin oxidoreductase subunit CD [Chlorobium phaeobacteroides DSM 266]**	**BChl *e* cluster-bchF3**
fig|319225.9.peg.1951	**Contig41**	**453**	**94**	**99**	**radical SAM domain-containing protein [Chlorobium phaeobacteroides DSM 266]**	**BChl *e* cluster-bchQ2**
fig|319225.9.peg.1953	**Contig41**	**204**	**86**	**100**	**proto-chlorophyllide reductase 57 kD subunit [Chlorobium phaeobacteroides DSM 266]**	**BChl *e* cluster**
fig|319225.9.peg.1954	**Contig41**	**60**	**92**	**100**	**chlorosome envelope protein B [Chlorobium phaeobacteroides DSM 266]**	**BChl *e* cluster**
fig|319225.9.peg.1955	**Contig41**	**54**	**-**	**-**	**Hypothetical protein (without blast)**	**BChl *e* cluster**
fig|319225.9.peg.1965	Contig41	78	86	99	hypothetical protein Cvib_1657 [Chlorobium phaeovibrioides DSM 265]	
fig|319225.9.peg.1969	Contig41	46	-	-	Hypothetical protein (without blast)	
fig|319225.9.peg.1974	Contig27	59	-	-	Hypothetical protein (without blast)	
fig|319225.9.peg.1981	Contig27	39	38	82	hypothetical protein partial [[Clostridium] difficile]	
fig|319225.9.peg.1997	Contig27	39	84	100	hypothetical protein Clim_2404 [Chlorobium limicola DSM 245]	
fig|319225.9.peg.1999	Contig27	57	-	-	Hypothetical protein (without blast)	
fig|319225.9.peg.2031	Contig27	40	-	-	Hypothetical protein (without blast)	
fig|319225.9.peg.2036	Contig27	39	-	-	Hypothetical protein (without blast)	
fig|319225.9.peg.2041	Contig27	54	38	89	possible N-carbamoyl-L-amino-acid hydrolase [Weissella paramesenteroides]	
fig|319225.9.peg.2059	Contig27	435	100	100	transposase IS4 family protein [Chlorobium phaeobacteroides DSM 266]	

Table A.C5.3: Direct repeat and spacer regions of the CRISPR locus identified in *Chl. luteolum* CIII.

Crispr_begin_position: 1350611 Crispr_end_position: 1351470
>Direct_repeat_length_32 _Number_of_spacers_12
GTCGCGCCCCACGCGGGCGCGTGGATTGAAAC
>spacer1
CTGGAAAGGTCGCGCCCCACGCGGGCGCGTGGATTGAAACTATCTACGCCGCGTTCGTGCAAC
CATACACGGTAA
>spacer2
ACACACTTGCAGAACTCCCTATCCCGGAAGGC
>spacer3
AGGTACAATATAGCCTTATCTTCGGGTTTCGTT
>spacer4
TCTCAGCCCAGCCCGCATCAGTGAAGCCTACGT
>spacer5
TTCCAGTATGATTTCGTCGTGATTGACCCGCTTA
>spacer6
AACTATTCGGCAGCGCAGTACAAGGACAACTAC
>spacer7
CACCCATCGCATCGAAAAAGTCACCGAAGACAAA
>spacer8
TGGTTCAGCAGCTCGTACGACATACCCAGCACGGA
>spacer9
ATCGCCAGCATCGACGCATCACGGATGCCGGCAGG
>spacer10
CGATCTCCCGCCCGCTCCTTCCAGTGCCGCACA
>spacer11
GATCTGCTCAAGCAGGCTTGCTATGTCTCGGCC
>spacer12
ATCATGTCGGATAAAGGTCGCCAAGCCGTGGCGG

Table A.C5.4: Putative bacteriophage contigs.

	length	GC	GC%	CpG	CpG%	Read Depth
Contig1	65304	22741	0.348233	1504	0.023031	34.8x
Contig2	7907	3257	0.411913	702	0.088782	97.5x
Contig3	19838	6550	0.330174	960	0.048392	189.1x
Contig4	24185	10767	0.445193	2534	0.104776	111.1x
Contig5	106030	35289	0.332821	4668	0.044025	169.0x

Table A.C5.5: Predicted host-acquired auxiliary metabolic genes for putative bacteriophage contigs 3 and 5.

Putative Classification	ORF	Start	Stop	Orientation	% identity	al. length	Hit ID	Hit Annotation	Hit Taxa
Contig3	Contig3_1	1	252	-	57	75	MCA2930-NC_002977	prophage MuMc02, head decoration protein	Methylococcus capsulatus str. Bath
Myovirus	Contig3_2	1474	1875	-	31	122	JCVI_PEP_1113079352272-UDEL_CHESAPEAKE_VIROPLANKTON_SMPL		UDEL_CHESAPEAKE_VIROPLANKTON_SMPL
	Contig3_3	1903	4561	-	48	448	gi448936869-KC465899	terminasee large subunit	Pelagibacter phage HTVC008M
	Contig3_4	4563	6551	-	38	212	gi448936864-KC465899	proximal tail sheath stabilization	Pelagibacter phage HTVC008M
	Contig3_5	6634	7257	-	41	165	gi113200614-NC_008296	14 neck protein	Synechococcus phage syn9
	Contig3_6	7261	8043	-	29	190	JCVI_PEP_1113079359376-UDEL_CHESAPEAKE_VIROPLANKTON_SMPL		UDEL_CHESAPEAKE_VIROPLANKTON_SMPL
	Contig3_7	8058	9824	-	40	142	SAK_0759-NC_007432	prophage LambdaSa04, minor structural protein	Streptococcus agalactiae A909
	Contig3_8	9858	13594	-	35	271	gi448936843-KC465899	baseplate wedge	Pelagibacter phage HTVC008M
	Contig3_9	13598	14008	-	37	124	gi58532890-NC_006820	25 tail lysozyme	Synechococcus phage S-PM2
	Contig3_10	14539	17122	-	26	284	gi448936818-KC465899	structural protein	Pelagibacter phage HTVC008M
Contig5	Contig5_1	1	825	+	45	168	gi448936853-KC465899	hypothetical protein	Pelagibacter phage HTVC008M
Myovirus	Contig5_2	1953	4884	-	37	464	gi113200684-NC_008296	41 41 helicase	Synechococcus phage syn9
	Contig5_3	4892	5789	-	68	134	HMPREF0381_0731-NZ_AEPW01000024	dUTP diphosphatase	Eubacterium saburreum DSM 3986
	Contig5_4	7687	8534	+	34	234	gi448936812-KC465899	baseplate hub subunit	Pelagibacter phage HTVC008M
	Contig5_5	12302	13156	-	42	247	gi58533011-NC_006820	32 single-stranded DNA binding protein	Synechococcus phage S-PM2
	Contig5_6	14114	16014	-	49	191	jgi_96647_7147.m000009-Volca1	hypothetical protein	Volvox carteri
	Contig5_7	16072	18892	-	60	138	JCVI_PEP_1113079336300-UDEL_CHESAPEAKE_VIROPLANKTON_SMPL		UDEL_CHESAPEAKE_VIROPLANKTON_SMPL
	Contig5_8	18949	19923	-	62	224	JCVI_PEP_1113079330680-UDEL_CHESAPEAKE_VIROPLANKTON_SMPL		UDEL_CHESAPEAKE_VIROPLANKTON_SMPL
	Contig5_9	19942	22297	-	31	285	gi38640254-NC_005260	rnh RnaseH	Aeromonas phage Aeh1
	Contig5_10	22330	24590	-	36	311	gi412993653-FO082278	COG0438: Glycosyltransferase (ISS)	Bathycoccus prasinos
	Contig5_11	31336	31797	+	45	136	gi18071215-NC_003324	hypothetical protein	Sinorhizobium phage PBC5
	Contig5_12	34000	34405	+	42	139	gi312281419-NC_006884	glutamine-dependent NAD(+) synthetase	Prochlorococcus phage P-SSM4
	Contig5_13	34423	35437	-	30	342	gi113200699-NC_008296	61 DNA primase	Synechococcus phage syn9
	Contig5_14	35522	37252	+	40	425	gi448936870-KC465899	tail sheath protein	Pelagibacter phage HTVC008M
	Contig5_15	37658	38203	+	34	170	gi448936871-KC465899	tail tube monomer	Pelagibacter phage HTVC008M
	Contig5_16	38748	40827	+	42	482	gi113200635-NC_008296	20 portal vertex protein	Synechococcus phage syn9
	Contig5_17	43200	43833	+	43	202	gi61806308-NC_006884	21 prohead core scaffolding protein and protease	Prochlorococcus phage P-SSM4
	Contig5_18	48302	49441	+	28	319	gi61806006-NC_006883	22 prohead core protein	Prochlorococcus phage P-SSM2
	Contig5_19	49486	50817	+	44	441	gi448936880-KC465899	major capsid	Pelagibacter phage HTVC008M
	Contig5_20	50894	53715	+	34	213	gi161322921-ABIB01000021	glycosyltransferase, group 2 family	Kordia algicida OT-1
	Contig5_21	54075	54635	+	32	165	gi61806313-NC_006884	3 gp3	Prochlorococcus phage P-SSM4
	Contig5_22	54651	56889	+	36	311	gi91220154-NZ_AAPR01000540	UvsW	Psychroflexus torquis ATCC 700755
	Contig5_23	56893	59673	+	35	574	gi58532930-NC_006820	46 endonuclease subunit	Synechococcus phage S-PM2
	Contig5_24	61534	62666	+	29	257	Sala_1869-NC_008048	hypothetical protein	Sphingopyxis alaskensis RB2256
	Contig5_25	62687	64967	+	36	307	gi61806033-NC_006883	44 clamp loader small subunit	Prochlorococcus phage P-SSM2
	Contig5_26	64982	66768	+	48	206	EUR_29810-FP929042	thymidylate synthase, flavin-dependent	Eubacterium rectale DSM 17629
	Contig5_27	66775	67758	+	36	326	ViPhICP1_gp191-NC_015157	hypothetical protein	Vibrio phage ICP1
	Contig5_28	68120	70955	+	36	846	gi58532945-NC_006820	43 DNA polymerase	Synechococcus phage S-PM2

Table A.C5.5: *Continued*

Putative Classification	ORF	Start	Stop	Orientation	% identity	al. length	Hit ID	Hit Annotation	Hit Taxa
	Contig5_29	71604	72480	-	42	201	gi282599019-NC_013697	baseplate hub subunit and tail lysozyme; similar to YP_001469479.1 gp5 baseplate hub subunit and tail lysozyme	Deftia phage phiW-14
	Contig5_30	73075	73584	+	36	164	HMPREF0983_02337-NZ_ACTJ01000053	putative hydrolase protein	Erysipelotrichaceae bacterium 3_1_53
	Contig5_31	73588	75057	+	28	250	Acj61p202-NC_014661	gp30 DNA ligase	Acinetobacter phage Acj61
	Contig5_32	75068	75559	+	37	160	Rvan_3136-NC_014664	metallophosphoesterase	Rhodomicrobium vannielii ATCC 17100
	Contig5_33	75571	76386	+	49	160	Cpha266_0651-NC_008639	metallophosphoesterase	Chlorobium phaeobacteroides DSM 266
	Contig5_34	76719	80064	+	42	227	RER_24950-NC_012490	hypothetical protein; K07074	Rhodococcus erythropolis PR4
	Contig5_35	81939	82848	+	40	169	gi20066007-NC_003524||AC1_2808-NZ_ABDV01000026	Gp45 protein	Clostridium phage phi3626
	Contig5_36	82904	83621	+	44	152	RUMLAC_01904-NZ_ABOU02000045	hypothetical protein	Ruminococcus lactaris ATCC 29176
	Contig5_37	85018	87504	+	38	337	gi161326946-ABIB01000001	hypothetical protein || RNA ligase (ATP)	Kordia algicida OT-1
	Contig5_38	87546	88040	+	39	163	SRU_1190-NC_007677||SRM_01376-NC_014032||gi294507191-NC_014032	HNH endonuclease domain-containing protein||HNH endonuclease	Salinibacter ruber DSM 13855
	Contig5_39	88062	89229	+	44	359	Halhy_3676-NC_015510	RNA ligase, DRB0094 family	Haliscomenobacter hydrossis DSM 1100
	Contig5_40	91610	92350	+	39	233	GM21_3826-NC_012918	hypothetical protein	Geobacter sp. M21
	Contig5_41	92377	93466	+	40	144	gi33620690-NC_005066||gi238695014-NC_012740	4 head completion protein||head completion protein	Enterobacteria phage RB49
	Contig5_42	94040	94991	+	48	105	VR7_gp129-NC_014792	DenV endonuclease V N-glycosylase UV repair enzyme	Enterobacteria phage vB_EcoM-VR7
	Contig5_43	99618	100005	-	47	107	Runsl_3984-NC_015703	HNH endonuclease	Runella slithyformis DSM 19594
	Contig5_44	104565	104825	+	60	84	gi318065996-NC_006820	Hypothetical-Protein | belonging to T4-LIKE GC: 780	Synechococcus phage S-PM2
	Contig5_45	104843	106030	+	39	104	mru_0296-NC_013790	hypothetical protein	Methanobrevibacter ruminantium M1

Red=DNA metabolism; Blue=Structural and packaging; Green=Lysis;Purple=Putative host derived

Figure A.C6.1: Maximum-parsimony phylogenetic tree of 16S rRNA gene bacterial sequences recovered from slush (SL), underlying water column (WC) and pond (P) of Lake Redon during winter (blue) and spring (red). The tree is based on maximum parsimony analysis of the dataset in the ARB program package (http://www.arb-home.de). Sequences of c. 900 nt were inserted into the optimized tree by using parsimony criteria without allowing changes in the overall tree topology. Sequences from this study are in bold and are representatives of each OTU at 97% identity (the number of sequences within each OTU is also shown). GenBank accession numbers are provided and the closest cultured relatives are included. The scale bar represents 10% estimated divergence.

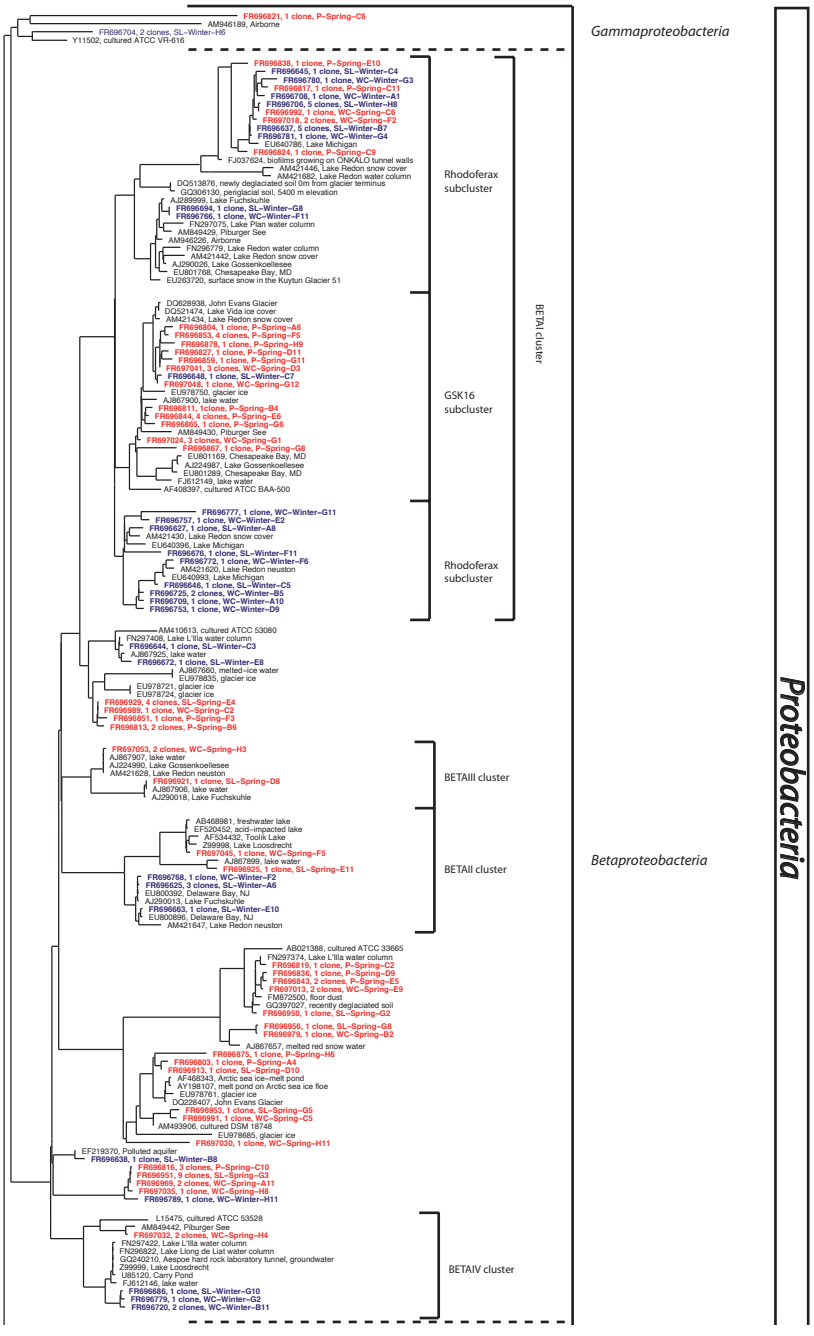

Figure A.C6.1: *Continued*

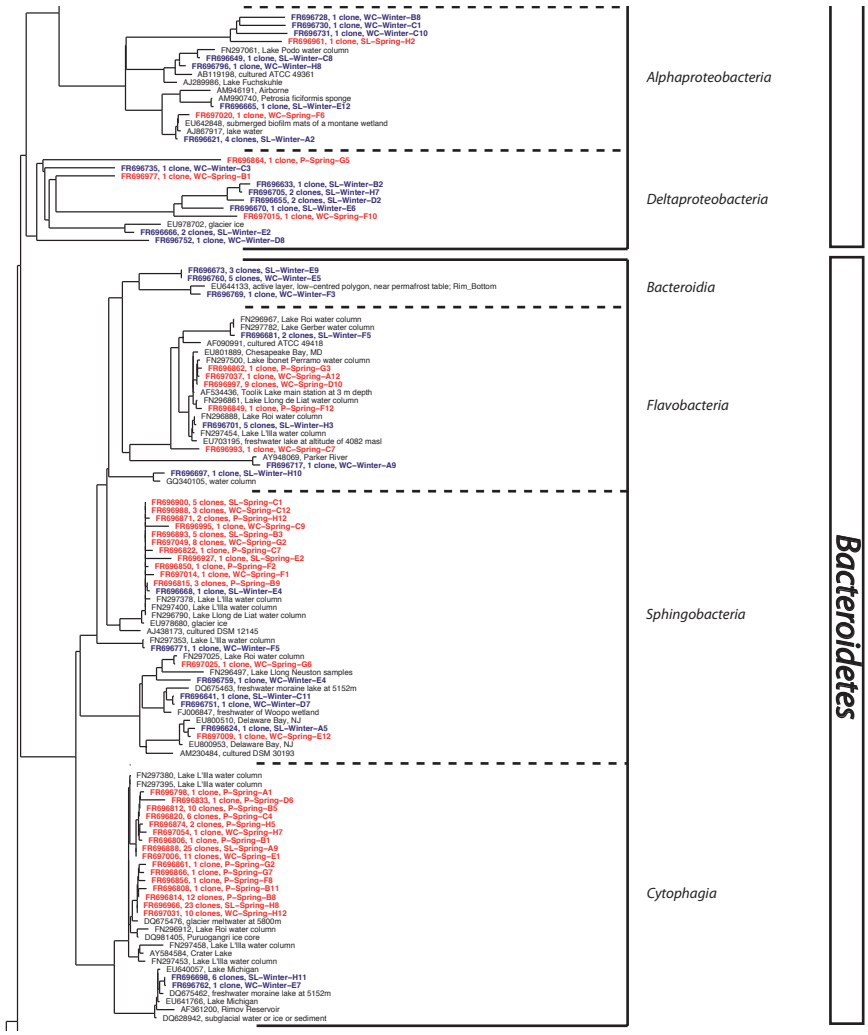

Figure A.C6.1: *Continued*

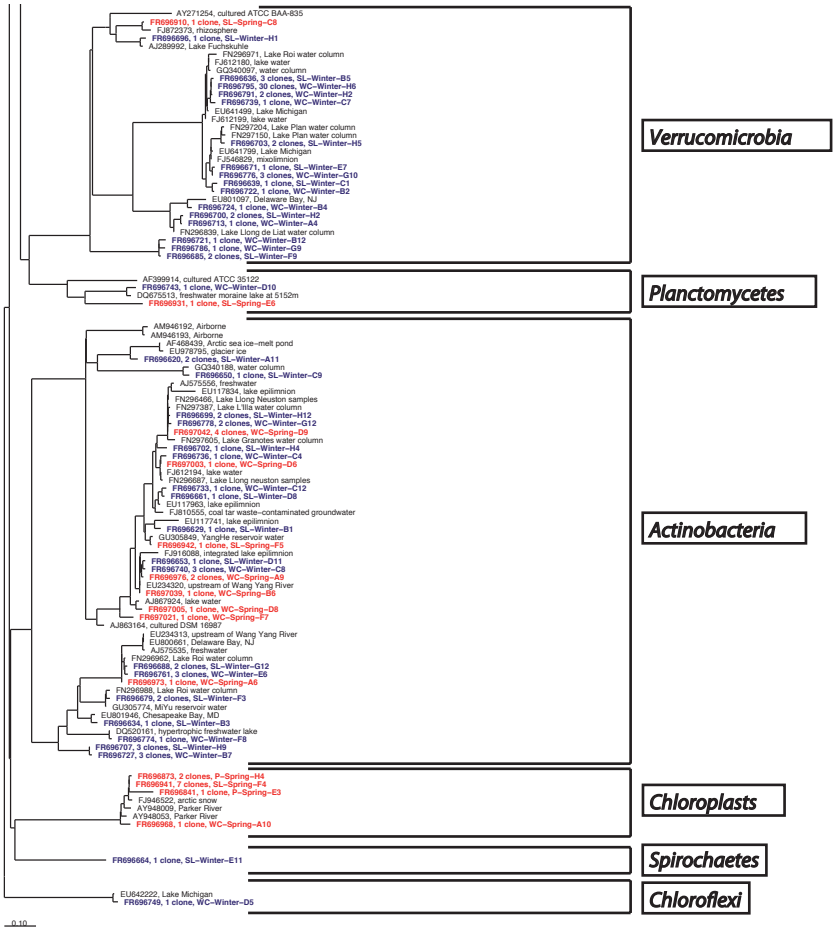

Table A.C6.1. Closest BLASTs of slush (SL), water column (WC) and pond (P) 16S rRNA gene OTUs. The isolation source of the closest BLAST was retrieved from the GenBank database.

OTUs				Closest BLAST		
Category	Accession nº	Clone id.	Nº of clones at 97%	Sequence	Isolation source	Identity (%)
Actino-bacteria	FR696942	SL-Spring-F5	1	GU305849	YangHe reservoir water	99,9
	FR696620	SL-Winter-A11	2	EU978795	Glacier ice	99,3
	FR696629	SL-Winter-B1	1	EU117741	lake epilimnion	98,5
	FR696634	SL-Winter-B3	1	EU801946	Chesapeake Bay, MD	98,8
	FR696650	SL-Winter-C9	1	GQ340188	Water column	98,5
	FR696653	SL-Winter-D11	1	FJ916088	Integrated lake epilimnion	99,1
	FR696661	SL-Winter-D8	1	EU117963	Lake epilimnion	98,6
	FR696679	SL-Winter-F3	2	FN296988	Lake Roi water column	98,7
	FR696688	SL-Winter-G12	2	EU800661	Delaware Bay, NJ	98,7
	FR696699	SL-Winter-H12	2	FN296466	Lake Llong Neuston samples	99,4
	FR696702	SL-Winter-H4	1	FJ810555	Contaminated groundwater	97,9
	FR696707	SL-Winter-H9	3	AY792234	Humic Lake	95,7
	FR696973	WC-Spring-A6	1	EU234313	Upstream of Wang Yang River	100,0
	FR696976	WC-Spring-A9	2	EU234320	Upstream of Wang Yang River	99,7
	FR697039	WC-Spring-B6	1	FJ916087	Integrated lake epilimnion	87,9
	FR697003	WC-Spring-D6	1	FJ612194	Lake water	99,8
	FR697005	WC-Spring-D8	1	AJ867924	Lake water	99,8
	FR697042	WC-Spring-D9	4	AJ575556	Freshwater	100,0
	FR697021	WC-Spring-F7	1	EU800576	Delaware Bay, NJ	96,4
	FR696727	WC-Winter-B7	3	AY792234	Humic Lake	95,0
	FR696733	WC-Winter-C12	1	EU117963	lake epilimnion	98,6
	FR696736	WC-Winter-C4	1	FN296687	Lake Llong Neuston samples	98,4
	FR696740	WC-Winter-C8	3	FJ916088	Integrated lake epilimnion	99,3
	FR696761	WC-Winter-E6	3	FN296962	Lake Roi water column	98,7
	FR696774	WC-Winter-F8	1	DQ520161	Hypertrophic freshwater lake	99,1
	FR696778	WC-Winter-G12	2	FN297605	Lake Granotes water column	98,7
Bacteroide-tes (class *Bacteroidia*)	FR696673	SL-Winter-E9	3	EF034416	Spitsbergen permafrost soil	96,6
	FR696760	WC-Winter-E5	5	EF034715	Spitsbergen permafrost soil	96,7
	FR696769	WC-Winter-F3	1	EU644133	Permafrost	97,2
Bacteroide-tes (class *Cytophagia*)	FR696698	SL-Winter-H11	6	EU641766	Lake Michigan	99,2
	FR696762	WC-Winter-E7	1	DQ675462	Freshwater moraine lake	99,1
	FR696798	P-Spring-A1	1	FN297458	Lake L'Illa water column	97,0

Table A.C6.1. *Continued*

OTUs				Closest BLAST		
Category	Accession nº	Clone id.	Nº of clones at 97%	Sequence	Isolation source	Identity (%)
Bacteroidetes (class *Cytophagia*)	FR696806	P-Spring-B1	1	FN297352	Lake L'Illa water column	96,9
	FR696808	P-Spring-B11	1	FN297395	Lake L'Illa water column	97,3
	FR696812	P-Spring-B5	10	FN297458	Lake L'Illa water column	99,6
	FR696814	P-Spring-B8	12	FN296912	Lake Roi water column	99,6
	FR696820	P-Spring-C4	6	FN297458	Lake L'Illa water column	99,6
	FR696833	P-Spring-D6	1	FN297458	Lake L'Illa water column	93,0
	FR696856	P-Spring-F8	1	FN297451	Lake L'Illa water column	97,7
	FR696861	P-Spring-G2	1	DQ675476	Glacier meltwater	98,1
	FR696866	P-Spring-G7	1	FN297380	Lake L'Illa water column	98,3
	FR696874	P-Spring-H5	2	FN297458	Lake L'Illa water column	97,5
	FR696888	SL-Spring-A9	25	AY584584	Crater Lake, Oregon	100,0
	FR696966	SL-Spring-H8	23	DQ981405	Puruogangri ice core	99,6
	FR697006	WC-Spring-E1	11	AY584584	Crater Lake, Oregon	100,0
	FR697031	WC-Spring-H12	10	DQ981405	Puruogangri ice core	99,6
	FR697054	WC-Spring-H7	1	AY584584	Crater Lake, Oregon	97,2
Bacteroidetes (class *Flavobacteria*)	FR696697	SL-Winter-H10	1	GQ340105	Water column	97,3
	FR696717	WC-Winter-A9	1	AY948069	Parker River, Massachusetts	98,2
	FR696681	SL-Winter-F5	2	FN296967	Lake Roi water column	99,1
	FR696701	SL-Winter-H3	5	FN297454	Lake L'Illa water column	99,2
	FR696849	P-Spring-F12	1	FN296861	Lake Llong de Liat water column	98,8
	FR696862	P-Spring-G3	1	FN297500	Lake Ibonet Perramo water column	97,3
	FR697037	WC-Spring-A12	1	EU801889	Chesapeake Bay, MD	98,4
	FR696993	WC-Spring-C7	1	DQ514307	Marine sediments (Arctic)	90,2
	FR696997	WC-Spring-D10	9	EU801889	Chesapeake Bay, MD	99,1
Bacteroidetes (class *Sphingobacteria*)	FR696624	SL-Winter-A5	1	EU800953	Delaware Bay, NJ	98,7
	FR696641	SL-Winter-C11	1	FJ006847	freshwater of Woopo wetland	97,1
	FR697009	WC-Spring-E12	1	EU800510	Delaware Bay, NJ	99,3
	FR697025	WC-Spring-G6	1	FN297025	Lake Roi water column	99,7

Table A.C6.1. *Continued*

OTUs				Closest BLAST		
Category	Accession nº	Clone id.	Nº of clones at 97%	Sequence	Isolation source	Identity (%)
Bacteroidetes (class *Sphingobacteria*)	FR696751	WC-Winter-D7	1	DQ675463	freshwater moraine lake	97,5
	FR696759	WC-Winter-E4	1	FN296497	Lake Llong Neuston samples	98,4
	FR696668	SL-Winter-E4	1	FN296790	Lake Llong de Liat water column	99,2
	FR696771	WC-Winter-F5	1	FN297353	Lake L'lla water column	99,3
	FR696815	P-Spring-B9	3	FN296790	Lake Llong de Liat water column	99,6
	FR696822	P-Spring-C7	1	FN297378	Lake L'lla water column	97,8
	FR696850	P-Spring-F2	1	FN297400	Lake L'lla water column	97,9
	FR696871	P-Spring-H12	2	FN297378	Lake L'lla water column	98,6
	FR696893	SL-Spring-B3	5	FN297400	Lake L'lla water column	100,0
	FR696900	SL-Spring-C1	5	FN297378	Lake L'lla water column	99,8
	FR696927	SL-Spring-E2	1	EU978680	glacier ice	100,0
	FR696988	WC-Spring-C12	3	FN297378	Lake L'lla water column	99,8
	FR696995	WC-Spring-C9	1	EU978704	glacier ice	96,7
	FR697014	WC-Spring-F1	1	FN297400	Lake L'lla water column	97,5
	FR697049	WC-Spring-G2	8	AB267722	Soil of the ginseng field	98,1
Chloroflexi	FR696749	WC-Winter-D5	1	EU642222	Lake Michigan	98,2
Chloroplasts	FR696968	WC-Spring-A10	1	AY948053	Massachusetts, Parker River	97,4
	FR696841	P-Spring-E3	1	FJ946522	arctic snow	92,0
	FR696873	P-Spring-H4	2	FJ946522	arctic snow	98,0
	FR696941	SL-Spring-F4	7	AY948009	Massachusetts, Parker River	97,6
Planctomycetes	FR696931	SL-Spring-E6	1	GQ487924	soil polluted by heavy metals	93,9
	FR696743	WC-Winter-D10	1	DQ675513	freshwater moraine lake at 5152m	98,5
Proteobacteria (Class *Alphaproteobacteria*)	FR696621	SL-Winter-A2	4	EU642848	No isolation source	99,2
	FR696649	SL-Winter-C8	1	FN297061	Lake Podo water column	99,4
	FR696665	SL-Winter-E12	1	AM990740	Petrosia ficiformis sponge	99,3
	FR697020	WC-Spring-F6	1	AJ867917	lake water	99,8
	FR696731	WC-Winter-C10	1	GU230291	coastal water	87,3
	FR696796	WC-Winter-H8	1	AJ289986	Lake Fuchskuhle	98,8
	FR696961	SL-Spring-H2	1	EU640279	Lake Michigan	88,0
	FR696730	WC-Winter-C1	1	EU640279	Lake Michigan	84,4
	FR696728	WC-Winter-B8	1	EU640157	Lake Michigan	89,3

Table A.C6.1. *Continued*

OTUs				Closest BLAST		
Category	Accession nº	Clone id.	Nº of clones at 97%	Sequence	Isolation source	Identity (%)
Proteo-bacteria (Class *Beta-proteo-bacteria*)	FR697030	WC-Spring-H11	1	EU801264	Chesapeake Bay, MD	94,4
	FR696803	P-Spring-A4	1	EU978761	glacier ice	97,4
	FR696804	P-Spring-A6	1	EU978750	glacier ice	95,9
	FR696811	P-Spring-B4	1	EU801169	Chesapeake Bay, MD	96,9
	FR696813	P-Spring-B6	2	EU978835	glacier ice	97,7
	FR696816	P-Spring-C10	3	AJ867660	melted-ice water	99,5
	FR696817	P-Spring-C11	1	FJ037624	biofilms	98,3
	FR696819	P-Spring-C2	1	FN297374	Lake L'Illa water column	97,9
	FR696824	P-Spring-C9	1	GQ306130	periglacial soil, 5400 m elevation	97,5
	FR696827	P-Spring-D11	1	EU978750	glacier ice	95,8
	FR696836	P-Spring-D9	1	DQ228407	John Evans Glacier	97,0
	FR696838	P-Spring-E10	1	EU263720	surface snow in the Kuytun Glacier 51	98,5
	FR696843	P-Spring-E5	2	AY198107	melt pond on Arctic sea ice floe	98,2
	FR696844	P-Spring-E6	4	EU801169	Chesapeake Bay, MD	98,2
	FR696851	P-Spring-F3	1	EU978835	glacier ice	96,6
	FR696853	P-Spring-F5	4	EU978750	glacier ice	97,7
	FR696859	P-Spring-G11	1	EU978750	glacier ice	93,4
	FR696865	P-Spring-G6	1	AB519656	antarctic snow	96,0
	FR696867	P-Spring-G8	1	FM209305	sand soil	95,6
	FR696875	P-Spring-H6	1	FN297386	Lake L'Illa water column	93,7
	FR696878	P-Spring-H9	1	EF079081	freshwater reserve De Bruuk	94,6
	FR696913	SL-Spring-D10	1	DQ228407	John Evans Glacier	99,1
	FR696921	SL-Spring-D8	1	AJ867906	lake water	99,9
	FR696925	SL-Spring-E11	1	AJ867899	lake water	97,1
	FR696929	SL-Spring-E4	4	EU978835	glacier ice	99,9
	FR696950	SL-Spring-G2	1	AB074523	No isolation source	99,1
	FR696951	SL-Spring-G3	9	AJ867660	melted-ice water	100,0
	FR696953	SL-Spring-G5	1	EU978685	glacier ice	97,7
	FR696956	SL-Spring-G8	1	AJ867657	melted red snow water	99,5
	FR696625	SL-Winter-A6	3	EU800392	Delaware Bay, NJ	99,3
	FR696627	SL-Winter-A8	1	EU801768	Chesapeake Bay, MD	99
	FR696637	SL-Winter-B7	5	EU640747	Lake Michigan	99,5
	FR696638	SL-Winter-B8	1	EF219370	No isolation source	97,1
	FR696644	SL-Winter-C3	1	FN297408	Lake L'Illa water column	99,5
	FR696645	SL-Winter-C4	1	EU801480	Chesapeake Bay, MD	98,4
	FR696646	SL-Winter-C5	1	EU640993	Lake Michigan	99,6
	FR696648	SL-Winter-C7	1	AM849430	Piburger See	98,3
	FR696663	SL-Winter-E10	1	EU800896	Delaware Bay, NJ	99,1

Table A.C6.1. *Continued*

OTUs				Closest BLAST		
Category	Accession nº	Clone id.	Nº of clones at 97%	Sequence	Isolation source	Identity (%)
Proteo-bacteria (Class *Beta-proteo-bacteria*)	FR696672	SL-Winter-E8	1	AJ867925	lake water	98,7
	FR696676	SL-Winter-F11	1	AM849429	Piburger See	99,7
	FR696686	SL-Winter-G10	1	FN297422	Lake L'Illa water column	99,4
	FR696694	SL-Winter-G8	1	EU640396	Lake Michigan	99,6
	FR696706	SL-Winter-H8	5	AJ867930	lake water	99,6
	FR696969	WC-Spring-A11	2	AJ867660	melted-ice water	99,8
	FR696979	WC-Spring-B2	1	AJ867657	melted red snow water	99,4
	FR696989	WC-Spring-C2	1	EU978835	glacier ice	99,8
	FR696991	WC-Spring-C5	1	GQ397027	soil	97,0
	FR696992	WC-Spring-C6	1	AJ867905	lake water	99,5
	FR697041	WC-Spring-D3	3	AM849430	Piburger See	99,0
	FR697013	WC-Spring-E9	2	AY198107	melt pond on Arctic sea ice floe	99,7
	FR697018	WC-Spring-F2	2	GQ340350	water column	98,7
	FR697045	WC-Spring-F5	1	EU800896	Delaware Bay, NJ	99,8
	FR697024	WC-Spring-G1	3	AJ867900	lake water	99,9
	FR697048	WC-Spring-G12	1	AM849430	Piburger See	99,5
	FR697053	WC-Spring-H3	2	AJ224990	Lake Gossenkoellesee	99,2
	FR697032	WC-Spring-H4	2	AM849442	Piburger See	99,6
	FR697035	WC-Spring-H8	1	EU978724	glacier ice	98,8
	FR696708	WC-Winter-A1	1	AJ867918	lake water	96,9
	FR696709	WC-Winter-A10	1	EU640396	Lake Michigan	98
	FR696725	WC-Winter-B5	2	EU640396	Lake Michigan	98,4
	FR696753	WC-Winter-D9	1	EU640396	Lake Michigan	95,4
	FR696757	WC-Winter-E2	1	FN296779	Lake Redon water column	99,4
	FR696766	WC-Winter-F11	1	EU640396	Lake Michigan	99,1
	FR696768	WC-Winter-F2	1	EU800392	Delaware Bay, NJ	98,6
	FR696772	WC-Winter-F6	1	FN297075	Lake Plan water column	99
	FR696777	WC-Winter-G11	1	FN296779	Lake Redon water column	83,3
	FR696779	WC-Winter-G2	1	GQ240210	groundwater	99,2
	FR696780	WC-Winter-G3	1	FN296425	Lake Llong Neuston samples	98,4
	FR696781	WC-Winter-G4	1	EU640786	Lake Michigan	99,3
	FR696789	WC-Winter-H11	1	FN297408	Lake L'Illa water column	99,6
	FR696720	WC-Winter-B11	2	FJ612146	lake water	98,9
Proteo-bacteria (Class *Delta-proteo-bacteria*)	FR696633	SL-Winter-B2	1	EU640494	Lake Michigan	95,6
	FR696655	SL-Winter-D2	2	EU640494	Lake Michigan	96,0
	FR696670	SL-Winter-E6	1	EU640494	Lake Michigan	95,6
	FR696705	SL-Winter-H7	2	EU640494	Lake Michigan	97,7
	FR696864	P-Spring-G5	1	DQ337084	subsurface water	89,8
	FR696666	SL-Winter-E2	2	EU978702	glacier ice	99,4
	FR696735	WC-Winter-C3	1	AJ966227	Lake Geneva	92,6
	FR696977	WC-Spring-B1	1	EU803555	Lake Gatun	87,0
	FR696752	WC-Winter-D8	1	FJ745099	surface marine water	90,5
	FR697015	WC-Spring-F10	1	EU640494	Lake Michigan	98,0

Table A.C6.1. *Continued*

OTUs				Closest BLAST		
Category	Accession nº	Clone id.	Nº of clones at 97%	Sequence	Isolation source	Identity (%)
Proteo-bacteria (Class *Gamma-proteo-bacteria*)	FR696821	P-Spring-C6	1	EF520622	acid-impacted lake	84,4
	FR696704	SL-Winter-H6	2	AY580815	Marine water	90,8
Spiro-chaetes	FR696664	SL-Winter-E11	1	AB540019	lake	94,0
Verruco-microbia	FR696910	SL-Spring-C8	1	FJ872373	rhizosphere	99,0
	FR696636	SL-Winter-B5	3	FN296971	Lake Roi water column	99,3
	FR696639	SL-Winter-C1	1	FN296971	Lake Roi water column	96,7
	FR696671	SL-Winter-E7	1	FJ546829	mixolimnion	99,0
	FR696685	SL-Winter-F9	2	EF072607	GASP Watkinsville sampling site, Georgia, USA	89,2
	FR696696	SL-Winter-H1	1	AJ289992	Lake Fuchskuhle	98,0
	FR696700	SL-Winter-H2	2	FN296839	Lake Llong de Liat water column	99,2
	FR696703	SL-Winter-H5	2	FN297150	Lake Plan water column	99,1
	FR696713	WC-Winter-A4	1	FN296839	Lake Llong de Liat water column	99,7
	FR696721	WC-Winter-B12	1	EF072607	GASP Watkinsville sampling site, Georgia, USA	87,3
	FR696722	WC-Winter-B2	1	GQ340097	water column	97,7
	FR696724	WC-Winter-B4	1	EU801097	Delaware Bay, NJ	99,0
	FR696739	WC-Winter-C7	1	EU641499	Lake Michigan	97,8
	FR696776	WC-Winter-G10	3	FJ546829	mixolimnion	99,6
	FR696786	WC-Winter-G9	1	EF072607	GASP Watkinsville sampling site, Georgia, USA	88,2
	FR696791	WC-Winter-H2	2	GQ340097	water column	98,1
	FR696795	WC-Winter-H6	30	FN296971	Lake Roi water column	99,5

Table A.C7.1: Detailed list of the marker genes used in the present work for the carbon, nitrogen, sulfur and phosphorus cycles.

Cycle	Step	KEGG	Gene
CARBON	Aerobic C fixation (Calvin cycle) (K00855+K01602)/2	K00855	phosphoribulokinase
		K01602	RuBisCO small chain
	Aerobic CH4 oxidation	K08684	methane monooxygenase
	Aerobic respiration (K02256+K02262)/2 +(K02274+K02276)/2	K02256	cytochrome c oxidase subunit I (coxI)
		K02262	cytochrome c oxidase subunit III (coxIII)
		K02274	cytochrome c oxidase subunit I (coxA)
		K02276	cytochrome c oxidase subunit III (coxC)
	Anaerobic C fixation (Arnon:K00174,K00175, K00244,K01648. Reductive Acetil-CoA: K00194,K00197) (K00174+K00175+K00244 +K01648)/4+(K00194 +K00197)/2	K00174	2-oxoglutarate:ferredoxin oxidoreductase subunit alpha
		K00175	2-oxoglutarate:ferredoxin oxidoreductase subunit beta
		K00244	frdA; fumarate reductase flavoprotein subunit
		K01648	adenosinetriphosphate (ATP) citrate lyase
		K00194	CO dehydrogenase subunit delta
		K00197	CO dehydrogenase subunit gamma
	CO oxidation (K03518+K03519+K03520)/3	K03518	CO dehydrogenase small subunit (coxS)
		K03519	cutM, coxM; carbon-monoxide dehydrogenase medium subunit
		K03520	cutL, coxL; carbon-monoxide dehydrogenase large subunit
	Fermentation	K00016	L-lactate dehydrogenase
	Methanogenesis (K00400+K00401)/2	K00400	coenzyme M methyl reductase beta subunit (mcrB)
		K00401	methyl coenzyme M reductase system, component A2
NITROGEN	Ammonification K05904+K03385	K03385	formate-dependent nitrite reductase periplasmic cytochrome c552 (nrfA)
		K05904	cytochrome c nitrite reductase (nrfA)
	Anammox (SRAO)	K10535	hydroxylamine oxidoreductase/hydrazine oxidoreducatse (hao/hzo)
	Denitrification (K02305+K04561+K00376)/3	K00376	nitrous oxide reductase (nosZ)
		K02305	nitric-oxide reductase (norC)
		K04561	nitric-oxide reductase (norB)
	Nitrate reduction + Nitrite oxidation (K00370+K00371)/2	K00370	nitrate reductase alpha & nitrite oxidoreductase (narG/nxrA)
		K00371	nitrate reductase beta & nitrite oxidoreductase (narH/nxrB)
	Nitrate reduction (K02567+K02568)/2	K02567	periplasmic nitrate reductase (napA)
		K02568	cytochrome c-type protein (napB)
	Nitrification (K10944+K10945+K10946)/3	K10944	ammonia monooxygenase sub.A (amoA)
		K10945	ammonia monooxygenase sub.B (amoB)
		K10946	ammonia monooxygenase sub.C (amoC)

Table A.C7.1: *Continued*

Cycle	Step	KEGG	Gene
NITROGEN	Nitrogen assimilation (K00360+K00367+K01915+ K00265+K00284)/3	K00265	glutamate synthase (NADPH/NADH) large chain (gltB)
		K00284	glutamate synthase (ferredoxin-dependent) (gltS)
		K00360	assimilatory nitrate reductase
		K00367	assimilatory nitrate reductase
		K01915	glutamine synthetase (glnA)
	Nitrogen Fixation (K00531+K02586+K02588+ K02591)/4	K00531	nitrogenase
		K02586	nitrogenase molybdenum-iron protein alpha chain (nifD)
		K02588	nitrogenase iron protein (nifH)
		K02591	nitrogenase molybdenum-iron protein beta chain (nifK)
	Nitrogen Mineralization K00260+K00261+K00262	K00260	glutamate dehydrogenase
		K00261	glutamate dehydrogenase
		K00262	glutamate dehydrogenase
SULFUR	Assimilatory sulfate reduction (K00860+K00956+K00957)/3	K00860	adenylylsulfate kinase (cysC)
		K00956	sulfate adenylyltransferase subunit 1 (cysN)
		K00957	sulfate adenylyltransferase subunit 2 (cysD)
	Dissimilatory sulfate reduction and sulfide oxidation (K00394+K00395+K11180)/3	K00394	adenylylsulfate reductase subunit A (aprA)
		K00395	adenylylsulfate reductase subunit B (aprB)
		K11180	sulfite reductase (dsrA)
	Sulfur Mineralization K00456+K01011	K00456	cysteine dioxygenase
		K01011	3-mercaptopyruvate sulfurtransferase
	Polysulfide reduction	K08352	polysulfide reductase chain A (psrA)
PHOSPHORUS	Phosphate transport (K02038+K02036+K02037+ K02040)/4	K02038	phosphate transport system permease protein (pstA)
		K02036	phosphate transport system ATP-binding protein (pstB)
		K02037	pstC; phosphate transport system permease protein (pstC)
		K02040	phosphate transport system substrate-binding protein (pstS)
	Phosphonoacetate hydrolase	K06193	phosphonoacetate hydrolase (phnA)
	2-phosphonopropionate transporter	K04750	PhnB protein (phnB)
	Phosphonate transport (K02041+K02044+K02042)/3	K02041	phosphonate transport system ATP-binding protein (phnC)
		K02044	phosphonate transport system substrate-binding protein (phnD)
		K02042	phosphonate transport system permease protein (phnE)

Table A.C7.1: *Continued*

Cycle	Step	KEGG	Gene
PHOSPHORUS	Phosphonate metabolism (K02043+K06166+K06165+ K06164+K06163+K05781+ K05780+K06162+K05774)/9	K02043	GntR family transcriptional regulator, phosphonate transport system regulatory protein (phnF)
		K06166	a-D-ribose 1-methylphosphonate 5-triphosphate synthase sub. PhnG (phnG)
		K06165	a-D-ribose 1-methylphosphonate 5-triphosphate synthase sub. PhnH (phnH)
		K06164	a-D-ribose 1-methylphosphonate 5-triphosphate synthase sub. PhnI (phnI)
		K06163	a-D-ribose 1-methylphosphonate 5-phosphate C-P lyase (phnJ)
		K05781	phosphonate transport system ATP-binding protein (phnK)
		K05780	a-D-ribose 1-methylphosphonate 5-triphosphate synthase sub. PhnL (phnL)
		K06162	a-D-ribose 1-methylphosphonate 5-triphosphate diphosphatase (phnM)
		K05774	ribose 1,5-bisphosphokinase (phnN)
	2-aminoethylphosphonic acid pathway (K03430+K05306)/2	K03430	2-aminoethylphosphonate-pyruvate transaminase (phnW)
		K05306	phosphonoacetaldehyde hydrolase (phnX)
	Phosphate regulation (K07636+K02039+K07657+ K07658)/4	K07636	two-component system, OmpR family, phosphate regulon sensor histidine kinase PhoR (phoR)
		K02039	phosphate transport system protein (phoU)
		K07657	two-component system, OmpR family, phosphate regulon response regulator PhoB (phoB)
		K07658	two-component system, OmpR family, alkaline phosphatase synthesis response regulator PhoP (phoB1; phoP)
	Alkaline phosphatase (K01077+K01113)/2	K01077	alkaline phosphatase (phoA)
		K01113	alkaline phosphatase D (phoD)
	G3P transporter (K05814+K05813+K05816+ K05815)/4	K05814	sn-glycerol 3-phosphate transport system permease (ugpA)
		K05813	sn-glycerol 3-phosphate transport system substrate-binding (ugpB)
		K05816	sn-glycerol 3-phosphate transport system ATP-binding (ugpC)
		K05815	sn-glycerol 3-phosphate transport system permease (ugpE)
	Glycerophosphodiester phosphodiesterase	K01126	glycerophosphoryl diester phosphodiesterase (ugpQ; glpQ)
	Polyphosphate kinase	K00937	polyphosphate kinase (ppk)
	Exopolyphosphatase	K01524	exopolyphosphatase / guanosine-5'-triphosphate,3'-diphosphate pyrophosphatase (ppx-gppA)

Table A.C7.2: Specific taxonomic composition (Order level) for 16S and 18S rRNA gene (% relative abundance) in the metagenomic pool. EL: Epilimnion. HL: Hypolimnion.

rRNA gene	Phylum	Order	Slush	EL	ML
18S	Alveolata	BOLA914	0.0	0.5	0.7
	Alveolata	Ciliophora	2.5	16.1	7.9
	Alveolata	Dinoflagellata	0.2	6.0	0.5
	Alveolata	Protalveolata	0.0	0.3	10.6
	Alveolata	Unresolved Alveolata	0.0	1.3	2.3
	Chloroplastida	Charophyta	0.0	0.5	0.0
	Chloroplastida	Chlorophyta	0.0	3.8	2.3
	Chloroplastida	Unresolved Chloroplastida	0.0	1.7	0.2
	Cryptomonadales	Cryptomonas	0.2	1.0	30.5
	Discoba	Discicristata	0.0	0.0	0.2
	Fungi	Chytridiomycota	5.5	0.5	0.0
	Fungi	Basidiomycota	1.0	5.5	1.8
	Fungi	Ascomycota	0.0	4.3	2.8
	Fungi	Unresolved Fungi	0.0	0.2	0.2
	Holozoa	Choanomonada	0.0	0.0	2.1
	Holozoa	Metazoa	0.2	0.8	0.9
	Holozoa	Unresolved Holozoa	0.0	0.0	0.7
	Kathablepharidae	Kathablepharidae	0.0	0.8	0.0
	Nucletmycea	LKM11	0.0	0.0	6.7
	Nucletmycea	LKM15	0.0	0.0	0.7
	Nucletmycea	Unresolved Nucletmycea	0.0	0.0	1.6
	P1-31	P1-31	0.0	0.0	2.5
	Rhizaria	Cercozoa	0.5	5.9	3.5
	Stramenopiles	Bicosoecida	0.0	8.0	1.8
	Stramenopiles	Labyrinthulomycetes	0.0	0.0	0.2
	Stramenopiles	MAST-12	0.0	0.7	0.0
	Stramenopiles	MAST-2	0.0	0.0	0.2
	Stramenopiles	Bolidomonas	0.0	0.3	0.0
	Stramenopiles	Chrysophyceae	85.3	33.1	8.8
	Stramenopiles	Diatomea	0.0	0.0	0.2
	Stramenopiles	Dictyochophyceae	0.0	0.3	0.2
	Stramenopiles	Unresolved Stramenopiles	1.2	3.3	2.3
	Stramenopiles	Peronosporomycetes	0.0	0.3	0.2
	Telonema	Telonema	0.0	0.0	2.1
	Unclassified	Unclassified	3.2	4.2	4.6
	Unresolved Centrohelida	Unresolved Centrohelida	0.0	0.0	0.2
	Unresolved Opisthokonta	Unresolved Opisthokonta	0.0	0.0	0.2
	Unresolved SAR	Unresolved SAR	0.0	0.3	0.0
rRNA gene	Phylum	Order	Slush	EL	ML
16S	Acidobacteria	Acidobacteriales	0.0	0.0	0.0
	Acidobacteria	Holophagales	0.0	0.0	0.1
	Acidobacteria	Subgroup 3	0.0	0.0	0.8
	Acidobacteria	Unresolved Acidobacteria	0.0	0.0	0.0
	Actinobacteria	Acidimicrobiales	4.1	0.0	4.1
	Actinobacteria	Coriobacteriales	0.0	0.0	0.0
	Actinobacteria	Corynebacteriales	1.4	0.3	1.4

Table A.C7.2: *Continued*

rRNA gene	Phylum	Order	Slush	EL	ML
16S	Actinobacteria	Frankiales	0.0	19.1	24.5
	Actinobacteria	Gaiellales	0.0	0.0	0.5
	Actinobacteria	Micrococcales	0.0	1.1	0.4
	Actinobacteria	PeM15	0.0	0.0	0.1
	Actinobacteria	Propionibacteriales	1.4	0.3	0.2
	Actinobacteria	Solirubrobacterales	0.0	0.0	0.9
	Actinobacteria	Streptomycetales	0.0	0.0	0.0
	Actinobacteria	Unresolved Actinobacteria	0.0	2.4	3.1
	Actinobacteria	Unresolved Thermoleophilia	0.0	0.0	0.0
	Alphaproteobacteria	Caulobacterales	1.4	0.4	1.4
	Alphaproteobacteria	Parvularculales	0.0	0.0	0.0
	Alphaproteobacteria	Rhizobiales	0.0	1.5	0.8
	Alphaproteobacteria	Rhodobacterales	0.0	0.0	0.1
	Alphaproteobacteria	Rhodospirillales	2.7	0.1	0.8
	Alphaproteobacteria	Rickettsiales	0.0	0.1	0.4
	Alphaproteobacteria	SAR11 clade	0.0	0.1	0.1
	Alphaproteobacteria	Sphingomonadales	2.7	0.6	0.4
	Alphaproteobacteria	Unresolved Alphaproteobacteria	1.4	0.3	0.4
	Betaproteobacteria	Burkholderiales	34.2	48.7	7.9
	Betaproteobacteria	Hydrogenophilales	0.0	0.0	0.0
	Betaproteobacteria	Methylophilales	0.0	0.6	2.3
	Betaproteobacteria	Neisseriales	0.0	0.2	0.0
	Betaproteobacteria	Nitrosomonadales	0.0	0.0	0.7
	Betaproteobacteria	Rhodocyclales	0.0	0.0	0.1
	Betaproteobacteria	TRA3-20	1.4	0.0	0.2
	Betaproteobacteria	Unresolved Betaproteobacteria	2.7	1.7	1.4
	Deltaproteobacteria	Bdellovibrionales	0.0	0.0	0.1
	Deltaproteobacteria	Desulfobacterales	0.0	0.0	0.0
	Deltaproteobacteria	Desulfuromonadales	0.0	0.0	0.1
	Deltaproteobacteria	Myxococcales	0.0	0.1	2.2
	Deltaproteobacteria	Sh765B-TzT-29	0.0	0.0	0.0
	Deltaproteobacteria	Sva0485	0.0	0.0	0.0
	Deltaproteobacteria	Unresolved Deltaproteobacteria	0.0	0.0	0.2
	Epsilonproteobacteria	Campylobacterales	0.0	0.1	0.0
	Gammaproteobacteria	Aeromonadales	2.7	0.0	0.0
	Gammaproteobacteria	Alteromonadales	0.0	0.0	0.1
	Gammaproteobacteria	Chromatiales	0.0	0.0	0.0
	Gammaproteobacteria	Enterobacteriales	1.4	0.0	0.0
	Gammaproteobacteria	Legionellales	0.0	0.1	0.5
	Gammaproteobacteria	Methylococcales	0.0	0.0	2.4
	Gammaproteobacteria	NKB5	0.0	0.0	0.0
	Gammaproteobacteria	Oceanospirillales	0.0	0.0	0.0
	Gammaproteobacteria	Pseudomonadales	17.8	0.4	0.4
	Gammaproteobacteria	Thiotrichales	0.0	0.0	0.0
	Gammaproteobacteria	Xanthomonadales	0.0	0.1	0.1
	Gammaproteobacteria	Unresolved Gammaproteobacteria	0.0	0.1	0.6

Table A.C7.2: *Continued*

rRNA gene	Phylum	Order	Slush	EL	ML
16S	Proteobacteria	Unresolved Proteobacteria	0.0	0.4	0.9
	Armatimonadetes	Chthonomonadales	0.0	0.0	0.0
	Armatimonadetes	Unresolved Armatimonadetes	0.0	0.0	0.1
	Bacteroidetes	Bacteroidales	0.0	0.0	0.1
	Bacteroidetes	BSV13	0.0	0.0	0.0
	Bacteroidetes	Cytophagales	1.4	1.8	1.2
	Bacteroidetes	Flavobacteriales	1.4	9.3	5.5
	Bacteroidetes	Sphingobacteriales	2.7	5.0	6.2
	Bacteroidetes	Unresolved Bacteroidetes	0.0	0.3	0.6
	Bacteroidetes	vadinHA17	0.0	0.0	0.0
	Bacteroidetes	WCHB1-32	0.0	0.0	0.0
	BD1-5	BD1-5	0.0	0.0	0.0
	Candidate division JS1	Candidate division JS3	0.0	0.0	0.0
	Candidate division OD1	Candidate division OD1	0.0	0.1	3.8
	Candidate division OP11	Candidate division OP11	0.0	0.0	0.1
	Candidate division OP3	Candidate division OP3	0.0	0.0	0.2
	Candidate division TM7	Candidate division TM7	0.0	0.0	0.6
	Chlamydiae	Chlamydiales	2.7	0.0	0.3
	Chloroflexi	Chloroflexales	0.0	0.1	0.2
	Chloroflexi	S085	0.0	0.0	0.0
	Chloroflexi	SL56 marine group	0.0	0.0	0.2
	Chloroflexi	TK10	0.0	0.0	0.1
	Chloroflexi	Unresolved Chloroflexi	0.0	0.0	0.1
	Cyanobacteria	Gastranaerophilales	0.0	0.0	0.0
	Cyanobacteria	SubsectionI	1.4	0.1	0.0
	Cyanobacteria	SubsectionIV	0.0	0.0	0.0
	Cyanobacteria	Unresolved Cyanobacteria	0.0	0.5	0.1
	Elusimicrobia	Lineage IV	0.0	0.0	0.0
	Fibrobacteres	Fibrobacterales	0.0	0.0	0.0
	Firmicutes	Bacillales	0.0	0.3	0.1
	Firmicutes	Clostridiales	5.5	0.1	0.1
	Firmicutes	Lactobacillales	0.0	0.0	0.0
	Firmicutes	Unresolved Firmicutes	0.0	0.0	0.0
	Fusobacteria	Fusobacteriales	0.0	0.0	0.1
	Gemmatimonadetes	Gemmatimonadales	0.0	0.0	1.6
	Lentisphaerae	MSBL3	0.0	0.0	0.0
	Lentisphaerae	Oligosphaerales	0.0	0.0	0.0
	Lentisphaerae	Victivallales	0.0	0.0	0.0
	Nitrospirae	Nitrospirales	0.0	0.0	0.0
	NPL-UPA2	NPL-UPA2	0.0	0.0	0.1
	Planctomycetes	Phycisphaerales	0.0	0.0	2.1
	Planctomycetes	Planctomycetales	1.4	0.3	4.4
	Planctomycetes	Unresolved Planctomycetes	0.0	0.0	0.1
	Planctomycetes	vadinHA49	0.0	0.0	0.1
	SM2F11	SM2F11	0.0	0.0	0.0
	Spirochaetae	Spirochaetales	0.0	0.2	0.1

Table A.C7.2: *Continued*

rRNA gene	Phylum	Order	Slush	EL	ML
16S	Tenericutes	Anaeroplasmatales	0.0	0.0	0.0
	TM6	TM6	0.0	0.0	0.1
	Verrucomicrobia	Chthoniobacterales	2.7	0.0	1.6
	Verrucomicrobia	OPB35 soil group	0.0	0.0	2.4
	Verrucomicrobia	Opitutales	0.0	0.1	1.2
	Verrucomicrobia	Unknown Order	0.0	0.0	0.1
	Verrucomicrobia	Unresolved Opitutae	0.0	0.1	0.2
	Verrucomicrobia	Unresolved Verrucomicrobia	0.0	0.0	0.2
	Verrucomicrobia	vadinHA64	0.0	0.6	1.8
	Verrucomicrobia	Verrucomicrobiales	0.0	0.0	0.0
	WCHB1-60	WCHB1-60	0.0	0.0	0.0
	Euryarchaeota	Halobacteriales	0.0	0.0	0.1
	Euryarchaeota	Unresolved Euryarchaeota	0.0	0.0	0.0
	Unclassified	Unclassified	5.5	2.0	2.8

Table A.C7.3: Relative abundance of marker genes related to carbon, nitrogen and sulfur cycling as a proxy of the potential in situ relevance of the metabolic pathways. EL: Epilimnion. HL: Hypolimnion.

Cycle	Process	Slush %	EL %	HL %
CARBON	Aerobic C fixation	44.1	2.6	5.7
	Aerobic CH4 oxidation	0.9	0.0	0.0
	Aerobic respiration	51.9	65.5	62.4
	Anaerobic C fixation	0.9	2.1	11.8
	CO oxidation	2.2	29.1	18.9
	Fermentation	0.0	0.6	1.2
	Methanogenesis	0.0	0.0	0.02
NITROGEN	Ammonification	0.0	0.0	0.0
	Anammox	0.0	0.0	1.2
	Denitrification	1.8	0.2	1.4
	Nitrate reduction + Nitrite oxidation	8.6	0.9	5.5
	Nitrate reduction	5.1	0.1	0.1
	Nitrification	6.1	0.0	1.5
	Nitrogen assimilation	35.3	58.3	69.0
	Nitrogen fixation	1.2	0.03	1.1
	Nitrogen mineralization	41.9	40.4	20.3
SULFUR	Assimilatory sulfate reduction	53.8	79.1	65.6
	Sulfate reduction + Sulfur oxidation	0.0	0.0	0.5
	Sulfur mineralization	46.2	20.9	33.7
	Polysulfide reduction	0.0	0.0	0.1
PHOSPHATE	2-aminoethylphosphonic acid pathway	0.0	0.2	1.7
	2-phosphonopropionate transporter	4.5	0.7	0.8
	Alkaline phophatase	2.8	2.5	2.6
	Exopolyphosphatase	18.2	6.0	8.6
	G3P transporter	3.1	7.5	5.7
	Glycerophosphodiester phosphodiesterase	16.3	4.9	7.1
	Phosphate regulation	9.7	11.9	10.0
	Phosphate transport	11.8	23.9	22.5
	Phosphonate metabolism	3.0	8.1	2.9
	Phosphonate transport	13.8	20.5	11.9
	Phosphonoacetate hydrolase	7.0	1.9	5.3
	Polyphosphate kinase	9.9	12.0	20.9

Appendix B

environmental microbiology reports

Environmental Microbiology Reports (2012) **4**(1), 50–56 doi:10.1111/j.1758-2229.2011.00278.x

Winter to spring changes in the slush bacterial community composition of a high-mountain lake (Lake Redon, Pyrenees)

Tomàs Llorens-Marès, Jean-Christophe Auguet* and Emilio O. Casamayor

Limnological Observatory of the Pyrenees (LOOP) – Biogeodynamics & Biodiversity Group, Centro de Estudios Avanzados de Blanes, CEAB-CSIC, Accés Cala Sant Francesc, 14, 17300 Blanes, Girona, Spain.

Summary

Bacterial community composition was analysed in the slush layers of snow-covered Lake Redon (2240 m altitude, Limnological Observatory of the Pyrenees, LOOP, NE Spain) in winter and spring and compared with bacteria from the lake water column, using 16S rRNA gene clone libraries and CARD-FISH counts. The set of biological data was related to changes in bacterial production and to other relevant environmental variables measured in situ. In winter, up to 70% of the 16S rRNA sequences found in the slush were closely related to planktonic bacteria from the water column beneath the ice. Conversely, during spring ablation, 50% of the sequences had > 97% identity with bacteria from the cryosphere (i.e. globally distributed glaciers, snow and ice) and may have originated from remote aerosol deposition. The transition winter to spring was characterized by consistent community changes switching from assemblages dominated by *Betaproteobacteria*, *Verrucomicrobia* and *Bacteroidetes* during snowpack growth to communities essentially dominated by the *Bacteroidetes* of classes *Cytophagia* and *Sphingobacteria*. This strong bacterial composition switch was associated with consistent increases in bacterial abundance and production, and decreasing bacterial diversity.

Introduction

Ice cover and snowpacks in high-altitude lakes play a pivotal role in the dynamic of the pelagic system by preventing turbulence and reducing the exchange of light, heat, gases, liquid and particles between the atmosphere and the water column (Catalan, 1992; Wharton *et al*., 1993). The ice cover generally lasts 6 months or longer and is characterized by sandwich-like structures constituted by a superposition of snow, white ice and slush (i.e. a mixture of water and snow) layers on top of a sheet of black ice (Eppacher, 1966; Adams and Allan, 1987). Episodic events of flooding by lake water, melting and freezing drive dynamic changes in the physical structure and chemical characteristics of alpine ice covers (Catalan, 1989; Psenner *et al*., 1999). Microbial activities and biomasses in the slush layers are far larger than in the water column, with a great variety and density of morphologies including short rods and cocci-like bacteria, filaments, flagellate protists (autotrophic and heterotrophic), and ciliates (Felip *et al*., 1995; Felip *et al*., 1999).

While microbial communities from the remote cryospheres, such as sea ice (Bowman *et al*., 1997; Brinkmeyer *et al*., 2003), polar lakes (Priscu *et al*., 1999; Crump *et al*., 2003; Mosier *et al*., 2007) and glacier habitats (Zhang *et al*., 2008; 2009; Xiang *et al*., 2009), have been extensively documented, those thriving in nearer non-permanent ice covered alpine lakes have remained poorly studied. Most of such studies have been mainly focused on eukaryotic microorganisms by traditional microscopy methods, as in the case of Lake Redon (Felip *et al*., 1995; 1999; 2002), or in Lake Gossenköllessee, Tyrolean Alps, using general bacterial probes and FISH counts (Alfreider *et al*., 1996). In this work, we described the 16S rRNA gene composition of bacteria inhabiting the slush layers of an alpine lake both in winter during growing of the snowpack, and in spring during the melting phase. Overall, bacterial composition and functioning in Lake Redon were closely related to other ice-related ecosystems on Earth, suggesting that alpine areas are good models to improve the current understanding on the dynamics and functional role of cold adapted microorganisms facing climate variations.

Results and discussion

Samples were collected from different slush layers (see Fig. 1) and the lake water column (2 m depth beneath the ice sheet) of Lake Redon (Limnological Observatory of the Pyrenees, LOOP, NE Spain) both in winter during

Received 5 May, 2011; accepted 11 July, 2011. *For correspondence. E-mail jcauguet@ceab.csic.es; Tel. (+34) 972 336 101; Fax (+34) 972 337 806.

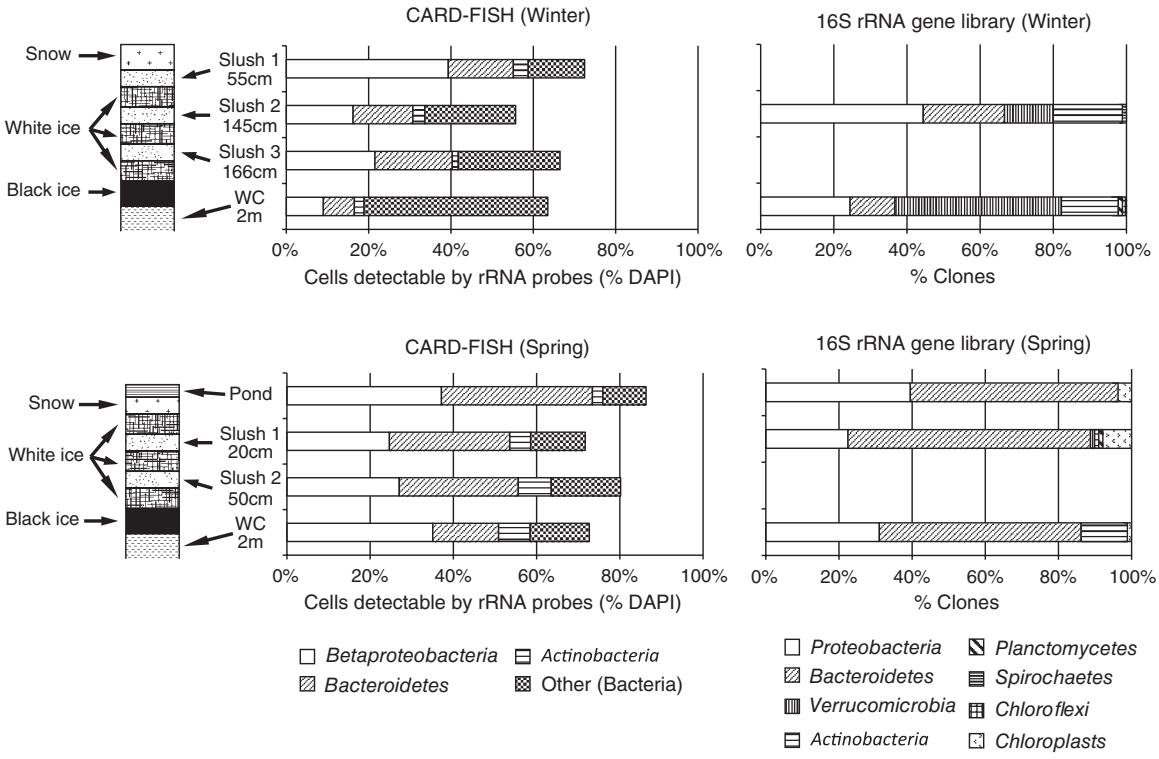

Fig. 1. Bacterial community structure in Lake Redon after CARD-FISH counts and 16S rRNA gene clone libraries. Populations are represented by relative abundances of clones in different phylogenetic groups. The ice-cover during winter (March) was 246 cm thick and composed by three slush layers at 55, 145 and 166 cm from the surface respectively. In spring (May) melting ponds were present on the ice-cover, which was only 70 cm thick and showed two slush layers at 20 and 50 cm from the surface. Water Column (WC) samples were collected 2 m depth from the black ice.

growth of the snowpack (20 March 2009; 246 cm cover thickness), and in spring during the ablation phase (27 May 2009; 70 cm cover thickness). One sample from a pool formed at the top of the snowpack in spring was also added to the study. The limnology of the lake and the different planktonic populations have been extensively studied for the last 25 years with traditional (Catalan *et al.*, 2006), and recently with DNA-based (Hervas and Casamayor, 2009) approaches. Water from the slush layer was pumped from small holes drilled in the cover (see more details in Felip *et al.*, 1995). Bacterial community composition was analysed by 16S rRNA gene clone libraries (Hervas and Casamayor, 2009) and CARD-FISH counts (Medina-Sanchez *et al.*, 2005). DNA extraction and cloning conditions were as previously reported (Dumestre *et al.*, 2002; Ferrera *et al.*, 2004). Overall, 437 sequences were analysed (see accession numbers FR696618 to FR697054 in GenBank and Table 1 for more details), and environmental information for each sample made publicly available (accession numbers ERS016138 to ERS016142 in GenBank). Bacterial activity was estimated by [3H]leucine incorporation according to the method described by Kirchman (1993) with slight modifications (Felip *et al.*, 1995).

The highest concentrations of NO_3 and NH_4 were found in the top slush layer in winter, and in the water column in spring (Table 1). NO_2 concentrations were similar in the water columns (WC), but increased significantly in the slush layers in spring. Interestingly, the highest concentration was found in the pond sample (1.04 μeq l^{-1}). Total dissolved phosphorus (TDP) and dissolved organic carbon (DOC) showed the highest concentrations closer to the surface (Table 1) both in winter (top slush layers) and spring (pond). We did not observe temporal changes in DOC concentrations but TDP doubled in the spring, probably due to frequent Saharan dust depositions on this area (Hervas *et al.*, 2009; Reche *et al.*, 2009). All concentrations were within previously reported ranges in this area (Felip *et al.*, 1995; 1999).

Total DAPI counts and bacterial production values in slush layers were similar to those found by Alfreider and colleagues (1996) and tended to be higher than in the water column (WC), except for DAPI counts during winter (Table 1). Slush layers offer better conditions for bacterial

Table 1. Concentration of nitrogen compounds, total dissolved phosphorous (TDP), dissolved organic carbon (DOC), bacterial abundance (DAPI counts) and production (BP) in the set of samples analysed, and diversity indicators obtained from clone libraries in slush (SL), water column (WC) and an ice-melting pond in Lake Redon.

	Layer	NO_3 (µeq l^{-1})	NH_4 (µeq l^{-1})	NO_2 (µeq l^{-1})	TDP (nmol l^{-1})	DOC (mg l^{-1})	DAPI ($\times 10^4$cells ml^{-1})	BP (pmol Leu $l^{-1}h^{-1}$)	Clone numbers	OTU (97%)	Coverage (%)	S_{Chao1}
Winter	SL 1	17	14.2	0.08	90	1.2	14.9	nd	nd	nd	nd	nd
	SL 2	**7**	**2.4**	**0.05**	**94**	**0.6**	**9.9**	**4.2 ± 0.2**	**90**	**50**	**68**	**81 ± 18**
	SL 3	7	3.4	0.05	68	0.6	16.5	nd	nd	nd	nd	nd
	WC	**6**	**2.8**	**0.07**	**44**	**0.5**	**42.5**	**1.2 ± 0.2**	**90**	**45**	**61**	**164 ± 93**
Spring	**POND**	**3**	**3.8**	**1.04**	**284**	**1.3**	**178.5**	**223.1 ± 5.2**	**81**	**42**	**63**	**114 ± 53**
	SL 1	**4**	**3.5**	**0.38**	**180**	**0.8**	**86.5**	**276.3 ± 11.0**	**89**	**18**	**88**	**73 ± nd**
	SL 2	4	3.2	0.28	123	0.6	76.1	nd	nd	nd	nd	nd
	WC	**15**	**9.6**	**0.07**	**60**	**0.7**	**68.8**	**78.0 ± 9.1**	**87**	**38**	**72**	**77 ± 29**

OTUs and diversity indices were calculated at 3% cut-off. Samples labelled in bold were selected for 16S rRNA gene clone libraries.
nd, not determined.

growth than the WC because the ice grains matrix with nutrient-rich interstitial water provides a better environment for bacterial activity, interaction between cells and substrate, and for the development of filamentous forms as previously discussed (Felip *et al*., 1995; 1999). We observed that *Bacteroidetes* were particularly favoured being twice more abundant in the slush layers than in the plankton as shown by CARD-FISH counts (Fig. 1). *Betaproteobacteria* cells were also found to be more abundant in the slush layers in winter. These results are in agreement with a previous CARD-FISH work carried out in Lake Gossenköllessee (Alfreider *et al*., 1996). As in this previous work, we also observed a shift towards bacteria that did not hybridize with any of the group-specific probes tested in the transition from the upper slush layer to the WC. Particularly in March, up to 70% of EUB338 positive cells did not hybridize with any of the group-specific probes tested, and the sum of the cells hybridized with probes BET42a (for *Betaproteobacteria*), HGC69a (for *Actinobacteria*) and CF319a (for *Bacteroidetes*) was particularly low. We could relate this fact to the abundance of *Verrucomicrobia* sequences in the WC (up to 46%, Fig. 1). Interestingly, bacterial production increased 72.2 ± 48.2-fold (Table 1) from winter to spring, and we observed significant increases in bacterial abundance (4.2 ± 2.6-fold, Table 1), mainly by *Bacteroidetes* (12 times more abundant in spring versus winter), *Betaproteobacteria* (9 times) and *Actinobacteria* (10 times) (Fig. 1). During the ablation phase, light availability increased promoting massive algae growth (Felip *et al*., 1999), further fuelling most of the bacterial activity detected. Glaciers, which hold 75% of the freshwater on the planet, are largely autotrophic systems (Anesio *et al*., 2009), and polar sea ice has also shown a net autotrophic activity integrated over an entire season although polar seas melting will probably exacerbate bacterial respiration (Kaartokallio, 2004). Ice-melting is therefore a major promoter of community transitions both in marine and in inland waters. Previous studies in Lake Redon (Pyrenees) and Lake Gossenköllesee (Tyrolean Alps) showed that temporal changes in eukaryotic assemblages were strongly affected by the physical transformation of the lake cover and the snowpack in the catchment (Felip *et al*., 1999; Felip *et al*., 2002). After 16S rRNA gene analyses, we observed drastic changes in the slush bacterial community composition (Fig. 1) and a decrease in bacterial diversity from winter to spring (Table 1). The vulnerability of the cryosphere (i.e. cold ecosystems) to climate change and its potential large influence in the emission of greenhouse gases will certainly promote more research on the ecology of the microbial communities inhabiting these habitats.

All the sequences obtained in this work fell into eight bacterial phyla (Fig. 1 and Fig. S1). Overall,

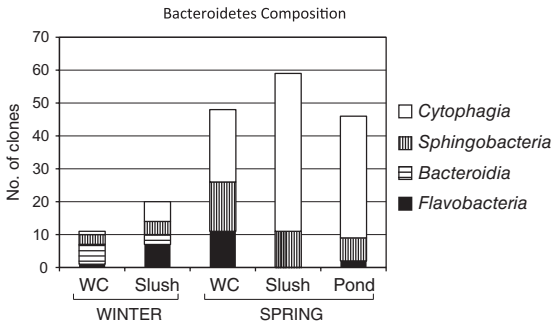

Fig. 2. Relative abundance of the different Classes within the phylum *Bacteroidetes* represented by the number of clones found in each layer.

Bacteroidetes was the most abundant (42% of all 16S rRNA gene sequences) and showed a marked winter to spring increase in abundance (17 ± 7 to 59 ± 6% respectively, Fig. 1); there was a clear phylogenetic segregation between the ice-growth phase in winter (mostly *Flavobacteria* and *Bacteroidia*) and the spring ablation period (mostly *Cytophagia* and *Sphingobacteria*) (Fig. 2 and Fig. S1). *Bacteroidetes* are abundant in inland waters (Barberán and Casamayor, 2010) and closely related to phytoplankton blooms, both using phytoplankton exudates during algal growth (Zeder *et al*., 2009) or complex DOM derived from senescent phytoplankton (Pinhassi *et al*., 2004; Teira *et al*., 2008). Algae were abundant in the spring sample as detected by microscopic observations, and the recovering of chloroplast sequences and probably *Bacteroidetes* were stimulated by the algal blooming. Indeed, *Bacteroidetes* is a very diverse chemoheterotrophic bacterial group with many aerobic members that can degrade biopolymers such as cellulose and chitin, and the high molecular mass fraction of the DOM (Kirchman, 2002), at relatively low temperatures (Mary *et al*., 2006).

Proteobacteria were also very abundant in the clone libraries with 32% of the sequences, and 80% of them being *Betaproteobacteria*. Most of these sequences fell into four previously described freshwater clusters, Beta-I-II-III-IV (Glockner *et al*., 2000; Zwart *et al*., 2002; Hervas and Casamayor, 2009), respectively, and in two new clusters essentially formed by sequences from the cryosphere (Fig. S1). As for *Bacteroidetes*, we also observed winter-to-spring phylogenetic segregation within the *Betaproteobacteria*. The GSK16 subcluster containing sequences mainly from freshwater ultraoligotrophic cold environments, subglacial environments and alpine and nival lakes was mainly detected in spring, whereas the *Rhodoferax* subcluster, a cosmopolitan freshwater group also very abundant in humic and eutrophic lakes (Zwart *et al*., 2002; Simek *et al*., 2005), was mostly detected in winter. As mentioned elsewhere (Hervas and Casamayor, 2009), these differences in temporal distributions suggest different ecologies or physiologies among closely related *Betaproteobacteria*.

Verrucomicrobia 16S rRNA sequences represented 12% of total clones, most of them only seen in winter. *Verrucomicrobia* have been found in cold environments such as Lake Vida, Antarctica (Mosier *et al*., 2007) or Lake Puma Yumco, Tibetan Plateau (Liu *et al*., 2009), but never at the relative abundances we found in the WC (42%) and slush (16%) of Lake Redon. Thus, alpine lakes might represent a suitable environment to further investigate this relatively unknown phylum (Sangwan *et al*., 2004). Finally, *Actinobacteria* (*c.* 10%), *Planctomycetes* (0.5%), *Spirochaetes* (0.5%) and *Chloroflexi* (0.2%) were also detected in the clone libraries.

Slush bacterial assemblages were very similar to the water column both in winter and spring (Fig. 3) and more than 70% of the 16S rRNA gene sequences during the snowpack growth phase had the closest match with sequences from lakes (Fig. 4). These results suggested initial colonization of the slush by bacteria from the same lake water and are in agreement with previous phytoplankton studies where initial slush algae originated from the phytoplankton-rich surface waters that flood the ice cover due to hydrostatic adjustment (Felip *et al*., 1995; 1999). Conversely, during spring ablation, 50% of the 16S rRNA gene slush sequences had the highest identity with sequences from the cryosphere (i.e. globally distributed glaciers, ice, snow and polar regions). A similar switch was previously described in the phytoplankton where non-planktonic species probably introduced by melting water coming from the snowpack were observed (Felip *et al*., 2002). In spring, the first meters of the lake water column were also influenced by melting waters and more than

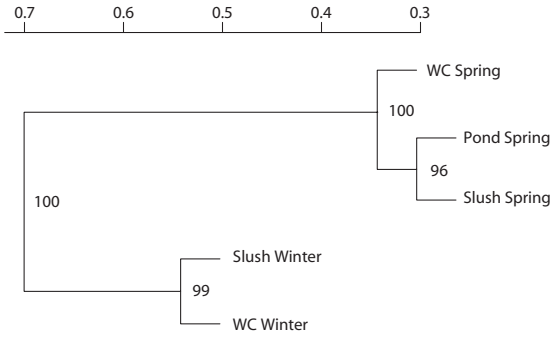

Fig. 3. Hierarchical clustering analysis (UPGMA algorithm with Jackknife supporting values, 100 replicates) carried out on the five libraries constructed in this study. Distances between clusters are expressed in UniFrac units: a distance of 0 means that two environments are identical and a distance of 1 means that two environments contain mutually exclusive lineages.

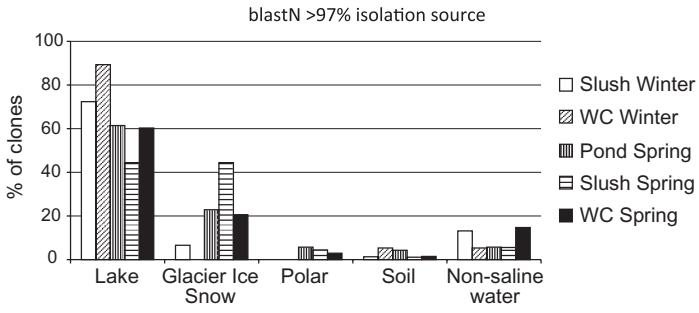

Fig. 4. Isolation sources of the closest BLAST match found in GenBank for each of the samples analysed. Only BLAST matches with more than 97% identity were considered.

20% of planktonic 16S rRNA gene bacterial sequences were closely related to sequences from the cryosphere (Fig. 4).

Overall *c.* 90% of the slush sequences were closely related (> 97% identity) either to cold freshwater lakes (66%), such as Lake Michigan (Mueller-Spitz *et al*., 2009), Crater Lake (Page *et al*., 2004) and Lake Fuchskuhle (Glockner *et al*., 2000) (see Table S1 for details and Fig. 4), or to polar or glacial environments (23%), such as Puruogangri Ice Core (Zhang *et al*., 2008) or an Arctic sea-ice melt pond (Brinkmeyer *et al*., 2003). These data are in agreement with the idea that aquatic bacteria in high-mountain regions are globally distributed (Zwart *et al*., 1998; Glockner *et al*., 2000; Liu *et al*., 2006; Sommaruga and Casamayor, 2009) but only develop in cold and oligotrophic habitats as alpine lakes, glaciers, snow or polar environments. As previously discussed (Hervas and Casamayor, 2009; Hervas *et al*., 2009), airborne dispersal is probably the mechanism that better explains the cosmopolitanism found in alpine areas. Despite their minor quantitative relevance in the whole cryosphere, these alpine areas are very convenient systems for surveying changes in microbial composition, dynamics, activity and fate following environmental perturbations.

Acknowledgements

We are thankful to Centre de Recerca d'Alta Muntanya, Universitat de Barcelona, Vielha for laboratory facilities. L Camarero, M Felip, M Vila-Costa, X Triadó and A Fernandez-Guerra are acknowledged for field and lab assistance and ancillary data. This research was supported by grants PIRENA CGL2009-13318 and GOS-LAKES CGL2009-08523-E to E.O.C., and CONSOLIDER grant GRACCIE CSD2007-00067 from the Spanish Office of Science and Innovation (MICINN). J.C.A. benefits from a Juan de la Cierva postdoctoral fellow (MICINN).

References

Adams, W.P., and Allan, C. (1987) Aspects of the chemistry of ice, notably snow, on lakes. In *Seasonal Snowcovers: Physics, Chemistry, Hydrology*. Jones, H.G., and Orville-Thomas, W.J. (eds). Dordrecht, The Netherlands: Reidel Publishing Company, pp. 393–466.

Alfreider, A., Pernthaler, J., Amann, R., Sattler, B., Glockner, F.O., Wille, A., and Psenner, R. (1996) Community analysis of the bacterial assemblages in the winter cover and pelagic layers of a high mountain lake by in situ hybridization. *Appl Environ Microbiol* **62:** 2138–2144.

Anesio, A.M., Hodson, A.J., Fritz, A., Psenner, R., and Sattler, B. (2009) High microbial activity on glaciers: importance to the global carbon cycle. *Glob Change Biol* **15:** 955–960.

Barberán, A., and Casamayor, E.O. (2010) Global phylogenetic community structure and beta-diversity patterns of surface bacterioplankton metacommunities. *Aquat Microb Ecol* **59:** 1–10.

Bowman, J.P., McCammon, S.A., Brown, M.V., Nichols, D.S., and McMeekin, T.A. (1997) Diversity and association of psychrophilic bacteria in Antarctic sea ice. *Appl Environ Microbiol* **63:** 3068–3078.

Brinkmeyer, R., Knittel, K., Jurgens, J., Weyland, H., Amann, R., and Helmke, E. (2003) Diversity and structure of bacterial communities in arctic versus antarctic pack ice. *Appl Environ Microbiol* **69:** 6610–6619.

Catalan, J. (1989) The winter cover of a high-mountain mediterranean lake (Estany-Redo, Pyrenees). *Water Resour Res* **25:** 519–527.

Catalan, J. (1992) Evolution of dissolved and particulate matter during the ice-covered period in a deep, high-mountain lake. *Can J Fish Aquat Sci* **49:** 945–955.

Catalan, J., Camarero, L., Felip, M., Pla, S., Ventura, M., Buchaca, T., *et al.* (2006) High mountain lakes: extreme habitats and witnesses of environmental changes. *Limnetica* **25:** 551–584.

Crump, B.C., Kling, G.W., Bahr, M., and Hobbie, J.E. (2003) Bacterioplankton community shifts in an arctic lake correlate with seasonal changes in organic matter source. *Appl Environ Microbiol* **69:** 2253–2268.

Dumestre, J.F., Casamayor, E.O., Massana, R., and Pedrós-Alió, C. (2002) Changes in bacterial and archaeal assemblages in an equatorial river induced by the water eutrophication of Petit Saut dam reservoir (French Guiana). *Aquat Microb Ecol* **26:** 209–221.

Eppacher, T. (1966) Umweltfaktoren und Lebewelt im Pelagial des Gossenköllesees (Kühtai, Stubaier Alpen, 2.413 m). PhD Thesis. Innsbruck, Austria: University of Innsbruck.

Felip, M., Sattler, B., Psenner, R., and Catalan, J. (1995) Highly active microbial communities in the ice and snow cover of high mountain lakes. *Appl Environ Microbiol* **61:** 2394–2401.

Felip, M., Camarero, L., and Catalan, J. (1999) Temporal changes of microbial assemblages in the ice and snow cover of a high mountain lake. *Limnol Oceanogr* **44:** 973–987.

Felip, M., Wille, A., Sattler, B., and Psenner, R. (2002) Microbial communities in the winter cover and the water column of an alpine lake: system connectivity and uncoupling. *Aquat Microb Ecol* **29:** 123–134.

Ferrera, I., Massana, R., Casamayor, E.O., Balagué, V., Sánchez, O., Pedrós-Alió, C., and Mas, J. (2004) High-diversity biofilm for the oxidation of sulfide-containing effluents. *Appl Microbiol Biotechnol* **64:** 726–734.

Glockner, F.O., Zaichikov, E., Belkova, N., Denissova, L., Pernthaler, J., Pernthaler, A., and Amann, R. (2000) Comparative 16S rRNA analysis of lake bacterioplankton reveals globally distributed phylogenetic clusters including an abundant group of actinobacteria. *Appl Environ Microbiol* **66:** 5053–5065.

Hervas, A., and Casamayor, E.O. (2009) High similarity between bacterioneuston and airborne bacterial community compositions in a high mountain lake area. *FEMS Microbiol Ecol* **67:** 219–228.

Hervas, A., Camarero, L., Reche, I., and Casamayor, E.O. (2009) Viability and potential for immigration of airborne bacteria from Africa that reach high mountain lakes in Europe. *Environ Microbiol* **11:** 1612–1623.

Kaartokallio, H. (2004) Food web components, and physical and chemical properties of Baltic Sea ice. *Mar Ecol Prog Ser* **273:** 49–63.

Kirchman, D.L. (1993) Leucine incorporation as a measure of biomass production by heterotrophic bacteria. In *Handbook of Methods in Aquatic Microbial Ecology*. Kemp, P.F., Sherr, B.F., Sherr, E.B., and Cole, J.J. (eds). Boca Raton, FL, USA: Lewis Publishers, pp. 509–512.

Kirchman, D.L. (2002) The ecology of Cytophaga-*Flavobacteria* in aquatic environments. *FEMS Microbiol Ecol* **39:** 91–100.

Liu, Y., Yao, T., Jiao, N., Kang, S., Zeng, Y., and Huang, S. (2006) Microbial community structure in moraine lakes and glacial meltwaters, Mount Everest. *FEMS Microbiol Lett* **265:** 98–105.

Liu, Y.Q., Yao, T.D., Zhu, L.P., Jiao, N.Z., Liu, X.B., Zeng, Y.H., and Jiang, H.C. (2009) Bacterial diversity of freshwater alpine lake puma yumco on the Tibetan plateau. *Geomicrobiol J* **26:** 131–145.

Mary, I., Cummings, D.G., Biegala, I.C., Burkill, P.H., Archer, S.D., and Zubkov, M.V. (2006) Seasonal dynamics of bacterioplankton community structure at a coastal station in the western English Channel. *Aquat Microb Ecol* **42:** 119–126.

Medina-Sanchez, J.M., Felip, M., and Casamayor, E.O. (2005) Catalyzed reported deposition-fluorescence in situ hybridization protocol to evaluate phagotrophy in mixotrophic protists. *Appl Environ Microbiol* **71:** 7321–7326.

Mosier, A.C., Murray, A.E., and Fritsen, C.H. (2007) Microbiota within the perennial ice cover of Lake Vida, Antarctica. *FEMS Microbiol Ecol* **59:** 274–288.

Mueller-Spitz, S.R., Goetz, G.W., and McLellan, S.L. (2009) Temporal and spatial variability in nearshore bacterioplankton communities of Lake Michigan. *FEMS Microbiol Ecol* **67:** 511–522.

Page, K.A., Connon, S.A., and Giovannoni, S.J. (2004) Representative freshwater bacterioplankton isolated from Crater Lake, Oregon. *Appl Environ Microbiol* **70:** 6542–6550.

Pinhassi, J., Sala, M.M., Havskum, H., Peters, F., Guadayol, O., Malits, A., and Marrase, C. (2004) Changes in bacterioplankton composition under different phytoplankton regimens. *Appl Environ Microbiol* **70:** 6753–6766.

Priscu, J.C., Adams, E.E., Lyons, W.B., Voytek, M.A., Mogk, D.W., Brown, R.L., *et al*. (1999) Geomicrobiology of subglacial ice above Lake Vostok, Antarctica. *Science* **286:** 2141–2144.

Psenner, R., Sattler, B., Wille, A., Fritsen, C.H., Priscu, J.C., Felip, M., and Catalan, J. (1999) Lake ice microbial communities in alpine and antarctic lakes. In *Cold Adapted Organisms*. Margesin, R., and Schinner, F. (eds). Heidelberg, Germany: Springer-Verlag, pp. 17–31.

Reche, I., Ortega-Retuerta, E., Romera, O., Pulido-Villena, E., Morales-Baquero, R., and Casamayor, E.O. (2009) Effect of Saharan dust inputs on bacterial activity and community composition in Mediterranean lakes and reservoirs. *Limnol Oceanogr* **54:** 869–879.

Sangwan, P., Chen, X.L., Hugenholtz, P., and Janssen, P.H. (2004) *Chthoniobacter flavus* gen. nov., sp nov., the first pure-culture representative of subdivision two, Spartobacteria classis nov., of the phylum *Verrucomicrobia*. *Appl Environ Microbiol* **70:** 5875–5881.

Simek, K., Hornak, K., Jezbera, J., Masin, M., Nedoma, J., Gasol, J.M., and Schauer, M. (2005) Influence of top-down and bottom-up manipulations on the R-BT065 subcluster of beta-proteobacteria, an abundant group in bacterioplankton of a freshwater reservoir. *Appl Environ Microbiol* **71:** 2381–2390.

Sommaruga, R., and Casamayor, E.O. (2009) Bacterial 'cosmopolitanism' and importance of local environmental factors for community composition in remote high-altitude lakes. *Freshw Biol* **54:** 994–1005.

Teira, E., Gasol, J.M., Aranguren-Gassis, M., Fernandez, A., Gonzalez, J., Lekunberri, I., and Alvarez-Salgado, X.A. (2008) Linkages between bacterioplankton community composition, heterotrophic carbon cycling and environmental conditions in a highly dynamic coastal ecosystem. *Environ Microbiol* **10:** 906–917.

Wharton, R.A., Lyons, W.B., and Marais, D.J.D. (1993) Stable isotopic biogeochemistry of carbon and nitrogen in a perennially ice-covered Antartic lake. *Chem Geol* **107:** 159–172.

Xiang, S.R., Shang, T.C., Chen, Y., Jing, Z.F., and Yao, T.D. (2009) Dominant bacteria and biomass in the kuytun 51 glacier. *Appl Environ Microbiol* **75:** 7287–7290.

Zeder, M., Peter, S., Shabarova, T., and Pernthaler, J. (2009) A small population of planktonic *Flavobacteria* with disproportionally high growth during the spring phytoplankton bloom in a prealpine lake. *Environ Microbiol* **11:** 2676–2686.

Zhang, X.F., Yao, T.D., Tian, L.D., Xu, S.J., and An, L.Z. (2008) Phylogenetic and physiological diversity of bacteria isolated from Puruogangri ice core. *Microbial Ecol* **55:** 476–488.

Zhang, X.J., Ma, X.J., Wang, N.L., and Yao, T.D. (2009) New subgroup of *Bacteroidetes* and diverse microorganisms in Tibetan plateau glacial ice provide a biological record of environmental conditions. *FEMS Microbiol Ecol* **67:** 21–29.

Zwart, G., Hiorns, W.D., Methe, B.A., Van Agterveld, M.P., Huismans, R., Nold, S.C., *et al*. (1998) Nearly identical 16S rRNA sequences recovered from lakes in North America and Europe indicate the existence of clades of globally distributed freshwater bacteria. *Syst Appl Microbiol* **21:** 546–556.

Zwart, G., Crump, B.C., Agterveld, M., Hagen, F., and Han, S.K. (2002) Typical freshwater bacteria: an analysis of available 16S rRNA gene sequences from plankton of lakes and rivers. *Aquat Microb Ecol* **28:** 141–155.

Supporting information

Additional Supporting Information may be found in the online version of this article:

Fig. S1. Maximum-parsimony phylogenetic tree of 16S rRNA gene bacterial sequences recovered from slush (SL), underlying water column (WC) and pond (P) of Lake Redon during winter (blue) and spring (red). The tree is based on maximum parsimony analysis of the data set in the ARB program package (http://www.arb-home.de). Sequences of *c.* 900 nt were inserted into the optimized tree by using parsimony criteria without allowing changes in the overall tree topology. Sequences from this study are in bold and are representatives of each OTU at 97% identity (the number of sequences within each OTU is also shown). GenBank accession numbers are provided and the closest cultured relatives are included. The scale bar represents 10% estimated divergence.

Table S1. Closest BLASTs of slush (SL), water column (WC) and pond (P) 16S rRNA gene OTUs. The isolation source of the closest BLAST was retrieved from the GenBank database.

Please note: Wiley-Blackwell are not responsible for the content or functionality of any supporting materials supplied by the authors. Any queries (other than missing material) should be directed to the corresponding author for the article.

The ISME Journal (2015) 9, 1648–1661

www.nature.com/ismej

OPEN

ORIGINAL ARTICLE

Connecting biodiversity and potential functional role in modern euxinic environments by microbial metagenomics

Tomàs Llorens-Marès[1], Shibu Yooseph[2], Johannes Goll[3], Jeff Hoffman[4], Maria Vila-Costa[1], Carles M Borrego[5,6], Chris L Dupont[4] and Emilio O Casamayor[1]

[1]*Integrative Freshwater Ecology Group, Center of Advanced Studies of Blanes–Spanish Council for Research (CEAB-CSIC), Blanes, Girona, Spain;* [2]*Informatics Group, J Craig Venter Institute, San Diego, CA, USA;* [3]*Informatics Group, J Craig Venter Institute, Rockville, MD, USA;* [4]*Microbial and Environmental Genomics Group, J Craig Venter Institute, San Diego, CA, USA;* [5]*Water Quality and Microbial Diversity, Catalan Institute for Water Research (ICRA), Girona, Spain and* [6]*Group of Molecular Microbial Ecology, Institute of Aquatic Ecology, University of Girona, Girona, Spain*

Stratified sulfurous lakes are appropriate environments for studying the links between composition and functionality in microbial communities and are potentially modern analogs of anoxic conditions prevailing in the ancient ocean. We explored these aspects in the Lake Banyoles karstic area (NE Spain) through metagenomics and *in silico* reconstruction of carbon, nitrogen and sulfur metabolic pathways that were tightly coupled through a few bacterial groups. The potential for nitrogen fixation and denitrification was detected in both autotrophs and heterotrophs, with a major role for nitrogen and carbon fixations in *Chlorobiaceae*. *Campylobacterales* accounted for a large percentage of denitrification genes, while *Gallionellales* were putatively involved in denitrification, iron oxidation and carbon fixation and may have a major role in the biogeochemistry of the iron cycle. *Bacteroidales* were also abundant and showed potential for dissimilatory nitrate reduction to ammonium. The very low abundance of genes for nitrification, the minor presence of anammox genes, the high potential for nitrogen fixation and mineralization and the potential for chemotrophic CO_2 fixation and CO oxidation all provide potential clues on the anoxic zones functioning. We observed higher gene abundance of ammonia-oxidizing bacteria than ammonia-oxidizing archaea that may have a geochemical and evolutionary link related to the dominance of Fe in these environments. Overall, these results offer a more detailed perspective on the microbial ecology of anoxic environments and may help to develop new geochemical proxies to infer biology and chemistry interactions in ancient ecosystems.
The ISME Journal (2015) **9,** 1648–1661; doi:10.1038/ismej.2014.254; published online 9 January 2015

Introduction

Linking microbial community composition and ecological processes such as carbon (CO_2 fixation and respiration), nitrogen (nitrification, denitrification and N_2 fixation) and sulfur cycling (sulfur assimilation, anaerobic sulfate respiration and sulfide oxidation) is a primary goal for microbial ecologists. This information is needed to improve our understanding on the structure and functioning of microbial communities, to properly guide experimental research efforts, to promote our ability to understand fundamental mechanisms controlling microbial processes and interactions *in situ* (Prosser, 2012) and to approach the study of earlier interactions of biosphere–hydrosphere–geosphere (Severmann and Anbar, 2009). However, a detailed comprehension of biological interactions in highly complex systems is however difficult (Bascompte and Sole, 1995).

Stratified lakes with euxinic (anoxic and sulfurous) bottom waters are simplified study systems to explore current biodiversity–biogeochemistry interactions because of their high activity, large biomass and low microbial diversity (Guerrero *et al.,* 1985). Usually, oxic–anoxic interfaces contain conspicuous blooms of photosynthetic bacteria that are often macroscopically visible because of the high

Correspondence: EO Casamayor, Integrative Freshwater Ecology Group, Center of Advanced Studies of Blanes–Spanish Council for Research (CEAB-CSIC), Accés Cala Sant Francesc, 14, Blanes, Girona 17300, Spain.
E-mail: casamayor@ceab.csic.es
or CL Dupont, Microbial and Environmental Genomics Group, J Craig Venter Institute, San Diego, CA 92037, USA.
E-mail: cdupont@jcvi.org
Received 19 March 2014; revised 17 November 2014; accepted 24 November 2014; published online 9 January 2015

intracellular content of pigments, and additional microbial populations also tend to accumulate (Pedrós-Alió and Guerrero, 1993). These blooms are, in fact, natural enrichment cultures that facilitate physiological studies *in situ* (Van Gemerden *et al.,* 1985). At such interfaces fine gradients of physicochemical conditions are present and tight coupling between different biogeochemical cycles (mainly carbon, nitrogen and sulfur) are established. Microbes adapted to such gradients are difficult to culture because *in situ* conditions are very difficult to mimic in the laboratory, and their study has improved perceptibly by culture-independent methods (Casamayor *et al.,* 2000).

Stratified euxinic lake systems may also provide potential modern day analogue ecosystems for the oceans during long periods of Earth history. The planet was essentially anoxic until 2.7–2.4 billion years ago, with a ferruginous ocean (Anbar, 2008; Reinhard *et al.,* 2013). With the advent of oxygenic photosynthesis, atmospheric oxygen began to rise, as did the oxygen content in the surface oceans. The deep oceans remained anoxic, but entered a period of temporal and spatial heterogeneity. Strong euxinic conditions might be expected in ancient coastal areas, with merely anoxic conditions in the open ocean, although high Fe deep ocean conditions would have been maintained (Reinhard *et al.,* 2013). In contrast, Fe is low in the deep waters of the modern ocean and, therefore, it is difficult to find appropriate ancient ocean analogue in the current marine realm. With this in mind, stratified aquatic systems with high Fe concentrations in deep waters could be more appropriate modern day analogues of the Proterozoic ocean. Karstic lacustrine systems with a gradient of organic carbon delivery and sulfide concentrations generated by sulfate reduction, and usually rich in iron, would provide reasonable biogeochemical analogues for ancient coastal to open ocean gradients.

In this study, we explored the oxic–anoxic interface (metalimnion) and bottom waters (hypolimnion) from two sulfurous lakes in the Banyoles karstic area (NE Spain) through shotgun metagenomics and *in silico* analysis of several metabolic pathways. In the framework of paleoreconstruction of anoxic conditions in ancient marine systems, one lake would be representative of strong euxinic conditions (Lake Cisó) and the other of low euxinia and an active iron cycle (basin III of Lake Banyoles). We explore the links between microbial composition and functionality for the carbon, nitrogen and sulfur cycling after phylogenetic and functional identification. The taxonomic identity assigned to each functional step was determined by the closest match in databases, and the relative abundance and distribution of marker genes was comparatively analyzed among samples as a proxy of the potential *in situ* relevance of these pathways under the specific environmental conditions studied. Because of the lack of oxygen, large microbial biomass and high contribution of deep dark fixation processes to overall CO_2 incorporation (Casamayor *et al.,* 2008, 2012; Casamayor, 2010), we hypothesized a high genetic potential for chemotrophic CO_2 fixation and a tight redox coupling between carbon, nitrogen and sulfur biogeochemical cycling. In addition, because of its euxinic nature we also expected a low contribution of both methanogens and ammonia oxidizers in the biogeochemical cycles prevailing in these environments.

Materials and methods

Environment and samples collection

Lake Cisó and basin III of Lake Banyoles (Banyoles C-III) are in the Banyoles karstic area, northeastern Spain (42°8'N, 2°45'E), and the microbial communities inhabiting these water bodies have been extensively studied by limnologists and microbial ecologists (see, for example, Guerrero *et al.,* 1980; Garcia-Gil and Abellà, 1992; Pedrós-Alió and Guerrero, 1993). The lakes were sampled on 8–9 May 2010. Vertical profiles of temperature, conductivity, oxygen and redox potential were measured *in situ* with a multiparametric probe OTT-Hydrolab MS5 (Hatch Hydromet, Loveland, CO, USA). The different water compartments (oxic epilimnion, metalimnion with the oxic–anoxic interface and anoxic hypolimnion) were determined for each lake according to the physicochemical profiles recorded *in situ* (Figure 1). For sulfide analyses, 10 ml of subsamples were collected in screw-capped glass tubes and immediately alkalinized by adding 0.1 ml of 1 M NaOH and fixed by adding 0.1 ml of 1 M zinc acetate. Sulfide was analyzed in the laboratory according to Trüper and Schlegel (1964). For pigments, water samples were processed as described by Guerrero *et al.* (1985) and analyzed by HPLC as previously reported (Borrego *et al.,* 1999). Iron (Fe^{+2}) concentrations were obtained from Garcia-Gil (1990).

These lakes are stratified and have incoming sulfate-rich water seeping in through bottom springs, resulting in deep waters rich in reduced sulfur compounds. An oxic–anoxic interface, or redoxcline, is established in the water column where light and sulfide usually coexist. Lake Banyoles is a gypsum karst spring area consisting of six main basins covering a surface area of 1.1 km^2. The basin III (C-III) is meromictic with a maximal depth of 32 m, and a redoxcline between 18 and 21 m, depending on the season. Blooms of brown-colored photosynthetic green sulfur bacteria (*Chlorobiaceae*) and purple sulfur bacteria (*Chromatiaceae*) have been periodically reported (Garcia-Gil and Abellà, 1992). Lake Cisó is a small monomictic lake (650 m^2), located 1 km away from Lake Banyoles with a maximum depth of 6.5 m. The thermocline is at 1.5 m, where different bacterial populations accumulate (Casamayor *et al.,* 2000). The presence of aerobic chemoautotrophic

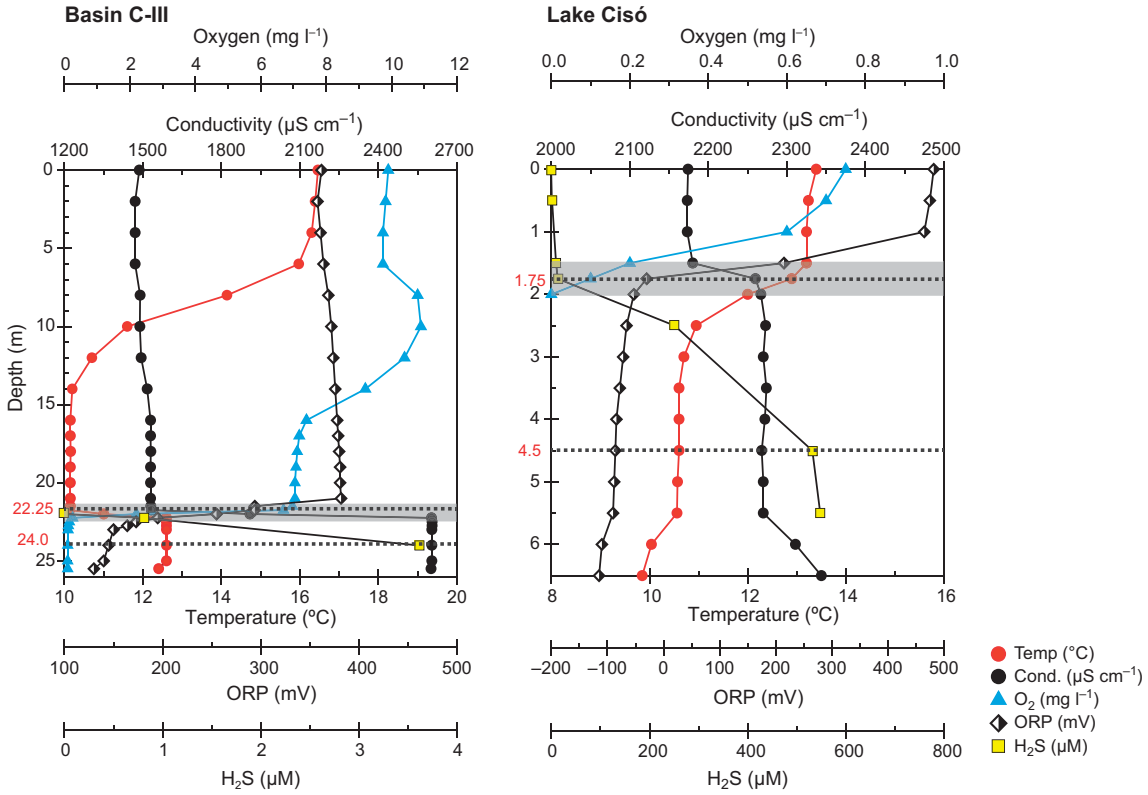

Figure 1 Vertical profiles of physicochemical data for Lake Banyoles basin C-III and Lake Cisó. Metagenomic analyses were carried out at two selected depths (dotted lines): the oxic–anoxic interface (shadowed areas indicate the redoxcline zone) and the anoxic and sulfurous (euxinic) hypolimnia.

sulfur-oxidizing bacteria and substantial fixation of CO_2 in the dark have been previously reported in sulfurous lakes (Casamayor, 2010). Lake Cisó is a small eutrophic water body fully surrounded by trees that strongly limit the incident irradiance on the lake and provide continuous allochthonous organic matter inputs both by leaching from the littoral zone and submerged vegetal debris. The system is therefore prone to a dominance of aerobic respiration and mineralization in surface layers overlying sulfate respiration, fermentation and anaplerotic pathways at depth. In addition, the conspicuous presence of photosynthetic organisms and dissolved and particulate organic matter causes a strong light extinction and quality filtering in the first 2 m that severely limits the development of oxygenic and anoxygenic green phototrophs (Vila and Abellà, 1994). Conversely, the open-basin Banyoles C-III is oligotrophic, with lower influence of the littoral zone. The basin maintains a stable, sharp chemocline that oscillates in depth between 19 and 21 m depending on the season, being shallower during summer. Active sulfate reduction occurring at the permanent anoxic monimolimnion causes sulfide accumulation below the chemocline, usually reaching concentrations of up to 1 mM during summer and late fall. Lower sulfide concentrations are common however during spring. Light intensities reaching the O_2/H_2S interface are generally low (between 1% and 0.1% of surface incident light in winter and summer, respectively) despite the transparency of the epilimnetic waters of Lake Banyoles. The brown-pigmented green sulfur bacteria are better adapted to low irradiances than the green-pigmented ones (Garcia-Gil and Abellà, 1992) and massively bloom in C-III.

The oxic–anoxic metalimnion interface and the euxinic (anoxic and sulfurous) hypolimnion samples for metagenomic analyses were determined *in situ* according to the vertical physicochemical profiles. Samples were prefiltered in the field through a 200 µm nylon mesh and kept in the dark in 25 l polycarbonate carboys until further processing in the lab 2–4 h later. The plankton was collected using serial filtration onto 3.0, 0.8 and 0.1 µm Supor 293 mm membrane disc filters (Pall Life Sciences, Port Washington, NY, USA) and stored in liquid nitrogen or −80 °C until DNA extraction. DNA extraction and pyrosequencing was carried out at the J Craig Venter Institute in

Rockville, MD, USA as recently reported (Zeigler Allen *et al.,* 2012).

DNA sequences analyses

A shotgun metagenomics approach was applied on all three size fractions of four samples from Lakes Cisó and Banyoles C-III. Identical reads were removed using CD-HIT (Li and Godzik, 2006). Annotation of metagenomic reads was conducted through the JCVI prokaryotic annotation pipeline (Tanenbaum *et al.,* 2010) using Uniref100, PFAM, TIGRfam and KEGG (Kyoto Encyclopedia of Genes and Genomes) Orthologs (KO) databases for taxonomic and functional annotation. JCVI Metagenomics reports (http://jcvi.org/metarep) were used for analysis and comparative metagenomics (Goll *et al.,* 2010). KO annotation was used for functional analysis and KO counts were normalized according to the length of the read and the length of the target gene (Sharon *et al.,* 2009). The communities and functional profiles found in each size fraction were highly similar (Supplementary Figure S1) and, therefore, we pooled all reads after normalizing for sequencing depth for subsequent analyses, which allows for a better comparison of metagenomes.

The functional analyses focused on the three main biogeochemical cycles for this type of lakes, that is, carbon (C), nitrogen (N) and sulfur (S) cycling. The genetic potential of the microbial community was analyzed following the C, N, and S marker genes (KOs) as reported by Lauro *et al.* (2011) with a few modifications. We amended this previous rubric by adding the anaerobic carbon fixation carried out through the Calvin cycle by *Chromatiaceae*, and additional genes for polysulfide reduction, nitrate reduction and nitrite oxidation. In addition, the genes *pyruvate:ferredoxin oxidoreductase* (*porA/B*) were not considered as marker genes for fermentation as in Lauro *et al.* (2011), because they are key genes in the reverse tricarboxylic acid cycle used for carbon fixation by *Epsilonproteobacteria* abundant in our study lakes (Campbell and Cary, 2004; Takai *et al.,* 2005). Because both sulfide oxidation and dissimilatory sulfate reduction pathways are mediated by the same set of genes (*aprA*, *aprB* and *dsrA*) but are found in different families of bacteria, we assigned metagenomic reads to each pathway according to phylogeny, that is, sulfate reduction for *Firmicutes* and *Deltaproteobacteria* reads, and sulfide oxidation for *Alphaproteobacteria*, *Betaproteobacteria*, *Chlorobiaceae* and *Chromatiaceae*. Finally, for the sulfur-oxidizing *Epsilonproteobacteria* of the order *Campylobacterales* we specifically searched for *sox* genes (coding for thiosulfate oxidation) not currently available in the KEGG database. Marker genes used in the present work are shown in Supplementary Table S1. Hierarchical clustering and heatmap plots were generated with R (R Development Core Team, 2012) using the library 'seriation'. Metagenomic data have been deposited at CAMERA (Sun *et al.,* 2011) under accession number CAM_P_0001174.

Results

Environmental parameters

At the time of sampling (spring 2010), the water column was thermally stratified with thermoclines spanning from 1.5 to 3 m in Lake Cisó, and 7–14 m in basin C-III (Figure 1). Chemical stratification was disconnected from thermal stratification in basin C-III, where a sharp chemocline was detected at 21 m depth based on the higher conductivity of incoming sulfate-rich waters. The epilimnion of C-III showed oxygen concentrations of $>6\,mg\,l^{-1}$, with rapid drawdowns in the hypolimnion, and the sharp oxic–anoxic interface caused an abrupt decrease in the redox potential and generation of a pronounced redoxcline (Figure 1, shaded area). In Lake Cisó, the epilimnion (0–1.5 m depth) was oxygen deficient ($0.2 - 1\,mg\,l^{-1}$) and the water column became completely anoxic below 2 m depth. In this case, the redoxcline and the oxic–anoxic interface were located in a narrow water layer of 0.5 m width (1.5–2 m depth). The concentration of nitrogen and sulfur species changed according to these physicochemical gradients with high concentrations of ammonia mainly in the hypolimnia (up to 60 μM) and sulfide concentrations ranging between 532 μM in Lake Cisó and <1 μM in C-III in agreement with redox potential (Eh) measurements (Table 1, and Supplementary Figure S2). The concentration of Chl *a* measured in the lakes agreed with their traditional trophic status (oligotrophic for C-III and

Table 1 Biogeochemical data for Lake Cisó and Banyoles basin C-III

	Cisó ML	*Cisó HL*	*C-III ML*	*C-III HL*
Depth (m)	1.75	4.5	22.25	24
Temperature (°C)	12.9	10.6	12.6	12.6
Conductivity ($\mu S\,cm^{-1}$)	2260	2268	2603	2604
Eh (mV)	−30	−86	195	145
Oxygen ($mg\,l^{-1}$)	0.10	0	0.25	0
H_2S (μM)	12.8	531.9	0.8	3.6
Light (% incident)	1%	<0.1%	1%	<0.1%
TOC ($mg\,l^{-1}$)	5	3	1.5	3
pH	7.40	7.23	7.14	7.15
TDP (μM)	1.05	2.83	0.33	0.37
NH_4 (μM)	44.39	50.99	25.04	37.52
NO_2 (μM)	0.75	b.d.l.	0.21	0.00
NO_3 (μM)	2.20	1.44	6.20	0.54
Urea (μM)	4.84	0.17	1.91	1.08
Si (μM)	185.0	168.1	144.8	114.5
Chl *a* ($\mu g\,l^{-1}$)	1.7	22.5	1.1	0.8
BChl *a* ($\mu g\,l^{-1}$)	2.4	123.7	1.1	1.6
BChl *c* and *d* ($\mu g\,l^{-1}$)	5.4	39.3	0	0
BChl *e* ($\mu g\,l^{-1}$)	0.8	13.6	25.8	40.6

Abbreviations: BChl, bacteriochlorophyll; b.d.l., below detection limits; Chl*a*, chlorophyll *a*; HL, hypolimnion; Eh, redox potential; ML, metalimnion; TOC, total organic carbon; TDP, total dissolved phosphorus.

mesotrophic for Lake Cisó). Biomarker pigments for green sulfur (BChl *c*, *d* and *e*) and purple sulfur bacteria (BChl *a*) were detected in the metalimnion and hypolimnion of Lake Cisó and basin C-III. Particularly, conspicuous concentrations of BChl *e*, the characteristic pigment of brown-colored species of *Chlorobium*, were measured between 22 and 24 m depth in basin C-III (Table 1). An active Fe^{2+} cycle has been previously reported in Lake Banyoles with concentrations of 8–10 μM in both the resurgence of groundwater (bottom spring) and water column of basin C-III, inflow velocity of 0.8 mmol total Fe per h, and concentrations of up to 8 mg total Fe per g of sediment (dw) (Garcia-Gil, 1990). Interestingly, we also observed substantial concentrations of nitrate in the bottom of the basin, coming from the groundwater, and high concentration in surface waters originated from the surrounding crop fields and farms (Supplementary Figure S2).

Taxonomic structure of the microbial communities

The overall taxonomic breakdown of the communities was assessed using the phylogenetic annotation of the metagenomic reads. The domain *Bacteria* numerically dominated the genetic composition of the microbial communities, both at the oxic–anoxic interfaces and at the anoxic hypolimnia (Table 2). More than 95% of all taxonomically assigned metagenomic reads matched bacteria, with a few representatives of archaea (range 0.7–3.5%), phages (0.8–4.0%) and eukaryotes (0.7–2.8%). Archaeal metagenomic reads were more abundant in the hypolimnion (2.67 ± 1.21% of total reads) than in the metalimnion (1.09 ± 0.47%). Most of the archaeal metagenomics reads matched methanogens within *Euryarchaeota* (c. 88%), with a few additional representatives within *Thermococci*, *Thermoplasmata*, *Archaeoglobi* and *Haloarchaea* (Supplementary Figure S3). The 16S rRNA gene in the metagenomics data set agreed with the broad taxonomic picture provided by the functional genes (Table 2), that is, 98–100% of the 16S rRNA gene affiliated to *Bacteria*, whereas Archaea were a minor component more abundant in the hypolimnion (1.4 ± 0.7%) than in the metalimnion (0.2 ± 0.2%).

Interestingly, we observed higher proportion of functional reads affiliated to *Crenarchaeota–Thaumarchaeota* at the oxic–anoxic interface (12.3 ± 0.4% of total archaeal reads) than at the anoxic and sulfurous bottom of the lakes (8.6 ± 0.5%). *Thaumarchaeota* metagenomic reads putatively assigned to ammonia oxidizers were 0.03% of total reads but were not detected in the 16S rRNA pool. Conversely, ammonia-oxidizing bacteria (AOB, *Nitrosomonadales*- and *Nitrosococcus*-like) and nitrite-oxidizing bacteria (*Nitrospirae*-like) metagenomic reads were detected at 10 times higher concentration (0.3% of total reads). AOB were also detected in the 16S rRNA pool at similar concentrations (0.1% of total 16S rRNA gene). Overall, the most abundantly recovered 16S rRNA gene from the metagenomic data set matched *Chlorobiales* (green sulfur bacteria; 20%, range 5–50%), *Campylobacterales* (Epsilonproteobacteria; 14%, range 11–21%), *Burkholderiales* (Betaproteobacteria; 12%, range 0.5–35%), OD1 (8%, range 4–13%) and *Frankiales* (Actinobacteria; 5%, range 0.3–12%), among others (Figure 2, and Supplementary Table S2). These populations were differentially distributed between layers and lakes (Figure 2, and see details in Supplementary Table S2) and yielded a taxonomic clustering according to the redox potential, with samples with higher redox (> -30 mV) and lower sulfide concentrations (sulfide <13 μM) closer to each other than to the most euxinic sample (Lake Cisó hypolimnion, sulfide >500 μM, redox -86 mV; Table 1).

Functional structure of the microbial communities

The metagenomic data set comprised four million reads of average length 377 bp and 54% of the metagenomic reads were taxonomically assigned based on the APIS or BLAST, whereas 22% could be assigned KO numbers and thus putative functions (*e*-value 10^{-5}). From the identified KOs, we selected marker genes related to C, N and S cycling

Table 2 Total number of metagenomic reads (averaged c. 1 million per sample) for Lake Cisó and Banyoles basin C-III

	Cisó ML	*Cisó HL*	*C-III ML*	*C-III HL*
Total number of reads	869 947	991 056	1 071 206	1 077 431
Taxonomically assigned reads (%)	46.7	53.5	54.2	62.4
Bacteria (%)	92.5	94.6	91.9	93.7
Archaea (%)	0.7	3.5	1.4	1.7
Eukarya (%)	2.8	1.1	2.7	0.7
Viruses (%)	4.0	0.8	4.0	3.9
16S rRNA genes in the metagenomic pool	465	578	690	787
Bacteria (%)	99.6	97.9	100	99.4
Archaea (%)	0.4	2.1	0	0.6
Functionally assigned metagenomic reads (%)	25.8	27.5	30.5	32.6
Reads of key genes in C, N and S cycles	2392	3574	4773	5162

Abbreviations: HL, hypolimnion; ML, metalimnion.

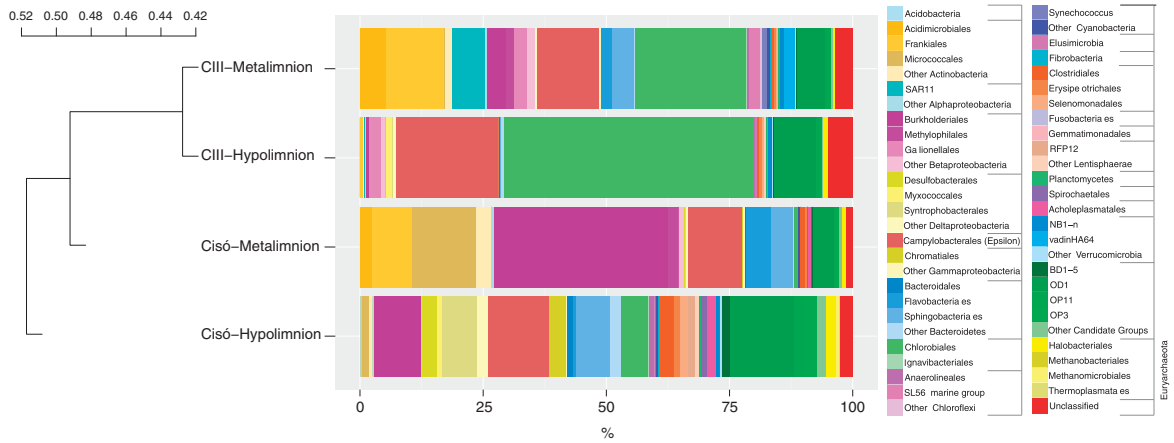

Figure 2 Prokaryotic community structure (relative abundances at the Order level) of Lake Banyoles basin C-III and Lake Cisó obtained from the 16S rRNA gene present in the metagenomic pool. See detailed information in Supplementary Table S2. Hierarchical clustering based on Bray–Curtis dissimilarity matrices.

(Supplementary Table S1). Anaerobic C fixation, nitrogen fixation and assimilatory sulfate reduction genes accounted for a substantial percentage of annotated reads in the hypolimnia, whereas genes for aerobic respiration, nitrogen assimilation and sulfur mineralization were more abundant at the oxic–anoxic interfaces (Supplementary Table S3). Other less abundant metabolic pathways such as ammonification, anammox–SRAO (sulfate-reducing anaerobic ammonia oxidation; Rikmann *et al.,* 2012) and dissimilatory sulfate reduction were detected, mostly in the hypolimnion of Lake Cisó. Such differences were globally captured by a functional-level (C, N and S pathways examined) hierarchical analysis that grouped the samples according to presence/absence of oxygen (Figure 3). This clustering analysis produced the same result using multiple other functional annotations, including KEGG (EC), Gene Ontology terms and MetaCyc. Similarly, repeating this analysis with all size fractions as separate libraries (data not shown) and housekeeping genes (Supplementary Figure S4) gave similar results, with redox being a more structuring factor than geographical distribution.

As Bacteria and Archaea accounted for most of total metagenomic reads, we focused on the prokaryotes for a comparative study of the geochemistry of carbon (Figure 4), nitrogen (Figure 5) and sulfur (Figure 6) along the redoxcline. We used the relative abundance of the detected functional genes as a proxy of the potential relevance of each pathway *in situ* without considering the role of microscopic algae. For the C cycling, the main pathway detected in the oxic–anoxic interface was aerobic respiration by heterotrophic *Actinomycetales* and *Burkholderiales* in Lake Cisó, and by *Actinomycetales* and *Pelagibacterales* (SAR11-like) in Lake Banyoles C-III. In the hypolimnion, the abundant pathways were various forms of anaerobic carbon fixation: by *Chromatiales* (anoxygenic phototrophy by the Calvin cycle), *Bacteroidales* (probably anaplerotic) and sulfate-reducing bacteria (SRB) (probably the reductive citric acid cycle/Arnon pathway; Fuchs, 2011) in Lake Cisó, and *Chlorobiales* (anoxygenic phototrophy by the Arnon cycle) in Banyoles C-III (Table 3). Chemolithotrophic aerobic carbon fixation via the Calvin cycle, which was rare, was mostly related to *Betaproteobacteria* of the genus *Hydrogenophilales* (*Thiobacillus*-like) and *Gallionellales* (*Syderoxydans*-like). Chemolithotrophic *Epsilonproteobacteria* with genes for the Arnon cycle (*Campylobacterales* on Figure 4) were found related to the genera *Arcobacter*, *Sulfuricurvum* and *Sulfurimonas* (Table 3). Carbon monoxide (CO) oxidation marker genes were also present (3–14% of those targeted marker genes selected for the carbon cycle, Supplementary Table S3) and related to heterotrophic bacteria. The potential for fermentation was mostly observed in Lake Cisó. Both methanogenesis and methane oxidation-specific marker genes had low abundances in all four environments, and even in those samples where such genes were not specifically detected (Figure 4, dotted lines) we found additional metagenomic reads taxonomically matching methanogens and methane oxidizers clades.

For the nitrogen cycle, most of the detected marker genes catalyzed N assimilation and mineralization (Figure 5 and Supplementary Table S3). Denitrification was observed in low abundance in all the cases (c. 3% of the nitrogen functional reads selected), and the main taxa involved were *Campylobacterales* (autotrophic *Sulfurimonas* and *Arcobacter*), *Oceanospirillales* (heterotrophs) and *Gallionellales* (autotrophic *Sideroxydans*). Conversely, the potential for nitrogen fixation (*nif* genes)

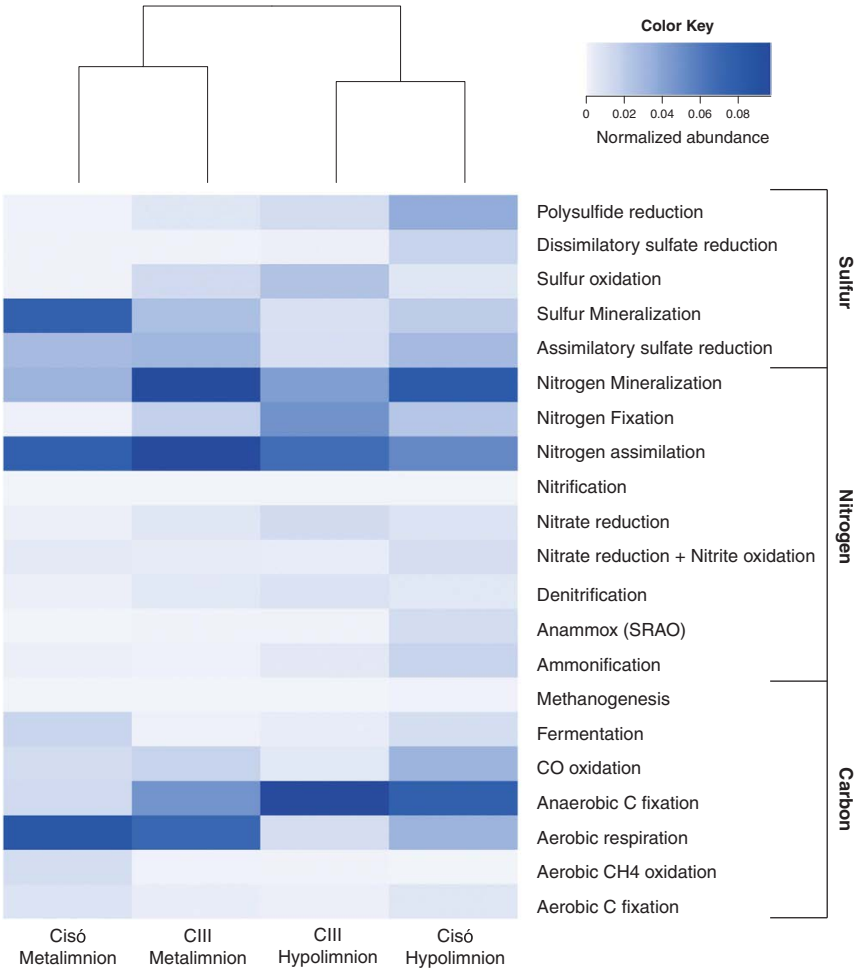

Figure 3 Heatmap plot and functional clustering of the selected KEGG Orthologs for the predicted open reading frames (ORFs) from the metagenomic reads for Lake Cisó and Banyoles basin C-III.

was observed in all the cases, although in higher abundance under euxinia (18 ± 11%) than in the oxic–anoxic interfaces (4 ± 4%). The *nif* genes were most related to *Chlorobium* in Lake Banyoles, whereas in Lake Cisó they were most similar to *Syntrophobacterales*. Under the most euxinic conditions, c. 6% of the total nitrogen marker genes examined were the anammox catalyzing enzyme hydrazine oxidoreductase, although these were associated with *Syntrophobacterales* instead of the planctomycetales found in oceanic anoxic zones. Both aerobic ammonia oxidation and nitrification marker genes had very low abundance, and were only properly detected in Lake Banyoles C-III hypolimnion (*amoC* gene 97% identical to *Nitrosospira multiformis*). However, metagenomic reads matching *Thaumarchaeota* (ammonia-oxidizing archaea (AOA)), *Nitrosomonadales* and *Nitrosococcus* (AOB) and *Nitrospirae* nitrite-oxidizing bacteria were detected in all lakes and water layers (Figure 5, dotted lines), pointing out that the genetic potential to close the nitrogen cycle was there, but at very low abundance as compared with other pathways in the cycle.

Finally, in the S cycle (Figure 6 and Supplementary Table S3) the highest percentage of the reads matched assimilatory sulfate reduction (28 ± 9% of those targeted sulfur marker genes) and sulfur mineralization (35 ± 25%), mostly driven by the predominant heterotrophic organisms found in each water layer (*Actinomycetales* and *Burkholderiales*). Most sulfide oxidation genes likely originated from *Chlorobiales* in Lake Banyoles C-III, and *Chromatiales* in Lake Cisó, with further contributions from chemolithotrophs *Gallionellales*, *Hydrogenophilales* and *Campylobacterales*. The potential for planktonic sulfate reduction was only observed in strong euxinia (Lake Cisó

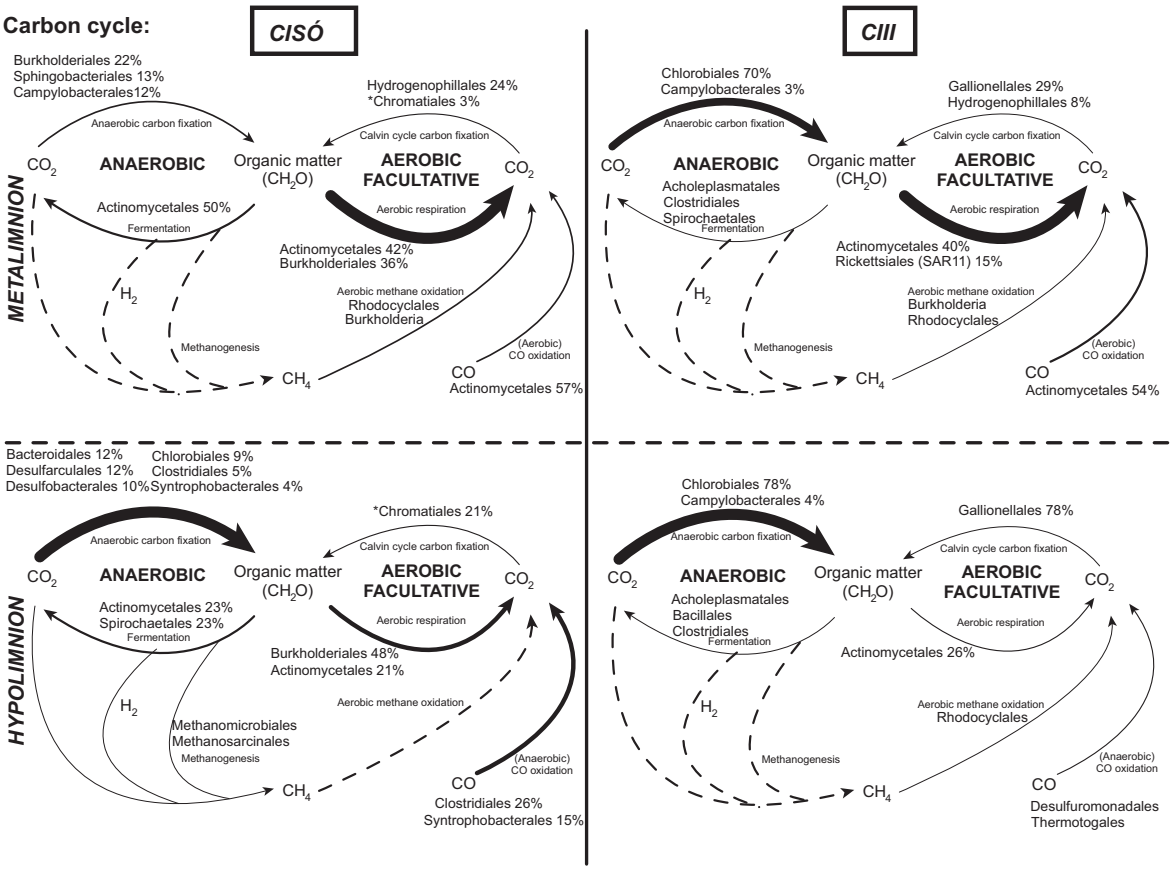

Figure 4 Genetic potential for several steps of the carbon cycle in Lake Cisó and Banyoles basin C-III using a combination of normalized marker genes. Arrow size proportional to the potential flux of the carbon pathways (100% value, see Supplementary Table S3). Dotted lines: not detected marked genes but putative presence of the pathway (see main text). Relative abundances for the main microbes potentially driving each conversion step are shown (only for those that contributed >1% of the marker genes mixture). **Chromatiales*: anoxygenic phototrophy through the Calvin cycle.

hypolimnion, 16% of targeted sulfur reads as compared with 1.4 ± 1% in the remaining samples), with reads likely originating from *Desulfobacterales* and most probably *Syntrophobacterales*, although members of this group may carry out both reductive and oxidative parts of the sulfur cycle. Interestingly, we observed a high richness of sulfate-reducing bacteria genera (Table 3) with the potential to degrade a wide variety of carbon compounds to help to maintain the high sulfide concentrations found in Lake Cisó.

Although the metagenomic data set does not contain transcriptome or proteome data, and thus only indicates potential function, we observed a direct linear relationship between relative abundance of dissimilatory sulfate reduction genes and *in situ* sulfide concentrations ($r = 0.998$, $P = 0.002$). Although this comparison should be carefully interpreted because of the low number of samples compared, it suggests a close link between both the abundance of planktonic SRB and sulfide production. We also observed significant direct linear relationships between the relative abundance of anaerobic carbon fixation genes from bacterial chemotrophs and denitrification ($r = 0.958$, $P = 0.042$), suggesting a close link between chemoautotrophy and the nitrogen cycle.

Discussion

Stratified planktonic environments with sharp chemical gradients and sulfide-rich bottom waters are valuable current windows on past Earth conditions. Anoxic and euxinic conditions were common but spatially and temporally heterogeneous in ancient oceans during Proterozoic (Reinhard *et al.,* 2013; Lyons *et al.,* 2014), and may have played an important role in mass extinctions during Phanerozoic (Meyer and Kump, 2008). The presence of marker pigments for photosynthetic sulfur bacteria (that is, isorenieratene and okenone) have been often

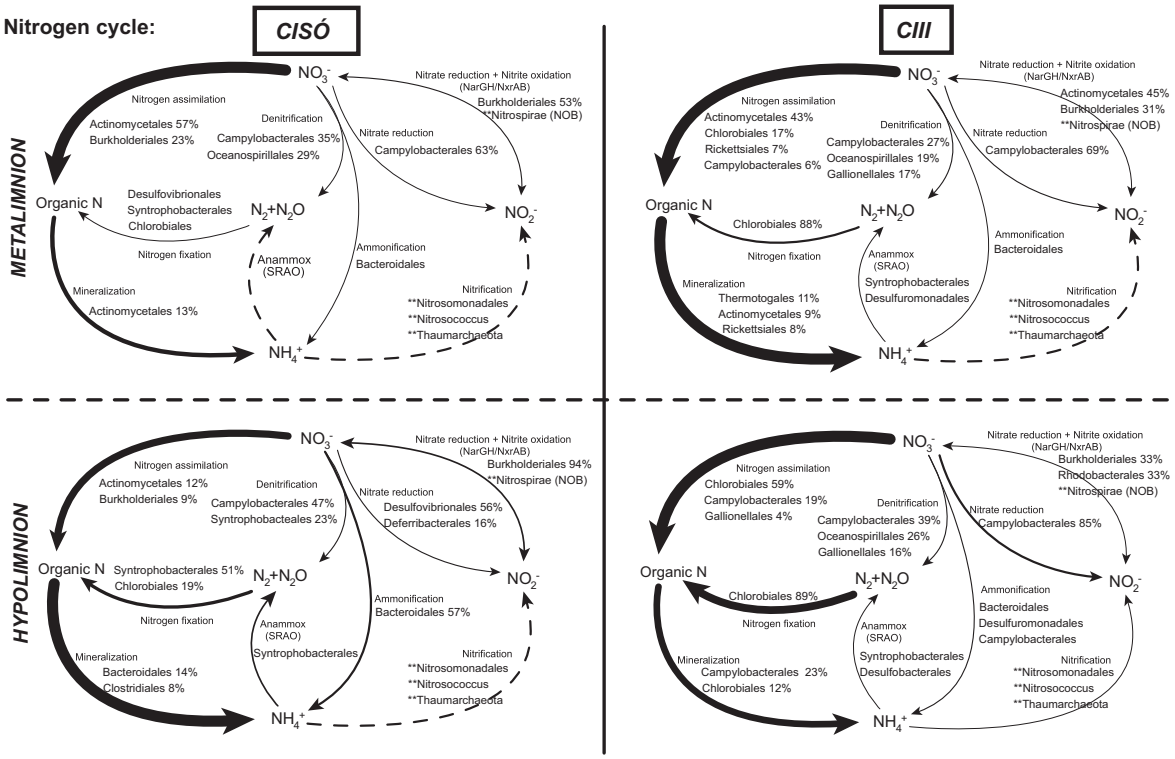

Figure 5 Genetic potential for several steps of the nitrogen cycle in Lake Cisó and Banyoles basin C-III using a combination of normalized marker genes. Arrow size proportional to the potential flux of the nitrogen pathways (100% value, see Supplementary Table S3). Dotted lines: not detected marked genes but putative presence of the pathway (see main text). Relative abundances for the main microbes potentially driving each conversion step are shown (only for those that contributed >1% of the marker genes mixture). **Presence of AOA, AOB and nitrite-oxidizing bacteria (NOB) reads in the metagenomic pool.

reported as evidence of euxinic conditions in ancient oceans (Damsté and Köster, 1998; Brocks *et al.,* 2005). These conditions are not common nowadays, although persistent euxinia can be found in deep silled basins such as the Black Sea, Baltic Sea and Cariaco Basin (Millero, 1991; Stewart *et al.,* 2007). Future climate change scenarios predict, however, an increasing of euxinia phenomena, mainly in coastal marine ecosystems (Diaz and Rosenberg, 2008). The study of stratified sulfurous lakes has, therefore, an additional interest to predict biogeochemical functioning and microbial interactions in such future scenarios. In the present study, we explored the community composition and functional gene content along a gradient of redox conditions in a karstic sulfurous area. Continental systems are cheaper and easier to sample than marine basins, and a large variety of photo- and chemolithotrophs organisms, sulfide-oxidizing and sulfate-reducing bacteria, fermenters, denitrifying microbes, methanogens and methane oxidizers are expected to be found, among others, according to previous studies (see, for example, Casamayor *et al.,* 2000; Barberán and Casamayor, 2011). The metabolisms harbored by these microorganisms have the potential to provide insights into the ecosystems operating in euxinic early stages of Earth. The strong euxinic conditions found in Lake Cisó may match biogeochemistry in ancient coastal areas, whereas basin C-III in Lake Banyoles may represent the transition from euxinic coastal areas to merely anoxic and rich Fe conditions in the ancient open ocean (Figure 7).

The very low abundance of genes for nitrification, the minor presence of anammox genes, the high potential for nitrogen fixation and mineralization and the potential for chemotrophic CO_2 fixation and CO oxidation all provide potential clues on the ancient oceanic anoxic zones functioning. The low abundance of ammonia oxidizers (AOA and AOB) agrees with the high ammonia accumulation in the anoxic bottom of the lakes, the lack of oxygen and presence of potentially toxic sulfide. We observed, however, a higher gene abundance of AOB relative to AOA in the metagenomic pool that may have a geochemical link related to the abundance of Fe in these environments. AOA have a highly copper-dependent system for ammonia oxidation and electron transport (Walker *et al.,* 2010), completely different from the iron-dependent system present in

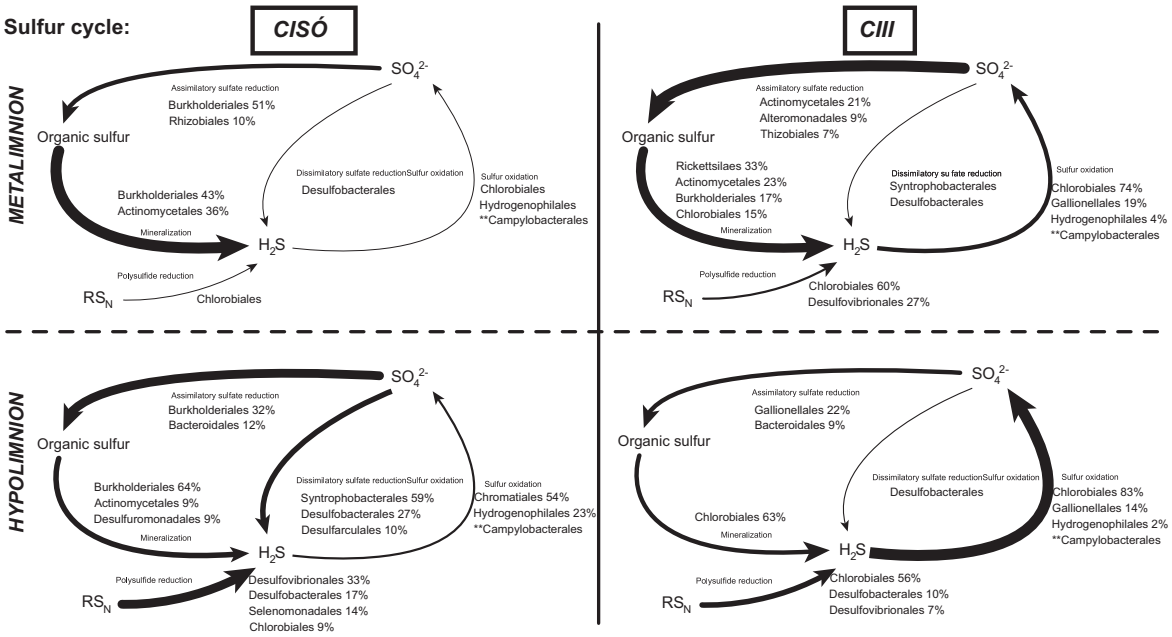

Figure 6 Genetic potential for several steps of the sulfur cycle in Lake Cisó and Banyoles basin C-III using a combination of normalized marker genes. Arrow size proportional to the potential flux of the sulfur pathways (100% value, see Supplementary Table S3). Relative abundances for the main microbes potentially driving each conversion step are shown (only for those that contributed >1% of the marker genes mixture). ***Campylobacteraceae* contributed through *sox* genes not reported in KEGG database.

Table 3 Carbon fixation cycles and main metabolic traits of the C-fixing microorganisms found in this study

Taxa/phylogeny	*C-fixation pathway*	*Traits*	*Main genera identified in Lakes Cisó and C-III from the 16S rRNA gene present in the metagenomic pool*
Gallionellales *Betaproteobacteria*	Calvin	Facultative Chemolithoautotroph Energy sources: Fe(II)/sulfide Denitrification	*Sideroxydans*
Hydrogenophilales *Betaproteobacteria*	Calvin	Chemolithoautotroph Sulfide oxidation	
Campylobacterales *Epsilonproteobacteria*	Arnon[a]	Chemolithoautotroph Denitrification Sulfide oxidation	*Arcobacter, Sulfuricurvum, Sulfurimonas*
Chromatiales *Gammaproteobacteria*	Calvin	Photolithoautotroph Anaerobic Tolerates oxygen	*Lamprocystis*
Chlorobiales *Chlorobi*	Arnon[a]	Photolithoautotroph Anaerobic (strict) N fixation	*Chlorobium luteolum*
Desulfobacterales *Deltaproteobacteria*	Arnon[a] Reductive acetyl-CoA[b]	Heterotroph Sulfate reducers	*Desulfatiferula, Desulfobulbus, Desulfocapsa, Desulfosalsimonas*
Syntrophobacterales *Deltaproteobacteria*	Arnon[a] Reductive acetyl-CoA(?)[b]	Heterotroph Sulfate reducer/ sulfide oxidation SRAO	*Desulfomonile*
Desulfuromonadales *Deltaproteobacteria*	Reductive acetyl-CoA[b]	Nitrate dependent Fe(II) oxidation with production of ammonium (Weber *et al.,* 2006)	

Abbreviation: SRAO, sulfate-reducing ammonium oxidation.
[a]Also known as reverse Krebs cycle, reverse tricarboxylic acid cycle (rTCA) and reverse citric acid cycle.
[b]Also known as Wood–Ljungdahl pathway.

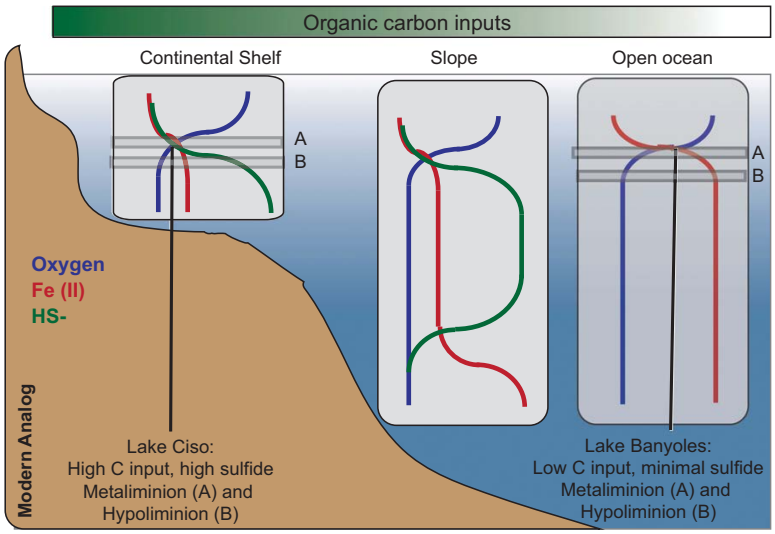

Figure 7 Lake Cisó and basin C-III of Lake Banyoles as modern analogs of anoxic conditions prevailing in the ancient ocean. The illustration shows the geochemical distributions of Fe, S, C and O_2 in depth profiles and along different oceanic regimes (shelf, slope, open ocean) during Proterozoic (Lyons *et al.,* 2014). Lake Cisó would be closer to coastal and continental shelf areas, whereas Banyoles C-III would be a more open ocean analogue.

AOB. The tradeoff in Fe- vs Cu-rich ammonia oxidation enzymatic systems would suggest that AOA evolved relatively recently (<550 million years ago) and that the Proterozoic oceans, which would have been Fe rich, would have been AOB dominated. Interestingly, the evolutionary dynamics of the *amoA* gene cladogenesis events visualized using lineage through time plots displays a different scenario for AOA and AOB, with AOB showing a more constant cladogenesis through the evolutionary time, whereas AOA experienced two fast diversification events separated by a long steady-state period (Fernàndez-Guerra and Casamayor, 2012).

The potential for nitrogen fixation and denitrification was detected in both autotroph and heterotroph microbial lineages, suggesting a diverse range of potential overlaps between carbon and nitrogen cycling in the ancient ocean, and an active nitrogen cycle in anoxic systems. Our results show a potential major contribution to nitrogen fixation by *Chlorobiaceae* under euxinic conditions. *Chlorobiaceae* were also the major contributors to carbon fixation in Banyoles C-III coupled to sulfide oxidation through the Arnon cycle. Therefore, the reported presence of *Chlorobiaceae* in the ancient ocean (Damsté and Köster, 1998; Brocks *et al.,* 2005) would have been of major relevance not only for the carbon but also for the nitrogen cycling. *Campylobacterales* (*Epsilonproteobacteria*) accounted for a large percentage of the denitrification genes in the anaerobic layers of both lakes, but were taxonomically segregated (*Arcobacter* dominated in Cisó, *Sulfurimonas* was present in C-III). Both genera respire nitrate coupled to C fixation in the dark through the reverse tricarboxylic acid cycle (Labrenz *et al.,* 2005; Burgin and Hamilton, 2007; Grote *et al.,* 2012), being potentially able to couple denitrification to sulfur oxidation (Ghosh and Dam, 2009). The other important group involved in denitrification was the chemolithoautotrophic *Gallionellales* oxidizing sulfide or Fe^{2+} while respiring nitrate and producing NH_4^+ or N_2. The presence of *Gallionellales* exclusively in C-III is probably because of their close relation with the iron cycle (Weber *et al.,* 2006), and by the fact that an active Fe^{2+} cycle has been previously detected in Lake Banyoles (Garcia-Gil *et al.,* 1990). The potential role of *Gallionellales* in ancient oceans with an active iron cycle is therefore of major interest.

The case of *Bacteroidales* also deserves to be mentioned. *Bacteroidales* have been typically considered aerobic or microaerophilic chemoorganoheterotrophic bacteria (Reichenbach, 2006), and have been recurrently detected in the Banyoles area (Casamayor *et al.,* 2000; Casamayor *et al.,* 2002; Casamayor *et al.,* 2012) and in the marine realm (Fernández-Gómez *et al.*, 2013). However, their role in anaerobic, sulfide-rich layers was not elucidated. Here, we assigned *Bacteroidales* as potentially catalyzing DNRA (dissimilatory nitrate reduction to ammonium), coupling the electron flow from organic matter to the reduction of nitrate. Thus, we would expect a potential gradient of distribution for anaerobic *Bacteroidales* in the ancient ocean being more abundant in the organic carbon- and sulfide-rich coastal zones (Figure 7) than in the anoxic and more oligotrophic open ocean. We also noticed the low abundance of key processes in the anaerobic carbon cycle such as CH_4 cycling, probably because

in the presence of high levels of sulfate, methanogens are generally poor competitors with sulfate reducers in stratified natural environments (Raskin *et al.,* 1996). Sulfate reduction normally occurs in fully anoxic sediments by SRB (Holmer and Storkholm, 2001). However, as shown here, a water column with euxinic conditions and a high availability of organic carbon is also suitable for the growth of an important community of planktonic SRB.

Previous studies in Banyoles area measured unexpected high rates of dark carbon fixation at the oxic–anoxic interface and the hypolimnetic waters, accounting for 58% of total annual fixed carbon in Lake Cisó (Garcia-Cantizano *et al.,* 2005). It was proposed that photosynthetic bacteria could be partly carrying out dark carbon incorporation *in situ* (Casamayor *et al.,* 2008), and *Thiobacilli* may actively fix CO_2 at certain depths (Casamayor, 2010). However, the ecological factors modulating the process and the microbial populations performing dark carbon fixation are still not well understood (Casamayor *et al.,* 2012). In the present investigation, we detected the potential for chemotrophic CO_2 fixation mainly through the reverse tricarboxylic acid cycle (K00174, K00175 and K00244 from *KEGG* Orthology) in *Bacteroidales*, *Campylobacterales* and *Desulfarculales*. In addition, other SRB such as *Desulfobacterales* may also participate through the anaerobic C_1-pathway (Wood–Ljungdahl pathway, K00194 and K00197) yielding formate assimilation and CO_2 fixation (Hugler *et al.,* 2003; Sun *et al.,* 2010; Fuchs, 2011). Interestingly, the diversity of taxa potentially participating in carbon fixation in the dark was larger in Lake Cisó than in C-III, in agreement with *in situ* measurements carried out in former investigations (Garcia-Cantizano *et al.,* 2005; Casamayor, 2010). These findings would suggest an active carbon-fixing activity in ancient euxinic oceans beyond the euphotic zone that certainly deserves further investigations.

In addition, the oxidation of CO generates adenosine triphosphate and CO_2 that may be further processed through one of the reductive CO_2 fixation pathways to be used as C source (Ragsdale, 2004; King and Weber, 2007). Some studies indicate that organisms using CO as both energy and C source can be viewed as the extant survivors of early metabolic processes (Huber and Wächtershäuser, 1997). In the hypoxic layers we found that the heterotrophic group of *Actinomycetales* accounted for most of monooxygenase CO genes in agreement with their mixotrophic lifestyle (Schmidt and Conrad, 1993). More interestingly, in the anoxic depths of Lake Cisó we found that CO oxidation genes were mainly related to SRB from *Deltaproteobacteria* group (*Geobacter* and deltaproteobacterium NaphS2) and to *Firmicutes* (*Carboxidothermus hydrogenoformans, Moorella thermoacetica* and *Clostridium* spp.). This finding suggests that the fate of the reducing equivalents from CO oxidation in anaerobic conditions could be coupled to sulfate reduction (carried out by SRB) to produce sulfide, or to CO_2 reduction to produce acetate (SRB and Firmicutes) (Roberts *et al.,* 2004; King and Weber, 2007). To check whether CO oxidation could be coupled to CO_2 reduction to yield acetate (Ragsdale, 2004; Roberts *et al.,* 2004), we identified the phylogenetic affiliation of acetyl-CoA synthase genes (ACS, K14138), and found that *Desulfobacterales* and *Firmicutes* had the potential to use the Wood–Ljungdahl pathway to obtain energy and fix carbon from CO in the hypolimnion of Lake Cisó. However, although the CO-oxidizing genes were detected, we cannot assess their relevance in the lake or the ancient oceans because CO-oxidizing bacteria carry out a facultative mixotrophic metabolism (Gadkari *et al.,* 1990).

Overall, the metagenomics approach unveiled the interrelationships between microbes and biogeochemical cycling in a comparative framework of two lakes that are modern analogs of ancient ocean conditions. These results may also help to develop new geochemical proxies to infer ancient ocean biology and chemistry. A major pitfall in our metagenomic approach is the reliance on the assumption that the genes come from a particular bacteria or archaea according to phylogentic annotation; lateral gene transfer would compromise the direct link of phylogeny to a metabolic pathway. In most of the cases we found the 16S rRNA gene counterpart present in the metagenomic data pool, giving additional support to such links. Obvious next steps include an experimental quantification of the energy and matter fluxes involved in each of the metabolic pathways to get a complete picture on the tight coupling between microbes and biogeochemical cycling in anoxic ecosystems.

Conflict of Interest

The authors declare no conflict of interest.

Acknowledgements

JC Auguet, M Llirós, F Gich, FM Lauro and JM Gasol are acknowledged for field and lab assistance and ancillary data. We sincerely appreciate insightful comments and suggestions from anonymous reviewers and the editor. This research was funded by Grants GOS-LAKES CGL2009-08523-E and DARKNESS CGL2012-32747 to EOC from the Spanish Office of Science (MINECO), from financial support by the Beyster Family Fund of the San Diego Foundation and the Life Technologies Foundation to the J Craig Venter Institute, and the NASA Astrobiology Institute to CLD.

References

Anbar AD. (2008). Oceans elements and evolution. *Science* **322**: 1481–1483.

Barberán A, Casamayor EO. (2011). Euxinic freshwater hypolimnia promote bacterial endemicity in continental areas. *Microb Ecol* **61**: 465–472.

Bascompte J, Sole RV. (1995). Rethinking complexity - modeling spatiotemporal dynamics in ecology. *Trends Ecol Evol* **10**: 361–366.

Borrego CM, Baneras L, Garcia-Gil J. (1999). Temporal variability of *Chlorobium phaeobacteroides* antenna pigments in a meromictic karstic lake. *Aquat Microb Ecol* **17**: 121–129.

Brocks JJ, Love GD, Summons RE, Knoll AH, Logan GA, Bowden SA. (2005). Biomarker evidence for green and purple sulphur bacteria in a stratified Palaeoproterozoic sea. *Nature* **437**: 866–870.

Burgin AJ, Hamilton SK. (2007). Have we overemphasized the role of denitrification in aquatic ecosystems? A review of nitrate removal pathways. *Front Ecol Environ* **5**: 89–96.

Campbell BJ, Cary SC. (2004). Abundance of reverse tricarboxylic acid cycle genes in free-living microorganisms at deep-sea hydrothermal vents. *Appl Environ Microbiol* **70**: 6282–6289.

Casamayor EO, Schafer H, Baneras L, Pedrós-Alió C, Muyzer G. (2000). Identification of and spatio-temporal differences between microbial assemblages from two neighboring sulfurous lakes: comparison by microscopy and denaturing gradient gel electrophoresis. *Appl Environ Microbiol* **66**: 499–508.

Casamayor EO, Pedrós-Alió C, Muyzer G, Amann R. (2002). Microheterogeneity in 16S ribosomal DNA-defined bacterial populations from a stratified planktonic environment is related to temporal changes and to ecological adaptations. *Appl Environ Microbiol* **68**: 1706–1714.

Casamayor EO, Garcia-Cantizano J, Pedrós-Alió C. (2008). Carbon dioxide fixation in the dark by photosynthetic bacteria in sulfide-rich stratified lakes with oxic-anoxic interfaces. *Limnol Oceanogr* **53**: 1193–1203.

Casamayor EO. (2010). Vertical distribution of planktonic autotrophic thiobacilli and dark CO2 fixation rates in lakes with oxygen-sulfide interfaces. *Aquat Microb Ecol* **59**: 217–228.

Casamayor EO, Llirós M, Picazo A, Barberán A, Borrego CM, Camacho A. (2012). Contribution of deep dark fixation processes to overall CO2 incorporation and large vertical changes of microbial populations in stratified karstic lakes. *Aquat Sci* **74**: 61–75.

Damsté JSS, Köster J. (1998). A euxinic southern North Atlantic Ocean during the Cenomanian/Turonian oceanic anoxic event. *Earth Planet Sci Lett* **158**: 165–173.

Diaz RJ, Rosenberg R. (2008). Spreading dead zones and consequences for marine ecosystems. *Science* **321**: 926–929.

Fernández-Gómez B, Richter M, Schüler M, Pinhassi J, Acinas SG, González JM *et al.* (2013). Ecology of marine Bacteroidetes: a comparative genomics approach. *ISME J* **7**: 1026–1037.

Fernàndez-Guerra A, Casamayor EO. (2012). Habitat-associated phylogenetic community patterns of microbial ammonia oxidizers. *PLoS One* **7**: e47330.

Fuchs G. (2011). Alternative pathways of carbon dioxide fixation: insights into the early evolution of life? In: Gottesman S, Harwood CS (eds) *Annual Review of Microbiology* vol. 65. Annual Reviews: Palo Alto, p 631.

Gadkari D, Schricker K, Acker G, Kroppenstedt RM, Meyer O. (1990). Streptomyces thermoautotrophicus sp. nov., a thermophilic CO- and H(2)-oxidizing obligate chemolithoautotroph. *Appl Environ Microbiol* **56**: 3727–3734.

Garcia-Cantizano J, Casamayor EO, Gasol JM, Guerrero R, Pedrós-Alió C. (2005). Partitioning of CO_2 incorporation among planktonic microbial guilds and estimation of in situ specific growth rates. *Microb Ecol* **50**: 230–241.

Garcia-Gil LJ. (1990). *Phototrophic bacteria and iron cycle in Lake Banyoles. PhD thesis*. Autonomous University of Barcelona, (in Spanish).

Garcia-Gil LJ, Salagenoher L, Esteva JV, Abellà CA. (1990). Distribution of iron in lake Banyoles in relation to the ecology of purple and green sulur bacteria. *Hydrobiologia* **192**: 259–270.

Garcia-Gil LJ, Abellà CA. (1992). Population dynamics of phototrophic bacteria in three basins of Lake Banyoles (Spain). In: Ilmavirta V, Jones R (eds) *The Dynamics and Use of Lacustrine Ecosystems*. Springer: The Netherlands, pp 87–94.

Ghosh W, Dam B. (2009). Biochemistry and molecular biology of lithotrophic sulfur oxidation by taxonomically and ecologically diverse bacteria and archaea. *FEMS Microbiol Rev* **33**: 999–1043.

Goll J, Rusch DB, Tanenbaum DM, Thiagarajan M, Li K, Methe BA *et al.* (2010). METAREP: JCVI metagenomics reports–an open source tool for high-performance comparative metagenomics. *Bioinformatics* **26**: 2631–2632.

Grote J, Schott T, Bruckner CG, Glockner FO, Jost G, Teeling H *et al.* (2012). Genome and physiology of a model Epsilonproteobacterium responsible for sulfide detoxification in marine oxygen depletion zones. *Proc Natl Acad Sci USA* **109**: 506–510.

Guerrero R, Montesinos E, Esteve I, Abellà C. (1980). Physiological adaptation and growth of purple and green sulfur bacteria in a meromictic lake (Vila) as compared to a holomictic lake (Siso). In: Dokulil M, Metz H, Jewson D (eds) *Shallow Lakes Contributions to their Limnology*. Springer: The Netherlands, pp 161–171.

Guerrero R, Montesinos E, Pedrós-Alió C, Esteve I, Mas J, Van Gemerden H *et al.* (1985). Phototrophic sulfur bacteria in two Spanish lakes: vertical distribution and limiting factors. *Limnol Oceanogr* **30**: 919–931.

Holmer M, Storkholm P. (2001). Sulphate reduction and sulphur cycling in lake sediments: a review. *Freshw Biol* **46**: 431–451.

Huber C, Wächtershäuser G. (1997). Activated acetic acid by carbon fixation on (Fe,Ni)S under primordial conditions. *Science* **276**: 245–247.

Hugler M, Huber H, Stetter KO, Fuchs G. (2003). Autotrophic CO2 fixation pathways in archaea (Crenarchaeota). *Arch Microbiol* **179**: 160–173.

King GM, Weber CF. (2007). Distribution, diversity and ecology of aerobic CO-oxidizing bacteria. *Nat Rev Microbiol* **5**: 107–118.

Labrenz M, Jost G, Pohl C, Beckmann S, Martens-Habbena W, Jurgens K. (2005). Impact of different in vitro electron donor/acceptor conditions on potential chemolithoautotrophic communities from marine pelagic redoxclines. *Appl Environ Microbiol* **71**: 6664–6672.

Lauro FM, DeMaere MZ, Yau S, Brown MV, Ng C, Wilkins D *et al.* (2011). An integrative study of a meromictic lake ecosystem in Antarctica. *ISME J* **5**: 879–895.

Li WZ, Godzik A. (2006). Cd-hit: a fast program for clustering and comparing large sets of protein or nucleotide sequences. *Bioinformatics* **22**: 1658–1659.

Lyons TW, Reinhard CT, Planavsky NJ. (2014). The rise of oxygen in Earth's early ocean and atmosphere. *Nature* **506**: 307–315.
Meyer KM, Kump LR. (2008). Oceanic euxinia in Earth history: causes and consequences. *Annu Rev Earth Planet Sci* **36**: 251–288.
Millero FJ. (1991). The oxidation of H2S in Framvaren fjord. *Limnol Oceanogr* **36**: 1006–1014.
Pedrós-Alió C, Guerrero R. (1993). Microbial ecology in Lake Cisó. *Adv Microb Ecol* **13**: 155–209.
Prosser JI. (2012). Ecosystem processes and interactions in a morass of diversity. *FEMS Microbiol Ecol* **81**: 507–519.
R Develppment Core Team (2012). *R: A Language and Environment for Statistical Computing*. R Foundation for Statistical Computing: Vienna, Austria.
Ragsdale SW. (2004). Life with carbon monoxide. *Crit Rev Biochem Mol Biol* **39**: 165–195.
Raskin L, Rittmann BE, Stahl DA. (1996). Competition and coexistence of sulfate-reducing and methanogenic populations in anaerobic biofilms. *Appl Environ Microbiol* **62**: 3847–3857.
Reichenbach H. (2006). The order Cytophagales. In: Dworkin M, Falkow S, Rosenberg E, Schleifer K-H, Stackebrandt E (eds) *Prokaryotes*. Springer: Berlin, pp 549–590.
Reinhard CT, Planavsky NJ, Robbins LJ, Partin CA, Gill BC, Lalonde SV *et al.* (2013). Proterozoic ocean redox and biogeochemical stasis. *Proc Natl Acad Sci USA* **110**: 5357–5362.
Rikmann E, Zekker I, Tomingas M, Tenno T, Menert A, Loorits L *et al.* (2012). Sulfate-reducing anaerobic ammonium oxidation as a potential treatment method for high nitrogen-content wastewater. *Biodegradation* **23**: 509–524.
Roberts GP, Youn H, Kerby RL. (2004). CO-sensing mechanisms. *Microbiol Mol Biol Rev* **68**: 453–473.
Schmidt U, Conrad R. (1993). Hydrogen, carbon-monoxide, and methane dynamics in Lake Constance. *Limnol Oceanogr* **38**: 1214–1226.
Severmann S, Anbar AD. (2009). Reconstructing paleoredox conditions through a multitracer approach: the key to the past is the present. *Elements* **5**: 359–364.
Sharon I, Pati A, Markowitz VM, Pinter RY. (2009). A statistical framework for the functional analysis of metagenomes. In: Batzoglou S (ed) *Research in Computational Molecular Biology, Proceedings*. Springer: Berlin, Heidelberg, Germany, pp 496–511.
Stewart K, Kassakian S, Krynytzky M, DiJulio D, Murray J. (2007). Oxic, suboxic, and anoxic conditions in the Black Sea. In: Yanko-Hombach V, Gilbert A, Panin N, Dolukhanov P (eds) *The Black Sea Flood Question: Changes in Coastline, Climate, and Human Settlement*. Springer: The Netherlands, pp 1–21.
Sun H, Spring S, Lapidus A, Davenport K, Del Rio TG, Tice H *et al.* (2010). Complete genome sequence of *Desulfarculus baarsii* type strain (2st14(T)). *Stand Genomic Sci* **3**: 276–284.
Sun SL, Chen J, Li WZ, Altintas I, Lin A, Peltier S *et al.* (2011). Community cyberinfrastructure for Advanced Microbial Ecology Research and Analysis: the CAMERA resource. *Nucleic Acids Res* **39**: D546–D551.
Takai K, Campbell BJ, Cary SC, Suzuki M, Oida H, Nunoura T *et al.* (2005). Enzymatic and genetic characterization of carbon and energy metabolisms by deep-sea hydrothermal chemolithoautotrophic isolates of Epsilonproteobacteria. *Appl Environ Microbiol* **71**: 7310–7320.
Tanenbaum DM, Goll J, Murphy S, Kumar P, Zafar N, Thiagarajan M *et al.* (2010). The JCVI standard operating procedure for annotating prokaryotic metagenomic shotgun sequencing data. *Stand Genomic Sci* **2**: 229–237.
Trüper HG, Schlegel HG. (1964). Sulphur metabolism in Thiorhodaceae.1. Quantitative measurements on growing cells of Chromatium Okenii. *Anton Van Lee J M S* **30**: 225–22.
Van Gemerden H, Montesinos E, Mas J, Guerrero R. (1985). Diel cycle of metabolism of phototrophic purple sulfur bacteria in Lake Cisó (Spain). *Limnol Oceanogr* **30**: 932–943.
Vila X, Abellà CA. (1994). Effects of light quality on the physiology and the ecology of planktonic green sulfur bacteria in lakes. *Photosynthesis Res* **41**: 53–65.
Walker CB, de la Torre JR, Klotz MG, Urakawa H, Pinel N *et al.* (2010). Nitrosopumilus maritimus genome reveals unique mechanisms for nitrification and autotrophy in globally distributed marine crenarchaea. *Proc Natl Acad Sci USA* **107**: 8818–8823.
Weber KA, Achenbach LA, Coates JD. (2006). Microorganisms pumping iron: anaerobic microbial iron oxidation and reduction. *Nat Rev Microbiol* **4**: 752–764.
Zeigler Allen L, Allen EE, Badger JH, McCrow JP, Paulsen IT, Elbourne LD *et al.* (2012). Influence of nutrients and currents on the genomic composition of microbes across an upwelling mosaic. *ISME J* **6**: 1403–1414.

Supplementary Information accompanies this paper on The ISME Journal website (http://www.nature.com/ismej)